Patterns and drivers of leaf thermoregulation in rainforest trees of the Australian Wet Tropics

Kali Middleby
October 2024

This thesis is submitted in fulfilment of the requirements for the degree of Doctor of Philosophy in Natural and Physical Sciences, College of Science and Engineering, James Cook University, Nguma-Bada (Cairns), Queensland

‘My life now is just trees… trees… and champagne.’
– *Dame Judi Dench*

Acknowledgements

I would like to express my deepest gratitude to my supervisors, Lucas, Martin, and Darren, for their consistent support and for giving me the freedom to pursue my research interests over the past four years. I think I had the most relaxed yet supportive panel I could have imagined, and I am very aware of how fortunate that makes me.

A special thanks to Kristine for the incredible opportunity to participate in the leaf-warming experiment, to Maurizio for inviting me into your lab and giving me the tools to process genetic datasets, and to Rebecca for your invaluable guidance with the genotype association analysis, which I wouldn't have had the confidence to include without your reassurance.

To my friends and family, thank you for your endless encouragement and for always making me believe I can achieve anything. A particular shoutout to Mikey, who flew to Cairns to help with lab work when I ambitiously set out to measure *all the things.*

Finally, to Alex – my partner, co-author, and co-conspirator – thank you for your constant support.

Incorporated Publications

This thesis is in the form of a 'thesis by publication' and incorporates both published works and submitted chapters.

Publication status of each chapter

Chapter 2. Published: **Middleby, K.B.**, Cheesman, A.W., Cernusak, L.A. (2024). Impacts of elevated temperature and vapour pressure deficit on leaf gas exchange and plant growth across six tropical rainforest tree species. *New Phytologist, 243*(2), 648-661. https://doi.org/10.1111/nph.19822

Chapter 3. Not published: Trait acclimation to contrasting temperature and humidity conditions alters leaf thermoregulation in tropical rainforest saplings.

Chapter 4. Published: **Middleby, K.B.**, Cheesman, A.W., Hopkinson, R., Baker, L., Ramirez Garavito, S., Breed, M.F., & Cernusak, L.A. (2024). Ecotypic variation in leaf thermoregulation and heat tolerance but not thermal safety margins in tropical trees. *Plant, Cell, and Environment* [Early View]. https://doi.org/10.1111/pce.15141

Chapter 5. Submitted: **Middleby, K.B.**, Jordan, R., Cheesman, A.W., Rossetto, M., Breed, M.F., Crayn, D.M., & Cernusak, L.A. (unpublished). Local adaptation to climate drives leaf thermoregulation in tropical trees. Submitted to *Global Change Biology*.

Other publications related to the thesis

Middleby, K.B., Cernusak, L.A., Breed, M.F., Crayn, D.M., Laurance, S.G.W., Preece, N., van Oosterrzee, P., Engert, J., & Cheesman, A.W. (unpublished) Strong site and provenance effects on tropical tree growth and survival, but limited evidence for local adaptation. Submitted to *Biotropica.* Note: Included as an appendix (see Appendix D) as context for Chapter 4 but not a part of this thesis

Co-authored publications during this thesis

Doughty, C., Keany, J., Wiebe, B., Rey-Sanchez, C., Carter, K., **Middleby, K.B.**, Cheesman, A.W., Goulden, M., da Rocha, H., Miller, S., Malhi, Y., Fauset, S., Gloor, E., Slot, M., Oliveras Menor, I., Crous, K., Goldsmith, G., & Fisher, J. (2023). Tropical forests are approaching critical temperature thresholds. *Nature* 621, 105–111. https://doi.org/10.1038/s41586-023-06391-z

Crous, K., Cheesman, A.W., **Middleby, K.B.**, Rogers, E., Wujeska-Klause, A., Bouet, A., Ellsworth, D., Liddell, M., Cernusak, L., & Barton, C. (2023). Similar patterns of leaf temperatures and thermal acclimation to warming in temperate and tropical tree canopies. *Tree Physiology* 43(8), 1383–1399. https://doi.org/10.1093/treephys/tpad054

Statement on the contribution of others

Research funding
Holsworth Wildlife Research Endowment (3 years)

Skyrail Rainforest Foundation (3 years)

Australian Postgraduate/Research Training Award (4 years)

Thesis committee
Prof Lucas Cernusak, College of Science and Engineering, James Cook University, Cairns, Australia

A/Prof Martin Breed, College of Science and Engineering, Flinders University, Adelaide, Australia

Prof Darren Crayn, Australian Tropical Herbarium, James Cook University, Cairns, Australia

Data collection
Data collection for this thesis was conducted by Kali Middleby, with assistance from Alexander Cheesman, Mikey Middleby, Sebastian Ramirez-Garavito, Michael Bewley-Green, Rachael Walshe, Nara Vogado, Jayden Engert, Richard Hopkinson, and Leesa Baker.

Contribution of authors to each chapter

Chapter	Statement of contribution
Chapter 1: General introduction	KM wrote the chapter.
Chapter 2: Impacts of elevated temperature and vapour pressure deficit on plant growth and gas exchange	KM conceived the research. KM and AC collected the data. KM analysed the data and wrote the manuscript with feedback from AC and LC.
Chapter 3: Trait acclimation to contrasting temperature and humidity conditions alters leaf thermoregulation in tropical rainforest saplings	KM conceived the research and collected and analysed the data. KM wrote the manuscript with feedback from LC.
Chapter 4: Ecotypic variation in thermoregulation and heat tolerance but not thermal safety margins in tropical trees	KM conceived the research, collected and analysed the data, and wrote the manuscript with editorial inputs from LC, AC, and MB. RH, LB and SRG helped collect data.
Chapter 5: Local adaptation to climate drives thermoregulation in co-occurring tropical rainforest trees	KM conceived the research, collected and analysed the data, and wrote the manuscript with editorial inputs from LC, MB, AC, DC, MR, & RJ.
Chapter 6: General discussion	KM wrote the chapter.

Thesis Abstract

Globally increasing temperatures threaten to push tropical rainforests beyond their physiological limits. However, trees can show remarkable resilience to warming through a combination of thermal tolerance and avoidance strategies that maintain leaf temperatures within safe operating margins. Plant thermoregulation can be achieved through variation of functional traits that affect leaf energy balance, potentially resulting in enhanced leaf cooling in warmer environments. Yet, evidence of this thermoregulatory ability within a species and the relative roles of plasticity (i.e. through acclimation on the scale of days to months) and genetic variation (e.g. local adaptation) remains limited. The aim of this thesis was to investigate the role of intraspecific trait variation in mediating leaf thermoregulation in tropical forests. By using a combination of experimental and field-based approaches, I explored the patterns of thermal trait variation across species distributions, whether these are a direct response to contrasting temperatures or other covarying environmental variables, and to what extent variation was driven by acclimation or adaptation.

In Chapter 2, to identify whether leaf trait variation responded directly to temperature and isolate the effect of acclimation, I conducted a glasshouse experiment to control for the effect of other variables. In this experiment, six tropical tree species of varying life history strategies were grown under different temperature and vapour pressure deficit treatments. After 6 months under the three climate treatments, I found that when controlling for vapour pressure deficit, an increase in growth temperature had a positive effect on plant growth, whereas vapour pressure deficit had the opposing effect, and thereby limited growth. All species showed consistent acclimation of photosynthetic biochemistry and thermal tolerance in response to temperature, whereas species acclimated their stomatal and minimum conductance and leaf traits differently. The main finding was that stomatal limitation associated with elevated vapour pressure deficit was likely responsible for constraining plant growth to elevated temperatures. This was one of the first studies to investigate the direct responses of gas exchange to elevated temperatures when simultaneously controlling for vapour pressure deficit in tropical trees.

In Chapter 3, working with the same plants from the experiment in Chapter 2, I aimed to determine whether acclimation of leaf thermal traits in response to temperature and vapour pressure deficit (VPD) treatments resulted in leaf thermoregulation. Specifically, I investigated whether plants grown under warmer or drier climates acclimate their leaf traits and physiology to help cool their leaves and avoid lethal operating temperatures. To do this, leaf traits measured in Chapter 2 were used to calculate the leaf-air temperature offset and thermal time constant using a steady-state leaf energy balance model. In this chapter, I found that leaf thermoregulation is both species-specific and context dependent. While some species demonstrated trait coordination supporting limited homeothermy, acclimation to elevated temperature and VPD affected the balance between leaf cooling and water conservation. Notably, VPD-induced acclimation appeared to reduce the capacity for limited

homeothermy in certain species, suggesting that plants prioritize water conservation over leaf cooling under high VPD conditions.

In Chapter 4, to identify if there was ecotypic variation in thermal tolerance and leaf temperatures in tropical trees, I measured leaf and canopy temperatures, thermal tolerance, and leaf thermal traits in lowland and upland provenances of four species planted in a common garden experiment. This revealed highly species-specific provenance differentiation in thermal tolerance and leaf thermal traits, with only one of the four species exhibiting the expected patterns of enhanced leaf cooling capacity for warm-adapted plants. Importantly, this study found that despite ecotypic variation in leaf temperatures and thermal tolerance, none of the species had substantial provenance differences in thermal safety margins.

Finally, Chapter 5 looks more closely at patterns and drivers of thermoregulation across the tropical distribution of three species. I combined measurements of leaf thermal traits from field campaigns with analyses of genomic variation to identify signals of selection and supported this with a glasshouse experiment. In this study, I found that covariation of leaf thermal traits resulted in enhanced leaf cooling for plants in warmer parts of their distributions in two of the three species, supporting results from Chapter 3. Genetic data suggested this variation was not solely due to acclimation, with signals of selection to temperature and precipitation linked to variation in leaf thermal traits for two of the three species. Looking closer at one species in a climate-controlled glasshouse experiment, I found strong evidence that variation in functional traits that impact the thermal response of leaves was driven strongly by both local adaptation and acclimation.

The findings of my thesis show that trait coordination resulting in enhanced leaf cooling was observed both as an acclimation response to warmer growth conditions (Chapters 2 and 3), and as an adaptive response in populations originating from warmer sites (Chapters 4 and 5). However, patterns differed across species, raising the question of how common plant thermoregulation is across tropical trees. Given the speed at which climate change is occurring, these results suggest that species with limited capacity to acclimate or adapt their thermal safety margins may be at risk.

Table of Contents

List of Tables and Figures

Chapter 1: General Introduction

How temperature affects plant functioning

Plant performance is strongly influenced by temperature. Temperature controls the enzymatic reaction rates of photosynthesis and respiration, the expression of heat shock proteins, the production of reactive oxygen species, and the fluidity of thylakoid membranes (Wahid et al., 2007). Indirectly, through its influence on vapour pressure deficit, temperature also influences the evaporative demand at both the leaf and soil levels, affecting water availability and demand. Global warming has caused rapid increases in both air temperature and vapour pressure deficit (IPCC, 2022) that outpace the adaptive capacity of trees which have long generation times. These effects have contributed to a rise in global tree mortality (Hammond et al., 2022), limited tree growth (Bauman et al., 2022a), constrained gross primary productivity (Yuan et al., 2019) and increased global land evapotranspiration (Wang et al., 2022).

Importance of tropical rainforests

Tropical rainforests host a significant portion of the earth's terrestrial biodiversity and provide critical ecosystem services such as carbon sequestration and water cycling (Mitchard, 2018). As such, environmental changes in these ecosystems substantially affect global carbon and water cycles (Armstrong Mckay et al., 2022). With historically low climate variability, tropical rainforests have adapted to narrower climatic niches (Fordham et al., 2019; Corlett, 2011) and already experience temperatures at or above their physiological optima (Doughty et al., 2023b; Mau et al., 2018). A number of studies show that while many tropical tree species are shifting their geographic ranges in response to warming, these migration rates appear slower than needed to keep pace with modern climate change (Colwell & Feeley., 2024; Esquivel-Muelbert et al., 2019; Feeley et al. 2011), leaving tropical forests critically vulnerable to warming.

Coping with heat

As plants are exposed to temperatures above their photosynthetic optima, the rate of carbon uptake is reduced. High temperatures disrupt electron transport in photosystem II which displaces light-harvesting complexes (Mathur et al., 2014). While photo-protective mechanisms can repair functioning over time, depending on the threshold and the cumulative stress exposure, (Cook et al., 2024) this can limit carbon uptake, or even result in leaf death. Photosynthetic heat tolerance varies significantly across species and biomes (Geange et al., 2021), and also within species due to acclimation or adaptation. Among tropical trees, critical temperature thresholds, such as T_{crit} (the temperature causing a 5% decline in photosynthetic efficiency) range from 35–57°C, and T_{50} (the temperature causing a 50% decline) ranges from 44–56°C (O'Sullivan et al., 2017; Slot et al., 2021). Although species can adjust photosynthetic heat tolerance by ~

0.24–0.60°C per 1°C increase in mean annual temperature (O'Sullivan et al., 2017; Slot et al., 2021; Zhu et al., 2018), studies suggest that this adjustment often does not fully maintain thermal safety margins in warmer climates (Kitudom et al., 2022; Perez & Feeley, 2020).

Leaf temperature

In addition to modifying heat tolerance, plants may employ a 'heat avoidance' strategy through the acclimation or adaptation of leaf traits that affect leaf energy balance. Traits such as absorptance, angle, emissivity, thickness, width, and stomatal conductance influence sensible and latent heat fluxes and net radiation, which in turn affect the offset between leaf and air temperature. These mechanisms contribute to substantial variation in leaf temperature among co-occurring species (Fauset et al., 2018; Guo et al., 2022; Leuzinger & Korner, 2007), while also helping to explain partial convergence in effective leaf temperatures across thermal gradients (Helliker et al., 2018; Liancourt et al., 2020; Zhou et al., 2023). Since leaf temperature, not air temperature, directly controls leaf metabolism, regulating leaf temperature provides an important strategy for maintaining thermal safety margins in warmer climates.

Plant thermoregulation

The concept that plants regulate leaf-to-air temperature differentials ($\Delta T_{leaf\text{-}air}$) via rapid changes in stomatal behaviour or long-term acclimation and adaptation has gained significant research attention. The 'limited homeothermy' hypothesis describes how partial maintenance of leaf temperature optimizes carbon gain (Mahan & Upchurch, 1988; Michaletz et al., 2015). Limited homeothermy is usually assessed by comparing the slope coefficient (β) of leaf versus air temperature, where a $\beta \sim 1$ indicates poikilothermy, $\beta < 1$ indicates limited homeothermy, and $\beta > 1$ indicates megathermy. Subsequent work has expanded this theory (Michaletz et al., 2015; 2016) and tested it using directly by measuring leaf and canopy temperatures in situ (Blonder et al., 2020; Fauset et al., 2018; Still et al., 2022), or indirectly using oxygen stable isotopes (Helliker et al., 2018; Liancourt et al., 2020) and energy balance theory (Dong et al., 2017; Guo et al., 2022). While these studies highlight the importance of leaf traits in regulating temperatures, most focus on comparisons between species in single environments, or their composition across biomes. This leaves a significant gap in our understanding of intraspecific variation and the roles of acclimation and adaptation.

The role of intraspecific variation (acclimation and adaptation)

Intraspecific trait variation can rival that observed between species (Zuleta et al., 2022). Understanding the extent and drivers of this variation in photosynthetic heat tolerance and leaf thermoregulation is essential for predicting tree responses to climate change. Acclimation, a type of phenotypic plasticity, occurs over a time scale of days to weeks. It includes both short-term physiological

responses and longer-term morphological adjustments. Acclimation enables plants to modify their traits in response to environmental changes. For example, plants might alter stomatal conductance or leaf orientation to mitigate heat stress. If environmental changes persist, new leaves may develop with modified traits, such as changes in leaf width or thickness. Acclimation can enhance leaf cooling and maintain carbon uptake during heat stress, which can then be allocated to growth, reproduction, or survival, providing a short-term fitness advantage. Over time, this can lead to local adaptation, where populations become genetically differentiated as they evolve traits that are better suited to their specific environmental conditions.

Conversely, trait variation can result in a convergence of leaf temperatures across contrasting climates (Helliker et al., 2018), creating a more uniform selective environment (Muñoz, 2022). This idea aligns with the Bogert effect, which suggests that thermoregulatory behaviour may homogenize selective pressures and potentially slow physiological evolution (Muñoz & Bodensteiner, 2019). While this theory is almost exclusively studied in animals, this might explain the limited evidence of adaptation in photosynthetic biochemistry (Kumarathunge et al., 2019) or thermal tolerance thresholds (Gimeno et al., 2008; Marias et al., 2016) and why leaf morphology often exhibits more pronounced adaptive changes compared to physiology and gas exchange (Bison & Michaletz, 2024; Everingham et al., 2024).

The interplay between acclimation and adaptation in thermal tolerance and leaf temperature regulation is complex. Acclimation can buffer populations against immediate thermal stress, supporting short-term survival in dynamic environments. However, these responses can also mask or constrain the longer-term evolutionary adaptations that are necessary to cope with sustained environmental changes. Meanwhile, local adaptation can drive genetic divergence in thermal safety margins among populations, but its success depends on the extent of environmental variation experienced over time.

Trait trade-offs across complex environmental gradients

Temperature variations across species distributions, driven by latitudinal or elevational gradients, often coincide with shifts in precipitation, humidity, and soil nutrient availability. These environmental gradients shape plant trait trade-offs, which in turn affect the leaf-to-air temperature differential ($\Delta T_{leaf\text{-}air}$) and leaf temperature. For instance, soil moisture availability may influence thermal responses, with water-limited plants exhibiting higher $\Delta T_{leaf\text{-}air}$ due to prioritizing water conservation over thermoregulation or carbon uptake. The expression of multiple traits may interact to balance these trade-offs. For example, while leaf width may increase with elevation, leading to a higher $\Delta T_{leaf\text{-}air}$ in cooler climates, an increase in another trait such as stomatal conductance may counterbalance the warming effect of broader leaves. These multivariate responses can be examined mechanistically by parameterizing a leaf energy balance model to assess how coordinated trait expression in response to growing temperatures influences leaf temperatures. If air temperature acts as a significant selective force across tropical tree distributions, then maintaining

T_{leaf} within acceptable limits – especially in warmer regions – through coordinated variation in leaf traits should be favoured over trait variation driven by other environmental factors.

Importance of considering intraspecific variation in plant thermoregulation

Understanding how leaf traits are coordinated within-species, and the implications on leaf temperatures can improve our ability to predict the fate of tropical forests in a changing climate and develop effective management strategies. Leaf traits influence plant fitness indirectly by altering temperature extremes experienced at the leaf surface, affecting processes such as photosynthesis and water use. While leaf damage from extreme temperatures may not always correlate with plant fitness, the ability to maintain leaf function under stress is a key component of plant survival and reproduction in changing environments.

Incorporating leaf temperature into ecological studies provides a more accurate assessment of the temperature extremes experienced by plants. For example, leaf energy balance models, which estimate leaf temperature based on physiological traits and environmental conditions, have been used to improve predictions of photosynthesis and drought stress in crop species (Perera et al., 2020) and to infer habitat preferences in early angiosperms (Lee et al., 2015), demonstrating the utility of mechanistic approaches for understanding plant-environment interactions. Other areas that could benefit from integrating leaf energy balance modelling include species distribution modelling (SDM), as trait- and physiology-based species distribution models (SDMs) have been shown to outperform traditional approaches (Gamliel et al., 2020).

Beyond modelling, intraspecific variation in thermoregulatory traits has practical implications for conservation and restoration. In rainforest restoration, selecting provenances that are pre-adapted to anticipated future climates can enhance restoration success. Provenances with traits suited to higher temperatures or altered moisture regimes are more likely to survive and thrive under future climatic conditions, improving ecosystem resilience and ensuring long-term conservation outcomes. By maintaining genetic diversity within and across restoration sites, this approach also supports the adaptive potential of tropical forests in the face of ongoing climate change. Ultimately, linking intraspecific trait variation to species distribution modelling and restoration strategies offers a pathway to more effectively predict and manage the impacts of climate change on tropical forests, emphasizing the need for a mechanistic understanding of how plants respond to climate extremes (Chardon et al., 2020; Westerband et al., 2021).

Objectives

To better predict the fate of tropical forests in a changing climate, and develop strategies to ensure their persistence, it is essential to understand how tropical trees can acclimate and adapt to environmental stressors. The overall aim of this thesis is to investigate how tropical rainforest trees regulate leaf

temperature in response to rising air temperatures and to identify the factors driving these responses. To achieve this aim, the specific objectives of the thesis are:

1. ***To identify patterns of leaf thermoregulation:*** Determine how leaf thermal traits vary within species across different temperature environments and assess whether this variation enhances cooling in warmer conditions.
2. ***To explore the roles of acclimation and genetic adaptation:*** Assess the relative contributions of short-term physiological acclimation and longer-term genetic adaptation to leaf thermoregulation.
3. ***To disentangle thermal trait variation that is due to temperature:*** Investigate how vapor pressure deficit and other environmental factors interact with temperature to affect leaf thermoregulation.

Thesis outline

To address these objectives (Obj), I combined field measurements, controlled experiments, molecular ecology, and leaf energy balance modelling. The thesis data chapters that address these objectives are summarised in Figure 1. 1, and organized as follows: In **Chapter 2,** I manipulated temperature and vapor pressure deficit in a climate-controlled growth experiment (Obj 3) to assess the physiological responses of selected tree species (Obj 2). In **Chapter 3**, I investigated how trait acclimation (Obj 2) to these treatments (Obj 3) affected both the leaf-air temperature offset and thermal time constant (Obj1). In **Chapter 4**, I switched to an assessment of ecotypic variation (Obj 2) in thermal safety margins (Obj 1), with saplings originating from high and low elevation sites grown in a lowland common garden. Finally, in **Chapter 5**, I explored the extent of intraspecific variation in leaf thermal traits and leaf temperatures (Obj 1) in natural populations across a wide thermal gradient across the Australian Wet Tropics. Using a combination of genotype-association analysis and a provenance trial in a climate-controlled glasshouse, I tested whether phenotypic divergence represented acclimation or local adaptation (Obj 2) in leaf thermoregulation.

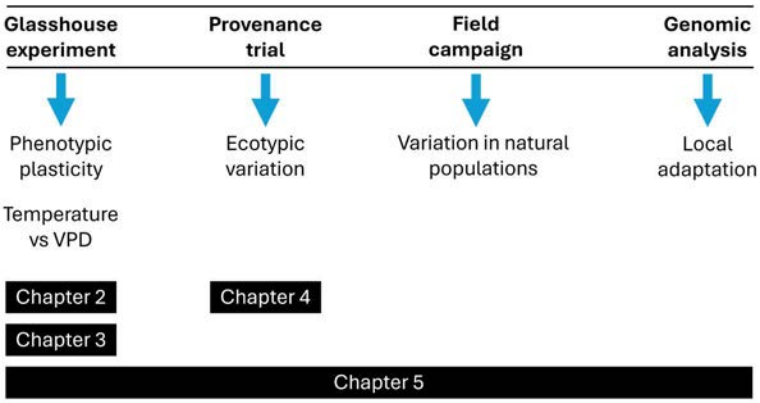

Figure 1. 1. Outline of methods incorporated to answer research questions throughout this thesis. Black boxes indicate in which chapters each approach is utilised. VPD = atmospheric vapour pressure deficit.

Chapter 2: Impacts of elevated temperature and vapour pressure deficit on leaf gas exchange and plant growth across six tropical rainforest tree species

2.1 Introduction

Tropical forests are critically important ecosystems for their role in carbon uptake and water cycling globally (Mitchard, 2018). These ecosystems already operate close to their critical temperature thresholds for photosynthesis, leaving them vulnerable to relatively small increases in temperature (Doughty et al., 2023b). As surface temperatures rise worldwide (IPCC, 2022), so does the vapour pressure deficit (VPD_{air}). The VPD_{air} has been increasing since the 1990s and is projected to continue in the coming decades (Fang et al., 2022). High VPD_{air} increases the atmospheric demand for water from plants, leading to atmospheric drought (Grossiord et al., 2020), and can exacerbate soil water deficit. Globally increasing VPD_{air} has resulted in gross primary productivity (GPP) declines partly offsetting the expected CO_2 fertilisation effect (Yuan et al., 2019). Furthermore, there is increasing evidence that hot, dry periods limit tropical tree growth (Bauman et al., 2022a) and drive higher rates of global forest mortality events (Bauman et al., 2022b; Hammond et al., 2022; Mcdowell et al., 2008). Characterising the relative roles of air temperature (T_{air}) and VPD_{air} on net primary productivity and leaf-level gas exchange in trees will allow us to understand better the trade-offs between opening stomata to increase carbon uptake and reduce heat stress (Sadok et al., 2021), and closing them to conserve water (Medlyn et al., 2011).

The temperature response of net photosynthesis (A_{net}) is a product of both the basal rates and thermal sensitivity of processes such as Rubisco carboxylation (V_{cmax}) and electron transport (J_{max}) in concert with the CO_2 concentration observed inside the leaf (c_i), which is influenced by stomatal conductance (g_s) (Farquhar et al., 1980). Both V_{cmax} and J_{max}, along with their thermal sensitivities acclimate to their environment, generally decreasing with increasing growth temperature (Fürstenau Togashi et al., 2018; Kumarathunge et al., 2019). These changes can be explained by the higher rate of enzyme activity under increased temperatures, causing plants to invest less nitrogen into photosynthetic enzymes like Rubisco (Prentice et al., 2014). Changes in nitrogen allocation and, consequently, photosynthetic biochemistry can also develop due to changes in leaf water status from decreased soil moisture (Zhou et al., 2013) or elevated VPD_{air} (Quebbeman & Ramirez, 2016; Walker et al., 2014; Yang et al., 2019). While the impact of VPD_{air} has received much less attention, a study in wheat showed that even short-term exposure to elevated VPD_{air} can decrease both V_{cmax} and J_{max} (Fakhet et al., 2021).

The response of A_{net} to warming is also constrained by stomata (Farquhar & Sharkey, 1982). Increasing temperature and VPD_{air} influence the instantaneous rate of g_s, and longer-term acclimation and

adaptation (Jarvis, 1976; Kruse et al., 2019; McAdam & Brodribb, 2015; Yamori et al., 2014). The short-term response of g_s to increasing temperature (and coincident VPD_{air}) follows a peaked pattern with reduced rates below and above their thermal optimum. This behaviour is due to increasing VPD_{air} resulting in stomatal closure (Peak & Mott, 2011) as well as optimal stomatal behaviour (Medlyn et al., 2011). However, there are now numerous reports that g_s can be decoupled from photosynthesis, increasing in response to high temperatures and resulting in cooler leaf temperatures (De Kauwe et al., 2019; Drake et al., 2018; Kumarathunge et al., 2019; Marchin et al., 2023; Urban et al., 2017b). Long-term warming studies in tropical trees report warmed plants having lower g_s measured under standard conditions than unwarmed plants (Crous et al., 2023; Fauset et al., 2019). However, with VPD_{air} generally not controlled in these experiments, this is likely a response to increasing VPD_{air} rather than a direct response to increasing T_{air}. Supporting this, a meta-analysis by Lopez et al. (2021) showed acclimation of plants to reduce g_s in response to increasing VPD_{air}, with implications on carbon uptake and plant growth. This generalised response may help prevent drought-induced cavitation, as a recent study in three temperate species shows that high VPD_{air} resulted in hydraulic damage in species that failed to reduce g_s (Schonbeck et al., 2022). Reduction in g_s as an acclimation response to warming suggests plants may opt to conserve water and avoid hydraulic damage, but at the cost of reduced carbon gain and increased vulnerability to thermal extremes at the leaf level due to reduced evaporative cooling (Blonder et al., 2023).

A change in g_s affects transpiration and modifies leaf energy balance (Bonan, 2008). Transpirational cooling, via maintained or increased g_s, can help avoid critical leaf temperatures when moisture is not limiting (Cook et al., 2021; Deva et al., 2020; Drake et al., 2020; Lapidot et al., 2019), or even despite soil drought (Marchin et al., 2023). This response may depend in part on the sensitivity of stomata to VPD_{air}, which varies between and within species (Grossiord et al., 2020). Tropical species originating from wetter biomes have higher sensitivity and exhibit an isohydric response, limiting water loss by closing stomata (Cunningham, 2004, 2005). According to leaf energy balance theory, all else being equal, this reduction in transpiration will increase T_{leaf} during the hottest part of the day (Bonan, 2008). However, increasing atmospheric VPD_{air} increases the vapour pressure difference between the leaf and air (VPD_L) – increasing the evaporation rate and passively reducing T_{leaf} (Massmann et al., 2019).

The integrated biochemical (V_{cmax25}, J_{max25}) and stomatal (g_s) responses to changes in both temperature and VPD_{air} will shape how trees respond to current and future warming. Characterising the relative impacts of temperature and VPD_{air} is important for tropical forests, given the variation in predicted climatic trajectories (Fang et al., 2022). Additionally, tropical species have higher sensitivities to both elevated T_{air} (Choury et al., 2022; Crous et al., 2022; Cunningham & Read, 2003) and VPD_{air} (Cunningham, 2004). Despite this, only one study has investigated tropical tree acclimation to VPD_{air} (Cunningham, 2005),

and only one study investigating the temperature response of GPP in tropical trees controlled for the associated increase in VPD_{air} (Smith et al., 2020).

I aimed to disentangle the impacts of T_{air} and VPD_{air} on growth and physiology in well-watered saplings of six tropical rainforest tree species using climate-controlled glasshouse chambers. I hypothesised; (H1) T_{air} and VPD_{air} would have contrasting impacts on plant growth, with increasing T_{air} having a positive effect, and increasing VPD_{air} having a negative effect under these treatment conditions, (H2) species with higher stomatal sensitivity to VPD_{air} would be more negatively affected by growth at elevated VPD_{air}, and (H3) photosynthetic biochemistry (e.g. V_{cmax} and J_{max}) would be impacted both directly by growth at elevated T_{air} and indirectly at elevated VPD_{air} through adjustment to lower operating c_i resulting from stomatal limitations, resulting in altered rates of gas exchange when assessed under common conditions.

2.2 Materials and Methods

2.2.1 Typical climate of study region

The Australian Wet Tropics bioregion is part of the humid tropics (Koppen-Geiger climate classification), with a hot-humid wet season from December to March and mild dry season from April to November. The range of mean VPD in the region is typical of other tropical wet forests (Bauman et al., 2022b), with a recent paper examining plant ecohydrological strategies across elevation at two well monitored sites (Binks et al., 2023) showing long term daily maximum VPD averaging 1.0 kPa at a site in the uplands (elevation 720 m) and 1.3 kPa at a site in the lowlands (elevation 86 m). It is important to note the daily maximum VPD at the lowland site rarely exceeded 2.5 kPa over 10 years of monitoring.

2.2.2 Study species

I examined six species, all woody trees from tropical rainforests of the Australian Wet Tropics: *Atractocarpus fitzalanii* (F. Muell.) Puttock *subsp. fitzalanii* (Rubiaceae), *Buckinghamia celsissima* F. Muell. (Proteaceae), *Endiandra microneura* C.T. White (Lauraceae), *Ficus racemosa* L. (Moraceae), *Melicope elleryana* (F. Muell.) T.G. Hartley (Rutaceae), and *Nauclea orientalis* (L.) L (Rubiaceae). Henceforth, these species are referred to by their genus name only. All plant material was obtained from local nurseries, originating from single source provenances of lowland populations in northeast Queensland, Australia. Three species (*Atractocarpus, Buckinghamia*, and *Endiandra*) are evergreen, late successional species, endemic to Queensland, Australia. The other three species (*Ficus*, *Melicope*, and *Nauclea*) are semi-deciduous, early successional species, more widely distributed with ranges including tropical Asia. These semi-deciduous species had not yet experienced a period of leaflessness.

2.2.3 Experimental setup and growth conditions

All seedlings (< one year old) were replanted into 8L pots containing a high organic matter potting mix augmented with a local volcanic stone, Quincan, to improve drainage. Prior to treatments, they were grown in a shade house (75% transmission) for one month to recover from possible transplant shock. At the experiment start, plants were placed into one of three glasshouse chambers. Treatments began in December 2022, coinciding with the onset of the Wet season, and lasted six months. Due to some limitations on total seedling numbers available, the number of individuals per species placed in each chamber varied from 5-11 (median 8). Individuals within each species were distributed so each treatment had similar-sized seedlings at the experiment start, with initial seedling heights ranging from an average (±1SD) of 16.4±2.6 cm in *Atractocarpus* to 40.4±4.1 cm in *Melicope*.

I applied three treatments to disentangle the physiological and morphological responses of saplings to realistic changes in growth temperature and VPD_{air}. These treatments included 1) low T_{air} and low VPD_{air}, 2) high T_{air} and low VPD_{air}, and 3) high T_{air} and high VPD_{air} (Table 2. 1, Figure 2. 1). A 6 °C difference was maintained between low and high-temperature chambers, with daytime (9 am to 3 pm) T_{air} averaging 26.6 (± 2.9) °C in the low-temperature chamber and 32.5 (± 2.9) °C in the high-temperature chambers (Table 2. 1, Figure 2. 1). A 0.7 kPa difference was maintained in the daytime average VPD_{air} of low and high VPD_{air} chambers, with daytime VPD_{air} averaging 0.72 (± 0.32) kPa in the low VPD_{air} chamber at high T_{air} and 1.4 (± 0.59) kPa in the high VPD_{air} chamber (Table 2. 1, Figure 2. 1). These conditions represent typical variations across elevation gradients in the Australian Wet Tropics. A fourth, low T_{air} low VPD_{air} treatment was not included a) because we only have access to three chambers, and b) given how these variables are positively correlated in nature, this combination is unrealistic. Glasshouse temperatures tracked external conditions measured outside the glasshouse with an offset applied between temperature treatments (Table 2. 1, Figure 2. 1) to maintain a realistic diel variation. T_{air} was controlled with the glasshouse climate control system, whereas VPD_{air} was controlled by manipulating relative humidity with an ultrasonic humidifier (JDH-03Z, Hangzhou Conloon Electric Co Ltd., Hangzhou, China) in the low VPD_{air} treatments and a dehumidifier (OADE20, Omega Altise, Victoria, Australia) in the high VPD_{air} treatment, with their action regulated by the relative humidity seen in each chamber.

Table 2. 1. Daytime (9am to 3pm) average treatment conditions over the 6-month experiment. Data represents mean ± 1 standard deviation and is based upon calibrated 10 min data recorded by glasshouse building management system (*n*=6344 observations per treatment).

Treatment	VPD_{air} (kPa)			T_{air} (°C)			RH (%)		
low T_{air} & low VPD_{air}	0.78	±	0.29	26.6	±	2.9	78	±	6.6
high T_{air} & low VPD_{air}	0.72	±	0.32	32.5	±	2.9	86	±	5.6
high T_{air} & high VPD_{air}	1.40	±	0.59	32.5	±	2.9	73	±	9.3

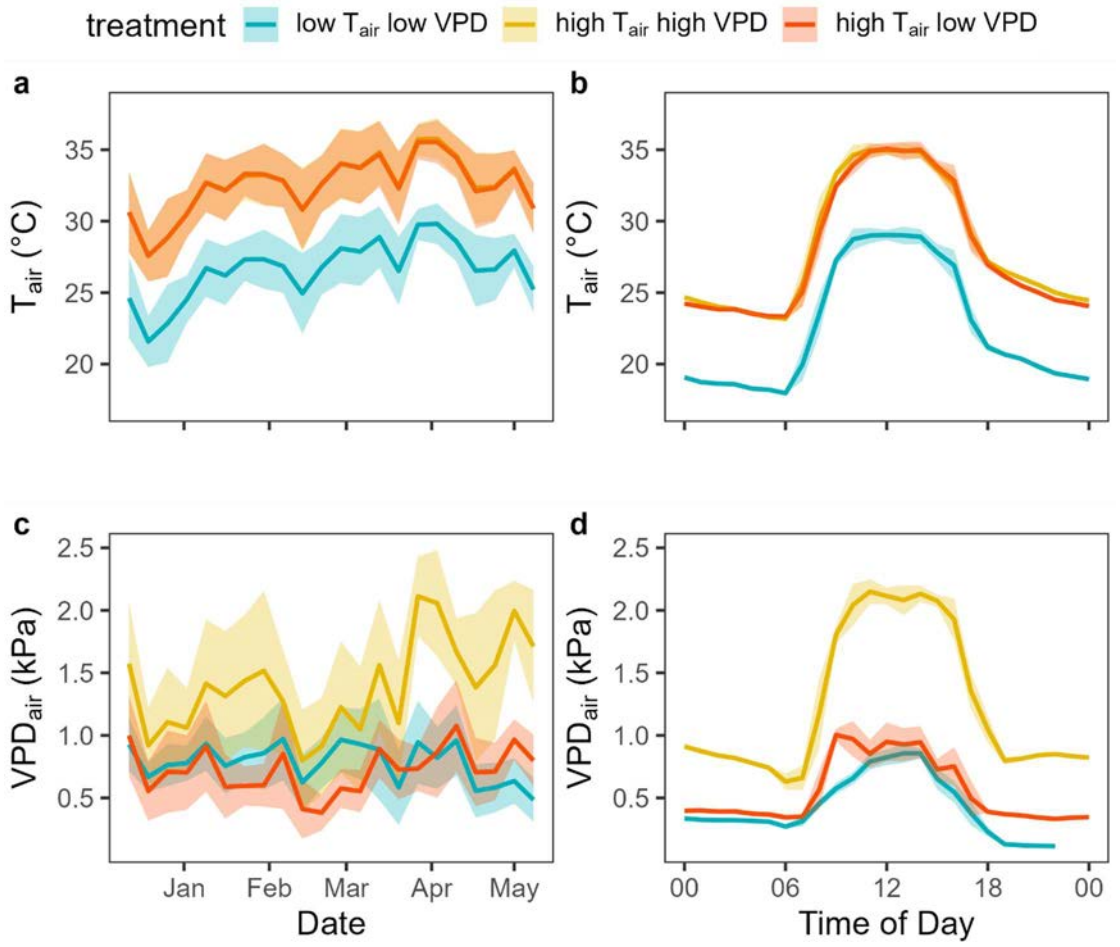

Figure 2. 1. Growth conditions during the experiment. Weekly averages of T_{air} (a) and VPD_{air} (c) during the day (9 am to 3 pm) throughout the growth experiment, and hourly averages of T_{air} (b) and VPD_{air} (d) for an example day on 29/04/2023. Solid lines represent means, and the shaded region represents one standard deviation. Colours represent different treatments but note in panels (a) and (b) they overlap for the two high T_{air} treatments.

I rotated treatments between chambers monthly to mitigate chamber effects. Plants were given slow-release fertilizer (Osmocote Native Formula, ScottsMicacle-Gro, Marysville, OH, USA) at the experiment start and again monthly for all species except *Buckinghamia*, which may be susceptible to phosphorus toxicity (Shane et al., 2004). Initially, all plants were irrigated daily using automated drip-line irrigation and watered to saturation once a week. As plants grew, this increased to automated watering twice daily with manual watering to saturation twice weekly. Toward the experiment end, I gave extra watering to both high-T_{air} treatments to ensure any impacts on plants could be attributed to atmospheric drought rather than soil moisture deficit.

The glasshouse uses horizontal shade screening (XLS-15 F Firebreak, Ludvig Svensson, Kinna Sweden) to create uniform light conditions in each chamber. This results in a 50 and 47% transmission of direct and diffuse PAR (i.e. 400-700 nm), as well as 35% transmission of IR load. Temperature and relative humidity in each chamber were recorded at 10 min intervals (RHP-2R2B Temperature and Humidity Probe, Dwyer Instruments, Michigan City, IN, USA) in the building management system, calibrated against a single humidity and temperature probe (HMP60, Vaisala, Finland).

2.2.4 Leaf temperature

T_{leaf} was monitored throughout the experiment to calculate the offset between leaf and air temperatures (ΔT) and the leaf-to-air vapour pressure difference (VPD_L). Abaxial T_{leaf} was measured using thermistors (LT-1T-SDI12, Edaphic Scientific Pty Ltd, Port Macquarie, Australia) with a ~ 1 mm^2 contact area and < 0.15 °C accuracy. I selected healthy, newly expanded mature leaves positioned horizontally (or if not, fixed horizontally using pipe-wire on the thermistor cable) with a slight north-facing tilt to minimise differences in radiation inputs that would impact ΔT. Due to limits on the number of thermistors available, T_{leaf} was monitored on two to three plants of different species per chamber at a time and thermistors were switched between plants after at least five days of measurements, resulting in eight measurement rounds. During data collection I ensured that a plant from each treatment of the same species was monitored simultaneously, resulting in a dataset for T_{leaf} from 3-5 plants (median 4) per species per treatment.

2.2.5 Gas exchange

Leaf gas exchange in a healthy, recently emerged, mature leaf was measured with a LI-6400xt portable photosynthesis system equipped with a 2×3 cm leaf cuvette with a red-blue LED light source (Li-Cor, Inc., Lincoln, NE, USA). For all gas exchange measurements, I measured one leaf per plant, and six plants per species per treatment on fully expanded and sun-exposed leaves, except for *Ficus* under the two low VPD_{air} treatments in which only five plants were available. Gas exchange measurements were performed under common environment conditions to allow for the determination of acclimation between plants grown under different environmental conditions. Plants were taken out of their growth chambers and into an antechamber where they acclimated for one hour before measurements. The room temperature averaged 28 °C during measurements and had a transparent glass roof so plants were exposed to solar radiation. The licor cuvette was set to a block temperature of 28 ±0.05 °C and VPD_{air} was controlled at 1 ±0.1 kPa for all plants. CO_2 concentration in the cuvette was set to 400 ppm, PAR to 1000 µmol m^{-2} s^{-1} (saturating light determined during preliminary light-response curves), and flow rate to 500 µmol s^{-1} unless stated otherwise. Once gas exchange rates stabilised (minimum 15 minutes), 10 measurements were taken, 30 seconds apart. These were averaged to get a plant-level mean for A_{net}, $g_{s,}$ and intrinsic water use efficiency ($iWUE = A_{net}/g_s$). The same gas exchange data were also used to determine g_1 (Medlyn et al.,

2011), with g_1 fit for each plant using the 'fitBBs' function in the 'plantecophys' package (Duursma, 2015), without fitting the intercept term g_0.

Following these measurements, on the same leaf, photosynthetic CO_2 response curves (A-C_i) were performed to obtain estimates of the maximum rates of Rubsico carboxylation (V_{cmax}) and the maximum rates of electron transport (J_{max}) and their ratio. V_{cmax} and J_{max} were fitted using the 'fitacis' function in the 'plantecophys' package in R (Duursma, 2015). Each curve was inspected for outliers. The curve for one plant could not be fit using the default method, so was removed from analysis. Model fitting was done on each curve. To account for the control over block temperature instead of T_{leaf} (T_{leaf} varied by up to *c*. 2 °C), the fitted parameters V_{cmax} and J_{max} were normalised to 25°C using temperature response parameters from Kelly (2014).

To determine if the impact of elevated VPD_{air} on growth was related to species-level stomatal sensitivity to VPD_{air}, I characterised this in plants grown under the high T_{air} and low VPD_{air} treatment. Stomatal insensitivity to VPD (φ) is a normalized response seen in transpiration across a change in VPD. It represents an index to examine stomatal responses to an imposed VPD change (Franks & Farquhar, 1999). Theoretically, the index ranges from 0, if stomata were to close completely following a change in VPD (while also assuming g_{min}=0), to 1, which would occur if there was no change in g_s following a change in VPD. I calculated φ by examining steady-state transpiration in leaves when exposed to a step change in VPD from 1 to 2 kPa in plants (n=6) grown under high T_{air} and low VPD_{air}. Leaf-level gas exchange in well-watered plants with a T_{leaf} of 28 °C (28.0 ± 0.1), PAR of 1000 µmol m^{-2} $s^{-1,}$ and VPD_L of 1 kPa (1.02 ±0.02 kPa) was allowed to equilibrate before data were logged every 30 sec for 5min. Then, a gradual (~5min ramping) change in VPD_L was imposed by increasing the proportion of air routed through the drierite until a VPD_L of 2 ±0.04 kPa was achieved. At this point, gas exchange was monitored, and once stable, data was once again logged every 30 sec for 5 min. Since φ will depend upon the incremental change in VPD experimentally applied, I first made minor adjustments to measured transpiration via extrapolation to standardise the VPD increment to exactly 1.0 kPa in all cases as per Franks & Farquhar (1999).

2.2.6 Minimum conductance

Leaf minimum conductance (g_{min}) was determined using the mass loss of detached leaves (MLD) (Pearcy et al., 1989; Sack & Scoffoni, 2007). For this, one fully expanded mature leaf per plant was sampled early in the morning before plants received full sunlight. Leaves were the same physiological stage as those used for leaf gas exchange. Petioles were sealed with parafilm, and leaves were placed into a zip lock bag within another opaque bag to keep samples in the dark. Leaves were taken immediately to the lab, scanned, weighed, and set up in the drying chamber. The drying chamber (with heating element off) contained two additional small fans directed upwards to increase air movement and allowed up to 16 leaves to be hung from the upper rail. A temperature-humidity sensor (HT-3015, Lutron Electronic Enterprise Co., Ltd.,

Taipei, Taiwan) recorded conditions during leaf drying. T_{air} and relative humidity in the drying chamber averaged 26.9 ±1.57 °C and 53.6 ±4.7 %, respectively. Fresh leaf mass was measured every 30 minutes with a 4-point balance until there were sufficient points (minimum 8) to observe the linear portion of the mass loss curve. To calculate g_{min}, I determined the transpiration rate (mass loss over time) divided by VPD, with VPD calculated per the Tetens equation (Monteith & Unsworth, 2013).

2.2.7 Photosynthetic heat tolerance

Photosynthetic heat tolerance was assessed using the rise of minimum fluorescence (F_o) with increasing temperature. Leaves were the same physiological stage as those used for leaf gas exchange and g_{min}. Leaves were dark adapted for 30 minutes then placed in a temperature-controlled chamber (3010-GWK1 Gas-Exchange Chamber, Walz, Heinz Walz GmbH, Effeltrich, Germany) connected to a portable gas exchange system (LiCor 6400xt, LiCor Inc., Lincoln, NE, USA). A chlorophyll fluorometer (PAM-2000, Walz, Heinz Walz GmbH, Effeltrich, Germany) measured fluorescence every 60 s with the fibre-optic sensor secured on the glass lid of the chamber. T_{leaf} was recorded using the Walz thermocouple, which has a stated accuracy of ± 0.2 °C. The initial chamber temperature was set to 30 °C, and once F_0 was stable, leaves were heated at 1 °C per min until T_{leaf} reached 60 °C. Leaves were kept in the dark during temperature ramping. This method is commonly used to determine the critical temperature (T_{crit}) threshold at which photosynthetic efficiency of PS-II begins to decline (Schreiber, 1986), which increases with growth temperature (Zhu et al., 2018). Here, T_{crit} is the breakpoint separating the slow and fast rise phases of the F_o versus T_{leaf} curve, determined from break-point regression using the 'segmented' Version 1.6-2 package in R (Muggeo, 2003). I determined T_{crit} on one leaf per plant for six plants per treatment on all six species, except for *Ficus* in the two low VPD_{air} treatments, which only had 5 plants available (106 curves).

2.2.8 Leaf morphology

Leaf traits were measured on all plants using a composite sample of 4-8 leaves per plant, including leaves used for T_{crit}, g_{min} and gas exchange measurements. I measured leaf fresh weight (g) using a 2-point balance, and scanned leaves (CanoScan, LiDE220, Canon Inc., Tokyo, Japan). ImageJ was used to calculate leaf area (cm^2) and effective leaf width (cm) – defined as the diameter of the largest circle that fits within the leaf lamina. Samples were oven-dried at 70 °C for three days to obtain dry weight (g). I calculated specific leaf area (SLA, $m^2\ kg^{-1}$), and leaf dry matter content (LDMC, $mg\ g^{-1}$). Petioles were not removed, and for species with compound leaves (*Melicope*), leaflets were treated as single leaves.

2.2.9 Biomass

Seedling height and diameter at the root collar were measured at the beginning and end of the experiment. Additionally, at the end of the experiment, all plants were harvested, partitioned, and dried (70 °C until constant mass) to get the dry biomass of leaf, stem, and roots. To analyse whether species-level

stomatal sensitivity to VPD could explain the different biomass responses to VPD across species, I calculated the response ratio of biomass to VPD as the average biomass of the high T_{air} low VPD_{air} treatment divided by the average biomass of the high T_{air} high VPD_{air} treatment for each species.

2.2.10 Data analysis

All analyses and graphical representations were performed using R version 4.2.2. To determine if six months of treatment duration had significantly impacted plant growth (total biomass), plant physiology (A_{net}, g_s, $_i$WUE, g_1, g_{min}, T_{crit}, V_{cmax25}, J_{max25}, and their ratio) and leaf morphology (SLA, LDMC, and leaf width), I ran a series of two-way ANOVA with species, treatment, and their interaction as explanatory variables, and type III sums of squares, with contrasts set to 'contr.sums'. To ensure assumptions of normality were met I cube root transformed g_s, and log transformed iWUE, g_{min}, SLA, and the ratio of J_{max25} to V_{cmax25}. Pairwise comparisons of treatments were assessed using the R package 'emmeans' (Lenth, 2022).

To examine if the species-level trait, φ (stomatal insensitivity to VPD) could explain observed differences in plant growth under elevated temperature but different VPD_{air} (i.e. high T_{air} low VPD_{air} and high T_{air} high VPD_{air}) I examined the correlation between φ and the response ratio of biomass to VPD_{air} using ordinary least squares regression.

To examine the impact of treatments on daytime (i.e. 9am to 3pm) VPD_L and ΔT across treatments, I fit a linear mixed effects model with either ΔT or VPD_L as the response variable, and species, treatment, and their interaction as fixed effects. I also included incoming radiation as a continuous covariate, to account for varying radiation within and across days. To account for the measurement design, plant ID nested within the measurement round was included as a random effect.

2.3 Results

2.3.1 Impacts on plant biomass

There were significant differences in total dry biomass across species and treatments, but their interaction was not significant (Table 2. 2). For plants grown under low VPD_{air}, biomass was higher in plants grown under higher T_{air}, with the increase in biomass averaging +28.9 % across species and ranging from +18.1 to +45.5 % (Table 2. 2, Figure 2. 2a). For plants grown under high T_{air}, biomass was lower in plants grown under high VPD_{air} than low VPD_{air}, with biomass −11.1 % lower in the high VPD_{air} compared to low VPD_{air} when averaging across species and ranging between +3.0 to −20.5 % (Table 2. 2, Figure 2. 2a). I found no evidence for a correlation between species-level stomatal sensitivity to VPD and the response ratio of biomass to elevated VPD ($p > 0.05$; Figure 2. 2b).

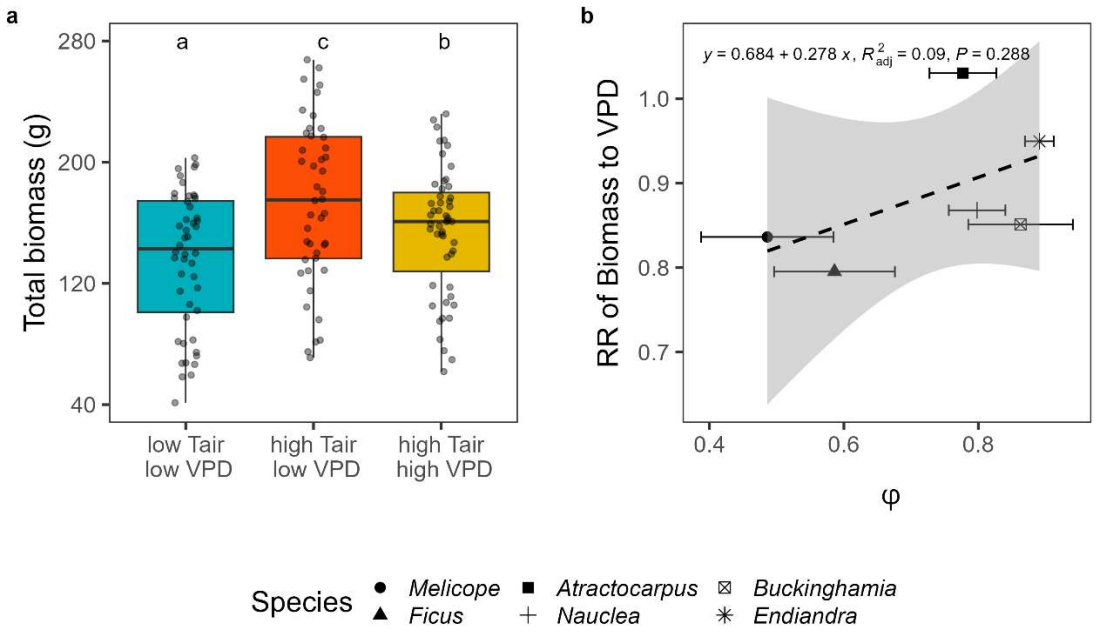

Figure 2. 2. Impact of treatments on total dry biomass accumulation (a) and correlation between stomatal insensitivity to VPD and the response ratio (RR) of biomass to elevated VPD_{air} (b). Each point in panel a represents a plant measurement. Box and whisker plots show the median, the 25th and 75th percentile, along with 1.5*the interquartile range. Colours represent the different treatments. Significant differences among treatments from Tukey Post Hoc results ($p < 0.05$) are denoted with letters. In (b) species with higher stomatal sensitivity to VPD have lower values on the x axis. Different species are represented with different shapes. Each point represents a species average and standard error for stomatal insensitivity to VPD, φ (n=5-6 per species), and the response ratio (RR) of biomass to VPD_{air} (n=5-10 per species). The RR was calculated as the mean biomass of the high T_{air} low VPD_{air} treatment divided by the mean biomass of the high T_{air} high VPD_{air} treatment. Grey shaded region represents the confidence interval (0.95) around the regression line, and the dashed line is the ordinary least squares regression.

2.3.2 Acclimation of leaf-level gas exchange

There was a statistically significant interaction between species and treatment on A_{net}, g_s, and iWUE (Table 2. 2). For most species, I found no evidence that growth temperature (at low VPD_{air}) affected A_{net}, g_s, or iWUE measured under standard conditions ($p > 0.05$; Table 2. 2, Figure 2. 3). The exception was *Nauclea*, where A_{net} was +40 % higher ($t(88) = 3.883$, $p < 0.001$), g_s was +281 % higher ($t(88) = 7.497$, $p < 0.0001$), and consequently, iWUE was −67 % lower ($t(88) = -6.552$, $p < 0.0001$), for plants grown under high T_{air} than low T_{air} (Table 2. 2, Figure 2. 3). I found evidence that elevated growth VPD_{air} (at high T_{air}) reduced g_s in *Melicope* ($t(88) = -4.855$, $p < 0.0001$), *Nauclea* ($t(88) = -5.024$, $p < 0.0001$), and *Buckinghamia* ($t(88) = -2.507$, $p < 0.05$; Table 2. 2, Figure 2. 3). In addition, iWUE was significantly higher for plants grown under high VPD_{air} than low VPD_{air}; for *Melicope* ($t(88) = 4.282$, $p < 0.001$), *Nauclea*

($t(88) = 4.583$, $p < 0.0001$), and *Buckinghamia* ($t(88) = 2.459$, $p < 0.05$; Table 2. 2, Figure 2. 3). Although average A_{net} was lower for plants grown under elevated VPD_{air} than low VPD_{air} for most species (Appendix A: Table 1), statistically significant differences were observed only for *Melicope* ($t(88) = -2.440$, $p < 0.05$; Table 2. 2, Figure 2. 3). When averaged across species this represented an −11 % reduction in A_{net}, a −41 % reduction in g_s, and a +58 % increase in iWUE for plants grown under elevated VPD_{air} than those grown under low VPD_{air} at the same growth temperature.

The trait g_1 averaged 4.6 (Range 0.8 to 15.5) across all species and treatments and was significantly affected by the interaction between species and treatment (Table 2. 2, Appendix A: Figure 1). Post-hoc analysis revealed similar trends to iWUE, with g_1 higher (indicating lower iWUE) in plants grown under high T_{air} compared to low T_{air} (at low VPD_{air}) for both *Melicope* ($t(88) = 2.648$, $p < 0.05$) and *Nauclea* ($t(88) = 7.429$, $p < 0.0001$) (Table 2. 2, Appendix A: Figure 1). VPD_{air} also impacted g_1, with plants grown under high VPD_{air} having a lower g_1 than those grown under low VPD_{air} for all species (Appendix A: Table 1), but statistically significant differences observed only for *Melicope* ($t(88) = -4.350$, $p < 0.001$) and *Nauclea* ($t(88) = -5.801$, $p < 0.0001$). In *Buckinghamia*, there was weak evidence for differences between the two VPD_{air} treatments under high T_{air} ($t(88) = -2.352$, $p = 0.054$), and additionally, g_1 in the high VPD_{air}, high T_{air} treatment was also significantly different than g_1 in the low VPD_{air}, low T_{air} treatment ($t(88) = -3.658$, $p < 0.01$) (Table 2. 2, Appendix A: Figure 1).

Table 2. 2. Two-way ANOVA results of treatment effects of physiology and biomass in six tropical woody species. DF means degrees of freedom. Significance denoted with "***", "**", and "*", are significant at P <0.001, P < 0.01, and P < 0.05, respectively.

Variable	Error	Treatment		Species		Treatment:Species	
	df	*df*	*F*	*df*	*F*	*df*	*F*
A_{net}	88	2	**5.17****	5	**48.08*****	10	**2.57****
$\sqrt[3]{g_s}$	88	2	**22.09*****	5	**42.55*****	10	**6.17*****
log10(iWUE)	88	2	**19.57*****	5	**30.32*****	10	**4.61*****
g_1	88	2	**21.03*****	5	**16.62*****	10	**5.73*****
V_{cmax25}	87	2	1.12	5	**27*****	10	1.37
J_{max25}	87	2	**12.86*****	5	**17.96*****	10	0.78
$\log10(J_{max25}/V_{cmax25})$	87	2	**12.21*****	5	**48.72*****	10	0.83
T_{crit}	88	2	**26.69*****	5	**22.63*****	10	1.76
$\log10(g_{min})$	88	2	0.1	5	**64.94*****	10	**2.37***
Total biomass	125	2	**29.33*****	5	**74.34*****	10	1.7
Leaf dry matter content	125	2	1.71	5	**181.69*****	10	1.08
log10(specific leaf area)	125	2	1.69	5	**193.61*****	10	0.92
Leaf width	125	2	**4.73***	5	**271.16*****	10	**5.05*****

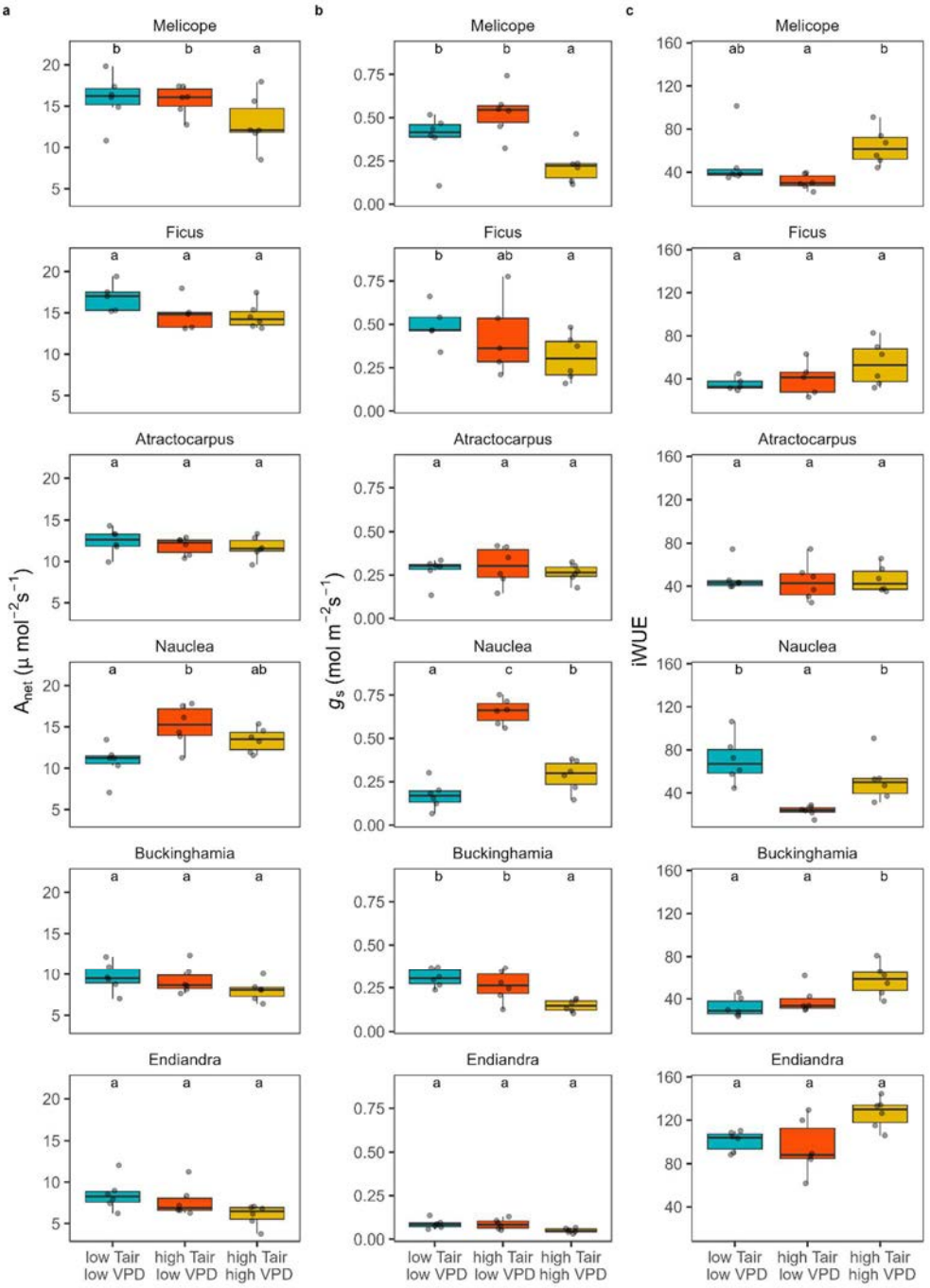

Figure 2. 3. Treatment impacts on gas exchange measured under common conditions for net photosynthesis, A_{net} (a), stomatal conductance, g_s (b), and intrinsic water use efficiency, iWUE (c). Species are ordered in decreasing stomatal sensitivity to VPD (top panel=high sensitivity, bottom panel=low sensitivity). Box and whisker plots show the median, 25th and 75th percentile, and 1.5*IQR. Colours represent the different treatments. Significant differences between treatments from Tukey Post Hoc results (p < 0.05) denoted with letters. Note that g_s and iWUE were transformed for analysis, but their untransformed values are presented here.

The average species g_{min} was 0.58 mmol m^{-2} s^{-1} and ranged from 0.04 to 3.54 mmol m^{-2} s^{-1} across all species and treatments (Table 2. 2, Appendix A: Figure 1). There was a significant interaction between species and treatment on g_{min} (Table 2. 2, Appendix A: Figure 1). For plants grown under low VPD_{air}, g_{min} decreased with elevated T_{air} for *Nauclea* ($t(88) = -2.418$, $p < 0.05$) but increased with elevated T_{air} for *Buckinghamia* ($t(88) = 2.541$, $p < 0.05$) and *Atractocarpus* ($t(88) = 2.312$, $p = 0.0593$) (Table 2. 2, Appendix A: Figure 1). For plants grown under high T_{air}, no species had significantly different g_{min} between plants grown under the low and high VPD_{air} treatments ($p > 0.05$).

2.3.3 Acclimation of photosynthetic biochemistry

Most species did not acclimate V_{cmax25} in response to treatments (Table 2. 2, Figure 2. 4, Appendix A: Figure 2). However, J_{max25} was −14.9 % lower on average in plants grown under high T_{air} compared to T_{air} (range −29.5 to −3.4 %) (Table 2. 2, Figure 2. 4, Appendix A: Table 1, Appendix A: Figure 2). Similarly, the ratio between J_{max25} and V_{cmax25} was −11.3 % lower on average in plants grown under high T_{air} than plants grown under low T_{air} but the same VPD_{air} (range −21.5 to −3.4 %) (Table 2. 2, Figure 2. 4, Appendix A: Table 1). No statistically significant differences were associated with VPD_{air} treatments (Table 2. 2, Figure 2. 4).

2.3.4 Acclimation of leaf thermal tolerance

T_{crit} averaged 47.4 °C (range 41.7 to 51.0 °C) across all species and treatments (Figure 2. 4, Appendix A: Figure 3). T_{crit} averaged 46.3 °C (range 41.7 to 49.8 °C) in the low T_{air} low VPD_{air} treatment, 48.1 °C (range 45.7 to 51) in the high T_{air} low VPD_{air} treatment, and 47.6 °C (range 44.6 to 50.1) in the high T_{air} high VPD_{air} treatment. Elevated T_{air} significantly affected T_{crit} (Table 2. 2), leading to a +0.31°C (range 0.06 to 0.57 °C) increase in T_{crit} per °C rise in T_{air} (Figure 2. 4). Most species also had a slightly higher T_{crit} for plants grown under low VPD_{air} than high VPD_{air} (average difference 0.8 °C, range −0.2 to 1.8 °C; Appendix A: Figure 3). However, this was not statistically significant (Table 2. 2, Figure 2. 4).

2.3.5 Acclimation of leaf morphology

LDMC and SLA were not affected by the treatments ($p > 0.05$, Table 2. 2, Figure 2. 4, Appendix A: Figure 3), whereas leaf width in *Atractocarpus* and *Nauclea* was (Table 2. 2, Appendix A: Figure 1). In *Atractocarpus*, plants grown under high T_{air} had narrower leaf widths on average than those grown under low T_{air} for both the low VPD_{air} treatment ($t(125) = -5.935$, $p < 0.0001$), and the high VPD_{air} treatment ($t(125) = -4.789$, $p < 0.0001$) (Table 2. 2, Appendix A: Figure 1). In *Nauclea*, the opposite trend was observed, with plants grown under low VPD_{air} having wider leaf widths when grown at high T_{air} compared to low T_{air} ($t(125) = 2.484$, $p < 0.05$). In *Nauclea*, leaf width was also impacted by the VPD_{air} treatment,

with narrower leaf widths observed for plants grown under high VPD_{air} compared to low VPD_{air}, at the same high T_{air} ($t(125) = -3.743$, $p < 0.001$) (Table 2. 2, Appendix A: Figure 1).

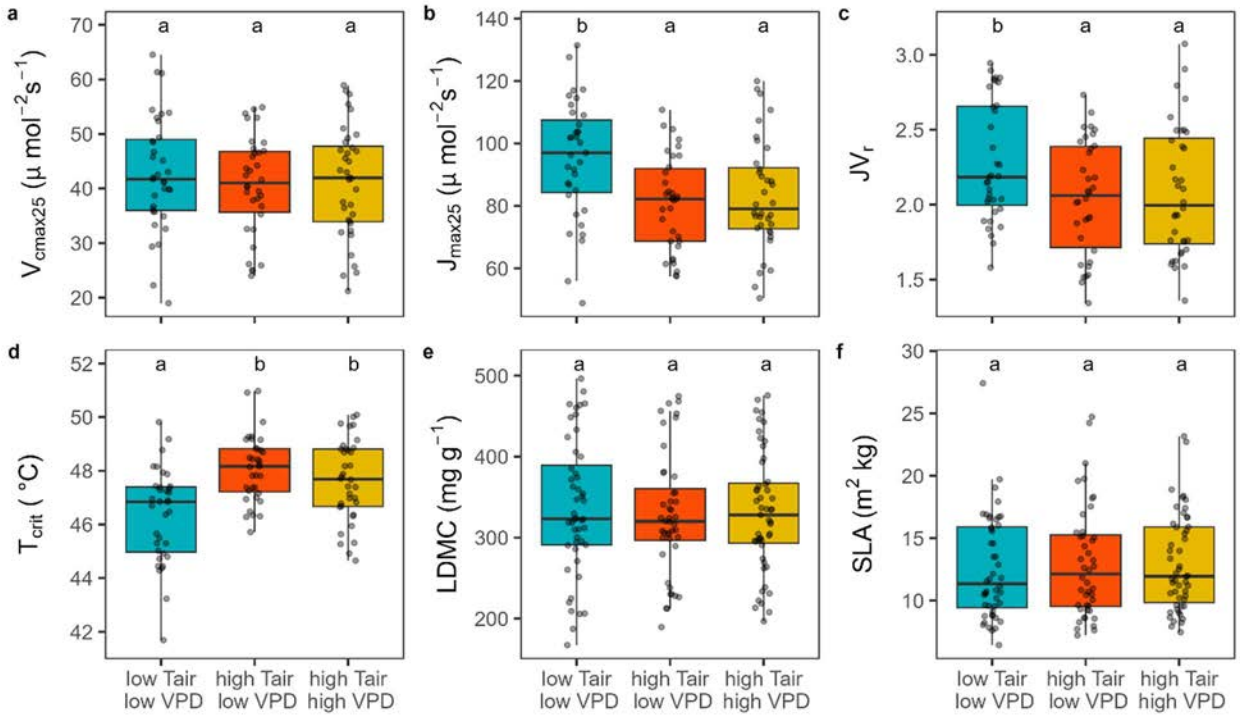

Figure 2. 4. Treatment impacts representing long-term acclimation for V_{cmax25} (a), J_{max25} (b), the ratio of J_{max25} to V_{cmax25}, JV_r (c), T_{crit} (d), leaf dry matter content, LDMC, (e) and specific leaf area, SLA, (f) across all species. Each point represents a plant measurement. Box and whisker plots show the median, the 25th and 75th percentile, along with 1.5*IQR. Colours represent the different treatments. Significant differences between treatments from Tukey Post Hoc results ($P < 0.05$) denoted with letters. Note that JV_r and SLA were transformed for analysis, but their untransformed values are presented here.

2.3.6 Impacts of treatment conditions on T_{leaf} and VPD_L

Daytime T_{leaf} was warmer than T_{air}, with ΔT (T_{leaf}–T_{air}) averaging +1.1 °C (range −1.3 to 4.3 °C) across all species and treatments (Figure 2. 5). ΔT was significantly higher for plants growing under low VPD_{air} than high VPD_{air}, with ΔT averaging 1.3 and 0.7 °C in the low and high VPD_{air} treatments, respectively (Figure 2. 5, Table 2. 3). Despite these differences in T_{leaf} between treatments, there were still significant differences in VPD_L between VPD_{air} treatments, with VPD_L averaging 1.3 and 1.9 kPa in the low and high VPD treatments, respectively (Figure 2. 5, Table 2. 3). There were no significant differences in VPD_L between low and high T_{air} treatments, growing under low VPD_{air} (Figure 2. 5, Table 2. 3). Thus, the pattern of VPD_L across treatments was similar to the pattern of VPD_{air}.

Table 2. 3. Differences in ΔT and VPD_L during the growth experiment. Results are from a linear mixed model to assess impacts of treatment, species, and their interaction on ΔT and VPD_L. The model included radiation as a covariate and plant nested within round as a random effect (1|round/plant).

		ΔT		VPD_L	
Parameter	df	F	*P*	F	*P*
treatment	2	11.44	< 0.001	65.69	< 0.0001
species	5	7.68	< 0.0001	2.56	< 0.05
radiation	1	57.16	< 0.0001	93.45	< 0.0001
treatment × species	10	0.72	ns	0.77	ns

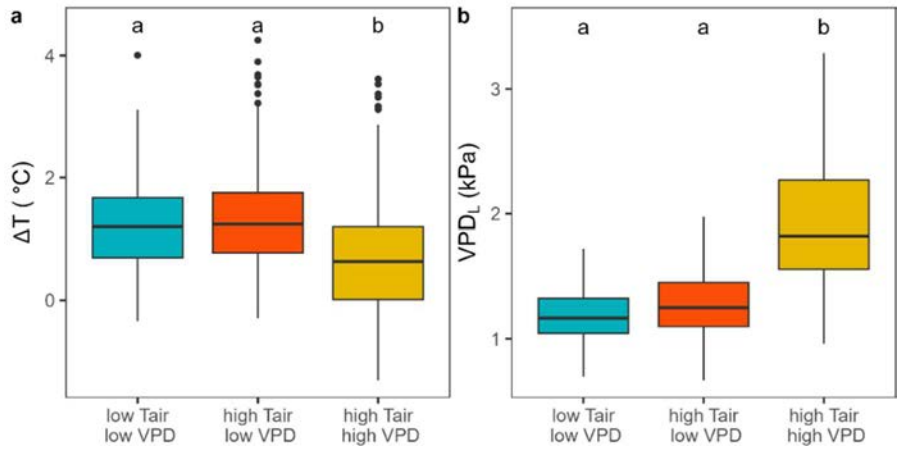

Figure 2. 5. Distribution of (a) leaf-air temperature differences (ΔT) and (b) leaf-air vapour pressure difference (VPD_L) in the different treatments for six species. Underlying data are from 10-minute averages, filtered to only include measurements during the daytime (9am-3pm). Letters denote significant differences between groups from pairwise comparisons.

2.4 Discussion

I utilised three climate-controlled chambers to disentangle the relative roles of T_{air} (at low VPD) and VPD_{air} (at high T_{air}) on integrated growth, leaf-level gas exchange, photosynthetic capacity, and thermal tolerance in saplings of six tropical tree species under well-watered conditions. I found that plant biomass increased under higher T_{air}, but that this positive impact was partially counteracted by elevated VPD_{air}. Contrary to expectation, variation in the response ratio of accumulated biomass to VPD across species was not associated with stomatal sensitivity to VPD, but the analysis was limited by a relatively small number of species. These results also show that different physiological traits acclimated to either T_{air} or VPD_{air}, with J_{max25} and thermal tolerance affected by T_{air}, and g_s and iWUE affected by VPD_{air}.

2.4.1 Interactive effects of T_{air} and VPD_{air} on growth.

Tropical tree growth increased in response to increasing growth temperature when considering non-extreme temperatures and non-limiting soil moisture, similar to other studies (Cheesman & Winter, 2013; Lin et al., 2010; Ramesh et al., 2023). Although I tested a 6 °C difference in growth temperatures, the absolute temperature of the high T_{air} treatment in this study was relatively conservative, with conditions comparable to those experienced by the focal species during summer across their lowland distributions in the Australian Wet Tropics. This study also revealed concurrent increases in VPD_{air} counteracted the stimulation of plant growth by increased growth temperatures. This supports recent findings that tropical tree growth and productivity is highly sensitive to increasing VPD (Bauman et al., 2022a; Smith et al., 2020), likely due to stomatal limitations on photosynthesis (Binks et al., 2023).

With the low number of species-replicates in the current study, I could not find a positive correlation between species-level sensitivity of stomata to VPD and plant biomass response ratio to elevated VPD_{air} (Figure 2. 2b). However, the two species (*Melicope* and *Ficus*) with the greatest biomass reduction under elevated VPD also had the highest stomatal sensitivity to VPD, highest SLA, and fastest growth rates, while species least affected by VPD (*Atractocarpus* and *Endiandra*) had amongst the least sensitive stomata, lowest SLA, and slowest growth rates. This suggests differential responses of fast- and slow-growing species to VPD changes, consistent with Bauman et al. (2022a), though the fast-slow continuum may not fully capture all variation in responses. Other traits, such as rooting patterns and water access strategies, may be decoupled from growth rates yet predictive of VPD responses. Further work would be needed to determine which functional trait drives the observed difference in VPD response across species. It should be noted that while I did not test if the stomatal sensitivity to VPD itself acclimated across treatments, other studies report a negative correlation between increasing VPD and stomatal sensitivity to VPD (Binks et al., 2023).

2.4.2 Reduction of leaf conductance with warming is a response to elevated VPD_{air}, but not T_{air}

Warming experiments often find lower g_s in leaves grown under higher temperatures than controls (Carter et al., 2021; Choury et al., 2022; Crous et al., 2023). However, with temperature and VPD_{air} often covarying, it is not always clear whether this response is to increasing growth temperature or the associated increase in VPD_{air}. I expected plants grown under high T_{air} would acclimate their physiology to reduce g_s only if also exposed to high VPD_{air}. While my results support this, an exceptional species in this study was *Nauclea*, which had a large increase in g_s and A_{net} under higher T_{air}. I am unsure of reasons why gas exchange was affected by growth temperature in this species and not others, but worth noting is that this species is found in particularly wet, swampy environments. For the other species in this study, g_s was only affected by VPD_{air}. It appears tropical woody species reduce g_s in response to increasing VPD_{air} to maintain

leaf water status and maintain hydraulic function, even at the expense of reduced carbon uptake. This contrasts with results from a similar study on three temperate species (Schonbeck et al., 2022), which found in response to elevated VPD there was no acclimation of g_s , but reduced leaf water potential, and increased signs of hydraulic dysfunction. These differences between species from temperate and tropical biomes are not surprising considering tropical species are generally more isohydric than temperate species (Cunningham, 2004). While these differences might suggest a biome-level distinction, the limited number of species in both studies means other factors, such as clade-specific traits or environmental conditions, could also explain the observed variation. This highlights the need for more extensive data to better understand these important differences.

I assessed leaf-level gas exchange under standard temperature and VPD_{air} to determine if plants had acclimated leaf function to their growth conditions. Gas exchange in these species acclimated more to long-term VPD_{air} than long-term T_{air}, with results showing tropical trees grown under higher VPD_{air} conditions shift to a more conservative water use strategy (higher iWUE) even without soil moisture deficit. This was driven by declining g_s rather than an increase in assimilation rate. This could be significant for modelling g_s, as the stomatal slope parameter (g_1), commonly used to represent dynamic changes in g_s in ecosystem models (Medlyn et al., 2011) is inversely related to iWUE. Although there has been discussion about the plasticity of g_1 as it pertains to soil moisture (Héroult et al., 2013; Wu et al., 2020), and across elevation where temperature and VPD covary (Mujawamariya et al., 2023), there have been no studies showing the plasticity of g_1 in plants acclimating directly to altered VPD. I show some tropical trees may modify g_1 in response to both higher VPD_{air} (g_1 decreasing in response) and when VPD is constant, higher T_{air} (g_1 increasing in response). These contrasting effects of T_{air} and VPD_{air} on acclimation of g_1 may account for the lack of acclimation to growth temperature observed in some studies covary (Mujawamariya et al., 2023). Furthermore, it is important to note the species variation not just in mean g_1, but in their range, with *Endiandra* varying relatively little (range 2.3) and *Nauclea* varying greatly (range 14). Further effort to disentangle the effects of temperature and VPD in a greater range of species would be helpful to establish both the generality of these observations, and potential drivers of species variation in acclimation capacity.

Water limitation from soil moisture deficit and higher VPD can cause a reduction in g_{min} (Duursma et al., 2019; Fanourakis et al., 2013; Schonbeck et al., 2022), however, in my study, g_{min} was not impacted by VPD_{air}. The mean daytime differences in T_{air} and VPD_{air} used in this study are within the range likely experienced by these species across their home-range distributions, which could explain the contrasting findings to Schönbeck et al. (2022), where g_{min} decreased with increasing VPD_{air} only at the highest growth temperature used in their study. In addition, while other studies held diel growth conditions constant during their experiments, I allowed temperature, and thereby VPD_{air}, to vary. The influence of dynamic VPD_{air} and acclimation to its range on g_{min} is poorly understood.

Two target species showed acclimation of g_{min} to growth T_{air}, with values higher for those grown under the warmer T_{air} treatments. This response may allow plants to avoid lethal temperatures under heat waves (Schuster et al., 2016; Slot et al., 2021) at the risk of increased vulnerability to hydraulic failure (Cochard, 2021). Although this contrasts with some reports of reduced g_{min} in response to long-term increases in temperature (Duursma et al., 2019), g_{min} is highly variable and responses are species-specific. In addition, other studies did not control for VPD_{air}, so the long-term response of g_{min} to growth temperature is still poorly understood.

2.4.3 Photosynthetic capacity acclimated to elevated T_{air}, but not VPD

Our results reveal photosynthetic biochemistry acclimated to elevated T_{air}, but not VPD_{air}. I expected V_{cmax25}, J_{max25}, or their ratio to change given the internal CO_2 concentration, c_i, will likely decrease at a higher VPD_{air} due to stomatal closure. This change in operating c_i could be expected to induce a change in either V_{cmax25} or J_{max25}, such that co-limitation of photosynthesis at the new operating c_i is maintained (Wang et al., 2017). Despite observing a reduction in g_s in response to elevated growth VPD_{air}, this did not translate into an associated impact on V_{cmax25} or J_{max25}, nor on A_{net}. There are very few studies reporting acclimation of photosynthetic biochemistry directly in response to growth VPD, with limited research done on tomato (Zhang et al., 2018), *Prosopis juliflora* (Shirke, 2004), and wheat (Fakhet et al., 2021), which report reduced rates of apparent V_{cmax} or nitrogen allocation to V_{cmax} in response to short-term increases of VPD_{air}. Substantially more studies report how growth VPD_{air} affects A_{net} (Lopez et al., 2021), with no change in photosynthetic rates between plants grown under low and high VPD when measured at common conditions. The sample size might not have been high enough to detect statistically significant differences in A_{net}, despite rates being lower on average in the high VPD_{air} treatment. However, these results on g_s indicate changes in A_{net} were likely due to stomatal limitation rather than changes in biochemistry. While I show a limited ability of tropical species to acclimate their biochemistry to growth VPD_{air}, further research is greatly needed to determine the effect in plants of contrasting biomes.

Growth temperature induced changes in J_{max25} and the ratio of J_{max25} to V_{cmax25}, but not V_{cmax25}. This is consistent with results from other studies (Kumarathunge et al., 2019) showing limited acclimation of V_{cmax25}, but a reduction of J_{max25} and the ratio of J_{max25} to V_{cmax25} in response to higher growth temperatures. Current meta-analyses suggest the positive correlation between the optimum temperature of photosynthesis and growth temperature observed in mature trees (Kumarathunge et al., 2019) to be driven by decreasing J_{max25} with increasing growth temperature, rather than changes in V_{cmax25} (Hikosaka et al., 2006).

2.4.4 Impact of VPD on leaf temperatures.

Daytime ΔT observed during the growth experiment was lower than reported in the field (Fauset et al., 2018; Rey-Sanchez et al., 2017). This is perhaps due to the glasshouse shade sail reducing radiation

inside the glasshouse and may account for the lack of variation in T_{crit} between high and low VPD_{air} treatments. In this study, T_{crit} increased 0.32 °C per 1 °C rise in T_{air}, comparable with the 0.34 °C found by Zhu et al. (Zhu et al., 2018). But with the difference in ΔT between the low and high VPD_{air} treatments being less than 1 °C, I would not expect to find large differences in T_{crit} due to VPD_{air}.

Increasing VPD has a complex impact on leaf energy balance, with the higher diffusion of water across the stomatal pore, and stomatal closure having opposing effects on latent heat flux (Gu et al., 2006). This results in a non-linear relationship between transpiration and VPD. Identifying when one process dominates over the other is critical to understanding how plant functioning will be impacted by warming. In this experiment, for plants grown at high T_{air}, those exposed to a higher VPD_{air} had a smaller or more negative ΔT. This was due to the higher atmospheric demand for water response to increasing VPD dominating over the decreased g_s response. Similarly, Massmann et al. (2019) demonstrated, using species traits combined with energy balance theory, that plant species from tropical biomes are likely to exhibit a positive transpiration trend in response to increasing VPD. In the range of VPD_{air} observed in this study, I found increasing VPD_{air} will not likely exacerbate heat stress experienced by tropical plants, so long as soil moisture is not limiting to transpiration. However, future work should explore whether acclimation to high VPD_{air} (i.e. reduced g_s) result in differences in ΔT when exposed to the same environmental conditions.

While I discuss the implications of these results broadly, caution should always be made when extrapolating findings from controlled glasshouse experiments conducted on saplings to mature trees in the field. Mature trees can have different hydrological strategies (Ryan & Yoder, 1997) to well-watered saplings and may therefore respond differently to changes in VPD. In addition, the glasshouse used light reducing shade sails to ensure light was distributed evenly to avoid leaf scorching. While sun and shade leaves can show different stomatal sensitivities to VPD (Hernández et al., 2020), this is often when comparing extremes in illumination (e.g. 5-20% full sunlight). In contrast, in this experiment direct PAR was only reduced by 50% from full tropical sunlight. If moderately reduced radiation during growth did impact stomatal response to VPD, this would mean my results underestimate the impact of VPD on plant growth in mature plants exposed to full sun.

2.5 Conclusion

This study demonstrates how both T_{air} (independent of VPD_{air}) and VPD_{air} (at high T_{air}) directly impact leaf gas exchange and growth in tropical tree species. Under future climate change, understanding the relative role changing temperature and VPD will have on plant growth is of critical importance to predicting the fate of tropical forests and global carbon cycling. Across the six species tested, I show how reduced conductance in response to elevated VPD led to reduced productivity. Further work across a broader range of species and growth conditions would be needed to establish the generality of this, and whether species-level stomatal sensitivity to VPD can help predict long term growth trends among species.

Chapter 3: Trait acclimation to contrasting temperature and humidity conditions alters leaf thermoregulation in tropical rainforest saplings

3.1 Introduction

Sun-exposed outer canopy, leaf temperatures (T_{leaf}) can be substantially different from surrounding air temperature (T_{air}), with reports of T_{leaf}-to-T_{air} offsets ($\Delta T_{leaf\text{-}air}$) of up to ± 20.0 °C (Ansari & Loomis, 1959; Blonder & Michaletz, 2018). Under steady-state conditions, equilibrium T_{leaf} represents the surface temperature at which net radiation exchange is balanced with fluxes of sensible and latent heat (Bonan, 2008). These fluxes are determined by the interaction of microclimate variables (such as solar radiation, wind speed, air temperature, vapour pressure deficit) with morphological and physiological characteristics of leaves (including leaf size, angle and orientation, absorption to solar radiation, and stomatal conductance).

Plant thermoregulation refers to changes in $\Delta T_{leaf\text{-}air}$ across thermal gradients, driven either by rapid adjustments in stomatal conductance or through acclimation and adaptation of key functional leaf traits. The *limited-homeothermy* hypothesis was initially proposed to explain how T_{leaf} covaries with T_{air}, suggesting that plants actively modified the relationship between T_{air} and T_{leaf} to maintain optimal functioning, resulting in T_{leaf} being higher than might be expected under infra-optimal temperatures and lower than expected under supra-optimal conditions (Gates et al., 1964; Mahan & Upchurch, 1988). Subsequent research has expanded upon this theory (Michaletz et al., 2016; Michaletz et al., 2015) and tested it through direct measurements of leaf and canopy temperature in situ (Blonder et al., 2020; Fauset et al., 2018; Still et al., 2022), or indirect assessments using oxygen stable isotopes (Helliker et al., 2018; Liancourt et al., 2020) and energy balance theory (Dong et al., 2017; Guo et al., 2022). These studies report a large range of $\Delta T_{leaf\text{-}air}$ and how this changes with T_{air} within and across biomes, however support for limited-homeothermy as envisaged by Mahan and Upchurch (1988) and codified by Blonder & Michaletz (2018) varies considerably, with support reported in some studies (Blonder et al., 2020; Michaletz et al., 2015; Perera et al., 2020), but refuted in others (Doughty et al., 2023b; Guo et al., 2023; Still et al., 2022). Given the range of methods and approaches used to test limited homeothermy, it remains unclear whether the differing results are due to measuring responses at different scales, applying varying definitions of thermoregulation, or reflecting genuine biological differences across species and environments. Ultimately, the basis of leaf thermoregulation lies in the modification of leaf traits, meaning that this phenomenon can be assessed through energy balance modelling to evaluate trait coordination and disentangle this from environmental affects, rather than relying solely on measured leaf temperature.

Over the longer-term (weeks to months) plants may regulate observed $\Delta T_{leaf\text{-}air}$ through the modification of leaf morphological and physiological traits (i.e., LMA, leaf lamina size, canopy architecture) that impact either steady-state or dynamic leaf temperatures. Steady-state leaf temperature refers to the equilibrium temperature achieved under the assumption that variables, such as radiation and heat fluxes, remain constant over time, allowing the system to reach a balance without considering transient changes. In contrast, dynamic leaf temperature accounts for the time-dependent accumulation or loss of mass and energy within the system, capturing transient responses to rapid environmental fluctuations, such as changes in light, wind, or temperature gradients. The thermal time constant (τ) represents the time it takes for a leaf to adjust its temperature in response to changes in the surrounding environment (Michaletz et al., 2015). It is influenced by the leaf's physical characteristics, such as its mass, thickness, and surface area, which in turn determine the rate at which heat is absorbed or lost. A higher thermal time constant indicates that a leaf heats or cools more slowly, allowing for greater thermal stability, while a lower time constant leads to more rapid changes in leaf temperature in response to microclimatic fluctuations. In the context of contrasting growth temperatures, plants growing in cooler environments (such as high elevation montane forests) are expected to develop traits (such as increased leaf thickness) that prolong heat retention, leading to a higher thermal time constant, whereas plants in warmer conditions (i.e. lowland forests) may acclimate by developing traits that facilitate faster heat dissipation, resulting in a lower thermal time constant. Although these acclimatory shifts in leaf morphology and physiology may reflect responses to other pressures (i.e. frost damage, desiccation stress, herbivory), they also have critical impacts on leaf energy balance and thermoregulation across diverse environmental conditions.

Given the individual importance of multiple traits on leaf energy balance, and the trade-offs/covariations often existing across suites of leaf functional traits in different environments (Conti et al., 2023), it is essential to consider multivariate trait acclimation when assessing the impact on leaf thermal responses. To date only a few studies have reported trait variation corresponding to higher $\Delta T_{leaf\text{-}air}$ in cooler environments and lower $\Delta T_{leaf\text{-}air}$ in warmer environments (Kullberg et al., 2023; Perez & Feeley, 2020). However, these studies are conducted in the field where other variables such as vapour pressure deficit, soil moisture, and soil nutrients can covary. Therefore, the co-acclimation of leaf thermal traits directly in response to temperature is not well understood.

In this study, I aimed to test whether tropical rainforest trees show evidence of leaf thermoregulation – the modification of traits or function that result in a modified $\Delta T_{leaf\text{-}air}$ or thermal time constant. To do so I assessed how the acclimation of leaf morphological and physiological traits to different temperature and VPD regimes from Chapter 2 affects the leaf thermal time constant and steady-state leaf energy balance. I hypothesised that acclimation would contribute to limited homeothermy, with plants grown under higher T_{air} having leaf traits that decrease $\Delta T_{leaf\text{-}air}$ and/or the thermal time constant compared

to plants grown under cooler T_{air} (H1). I also hypothesised that this response would only be observed when grown under similar low vapour pressure deficit, with acclimation to elevated VPD causing either poikilothermy or megathermy as plants trade off leaf cooling with a more conservative water use strategy (H2).

3.2 Materials and Methods

3.2.1 Plant material

This experiment further utilized plant material grown and measured in Chapter 2. Briefly, saplings of six trees from the Australian Wet Tropics: *Atractocarpus fitzalanii* (Rubiaceae), *Buckinghamia celsissima* (Proteaceae), *Endiandra microneura* (Lauraceae), *Ficus racemosa* (Moraceae), *Melicope elleryana* (Rutaceae), and *Nauclea orientalis* (Rubiaceae) were grown under three different combinations of low or high T_{air} and VPD. Daytime air temperatures averaged 26.6 (±2.9) °C in the low temperature chambers, and 32.5 (±2.9) °C for the two high temperature chambers, and VPD averaged 0.7 (±0.32) kPa for the two low VPD chambers and 1.4 (±0.59) kPa for the high VPD chamber (Table 2.1, Figure 2.1).

3.2.2 Leaf thermal time constant

The thermal time constant, τ (s), influences the time taken for leaves to heat up or cool down following a change in microclimate (Michaletz et al., 2015). This was calculated using the leaf traits LMA, LDMC, and leaf width, and by assuming air temperature of 28°C, air pressure of 1,012 hPa, and wind speed of 0.5 m s^{-1} to isolate the impact of any change in expressed leaf traits:

$$\tau = \varphi \cdot LMA \cdot \left(\frac{c_{pw}}{LDMC \cdot H} + \frac{c_{pd} - c_{pw}}{H}\right) \quad (eq\ 1)$$

where φ is the ratio of the projected to total leaf area, which is 0.5 for flat leaves, c_{pw} is the specific heat capacity of water (4,180 J kg^{-1} K^{-1}), c_{pd} is the specific heat capacity of dry leaf matter (J kg^{-1} K^{-1}), which varies across species so I used a value of 2,814 J kg^{-1} K^{-1} which was the mean of seven tropical tree species in (Jayalakshmy & Philip, 2010) and has been previously used in other studies based in the tropics (Fauset et al., 2018; Slot et al., 2021). The heat transfer coefficient, H(W m^{-2} K^{-1}), was calculated using the formula:

$$H = \rho_a \cdot c_{p,a} \cdot g_h \quad (eq\ 2)$$

where ρ_a is air density (1.170685 kg m^{-3}), $c_{p,a}$ is the specific heat capacity of air at a constant pressure (1004.78 J kg^{-1} K^{-1}), and g_h (m s^{-1}) is the heat conductance which was calculated for a flat plate under laminar forced convection conditions as per Jones (2013):

$$g_h = 1.5 \cdot 0.00662 \cdot \sqrt{\frac{U}{w}} \qquad (eq\ 3)$$

where outdoor turbulence is accounted for by a factor of 1.5, U is the wind speed (m s^{-1}), and w is the leaf width (m). The thermal time constant was not incorporated into steady state leaf energy balance modelling but was analysed as a response variable independently.

3.2.3 Leaf Energy Balance

To examine how trait acclimation was likely to impact the leaf-air temperature offset ($\Delta T_{leaf\text{-}air}$) I estimated T_{leaf} by parameterising a steady-state leaf energy balance model with observed variation in leaf traits but common microclimate inputs ($\Delta T_{mod\text{-}air}$). The model combines a Penman-Monteith leaf energy balance model (Jones, 2013) with a C_3 plant photosynthesis model (Farquhar et al., 1980) and unified stomatal optimization model (Medlyn et al., 2011) as implemented with the PhotosynEB function in the 'plantecophys' package (Duursma, 2015). Plant traits used included leaf width, V_{cmax25}, J_{max25}, g_1, and g_{min}, which were measured and reported in Chapter 2. Because g_{min} was not always measured on the same plants that had gas exchange measurements I used species-mean g_{min}. I used temperature response parameters for V_{cmax} and J_{max} of tropical species as per Kelly (2014), resulting in activation energies for V_{cmax} (EaV) and J_{max} (EaJ) being 103600 and 31500 J mol^{-1} respectively, ΔS (delsC) of 640.8 J mol^{-1} K^{-1}, entropy term (delsJ) of 632.2 J mol^{-1} K^{-1}, and parameters controlling the peakedness of curves for both V_{cmax} and J_{max} (EdVC and EdVJ) equal to 200000. Microclimate inputs for all plants were T_{air} = 28 °C, VPD = 1 kPa, PPFD = 1500 µmol m^2 s^{-1} and Wind = 0.5 m s^{-1}.

3.2.4 Data analysis

All analyses were conducted using R v.4.2.2. To assess differences in the coordination of leaf thermal traits, I assessed the effect of species and treatment on the modelled leaf-air temperature differential ($\Delta T_{mod\text{-}air}$) and the leaf thermal time constant using a linear model. A two-way analysis of variance (ANOVA) was performed to test for significant interactions between species and treatment. To further explore significant interactions between species and treatments, I conducted post-hoc pairwise comparisons using estimated marginal means (EMM), calculated with the emmeans() function (Lenth, 2022), and compact letter displays (CLD) were generated to denote statistically significant differences between groups.

3.3 Results

3.3.1 Steady-state leaf energy balance

Across all individuals, mean $\Delta T_{mod\text{-}air}$ was 9.4 °C, ranging from 4.9 to 16.4 °C (Figure 3. 1). A two-way ANOVA (adjR^2 = 0.69) revealed significant species × treatment interactions for $\Delta T_{mod\text{-}air}$ ($F_{(10,88)}$ = 4.27, P < 0.0001), indicating that species responded differently to treatment conditions (Table 3. 1). Plants in the low T_{air} low VPD_{air} group had a higher mean $\Delta T_{mod\text{-}air}$ than those in the high T_{air} low VPD_{air} group for *M. elleryana*, *A. fitzalanii*, and *N. orientalis*, but this was only significant for *N. orientalis*. Plants in the high T_{air} high VPD_{air} group had a higher mean $\Delta T_{mod\text{-}air}$ than those in the high T_{air} low VPD_{air} group for *M. elleryana*, *N. orientalis*, *B. celsissima*, and *E. microneura* but this was only significant for *M. elleryana* and *N. orientalis*.

Table 3. 1. Anova Table (Type III tests) for modelled leaf-air temperature differences

Term	Sum Sq	Df	*F* value	*P*
Intercept	386.25	1	177.93	<0.0001
Species	272.18	5	25.08	<0.0001
Treatment	18.70	2	4.31	0.01643
Interaction	92.73	10	4.27	<0.0001
Residuals	191.03	88		

3.3.2 Thermal time constant

The mean thermal time constant across all individuals was 15.9 (s) and ranged from 6.2 to 32.3 (s) (Figure 3. 1). A two-way ANOVA (adjR^2 = 0.92) indicated significant species × treatment effects for the thermal time constant ($F_{(10,125)}$ = 2.80, P = 0.0037) (Table 3. 2). Post-hoc comparisons revealed significant differences between treatments for two species: For *A. fitzalanii*, the low T_{air} low VPD_{air} group had a significantly higher thermal time constant compared to both the high T_{air} low VPD_{air} and high T_{air} high VPD_{air}. *N. orientalis* exhibited higher thermal time constants in both the low T_{air} low VPD_{air} and high T_{air} low VPD_{air} groups compared to the high T_{air} high VPD_{air} group.

Table 3. 2. Anova Table (Type III tests) for thermal time constant

Term	Sum Sq	Df	*F* value	*P*
Intercept	1047.00	1	257.76	<0.0001
Species	3148.48	5	155.02	<0.0001
Treatment	1.97	2	0.24	0.7853
Interaction	113.79	10	2.80	0.0037
Residuals	507.74	125		

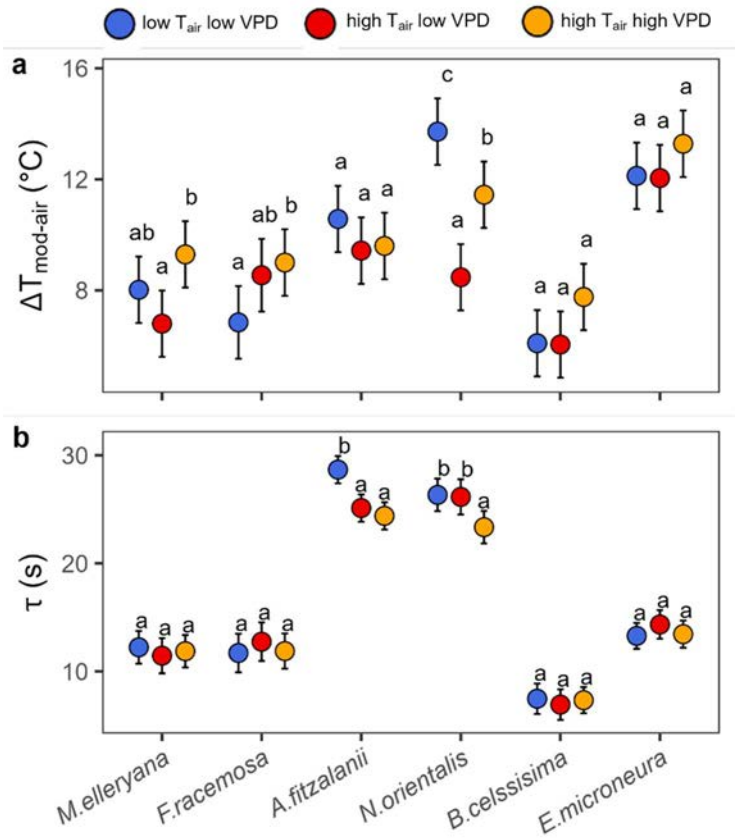

Figure 3. 1. Assessment of leaf thermal trait coordination. Points show the estimated marginal means and 95% confidence intervals for (a) modelled leaf-air temperature differences using common microclimate inputs, $\Delta T_{mod\text{-}air}$; and (b) the thermal time constant, τ. Letters denote significant differences between treatment groups for each species. Microclimate inputs for the leaf energy balance model were T_{air} = 28°C, VPD = 1 kPa, PPD = 1500 µmol m^2 s^{-1} and Wind = 0.5 m s^{-1}.

3.4 Discussion

Although plant thermoregulation is often measured using observed leaf temperature measurements and assessing the slope between T_{leaf} and T_{air} and whether this is greater than or less than 1 (Crous et al., 2023; Michaletz et al., 2015), limited homeothermy does not require having a slope less than 1 (Guo et al., 2023). This is because external environmental conditions (such as increased radiative load, reduced wind speed, or altered vapour pressure deficit) can cause leaf temperature to increase irrespective of plant trait adjustments (Leigh et al., 2012; Perez & Feeley, 2018). As such, limited homeothermy can manifest through trait coordination that enhances leaf cooling, even if leaf temperatures remain above air temperature. This chapter aimed to evaluate whether leaf thermoregulation, defined by the capacity to modify the leaf-air temperature differential ($\Delta T_{leaf\text{-}air}$) through trait acclimation, occurred in tropical saplings exposed to contrasting growth temperature and humidity regimes. Specifically, the study tested two hypotheses: (1)

that saplings grown in warmer conditions would exhibit traits that decrease $\Delta T_{leaf\text{-}air}$ or the thermal time constant, reflecting limited homeothermy, and (2) that under high vapour pressure deficit (VPD), plants would show reduced thermoregulation, potentially adopting poikilothermic or megathermic strategies as they balance water use with heat dissipation. The results provide partial support for these hypotheses, with substantial variation among species in their responses to environmental conditions, suggesting that leaf thermoregulation in tropical rainforest saplings is both species-specific and context dependent.

Does longer-term trait acclimation support the limited homeothermy hypothesis? (H1)

Some of the traits known to influence leaf energy balance are also shown to have high plasticity in response to their environment. Since temperature is a significant factor determining growth and survival this should exert some influence over optimal trait combinations to avoid lethal operating temperatures. I expected that plants acclimated to warmer growth conditions, would have leaf trait combinations that helped to maintain cooler leaf temperatures for a given air temperature when compared to plants grown under cooler conditions. However, the results provide only limited support for this (2/6 species). While other studies assessing $\Delta T_{leaf\text{-}air}$ in the field found some evidence of this with observed leaf temperatures (Kitudom et al., 2022) and energy balance modelled leaf temperatures (Kullberg et al., 2023), results are species specific.

Two species exhibited the expected pattern of thermal time constant variation with growth temperature, showing higher values in plants grown under cooler conditions. In contrast, Slot et al. (2021) found no relationship between the thermal time constant and elevation across 147 tropical tree species, though their study focused primarily on inter-specific differences rather than intraspecific variation. The findings in this chapter also contrast with those from Curtis et al. (2019), who observed that longer thermal time constants in lower, north-facing canopy positions were associated with lower wind speeds and a higher likelihood of reaching extreme temperatures within the canopy of the desert tree *Acacia papyrocarpa*. The traits influencing the thermal time constant – such as leaf width, leaf mass per area, and leaf dry matter content – are commonly measured functional traits that also affect carbon economics. However, few studies have measured or estimated the thermal time constant, making it difficult to place these results in a broader context and understand the extent of acclimation and adaptation of this trait.

In Chapter 2, stomatal conductance and water use efficiency did not differ substantially between plants grown under contrasting temperatures but similar low vapour pressure deficit. Instead, acclimation to elevated vapour pressure deficit affected stomatal conductance. However, leaf width did differ between the low and high temperature treatments for two species, as a result the differences in modelled $\Delta T_{leaf\text{-}air}$ and thermal time constant observed here are likely due to leaf width rather than gas exchange or other leaf traits.

Does acclimation to elevated vapour pressure deficit mask limited homeothermy? (H2)

In natural systems, higher air temperatures typically coincide with higher VPD. As a result, plants must balance trait acclimation that optimizes carbon uptake and/or leaf cooling with the need to reduce water loss in environments with higher evaporative demand. I expected that plants acclimated to both high temperature and elevated VPD would exhibit warmer leaf temperatures when modelled under common microclimate conditions, due to a more conservative water use strategy. This hypothesis was supported in only two of the six species studied, suggesting that the capacity for thermoregulation, while limited, can sometimes be masked by acclimation to VPD. These findings indicate that tropical trees vary widely in their responses to high VPD, highlighting the complexity of these trade-offs. The observed heterogeneity reinforces the need for further research across a larger number of species to assess whether generalities in VPD response exist and to refine our understanding of the mechanisms driving these differences.

Acclimation to both elevated temperature and VPD has important implications for plant survival during heat stress events. In conditions of high VPD, tropical trees may prioritize water conservation over leaf cooling, potentially increasing the risk of heat damage. This indicates that tropical tree mortality during extreme heat events (Bauman et al., 2022b) could arise more from thermal stress or carbon starvation than hydraulic failure (Mcdowell et al., 2008), as tropical trees are generally isohydric and close their stomata to limit water loss (Cunningham, 2004). However, this relationship is complex: while reduced stomatal conductance at high VPD could lead to higher leaf temperatures, the higher evaporative demand associated with elevated VPD can also cool leaf temperatures, even when stomatal conductance decreases. This was observed in Chapter 2, where leaf-air temperature offsets were lower in chambers with elevated VPD compared to those with normal VPD. Whether plants are more vulnerable to heat damage or hydraulic dysfunction during heatwaves will depend on how these opposing processes – reduced stomatal conductance driving higher leaf temperatures and elevated VPD driving cooler temperatures – interact to affect the overall leaf energy balance (Massmann et al., 2019). Overall, the findings suggest that VPD-induced acclimation can reduce the capacity for limited homeothermy in some tropical species, and future studies should explore the degree to which these trade-offs affect long-term survival and performance in natural environments.

Limitations

In this study, I assessed trait coordination using energy balance modelling to calculate leaf-air temperature offset and the thermal time constant, but these are indices rather than direct measurements of leaf temperature. Although these models generally show a good ability to predict leaf temperature (Fauset et al., 2018; Guo et al., 2022; Perez & Feeley, 2020), their implementation across larger gradients, where stomatal conductance cannot be directly assessed, relies on assumptions that stomatal conductance is well predicted by the parameters V_{cmax25} J_{max25} and g_1. It is important to note that in Chapter 2, the temperature

response of these parameters (i.e. activation energy and entropy) was not measured, which is one way in which plants can acclimate to different growth temperatures and alter the temperature response of gas exchange (Kumarathunge et al., 2019). Thus, while the leaf-air temperature differences between the low T_{air} low VPD_{air} and high T_{air} low VPD_{air} treatments in this experiment likely reflected differences in leaf width rather than stomatal conductance, actual measurements of leaf temperatures may deviate from those estimated here. Additionally, this is a steady-state energy balance model and does not directly integrate the thermal time constant. Despite these limitations, it provides a useful approach to understanding leaf temperature variation likely caused by plant traits rather than external environmental factors.

Another important consideration is that trait coordination and acclimation to temperature may not always be driven directly by energy balance optimization or leaf thermoregulation. Instead, these shifts could reflect indirect responses to other selection pressures, such as water use efficiency, carbon uptake, or nutrient acquisition, which may covary with temperature in natural settings. For example, changes in traits like leaf width or leaf mass per area might primarily enhance resource use strategies rather than directly regulate leaf temperatures. If this alternate hypothesis is correct, observed effects on τ or $\Delta T_{leaf\text{-}air}$, while real, may lack direct functional significance for thermoregulation. This raises broader questions about the validity of the underlying hypothesis that leaf thermoregulation is the main driver of trait plasticity or selection in leaves. While this study controlled environmental factors to isolate temperature and VPD effects, future research should explore whether leaf thermoregulation itself is a target of selection or simply a byproduct of broader adaptive strategies to environmental gradients.

Conclusions

This study highlights the species-specific and context-dependent nature of leaf thermoregulation in tropical saplings, with acclimation to elevated temperature and vapour pressure deficit affecting the balance between leaf cooling and water conservation. While some species demonstrated trait coordination supporting limited homeothermy, substantial heterogeneity in responses to temperature and VPD was observed, suggesting that general patterns may be difficult to identify without measuring more species. Additionally, VPD-induced acclimation may reduce this capacity, with potential consequences for plant survival under increasing climate variability. Future research should further explore the role of these trade-offs in shaping long-term resilience to heat stress.

Chapter 4: Ecotypic variation in leaf thermoregulation and heat tolerance but not thermal safety margins in tropical trees

4.1 Introduction

The conservation of existing forests and active reforestation are pivotal to mitigating the worst impacts of climate change (Girardin et al., 2021; Griscom et al., 2017). However, periodic heat stress, induced by rapid climate change (IPCC, 2022) threatens forest function and thereby the future success of these conservation efforts (Jordan et al., 2024). Increased frequency of hot, dry conditions has driven declines in forest tree populations (Hammond et al., 2022) and associated carbon accumulation in biomass (Anderegg et al., 2016; Brienen et al., 2015). Tropical rainforests may be particularly susceptible, given their canopies already experience temperatures exceeding their thermal limits for maximum photosynthesis (Mau et al., 2018). With the frequency of lethal temperatures predicted to increase with future global warming (Doughty et al., 2023b), it is essential to understand the capacity of species to tolerate or avoid heat stress

The leaf thermal safety margin describes the difference between observed maximum leaf temperatures and thermal tolerance of photosynthesis, and as such is a useful proxy to determine vulnerability of ecosystems, species, or populations to climate warming. Photosynthetic heat tolerance is often determined by assessing damage to leaf photosystem II using chlorophyll fluorescence (Maxwell & Johnson, 2000). Two commonly used metrics are T_{crit} and T_{50}, representing the temperatures at which there is a 5% and 50% decline in photosystem II functioning. The ability to acclimate photosynthetic heat tolerance to warmer leaf temperatures is a common adaptation (Perez & Feeley, 2020), with higher values generally found in leaves exposed to higher ambient temperatures (Geange et al., 2021; O'Sullivan et al., 2017), lower soil moisture (Cook et al., 2021), and higher radiation (Slot et al., 2019). While species originating from warmer habitats exhibit higher T_{crit}, the increase observed across an increase in growth temperature is modest, ranging from 0.24°C to 0.60°C increase per 1°C increase in mean annual temperature (O'Sullivan et al., 2017; Slot et al., 2021; Zhu et al., 2018). Consequently, higher observed leaf temperatures in warmer climates such as lowland tropical forests result in them having a narrower thermal safety margin, which has been observed across species in contrasting biomes (Kitudom et al., 2022; Perez & Feeley, 2020) and within species (Kullberg et al., 2023).

Forest canopy leaf temperatures can be substantially different from ambient air temperatures (Blonder & Michaletz, 2018; Crous et al., 2023; Fauset et al., 2018). Leaf temperature is a result of the balance of sensible and latent heat fluxes, along with net incoming radiation, and is impacted by a broad suite of morphological and physiological traits that interact with the microclimate of the leaf (Campbell & Norman, 1998; Jones, 2013). Fully illuminated sunlit leaves are typically warmer than ambient air

temperatures (Zhou et al., 2023), with the magnitude of this offset (ΔT) varying due to differences in leaf thermal traits (Blonder & Michaletz, 2018), such as effective leaf width, solar absorptance profile, inclination angle and orientation, and dynamic stomatal conductance (g_s) (Fauset et al., 2018; Guo et al., 2022; Perez & Feeley, 2020). Trait variation resulting in enhanced leaf cooling is an important strategy to avoid heat stress (Deva et al., 2020; Drake et al., 2018). Indeed, there is growing evidence that communities of plant species grown under warmer conditions preferentially express leaf trait combinations that decrease leaf warming compared to those grown under cooler conditions (Kitudom et al., 2022; Kullberg et al., 2023; Leigh et al., 2012; Posch et al., 2022; Wright et al., 2017), providing some support to the idea of plant thermoregulation and limited homeothermy (Blonder & Michaletz, 2018; Michaletz et al., 2016).

However, it is unclear to what extent intra-specific genetic variation may also show similar patterns of limited homeothermy. A recent study in sage-brush reported lower canopy temperatures of warm origin populations, attributing this to differences in plant height altering canopy microclimate (Olsoy et al., 2023). Similarly, warm origin genotypes of *Populus fremontii* exhibited higher transpiration rates and consequently lower leaf temperatures compared to cool origin genotypes (Hultine et al., 2020). In addition, enhanced leaf cooling has been associated with more heat tolerant genotypes in *Phaseolus vulgaris* (Deva et al., 2020). On the other hand, evidence for increased thermal tolerance of warm-origin genotypes is mixed (Chen et al., 2016; Coast et al., 2022; Gimeno et al., 2008; Marias et al., 2016), with some studies suggesting a physiological limit to the high temperature acclimation of thermal tolerance (Neri et al., 2024; Slot et al., 2021; Tiwari et al., 2020). If tropical trees do exhibit a simultaneous increase in thermal tolerance and decrease in leaf temperatures of warm origin provenances, there is potential for warm origin genotypes to have greater thermal safety margins when planted under common conditions, such as in restoration plantings. However, if T_{crit} acclimates to T_{leaf} across populations as it does across species and biomes (Perez & Feeley, 2020), this may ultimately lead to a convergence of thermal safety margins. Therefore, understanding how these two variables covary across provenances is important for the conservation and management of tropical rainforests.

Here I tested whether upland and lowland provenances of four tropical tree species differed in their thermal safety margins when grown in a lowland common garden. This was achieved by measuring photosynthetic heat tolerance, leaf and canopy temperatures, as well as leaf thermal traits which were then used to paramaterise a leaf energy balance model. I hypothesised that provenances from the warmer lowlands would have a lower ΔT compared to provenances from the cooler uplands (H1), and that this provenance variation could be explained by variation in both leaf thermal traits, and differences in microclimate in plants of differing canopy heights (H2). I also expected thermal tolerance to acclimate to T_{leaf}, such that T_{crit} and T_{50} would show similar patterns of provenance-differentiation as ΔT, leading to a convergence of thermal safety margins across provenances (H3).

4.2 Materials and Methods

4.2.1 Study site

This study was located in the Wet Tropics of Queensland, Australia, declared a UNESCO World Heritage Area in 1988 (UNESCO World Heritage Centre 1988), due to its high diversity, endemism, and relicts of Gondwanan plant lineages. The region covers just 8,900 km^2 but due to its mountainous terrain experiences steep environmental gradients across relatively short geographic distances. The lowland tropical rainforest community of this region was recently declared 'Endangered' due to a history of clearing resulting in substantial fragmentation leaving it susceptible to pressures exacerbated by current climate change (Threatened Species Scientific Comittee 2021).

The study site was a 1.5-year-old provenance trial established in March 2022 at James Cook University's Daintree Rainforest Observatory (DRO) in Cape Tribulation (−16.10449 °S, 145.4511 °E), Queensland, Australia. The provenance trial site has an area of 2,251 m^2 and is surrounded by mature secondary forest regrowth. The plot used in this study is one of three set up across the Australian Wet Tropics bioregion as part of the TropAdapt project (https://tropadapt.org) to determine differences in growth and survival across upland and lowland provenances in 16 rainforest tree species (Appendix D). At each site, 6- to 12-month-old saplings of 16 species and provenance (upland and lowland for each species) were planted in a randomised block design (n = 32 plants per block × 10 blocks at each site) at 3 × 3 m spacing. The DRO has a mean annual temperature (MAT) of 24.1 °C and a mean annual precipitation of 3516 mm (Karger et al., 2017). The soils are acidic, dystrophic, brown dermosol, formed in the colluvium from the metamorphic and granitic mountains to the west (Murtha, 1989).

4.2.2 Plant material

To ensure findings are useful both for understanding natural systems, and for informing restoration management, I chose tree species that are characteristic of rainforest communities in the Wet Tropics of Queensland (Goosem & Tucker, 1995; Threatened Species Scientific Comittee 2021), and among the most frequently used in regional rainforest tree plantings (Engert et al., 2020). Given how speciose the tropics are, and to gain insight into how generalisable potential patterns are across diverse species types, I included species that differ in plant families, life history strategies, and deciduousness. From the original 16 species planted, four species were selected as the focus for this work (Table 4. 1), including *Castanospermum australe* A.Cunn. ex Mudie (Fabaceae), *Homalanthus novo-guineensis* (Warb.) Lauterb. & K.Schum. (Euphorbiaceae), *Melicope elleryana* (F.Muell.) T.G.Hartley (Rutaceae), and *Terminalia microcarpa* Decne. (Combretaceae). All four species have a wide elevational distribution, are relatively abundant in the Wet Tropics of Queensland, and naturally occur throughout the tropical and subtropical Australian and Indo-Malesian floristic regions. Three of the species, *C. australe*, *H. novo-guineensis,* and *M. elleryana*,

are evergreen, whilst *T. microcarpa* is considered semi-deciduous with a period of leaflessness during the dry season (September or October) in mature trees. *H. novo-guineensis* is a fast-growing, shade intolerant pioneer species, while the other three are late secondary, shade tolerant species (Goosem & Tucker, 1995). Of the four species, *C. australe* has the slowest growth rates, highest wood density, and is a nitrogen fixer. While all four species are present in well-developed rainforest, *M. elleryana* and *C. australe* are characteristic upper canopy species, and *T. microcarpa* is often present as an emergent species in the canopy of mature forests in the region (Threatened Species Scientific Comittee 2021).

Table 4. 1. Provenance information for target species in this study. Climate data obtained from CHELSA v.2. 1981-2010 at 1km resolution.

Species	Provenance	Lat	Long	Elev[1]	MAT[2]	MTWM[3]	MAP[4]
Castanospermum australe	Upland	−17.34	145.50	763	20.3	27.7	1898
	Lowland	−16.47	145.36	83	24.3	29.2	2298
Homalanthus novo-guineensis	Upland	−17.52	145.57	1074	18.6	25.9	2874
	Lowland	−16.18	145.41	19	24.4	28.6	3334
Melicope elleryana	Upland	−17.30	145.46	782	19.9	27.3	1665
	Lowland	−16.18	145.41	19	24.4	28.6	3334
Terminalia microcarpa	Upland	−17.26	145.48	767	20.4	27.8	1604
	Lowland	−16.26	145.33	5	24.3	29.3	2354

[1] Elev = Elevation, m a.s.l

[2] MAT = Mean annual temperature (BIO1), °C

[3] MTWM = Max temperature of the warmest month (BIO5), °C

[4] MAP = Mean annual precipitation (BIO12), mm

Saplings were sourced from local nurseries (Tablelands Regional Council, Rainforest Rescue, and Douglas Shire Council), with the coordinates of seed source used to determine the climate of origin for the source populations (Table 4. 1, Appendix B: Figure 1, Figure 2). Saplings of upland origin were grown from seeds collected in the Atherton tablelands, while those of lowland origin were sourced from the Daintree Rainforest around Cape Tribulation and Diwan. The mean geographic distance between upland and lowland collection sites was 121 km (range 97 to 150 km) (Table 4. 1). The lowland collection site for all species is close both geographically and climatically to the DRO common garden site (Appendix B: Figure 1). While multiple nurseries were used to obtain seedlings, propagation and seedling hardening techniques follow standard practice developed by local reforestation practitioners (Goosem & Tucker, 1995). It should be noted that while provenance seed collection location information is verified, nurseries did not record the number of individual trees that seed were collected from. Nursery guidelines recommend a seed sourcing strategy of collecting from multiple individuals (Commander, 2021), however given the

potential for asynchronous phenology in species with only low native density in natural plantings I cannot confirm whether seeds from a particular provenance originated from one or more individuals from that locality.

4.2.3 Experimental design

To determine if leaf thermal traits, leaf temperatures and thermal tolerance differed between the lowland and upland provenances of the four selected species, I identified six replicate individuals per group (n = 6 individuals × 2 provenances per species) that had healthy and fully sun-exposed canopies on which to conduct all measurements. Plant heights ranged from 0.7 to 9.0 m (mean 4.46 m). Leaf morphological traits and thermal tolerance required destructive leaf sampling and were measured on leaves sampled from the top of the canopy using a pole pruner. Leaf temperature, stomatal conductance, and leaf angle were measured *in situ*, with the aid of a stepladder. As a result, these measurements were conducted at canopy heights of *c.* 2.5m, except in smaller stature trees which were measured at the top of their canopy.

Three of the species, *C. australe*, *H. novo-guineensis*, and *T. microcarpa* had provenance-level differences in plant growth, with trees from the lowland-origin provenance taller than trees from the upland-origin provenance. In contrast, plant height did not differ between provenances in *M. elleryana* (Appendix B: Figure 3). To determine if potential provenance differences in leaf morphological traits and thermal tolerance (measured at the top of the canopy) were due to the greater plant heights of lowland provenances, I chose a subset of individuals (n=5 per species) from *C. australe* and *H. novo-guineensis* to measure leaves from mid-canopy (but still fully sun-exposed) positions, at canopy heights similar to the upland provenance trees.

In situ measurements of leaf temperatures took place daily from the 19th until the 25th of October 2023, and then again from the 6th to the 8th of November 2023. Stomatal conductance was measured over three days, combined with leaf temperature measurements on the 25 October 2023 and 7 and 8 November 2023. Destructive leaf sampling for thermal tolerance assays and leaf morphological traits began on the 19 October 2023 and ended on the 25 October 2023. All leaves measured and sampled represented healthy, mature, fully sun-exposed leaf material of similar positioning and aspect, on the North side of the canopy. It rained frequently in the lead-up to our measurement campaign, so plants were not expected to be moisture-limited.

4.2.4 Leaf and canopy temperatures

Observed T_{leaf} and thereby observed leaf-to-air temperature differences (ΔT) were measured using two different methods: first by tracking individual T_{leaf} with point measurements taken over 10 days using an infrared thermometer, and subsequently by determining whole canopy temperature (T_{can}) using UAV-

based thermal imagery. Individual leaf temperatures were recorded using a dual laser infrared thermometer (MS6530, Mastech, Pittsburgh, Pennsylvania, US), with a spectral response of 8-14 μm, a distance to spot size ratio of 12:1, and an assumed emissivity at 0.95. Measurement campaigns for T_{leaf} took place between the times of 10:45 and 14:45 during cloud-free periods with low windspeed. Measurements were standardised across trees by taking measurements on 10 sun-exposed leaves on branches that were perpendicular to the solar angle to ensure maximum incoming radiation. This was repeated over multiple days and in a randomised order. The total number of leaves measured on each plant ranged from 30 to 50 (n = 1990). The difference between leaf and air temperatures (ΔT_{leaf}) for each plant was calculated by subtracting 10-min average air temperature.

For T_{can}, thermal images of whole tree canopies were taken using a drone (DJI Mavic 2 Enterprise Advanced, DJI Technology Co. Ltd, Shenzhen, China) fitted with a FLIR M2ED thermal camera (Teledyne Flir, Wilsonville, OR, USA) with a thermal spectral band ranging from 8 to 14 μm, an uncooled Vox microbolometer thermal sensor (with automated calibration), sensor resolution of 640 x 512 pixels, approx. 9 mm lens with a 57° horizontal field of view, and 30 Hz frame rate. The flight was completed on 11th December 2023 at 12:07 pm, with a 15 min flight time. Both thermal (IR) and true colour (RGB) images were taken simultaneously and flown with 50% overlap at 1.3 m s^{-1}. With a flight altitude of 27 m above the ground the pixel resolution was 4.2 cm $pixel^{-1}$. RGB images were captured at the same times and locations as the thermal images, with an image size of 5472 x 3648 pixels, 35 mm format equivalent lens length of 24 mm, and a horizontal field of view of 84°. An RGB orthophoto mosaic of the trial site with an average ground sample distance of 2.18cm was created using Pix4Dmapper (Pix4D S.A., Prilly, Switzerland).

Thermal images were converted to TIFF, with radiometric data converted to temperatures using the mean air temperature (29°C) and relative humidity (38 %) measured on the crane weather station during the flight, and an object distance of 27 m minus the target tree height, resulting in object distances ranging from 18.00 m to 26.34 m (mean 22.54). Images were analysed using ImageJ, with target tree canopies determined manually using polygons, and background temperatures of the ground excluded using threshold filtering. For each tree, calculations of the mean, standard deviation, median, minimum, maximum, and skewness of canopy temperatures were recorded. The mean of each individual canopy was used for analysis of T_{can}.

4.2.4 Stomatal conductance

Stomatal conductance (g_s) was measured on abaxial leaf sides using a leaf porometer (SC-1 Leaf Porometer, Decagon Devices Inc, Pullman, United States) with a measurement range of 0 to 1,000 mmol m^2 s^{-1} and a stated accuracy of ±10% of measurement from 0 to 500 mmol m^2 s^{-1}. Porometer measurements

took place over three days, with one leaf per plant measured each day (n = 3 measurements per plant), in conjunction with T_{leaf}. For analysis of provenance differentiation, I used the plant-level average of the 3 measurements per plant.

4.2.5 Leaf angle

Leaf inclination angle (°) – the angle of the leaf relative to the horizontal plane – was measured *in situ* on 10 leaves per plant using an electronic protractor using the plumb measuring mode from the 'Protractor' app (EXA Tools, Bielsko-Biała, Poland) within a cell phone (OPPO A74 5G Android smartphone, OPPO, Dongguan, China). This technique has shown similar accuracy compared to traditional manual and digitiser methods of measuring leaf angle (Escribano‐Rocafort et al., 2014).

4.2.6 Photosynthetic heat tolerance

Photosynthetic heat tolerance was measured using a chlorophyll fluorometer (PAM-2000, Walz) following a protocol (Leon-Garcia & Lasso, 2019) modified from Krause et al (2010). Leaf material was sampled early in the morning, from north facing branches within one metre of the top of the canopy. For a subset of individuals in the lowland provenance of *C. australe* and *H. novo-guineensis*, leaves were also sampled from lower in the canopy. The species and individuals that were measured each day were randomised, making sure to always include at least one replicate from each provenance of each species.

To ensure assessment at steady state with respect to the photosynthetic system, fresh leaf material was dark adapted for 30 minutes, and then the ratio of F_v/F_m was recorded. Subsequently a cork corer was used to cut 4 to 6 discs per leaf, which were pooled per tree. Leaf discs had a diameter of 8 mm for smaller leaved species (*C. australe* and *T. microcarpa*) and 10 mm for larger leaved species (*H. novo-guineensis* and *M. elleryana*). From this pool, six leaf discs were randomly assigned to each temperature treatment. Leaf discs were heated in a water bath for 15 min at temperatures of either 34, 38, 40, 42, 44, 46, 48, 50, 52, 54, or 58 °C. Control discs were kept in a water bath at ambient lab temperature of 25 °C. Treatment duration times of 15 min were selected as is common for other studies of thermal tolerance (Perez & Feeley, 2020; Slot et al., 2021; Tiwari et al., 2020). After the heat treatment, leaf discs were stored in the dark in petri dishes with their abaxial side face down on a moist paper towel. After 24 hours, F_v/F_m was measured on dark-adapted leaf discs to determine irreversible damage to photosystem II. The temperature response of F_v/F_m was fitted using the following equation:

$$\frac{F_v}{F_m} = \frac{\frac{F_v}{F_{m.max}}}{1 + e^{b(Tleaf - T50)}} \qquad (eq\ 4)$$

Where $F_v/F_{m.max}$ is the upper horizontal asymptote that represents the F_v/F_m of non-stressed, healthy leaves and T_{leaf} is the temperature treatment. The 'nls_multstart' function in the 'nls_multstart' package was used to fit curves and obtain estimates of T_{50} for each plant, whereas T_{crit} was defined as the temperature where the horizontal line indicating $F_v/F_{m.max}$ intersects with the line of the slope of the F_v/F_m decline at T_{50}.

4.2.7 Leaf morphological traits

Leaf morphological traits were measured according to standard protocols (Perez-Harguindeguy et al., 2013) and included leaf fresh weight (g), leaf area (cm^2), leaf width (m) and leaf dry mass following 3 days of drying at 60 °C. From these I calculated leaf mass per area, LMA (kg m^{-2}) and leaf dry matter content, LDMC (g g^{-1}). Leaf morphological traits were measured on 3 to 10 leaves (average 9) per plant. The thermal time constant, τ (s), was calculated using the same methodology described in Chapter 3 (eq 1, 2, and 3).

4.2.8 Meteorological data during campaign

Meteorological variables including air temperature (T_{air}), photosynthetic active radiation, wind speed, and relative humidity were recorded at nearby weather stations during the measurement campaign (Appendix B: Figure 4, Figure 5). Air temperature and wind speed at 1.3 m height was recorded 200 m away from the plot in a clearing using a permanently mounted weather station (WeatherMate 3000, Environdata, Warwick, QLD, Australia). In addition, a research grade weather station located on the jib of a 47m height canopy access crane recorded air temperature and relative humidity (HMP60, Vaisalla, Vantaa, Uusimaa, Finland), wind speed (YOUNG Model 05103 Wind Monitor, R.M.Young, Traverse City, MI, USA), incoming photosynthetic active radiation (SQ-521 full-spectrum quantum sensor, Apogee, Logan, UT, USA) and precipitation with a tipping bucket rain gauge (TB7, HyQuest Solutions, Warwick Farm, NSW, Australia) with data recorded every one min via a networked datalogger (CR310, Campbell Scientific, Logan, UT, USA). Gap filling of wind speed data from the clearing was carried out by calibration of extant data against crane meteorological station. Multiplying wind speed measured at the top of the canopy crane by a factor of 0.6 was a better predictor of wind speed in the clearing than using a logarithmic wind profile.

4.2.9 Leaf energy balance model

To determine whether there were provenance-level differences in how leaf thermal traits covaried, T_{leaf} was modelled using a leaf energy balance equation implemented using the FindTleaf function in the 'plantecophys' package in R (Duursma, 2015). The leaf trait inputs used were individual plant-averages of leaf width (m) measured at the canopy top, along with stomatal conductance (μmol m^2 s^{-1}) and leaf

inclination angle (°) measured at *c.* 2.5 m height. Microclimate inputs were set to their average conditions during the measurement campaign, with wind speed set to 2.3 m s^{-1}, T_{air} to 28.0 °C, and VPD to 1.7 kPa. While PPFD averaged 1545 µmol m^2 s^{-1} during the campaign, this value was modified to account for variation in the interception of incoming radiation with the measured mean leaf inclination angle of each plant using the 'insolation' package in R (Corripio, 2021).

4.2.10 Data analysis

To test whether provenances from the warmer lowlands have a lower ΔT_{leaf} compared to the cooler upland provenances (H1) I used a linear mixed effects model including fixed effects for 'provenance' and random effects for measurement days 'doy' as well as individual leaves nested within individual plants 'unique_id/leaf'. The underlying data was based on individual spot measurements of T_{leaf} minus measured T_{air} at that time. Models were fitted to each species separately using 'lme4' (Bates et al., 2015) and pairwise comparisons between provenances were assessed using 'emmeans' (Lenth, 2022).

Several analyses were conducted to assess whether ΔT_{leaf} could be explained by leaf thermal traits and plant canopy heights (H2). I tested for provenance differentiation in leaf traits (width, angle, conductance, thermal time constant) and leaf–air temperature differences based on leaf energy balance modelling (ΔT_{mod}) and canopy temperatures (ΔT_{can}). For this I performed a two-way unpaired Student's *t*-test on each species separately. I used plant averages as a single observation so that all tests had balanced designs with $n = 6$ plants for each group. Homogeneity of variance was tested using the Levene test and normality was tested using the Shapiro test. To determine whether provenance differentiation in traits was a result of systematic differences in plant height between provenances, I tested for differences in leaf traits and thermal tolerance between leaves sampled in the upper and lower canopy of the lowland provenance of *C. australe* and *H. novo-guineensis.* To do so I performed paired *t*-tests on five replicate plants per group. The leaf trait, LMA, did not meet assumptions of normality so data were log transformed for analysis. In addition, I examined the relationship between modelled and observed T_{leaf}, and plant height using linear regression with either T_{leaf}, or T_{mod} as the response variable, and plant height as an explanatory variable. I considered these analyses in combination when interpreting how well variation in leaf traits and canopy height explained observed variation in T_{leaf}.

To assess the impact of provenance differentiation on thermal tolerance and the consequences of this on thermal safety margins (H3), I first tested for provenance differences in T_{crit} and T_{50}, as well as the thermal safety margins (TSM), as per the other traits (using two-way unpaired Student's t-tests). The thermal safety margin (TSM) of each plant was calculated with either T_{crit} or T_{50} as the upper threshold. From this value, I subtracted the maximum air temperature observed during the study period, 32 °C, and then subtracted either the mean observed leaf-air temperature differences measured with the handheld IR

sensor (ΔT_{leaf}), the mean observed canopy-air temperature differences measured with UAV thermal imagery (ΔT_{can}), or the modelled leaf-air temperature differences calculated under common conditions from the traits leaf width, stomatal conductance, and leaf inclination angle (ΔT_{mod}). I then assessed correlations between T_{leaf} and T_{crit} using linear regression. All analyses were performed using R version 4.2.2. Throughout the manuscript provenance differences are reported as arithmetic means ± 1 SD.

4.3 Results

4.3.1 Provenance level differentiation in leaf traits and stomatal conductance

Provenance effects on leaf width differed across species. For *H. novo-guineensis*, there was strong evidence that provenances differed in leaf width ($t_{(10)} = -4.27$, $p = 0.00163$), with leaves from the lowland provenance substantially narrower than leaves from the upland provenance, averaging 10.0 cm ± 1.3 and 15.2 cm ± 2.7 respectively (Figure 4. 1a). There was no evidence of a provenance effect in leaf width for *C. australe* ($t_{(10)} = -0.16$, $p = 0.87$, Figure 4. 1a), *M. elleryana* ($t_{(10)} = 0.81$, $p = 0.44$), or *T. microcarpa* ($t_{(10)} = 0.49$, $p = 0.64$, Figure 4. 1a).

The mean stomatal conductance (g_s) measured around midday was 311 mmol m^2 s^{-1} and ranged from 71 to 700 mmol m^2 s^{-1} across all species and provenances (Figure 4. 1b). For all species, mean g_s was lower in the lowland provenance than the upland provenance, however moderate evidence for a provenance effect on g_s was found only in *T. microcarpa* ($t_{(10)} = -2.25$, $p = 0.0479$), in which g_s averaged 248 mmol m^2 s^{-1} ± 83 in the lowland provenance and 416 mmol m^2 s^{-1} ± 163 for the upland provenance (Figure 4. 1b).

Mean leaf inclination angle was 32.1 ° and ranged from 4.5 to 65.7 ° across all species and provenances (Figure 4. 1c). For *C. australe*, I found strong evidence that leaves from the lowland provenance had steeper leaf angles than the upland provenance ($t_{(10)} = 3.64$, $p = 00454$), averaging 51.7 ° ± 9.1 for the lowland provenance and 33.2 ° ± 8.5 for the upland provenance (Figure 4. 1c). In *H. novo-guineensis*, I found strong evidence for the opposite pattern ($t_{(10)} = -3.83$, $p = 0.00333$), with the lowland provenance having shallower leaf angles than the upland provenance, averaging 24.8 ° ± 14.7 and 52.9 ° ± 10.3 respectively (Figure 4. 1c). I found no evidence for a provenance effect on leaf inclination angle for *T. microcarpa* or *M. elleryana* ($p > 0.1$, Figure 4. 1c).

The mean thermal time constant was 7.5 s and ranged from 2.3 to 19.9 s. For all species, the thermal time constant of the lowland population was lower on average than the upland provenance (Figure 4. 1d). However, I found strong evidence of a provenance effect only for *H. novo-guineensis* ($t_{(10)} = -3.45$, $p = 0.00619$) which had a thermal time constant of 9.3 s ± 1.4 for the lowland provenance and 14.2 s ± 3.2 for the upland provenance.

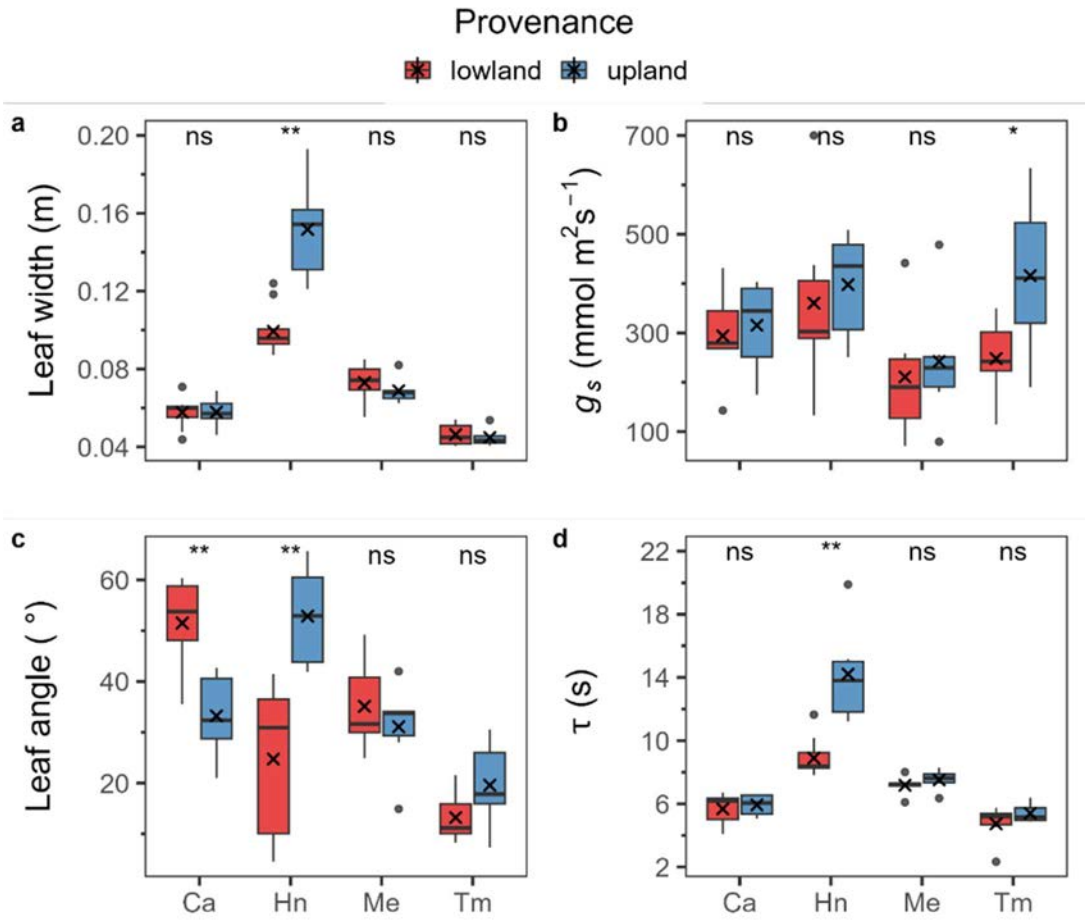

Figure 4. 1. Provenance differences in leaf functional traits of four tropical tree species grown under common environmental conditions. Panels show (a) leaf width, (b) stomatal conductance, g_s, (c) leaf inclination angle, and (d) thermal time constant, τ. Species include Ca = *Castanospermum australe,* Hn = *Homalanthus novo-guineensis,* Me = *Melicope elleryana,* and Tm = *Terminalia macrocarpa*. Data represent tree averages (n=6) presented as box and whisker plots showing median and interquartile range, with the average marked by ×. Results of intraspecific t-test of provenance differences indicated by subscript ns=not significant, * $p < 0.05$, and ** $p < 0.001$.

4.3.2 Provenance level differentiation in leaf and canopy temperatures

Temperatures of individual leaves recorded with handheld IR sensors ranged from 18.0 °C to 45.9 °C (Appendix B: Figure 6). When averaged to the plant level, mean T_{leaf} was 32.2 °C and ranged from 27.2 to 36.4 °C across all individuals. The mean leaf-to-air temperature difference, ΔT_{leaf}, was 4.1 °C and ranged from −0.7 to 8.1 °C (Figure 4. 2a). For most plants mean ΔT_{leaf} was positive, except for *H. novo-guineensis*, which had multiple occurrences of T_{leaf} cooler than T_{air} (Figure 4. 2a).

The mixed effects models found very strong evidence for provenance differences in ΔT_{leaf} for both *T. microcarpa* and *C. australe*. In *T. microcarpa,* ΔT_{leaf} was higher in the lowland provenance than the upland provenance ($t_{(124)} = 6.196$, $p < 0.0001$), with a mean of 5.2 °C ± 1.19 and 3.4 °C ± 1.35, respectively (Figure 4. 2a). The opposite was observed for *C. australe*, in which ΔT_{leaf} in the lowland provenance was lower than the upland provenance ($t_{(121)} = -3.788$, $p = 0.0002$), with a mean of 4.8 °C ± 1.42 and 6.0 °C ± 1.68 respectively (Figure 4. 2a). I found no evidence for provenance-differentiation in ΔT_{leaf} for *M. elleryana* or *H. novo-guineensis* ($p > 0.1$; Figure 4. 2a).

For ΔT_{can}, I found no evidence of provenance effects in any of the four species (Figure 4. 2b).

Modelled leaf-to-air temperature differences (ΔT_{mod}) represent the variation in potential leaf temperatures as resulting from the covariation between leaf width, leaf angle, and stomatal conductance. Across all individuals, mean T_{mod} was 29.1 °C and ranged from 27.1 to 31.0 °C (Figure 4. 2c). For *T. microcarpa,* I found moderate evidence for a provenance effect in ΔT_{mod} ($t_{(10)} = 2.39$, $p = 0.0381$), with ΔT_{mod} higher in the lowland provenance than the upland provenance averaging 1.6 °C ± 0.69 and 0.6 °C ± 0.78 respectively. For *H. novo-guineensis*, I found weak evidence for provenance differences ($t_{(10)} = 1.81$, $p = 0.0996$), with the lowland provenance also having a higher average ΔT_{mod} than the upland provenance, averaging 1.4 °C ± 1.0 and 0.3 °C ± 1.09 respectively. For the other two species, the data showed no evidence of provenance-differentiation in ΔT_{mod}.

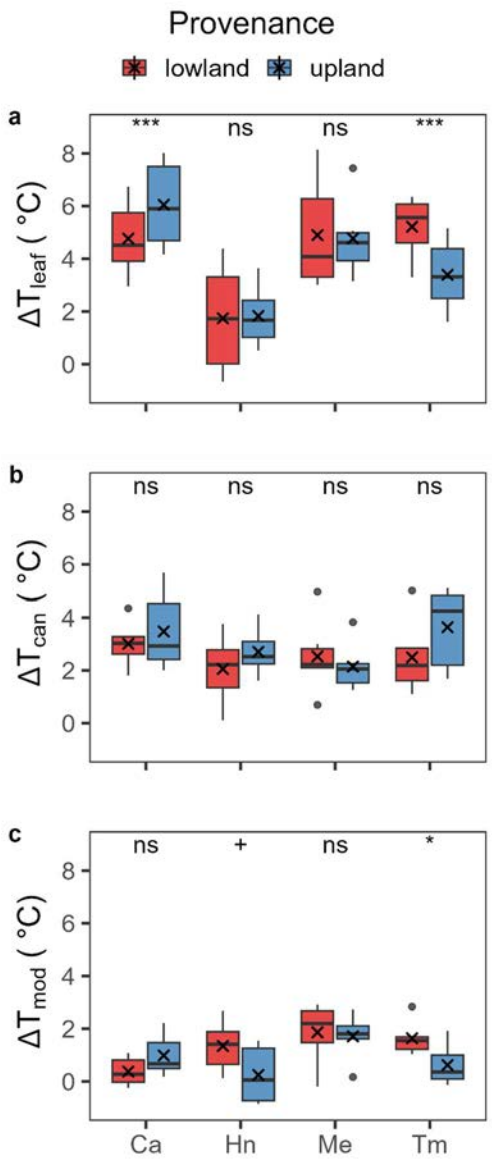

Figure 4. 2. Provenance differences in leaf-to-air temperature differences (ΔT) of four tropical tree species grown under common environmental conditions. Panels show ΔT calculated using (a) observed leaf temperatures ΔT_{leaf}, (b) observed canopy temperatures ΔT_{can}, (c) and trait modelling ΔT_{mod}. Ca = *Castanospermum australe,* Hn = *Homalanthus novo-guineensis,* Me= *Melicope elleryana,* and Tm = *Terminalia microcarpa*. Data is of tree averages (n=6) presented as a box and whisker plots showing median and interquartile range, with the average marked by ×. Results of intraspecific provenance differences indicated by subscript ns=not significant, + is marginally significant at $p < 0.1$, * $p < 0.05$, and *** $p < 0.0001$. Note that for panels a) and c) statistical analysis is based on unpaired t.test on the plant-level means, whereas for panel b) statistical analysis is based on mixed effects model including random effects of doy and individual plant, conducted on the individual leaf temperatures.

4.3.3 Correlation between modelled and observed leaf and canopy temperatures

Observed variation in ΔT_{leaf} was strongly predicted by the trait-based energy balance model (ΔT_{mod}), with an RMSE of 3.517 and MAE of 3.11 (Appendix B: Figure 7). However, ΔT_{mod} tended to underestimate ΔT_{leaf} for *C. australe*, and overestimate T_{leaf} for *H. novo-guineensis*. This was likely due to errors associated with the differences in T_{air} at the canopy height of each plant, versus from the clearing where T_{air} was measured at 2.5 m height. This is reflected in Appendix B: Figure 7b, where the difference between observed and modelled ΔT is correlated with plant height ($R^2 = 0.35$, $P < 0.0001$). This trend is driven by a decrease in measured ΔT_{leaf} with plant height (decreasing by 0.66 °C every 1m increase in plant height), and not by ΔT_{mod} (Appendix B: Figure 7c-d). The correlation between ΔT_{leaf} and ΔT_{mod} was improved when modifying air temperature and wind speed vertically through the canopy, however as this did not alter results of provenance-differentiation it is not included.

4.3.4 Provenance level differentiation in thermal tolerance

At the common garden experimental site, mean T_{crit} was 46.0 °C and ranged from 42.0 to 51.1 °C (Figure 4. 3a). For *C. australe*, I found moderate evidence of a provenance effect on T_{crit} ($t_{(10)} = -2.46$, $p = 0.0336$), with the lowland provenance having a lower T_{crit} than the upland provenance, averaging 46.6 °C ± 2.81 and 49.6 °C ± 1.05 respectively (Figure 4. 3a). For *T. microcarpa*, I found weak evidence for a provenance effect ($t_{(10)} = 1.85$, $p = 0.0947$), with T_{crit} averaging 47.7 °C ± 2.07 and 45.8 °C ± 1.41, for the lowland and upland provenance respectively (Figure 4. 3a). I found no evidence for a provenance effect on T_{crit} for *H. novo-guineensis* or *M. elleryana* ($p > 0.1$). The mean thermal tolerance metric T_{50} was 49.7 °C overall and ranged from 46.6 to 54.7 °C (Figure 4. 3b). I found no evidence for provenance-differentiation in T_{50} in any of the species ($p > 0.1$; Figure 4. 3b).

4.3.5 Within-canopy variation in leaf traits and thermal tolerance

To test whether provenance differences in thermal tolerance and leaf traits were due to differences in tree height between provenances, a subset of individuals from the lowland provenance of both *C. australe* and *H. novo-guineensis* were sampled at a mid-canopy position. There were no substantial differences in any leaf traits, or thermal tolerance metrics due to vertical canopy position (Appendix B: Figure 8).

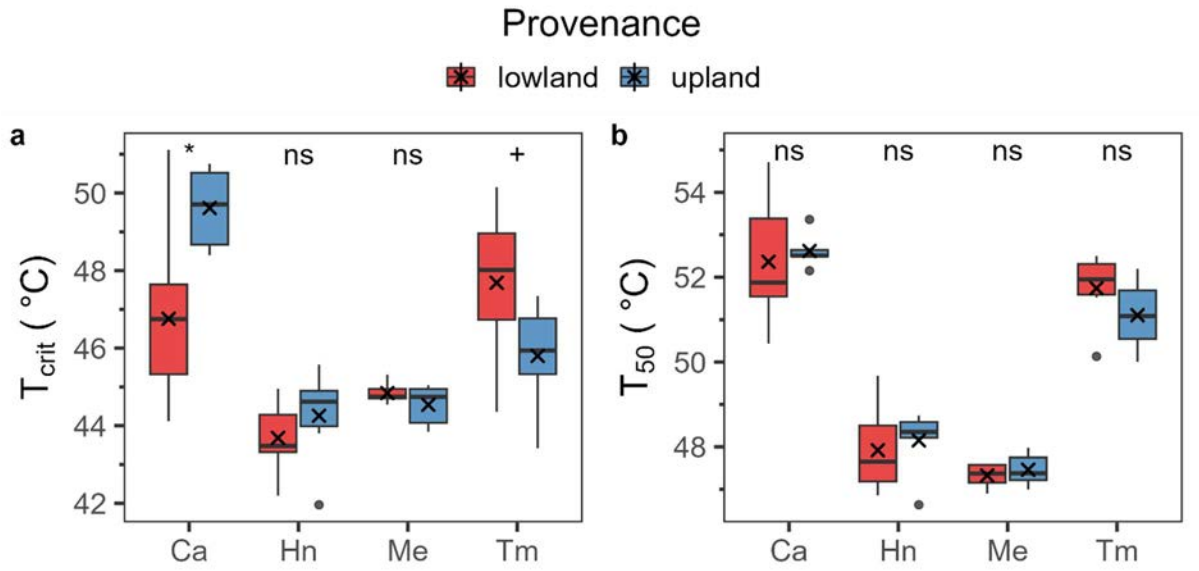

Figure 4. 3. Provenance differences in leaf thermal tolerance of four tropical tree species grown under common environmental conditions. Panels show (a) values for T_{crit} and (b) T_{50}). Ca = *Castanospermum australe,* Hn = *Homalanthus novo-guineensis,* Me= *Melicope elleryana,* and Tm = *Terminalia microcarpa*. Data is of tree averages (*n*=6) presented as a box and whisker plots showing median and interquartile range, with the average marked by ×. Results of intraspecific t-test of provenance differences indicated by subscript ns=not significant, + is marginally significant at $p < 0.1$ and * $p < 0.05$.

4.3.6 Provenance level differentiation in thermal safety margins

The mean thermal safety margin calculated using $T_{crit} - T_{leaf}$ ($TSM_{crit\text{-}leaf}$) was 9.8 °C and ranged from 4.4 to 14.2 °C across all species and provenances (Figure 4. 4a). I found no evidence of a provenance effect in any of the species ($p > 0.1$, Figure 4. 4a).

For thermal safety margins calculated using $T_{crit} - T_{can}$ ($TSM_{crit\text{-}can}$), I found weak evidence to support a provenance effect in *T. microcarpa* ($t_{(10)} = 2.23$, $p = 0.05$) (Figure 4. 4c).

The mean thermal safety margin calculated using $T_{crit} - T_{mod}$ ($TSM_{crit\text{-}mod}$) was 12.8 °C and ranged from 8.2 to 18.2 °C across all species and provenances (Figure 4. 4c). In *C. australe*, I found weak evidence for a provenance effect ($t_{(10)} = -1.90$, $p = 0.0861$), with $TSM_{crit\text{-}mod}$ of the lowland provenance lower than the upland provenance and averaging 14.2 °C ± 2.76 and 16.6 °C ± 1.40, respectively (Figure 4. 4c). I found no evidence for a provenance effect in $TSM_{crit\text{-}mod}$ for the other three species ($p > 0.1$; Figure 4. 4c).

No evidence of a provenance effect was observed in thermal safety margins calculated using T_{50} for any of the species ($p > 0.1$, Appendix B: Figure 9).

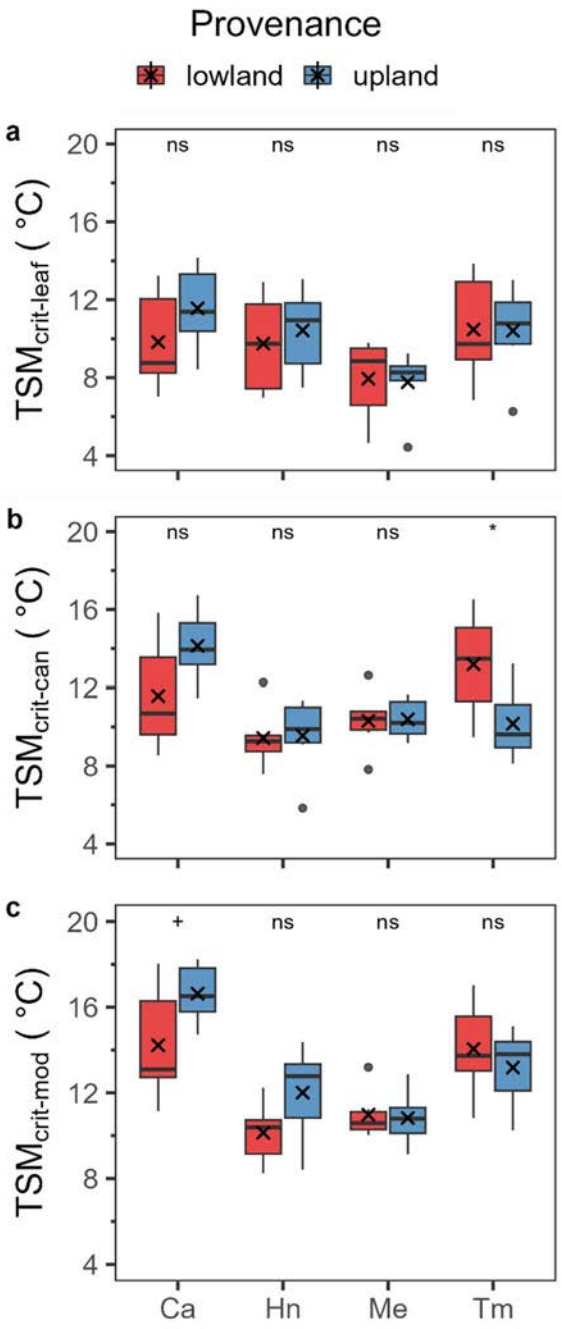

Figure 4. 4. Provenance differences in thermal safety margin (TSM) of four tropical tree species grown under common environmental conditions. TSM calculated using T_{crit} as upper threshold in all panels, with operating temperature defined as 32 °C (mean max air temperature of the site) plus ΔT_{leaf} in (a), ΔT_{can} in (b), and ΔT_{mod} in (c). Ca = *Castanospermum australe,* Hn = *Homalanthus novo-guineensis,* Me = *Melicope elleryana,* and Tm = *Terminalia microcarpa*. Data is of tree averages (n=6) presented as a box and whisker plots showing median and interquartile range, with the average marked by ×. Results of intraspecific t-test of provenance differences indicated by subscript ns=not significant, and * $p < 0.05$.

4.3.7 Contribution of T_{crit} and T_{leaf} to the thermal safety margin

Across all species and provenances, there was a significant, positive correlation between T_{crit} and T_{leaf} (R^2 = 0.11, $F_{1,46}$ = 6.90, p = 0.012, n = 48) that represented a 0.4 °C increase in T_{crit} per 1 °C increase in T_{leaf} (Appendix B: Figure 10). However, within-species, I did not find evidence for a correlation between T_{crit} and T_{leaf} in any of the four species (p > 0.1, Appendix B: Figure 10). Species differed in the absolute magnitude that either T_{crit} or T_{leaf} varied, as a result different variables contributed more to within-species variation in the thermal safety margin depending on the species (Figure 4. 5). In *C. australe* and *T. microcarpa*, the within-species range of T_{crit} was 1.3 and 1.4 times larger than the within-species range of T_{leaf} (respectively), and therefore contributed more to variation in the thermal safety margin for these species. In contrast, for *M. elleryana* and *H. novo-guineensis,* within-species variation in T_{crit} was the weaker driver of changes in thermal safety margins, as T_{crit} variation was 0.3 and 0.7 that of T_{leaf}.

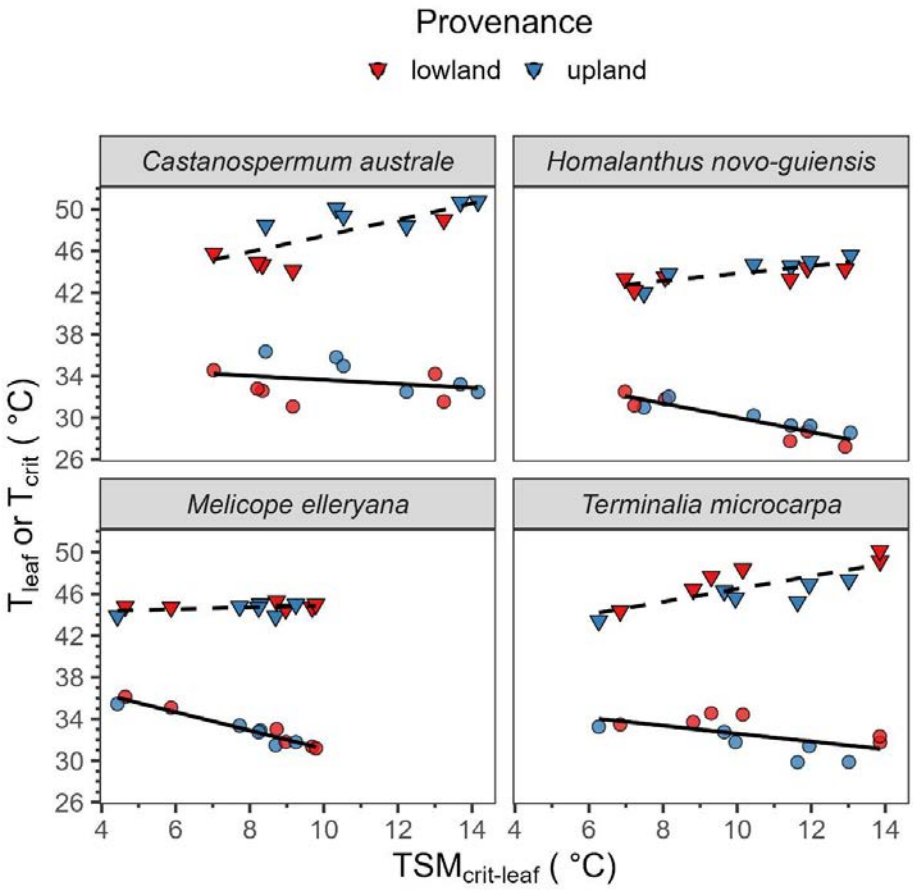

Figure 4. 5. Contribution of T_{leaf} and T_{crit} to thermal safety margins ($TSM_{crit-leaf}$) of four tropical tree species grown under common environmental conditions. Points represent plant-level averages of each variable and lines represent linear regressions. In each panel, T_{leaf} data are represented by circles for the individual points and solid lines for the regression, whereas T_{crit} data are represented by triangles for the points and a dashed line for the regression.

4.4 Discussion

Provenance trials in tropical tree species are relatively rare, and as such our understanding of how tropical forests acclimate or adapt to environmental change is limited. Here I established and utilised a provenance trial of tropical rainforest species in Queensland, Australia to assess whether trees originating from the cooler uplands and warmer lowlands differed in their leaf thermoregulatory traits, or thermal tolerance, and as a result operate with different thermal safety margins when grown under common environmental conditions.

With contrasting patterns of provenance-differentiation observed across the four species tested, I found only partial support for my first hypothesis that the lowland provenances would have cooler leaf temperatures than upland provenances when grown under common garden conditions (H1). Despite this, provenance-based variation of leaf thermal traits and plant height was consistent with variation in T_{leaf}, supporting my second hypothesis (H2). Finally, although limited within-species association between T_{leaf} and T_{crit} was observed, these variables covaried in such a way that thermal safety margins converged between provenances, supporting my third hypothesis (H3). Together, these results suggest that despite variation in either T_{crit} or observed T_{leaf}, there was no provenance-level difference in vulnerability to thermal stress as defined by the thermal safety margin.

4.4.1 Species-specific leaf thermoregulation provenance effects

In this study, provenance effects were observed in at least one thermal trait (i.e., leaf width, leaf angle, or g_s) in three of the four species, and provenance effects in measured T_{leaf} in two species. Assuming the expression of leaf thermal traits under common garden conditions would reflect underlying genetic adaptation associated with provenance, I expected higher T_{leaf} for cool-adapted, and lower T_{leaf} for warm-adapted provenances, which would be consistent with selective pressure to limit plant exposure to extreme leaf temperatures (Michaletz et al., 2016). However, patterns of provenance-differentiation in thermal traits and T_{leaf} followed expected trends (H1) only in one species, *C. australe*, with the opposite pattern observed for *T. microcarpa*, and no variation associated with provenance for the other two species. While this contrasts with other studies that have found warm-adapted plants to have a lower T_{leaf} compared to cool-adapted plants (Blasini et al., 2022; Kitudom et al., 2022; Kullberg et al., 2023), species-specific patterns in intra-specific variation of thermal traits have been reported previously (Kullberg & Feeley, 2022; Manishimwe et al., 2022). This suggests that different species may have different selection pressures, genetic history, or trait trade-offs resulting in contrasting patterns of provenance-associated variation in leaf thermoregulation. It is also interesting to note that the species that did exhibit the expected direction of provenance-differentiation in leaf thermoregulation, *C. australe*, was also the species that had the coolest realized thermal niche (Appendix B: Figure 1). As a result, the mean annual temperature of the lowland

provenance collection site, and the common garden planting location used were at the warmer limit of the species distribution. This is similar to the provenance-trial set up and findings of Blasini et al (2022), and partly supports the theory that selection pressures leading to local adaptation are stronger at the climate extremes of a species distribution (Rehm et al., 2015; Zimmermann et al., 2009). However, further work assessing variation in thermoregulation in multiple provenances, across sites, and in a broader range of species would be needed to establish if this could explain the contrasting patterns observed across the four species tested here.

4.4.2 Effects of leaf thermal traits and plant height on leaf temperature

I expected that provenance differences in ΔT_{leaf} could be explained by observed variation in leaf thermal traits, as well as the influence of plant height on microclimate. Leaf energy balance modelling proved a useful tool to explore the implications of coordinated shifts in multiple thermal traits, with observed and modelled ΔT_{leaf} showing close agreement, as in other studies (Fauset et al., 2018; Guo et al., 2022; Perez & Feeley, 2020). Deviations in the leaf energy balance modelling can probably be attributed to the scale of microclimate inputs coming as they do from a clearing 200m away. The provenance trial microclimate is partly buffered by the surrounding forest, which likely reduces wind speed compared to that observed in the clearing (Davies-Colley et al., 2000). As a result, modelled ΔT_{leaf} is generally lower than that observed. In addition, deviations between modelled and observed ΔT_{leaf} were associated with plant height. Despite these errors in absolute leaf temperature, the relative patterns of provenance differentiation in ΔT_{mod} was unaffected, therefore, leaf energy balance modelling can still be utilised to explore acclimation and adaptation of leaf thermoregulation to climate change.

C. australe:

Consistent with my expectations, T_{crit} and T_{leaf} were both higher in the upland provenance of *C. australe* compared to the lowland provenance. Leaves of the upland provenance had substantially shallower leaf angles than those from the lowland provenance. This likely resulted in an increased radiative load, resulting in warmer T_{leaf}, driving T_{crit} higher for the upland provenance. Leaf angle is often ignored in applications of leaf energy balance modelling, despite the strong effect it can have on modifying the net radiation term (Ponce De León & Bailey, 2024; Woods et al., 2018; Yang et al., 2023). This effect is partially reflected in the modelled leaf temperatures (T_{mod}); however, covariation of other thermal traits dampened the influence of leaf angle on T_{mod} resulting in no statistically significant differences in T_{mod} between provenances.

However, T_{crit} (measured on leaves sampled at the top of the canopy) still showed strong provenance differentiation, suggesting T_{leaf} at the top of the canopy in the upland provenance was indeed

warmer than for the lowland provenance. While this could indicate that leaf angles at the top of the canopy still differed sufficiently between provenances to impact leaf energy balance, another explanation is that the provenance-differentiation observed in T_{leaf} was also driven by systematic differences in microclimate due to plant height. The upland population, being smaller in stature compared to the lowland population, had a hotter thermal environment due to its proximity to the exposed ground with higher sensible heat/longwave radiation, as well as lower turbulence associated with wind speed. During the experiment, with the 3 × 3 m spacing between trees, the ground is exposed, and spot measurements revealed ground temperatures around 50 to 60 °C. In a provenance trial of sage-brush, Olsoy et al. (2023) also found that sub-species differences in T_{leaf} were associated with plant height, with shorter stature plants having higher T_{leaf}. With no compensatory changes in leaf traits with height within the canopy observed for *C. australe*, this could lead to higher T_{leaf} and T_{crit} in the smaller, upland provenance. This spatial pattern contrasts with what is observed in trees in a closed canopy where the lower canopy and ground are shaded and thus cooler than the upper canopy (Rey-Sanchez et al., 2017).

T. microcarpa:

In contrast, *T. microcarpa* had the opposite pattern to *C. australe*, with the lowland provenance having higher T_{mod}, T_{leaf} and T_{crit} than the upland provenance. This was likely driven by substantially lower g_s rates of the lowland provenance compared to the upland provenance.

Although an assumption of local adaptation of plant thermoregulation led to an expectation of higher g_s in lowland provenances, it is not surprising that *T. microcarpa* showed the reverse pattern. This is due to the likely trade-offs in gas exchange with temperature and vapour pressure deficit, which covary. The glasshouse experiment presented in Chapter 2 compared acclimation of gas exchange (including the stomatal function parameter g_1) under different temperature and VPD conditions, revealing tropical trees may decrease water use efficiency in response to increased air temperature but increase water use efficiency in response to increased VPD. Supporting this, a study assessing water use in a lowland and upland forest in this region showed the lowland forest with high VPD had lower canopy conductance and annual transpiration than the upland forest with low VPD (Binks et al., 2023). It is therefore possible the lower g_s of the lowland provenance in *T. microcarpa* is an adaptation to the higher evaporative demand of the seed source location, rather than temperature itself.

This pattern of provenance differences in T_{leaf} traits for *T. microcarpa* is particularly interesting considering, like *C. australe* and *H. novo-guineensis*, plants from the lowland provenance were taller than the upland provenance (Appendix B: Figure 3) and thus experience a cooler microclimate to the upland plants. The close relationship between T_{leaf} and T_{mod} suggests the measured variation in leaf thermal traits was adequate to explain these patterns, although it is also possible that the variation in thermal tolerance

and T_{leaf} was due to some unmeasured variable, as canopy architecture, including leaf clumping, can also play a large role in determining T_{leaf} (Gauthey et al., 2023; Leuzinger & Korner, 2007; Woods et al., 2018).

H. novo-guineensis:

Two species had no provenance-differentiation in T_{leaf} or T_{crit}, but for differing reasons. For *H. novo-guineensis*, strong provenance-differentiation was observed in leaf width, leaf inclination angle, and the thermal time constant, all of which were higher for the upland provenance than the lowland provenance. However, the net effect of variation in these traits - wider leaves would increase T_{leaf}, but steeper leaf angles would reduce T_{leaf} - led to a lack of provenance-differentiation in T_{mod} that was supported by measured T_{leaf}. This highlights the importance of considering the suite of leaf thermal traits in combination.

M. elleryana:

M. elleryana was the only species with no provenance effect in T_{leaf}, T_{can} or T_{crit}. Considering there was also no provenance-differentiation for any leaf thermal traits, nor in T_{mod}, it is highly likely that trait variation was not sufficient to cause a difference in T_{leaf} between provenances. In addition, this species had no provenance-level difference in plant height (Appendix B: Figure 3), so there were also no expected indirect differences due to microclimate.

4.4.3 Covariation between T_{leaf} and T_{crit} impacts thermal safety margin

Across all species T_{leaf} and T_{crit} were correlated, supporting other studies that suggest thermal tolerance (either T_{crit} or T_{50}) broadly acclimates to maximum T_{leaf} (Bison & Michaletz, 2024; Geange et al., 2021; Perez & Feeley, 2020; Tserej & Feeley, 2021). This represented a + 0.4 °C increase in T_{crit} per 1 °C increase in plant averaged T_{leaf} measured around midday, which is comparable to values reported with mean annual temperature in other studies (O'Sullivan et al., 2017; Slot et al., 2021; Zhu et al., 2018). I expected that this trend would also be evident within-species; however, no significant positive correlation was observed between T_{leaf} and T_{crit} for any of the measured species. This is similar to Kullberg & Feeley (2022) where only one of seven species had a significant correlation between T_{50} and max T_{air}, and none with T_{50} and modelled T_{leaf}. While this could reflect the importance of other variables besides T_{leaf} as drivers of variation in thermal tolerance (Lancaster & Humphreys, 2020), it could also be a result of a relatively low sample size compared to the variation of these traits and may require further study across an even larger gradient of T_{leaf}.

The strength of within species covariation between T_{leaf} and T_{crit} is important as it will determine patterns in the thermal safety margin, and thus how susceptible different provenances are to reaching critical leaf temperatures. While differences across provenances were observed in T_{leaf} and T_{crit}, no provenance-

differentiation was observed when considering these traits together through their thermal safety margins. This highlights that if attempting to consider vulnerability of provenances to heat stress for climate-matching of seed sources, an assessment based on either T_{leaf} or T_{crit} alone could misinform practitioners, resulting in a priority of one provenance over another. Although these findings suggest provenance-level variation in thermal safety margins may not be a high priority for climate matching of seed sources within species, a provenance effect was observed in other traits such as survival and growth rates (Appendix D). Climate-matching for provenance selection should therefore consider suites of leaf and whole plant traits and their potential trade-offs, rather than thermal safety margins alone.

4.4.4 Future recommendations

To achieve a comprehensive understanding of ecotypic variation, selected provenances should be representative of species-wide variation (Wadgymar et al., 2022). In this study I compared phenotypic variation between just two provenances, (i.e. upland and lowland) due to practical constraints when working in highly diverse tropical systems. Fruiting phenology varies widely across species distributions due to both climate and genetics (Abasolo et al., 2014; Stephens et al., 2022; Vogado et al., 2020) and gaining simultaneous access to a larger array of populations would require significant effort and/or the focusing on a smaller cadre of species. Nevertheless, the two provenances included (lowland sourced from the Daintree rainforest, and upland sourced from the Atherton Tablelands) represent the two primary regions of seed collection and rainforest restoration efforts in the Australian Wet Tropics. Accordingly, these results are well-aligned with current seed sourcing practices of regional restoration practitioners. Future efforts should include coordination among researchers, national parks management, and restoration and forestry practitioners to allow for comparison amongst different planting programs, and to include the collection of and incorporation of information on population genetics.

4.4.5 Conclusion

To avoid lethal leaf temperatures, plants may acclimate their thermal tolerance, or leaf thermal traits in such a way to enhance leaf cooling. While emerging evidence suggests plants in warmer environments have greater capacity to regulate their leaf temperatures (Blasini et al., 2022; Kitudom et al., 2022), I only found evidence of this intra-specific adaptation across provenances in one of the four species studied here. To understand whether tropical forests may be vulnerable to climate warming and determine appropriate seed sourcing strategies for tree-planting we urgently need more research assessing within-species variation in thermoregulation across a larger range of species, populations, and test sites. To achieve this, restoration and forestry practitioners and scientists should collaborate to establish a greater network of research trials in the tropics.

Chapter 5: Local adaptation to climate drives leaf thermoregulation in co-occurring tropical rainforest trees

5.1 Introduction

Global warming is rapidly increasing temperatures, raising concerns about the ability of species to adapt (IPCC, 2022). Tropical forest trees, vital for biodiversity, carbon sequestration and water cycling (Mitchard, 2018), may be particularly vulnerable due to their evolution in relatively stable thermal environments (Trew & Maclean, 2021). However, populations across different climates may respond differently to environmental change due to plasticity or local adaptation (Barton et al., 2020; Halbritter et al., 2018; Leites & Garzón, 2023; Matesanz & Ramirez-Valiente, 2019; Muehleisen et al., 2020). While local adaptation can enhance fitness in stable conditions, it may inhibit future persistence if climate change creates a mismatch between the historic conditions a population is adapted to and the new conditions (Jordan et al., 2024). Therefore, understanding how tropical trees have adapted to temperature is crucial for evaluating their resilience to global warming and informing effective management strategies.

Plants have evolved various mechanisms to cope with heat stress and maintain physiological function, such as altering biochemistry to increase their photosynthetic heat tolerance (Geange et al., 2021; Middleby et al., 2024). Such adjustments may help prevent leaf senescence and maintain carbon uptake during heatwaves (Drake et al., 2018) however recent studies indicate that this may be insufficient to preserve thermal safety margins in warmer environments (Kitudom et al., 2022; Kullberg et al., 2023; Perez & Feeley, 2020) or reveal tenuous links between heat tolerance metrics and visible leaf necrosis (Winter, et al. 2024). As such, species or populations near their thermal limits, such as those in lowland tropical forests, may be particularly vulnerable to even small temperature increases (Araujo et al., 2021; Doughty et al., 2023b; Pau et al., 2018).

Plants can also cope with thermal stress by avoiding high temperatures through morphological and physiological trait variations that influence leaf energy balance (Michaletz et al., 2015). Traits like leaf width, absorptance, leaf angle, and stomatal conductance interact with the canopy microclimate to influence the fluxes of sensible and latent heat and the interception of radiation (Campbell & Norman, 1998; Jones, 2013). This leads to significant differences between leaf and air temperatures ($\Delta T = T_{leaf} - T_{air}$), with variations ±20°C observed due to differences in water use strategies (Fauset et al., 2018), leaf size and shape (Leigh et al., 2017), and canopy architecture (Leuzinger & Korner, 2007; Woods et al., 2018). Given the importance of maintaining T_{leaf} within safe operating limits, it is hypothesised that traits influencing ΔT may undergo selection for enhanced leaf cooling in warmer environments (Mahan & Upchurch, 1988; Michaletz et al., 2015). While such thermoregulation has been noted across different ecosystems (Guo et

al., 2023; Kitudom et al., 2022), studies within species are limited (Kullberg et al., 2023; Kullberg & Feeley, 2022), and few have explored the roles of phenotypic plasticity and ecotypic variation.

Across species distributions, temperature often varies with other environmental factors such as precipitation, humidity, and soil nutrients, which can impact trait trade-offs and ΔT. For instance, in Chapter 4, a common garden trial comparing T_{leaf} in upland and lowland provenances of tropical rainforest species showed ecotypic differentiation, with varying provenance effects on T_{leaf}. This variation might result from competing pressures such as vapour pressure deficit (VPD) and temperature on stomatal conductance, observed in Chapters 2 and 3. While plant gas exchange must balance carbon uptake and water use, leaf cooling is also crucial (Blonder et al., 2023). If temperature strongly drives selection, traits that keep T_{leaf} within safe limits may be favoured in warmer regions.

Understanding local adaptation to temperature in tropical trees is essential for predicting their future vulnerability and guiding revegetation efforts to match provenance with future site conditions (Breed et al., 2013; Jordan et al., 2024). While common garden and reciprocal transplant experiments are ideal for studying local adaptation, they are resource-intensive (Sork et al., 2013), especially in remote areas. Population and ecological genomic methods, such as genotype-environment (GEA) and genotype-phenotype (GPA) associations, offer complementary insights into adaptative potential without extensive field trials (Arab et al., 2020; Breed et al., 2019; Shryock et al., 2021; Steane et al., 2014; Weigand & Leese, 2018) to support effective conservation (de Villemereuil et al., 2016; Faske et al., 2021).

This study investigates climate adaptation in tropical trees by examining intraspecific variation in leaf thermoregulation. I hypothesise that traits associated with leaf cooling are under selection. This hypothesis predicts that:

1) Within species, individuals exposed to warmer temperatures show coordination of leaf thermal traits that enhance leaf cooling.
2) Adaptive genetic variation associated with leaf thermal traits are positively correlated with mean annual temperature,
3) Patterns of leaf thermoregulation will be a result of both plasticity and ecotypic differentiation.

To test these predictions, I measured photosynthetic heat tolerance and leaf traits across a thermal gradient and predicted ΔT_{trait} with a leaf energy balance model. I defined leaf thermoregulation as intraspecific trait variation that leads to a change in ΔT (ΔT_{trait}) with an increase in mean annual temperature (MAT) or MAT of origin, with limited homeothermy present if the slope of ΔT_{trait} vs MAT is negative. I also produced genome-wide SNP genotype data and ran GEA and GPA analyses to explore genome-wide signals of selection and identify the environmental drivers of adaptive variation in thermoregulation using generalized dissimilarity modelling. Finally, I validated this approach using a climate-controlled genotype-environment trial in a common garden experiment.

5.2 Methods

5.2.1 Study system: Rainforest tree species in the Wet Tropics of Queensland, Australia

The Wet Tropics World Heritage Area (WTWHA) comprises 19,929 km^2 of mostly rainforest vegetation in northeastern Queensland, Australia. Its mountainous terrain creates geographic and spatial variation in climatic conditions across elevation within small distances that is ideal for exploring patterns of intraspecific trait variation and local adaptation. The WTWHA experiences warm temperatures year-round, with high but seasonal rainfall and periodic cyclone disturbance. I selected three tropical rainforest species - *Elaeocarpus grandis* F. Muell. (Elaeocarpaceae), *Cardwellia sublimis* F. Muell. (Proteaceae) and *Darlingia darlingiana (*F. Muell.) L.A.S. Johnson (Proteaceae) - that are relatively abundant, upper canopy species occurring across a wide elevational range (0-1300m) and commonly used in regional rainforest revegetation plantings (Engert et al., 2020). Both *C. sublimis* and *D. darlingiana* are endemic to the WTWHA, and have wind dispersed seeds, whereas *E. grandis* has a wider distribution extending into the Australian subtropics and has large fleshy fruits dispersed primarily by birds.

5.2.2 Field sampling

During October 2021 to May 2022, I sampled 3-10 individuals per population (median 6), spaced >100 m apart to avoid sampling closely related individuals (e.g. half- or full- siblings). I selected 16 sites in mature remnant forest, spanning an elevation range of 1299 m a.s.l (5 to 1304 m a.s.l), a mean annual temperature range of 7.1°C (18.6 to 25.8°C) and a mean annual precipitation range of 2940 mm (1355 to 4295 mm). I measured leaf traits on 105 *C. sublimis*, 96 *D. darlingiana,* and 104 *E. grandis* individuals, and generated genomic data for 98 *C. sublimis*, 96 *D. darlingiana* and 89 *E. grandis* individuals (Table 5. 1). Samples for genomic analysis were collected and dried on silica. Additionally, seeds were collected from 11 *E. grandis* individuals from six sites for the glasshouse experiment (Figure 5. 1, Table 5. 1).

5.2.3 Leaf traits

I measured leaf traits that impact leaf energy balance or are known to reflect trade-offs between resource acquisition and conservation (Wright et al., 2004). These included leaf mass per area (LMA, g m^{-2}), leaf dry matter content (LDMC, mg g^{-1}), leaf thickness (μm), leaf width (cm), leaf reflectance spectra including absorptance (Abs, %) and reflectance (Ref, %) to shortwave radiation, leaf carbon isotope composition ($\delta^{13}C$), leaf nitrogen (%), and the ratio of carbon to nitrogen. I also measured stomatal density (stomata mm^{-2}) and size (μm^2), to calculate theoretical maximum conductance (g_{max}, mol $m^{-2}s^{-1}$). Leaf traits were measured according to standard techniques on fully expanded sun-exposed leaves from each tree (Perez-Harguindeguy et al., 2013), with 10 leaf replicates per tree for leaf traits and 3 for absorptance and stomatal traits (for detailed measurement protocols, see Appendix C, Methods S1).

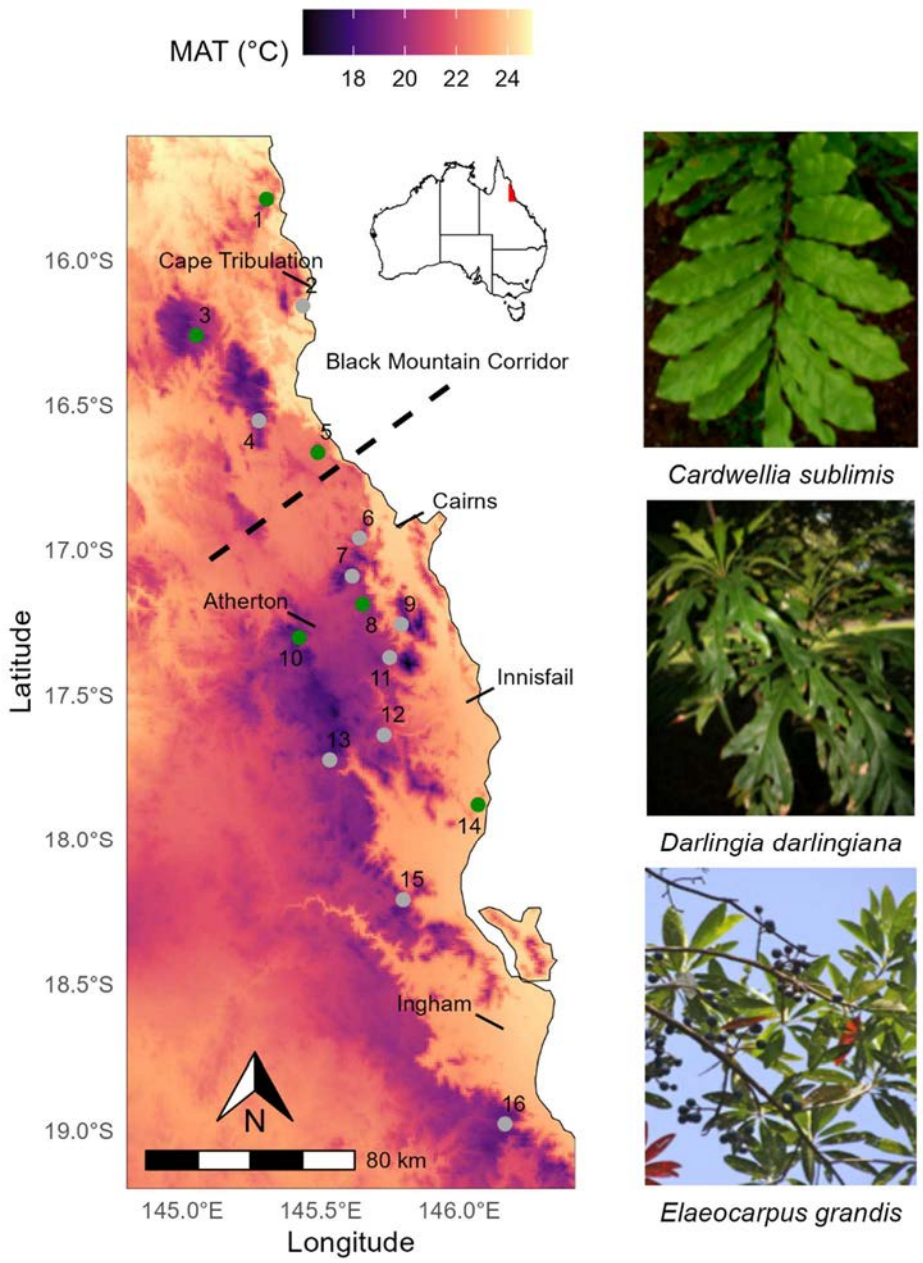

Figure 5. 1. Map of study region. Map colour shows Bio1, the mean annual temperature from 1981 to 2010 retrieved from CHELSA database at 1 km resolution. Solid black line indicates position of the Black Mountain corridor, a putative geographic barrier during glacial maxima. Grey points labelled with numbers indicate the populations where genetic and trait samples were collected for each of the three species shown to the right (see Table 5. 1 for further information on populations). Green points highlight populations where *E. grandis* seedlings were collected and used in the subsequent glasshouse experiment.

Table 5. 1. Site coordinates and means for environmental variables. Sites are ordered by decreasing latitude, and numbers correspond to those in Figure 5. 1. Sample size per population is given for trait measurements, and, where this differs, for the genetic dataset in brackets.

Population	Lat	Long	Elev (m)	MAT (°C)	MAP (mm)	Sample size per population		
						CS	DD	EG
1. Cedar Bay*	-15.79	145.3	172	23.8	2348	6	6	6
2. Daintree	-16.16	145.44	43	24.1	3296	6(5)	6	6(5)
3. Mt Windsor*	-16.26	145.05	1098	19.2	1651	6	6	6(5)
4. Mt Lewis	-16.55	145.28	1028	19.3	1790	9(8)	6	6
5. Kuranda*	-16.66	145.49	450	22.1	1957	6	6	6
6. Dinden	-16.96	145.64	493	21.7	1830	6	4	6
7. Mt Edith	-17.09	145.62	977	19.2	1907	6	6	3
8. Danbulla*	-17.19	145.65	770	20.0	2332	10(8)	9	10(6)
9. Goldsborough	-17.26	145.79	149	23.0	3072	0	6	6
10. Mt Baldy*	-17.3	145.42	1162	18.4	1555	7	6	5(4)
11. Topaz	-17.37	145.75	743	19.8	3680	6	0	6
12. South Johnstone	-17.64	145.73	540	20.6	3556	8(7)	8	8(6)
13. Tully Falls	-17.72	145.53	870	19.3	2123	6	6	6
14. Mission Beach*	-17.88	146.07	28	23.6	3545	10(7)	7	10(6)
15. Kirrama	-18.21	145.8	677	20.1	2548	6	6	6
16. Paluma Range	-18.98	146.17	832	19.2	1839	8	8	8(6)

Note: Lat = latitude, Long = longitude, Elev = Elevation (m a.s.l), MAT = mean annual temperature (Bio1, °C), MAP = mean annual precipitation (Bio12, mm). CS = *Cardwellia sublimis*, DD = *Darlingia darlingiana*, and EG = *Elaeocarpus grandis*. Sites with an * had *E. grandis* seedings included in the glasshouse trial.

5.2.4 Leaf temperature (T_{leaf}) modelling

I tested how covariation of leaf traits affects predicted leaf-to-air temperature differences (ΔT) across a thermal gradient and whether this helps maintain T_{leaf} within safe margins. T_{leaf} was predicted using a steady-state leaf energy balance model based on the Penman-Monteith equation (Jones, 2013; Monteith & Unsworth, 2013), requiring plant trait-based inputs (leaf width, absorptance to shortwave radiation, stomatal ratio, and conductance), and microclimate inputs (air temperature, vapour pressure deficit, radiation, and wind speed).

Microclimate inputs were paramaterised using the micro_global function in 'NicheMapr' v.3.2.0 (Kearney & Porter, 2020). Hourly estimates of each variable were obtained for the 15th of each month, using tree coordinates and elevation, with solar radiation adjusted for terrain (Maclean et al., 2019). This approach provided paired estimates of T_{air} and VPD. Note that canopy shading was set to 0 to simulate the sun-exposed outer canopy leaves we sampled. From this, tree-level means for daytime (09:00 to 15:00) T_{air}, VPD, and solar radiation (converted to photosynthetic photon flux density, PPFD) were calculated, as well as an overall species mean.

To separate changes in ΔT due to microclimate from those due to leaf trait covariation, I used two microclimate parameterizations. For ΔT based solely on leaf traits (hereafter ΔT_{trait}), microclimate inputs were set to overall means described above, with T_{air} = 24.8°C, VPD = 1.4 kPa, PPFD = 1403 μmol m^2 s^{-1}, and assuming calm conditions with wind speed of 0.5 m s^{-1}. For ΔT based on both traits and climate (ΔT_{clim}), I used observed tree-level microclimate means.

I implemented the leaf energy balance model using the PhotosynEB function in 'plantecophys' v.1.4-6 (Duursma, 2015), which couples an energy balance model to the Farquhar, von Caemmerer and Berry photosynthesis model (Farquhar et al., 1980) and the optimality-based unified g_s (USO) model (Medlyn et al., 2011), with T_{leaf} solved iteratively. For details on how parameters were obtained for stomatal conductance model see Appendix C, Methods S1.

To convert estimated T_{leaf} to ΔT, I used the same T_{air} values used as inputs for each respective model (i.e. a common T_{air} = 24.8°C for ΔT_{trait} and a varying T_{air} for ΔT_{clim}). For comparison with other studies, 'anatomical' ΔT_{trait} was also calculated using stomatal anatomy to derive g_s (Appendix C: Method S1). However, in downstream genetic analyses, I used ΔT_{trait} calculated using the PhotosynEB function, with other parameterisations presented purely for context or comparison.

5.2.5 Photosynthetic heat tolerance

Photosynthetic heat tolerance was assessed by examining the decline in maximum photosynthetic efficiency of photosystem II with increasing temperature. To do so, the ratio of variable fluorescence (F_v) to maximum fluorescence (F_m) was measured following an established protocol (Leon-Garcia & Lasso,

2019) modified from Krause et al. (2013). For each tree, 15-20 leaves were sampled, and six 9 mm leaf discs per leaf were pooled and randomly assigned to heat treatments. Discs were incubated for 30 minutes in water baths at 36, 40, 42, 44, 46, 48, 50, 52, 54, and 58°C, with an untreated control at ~24°C. After a 24-hour dark incubation, chlorophyll fluorescence was measured using a PAM-2000 chlorophyll fluorometer (PAM-2000, Heinz Walz GmbH, Effeltrich, Germany). Five sites (six for *E. grandis*) at varying elevations were measured during October-November 2021. Individuals showing photoinhibition (control Fv/Fm < 0.6) were excluded from analysis. A 4-parameter log-logistic curve was fitted using 'drc' v.3.0-1 (Ritz et al., 2015), with the lower asymptote set to 0. Thermal tolerance metrics including T_{crit} (T_{leaf} at 5% decline in F_v/F_m) and T_{50} (T_{leaf} at 50% decline in F_v/F_m), were obtained from the curves.

5.2.6 Quantification of thermal safety margins

To determine how intraspecific trait variation influences thermal safety margins (TSM) across species distributions, TSMs were calculated by subtracting modelled T_{leaf} (=$\Delta T + T_{air}$) from the thermal tolerance metric T_{50}. I calculated TSMs using both ΔT_{trait} and ΔT_{clim}, where ΔT_{trait} assesses the contribution of trait variation to TSMs, and ΔT_{clim} evaluates if this variation counteracts environmental changes. These TSM values overestimate those from direct T_{leaf} measurements, partly due to using T_{50} as the upper threshold instead of T_{crit}. Canopy leaves of tropical forests already surpass T_{crit} (Doughty et al., 2023b), and while some photosynthetic function can recover after a single T_{crit} exposure, recovery is less likely after T_{50} exposure (Cook et al., 2024; Tarvainen et al., 2022). Additionally, microclimate inputs (e.g. T_{air}) used for modelling T_{leaf} are seasonal and daytime averages (09:00 to 15:00). Although selection is driven by climate extremes rather than means (Zimmermann et al., 2009), this conservative approach is suitable for modelling relative ΔT_{trait} across a species distribution. To compare with other studies, TSMs were also calculated using 'anatomical' ΔT_{trait} and ΔT_{clim} using stomatal traits to derive g_s (Appendix C: Method S1).

5.2.7 Climate and Environmental Variables

To explore environmental drivers of trait and genomic variation, I retrieved gridded maps of bioclimatic variables, as well as wind speed and relative humidity for the Wet Tropics from the CHELSA database at 1km resolution, averaged for 1981-2010 (Brun et al., 2022; Karger et al., 2017). Gridded soil data products at 5–15 cm depth, 30m resolution, for the period 1950–2013 were obtained from the Soil and Landscape Grid of Australia and resampled to 1 km resolution using 'raster' v.3.6-11 (R. Hijmans, 2022) to match the bioclimatic data. To avoid multicollinearity and ensure interpretability, I selected uncorrelated variables ($r < 0.7$, calculated using values for the sampled sites) relevant to tropical tree functioning: mean annual temperature (Bio1,°C), precipitation of the driest month (Bio14, mm), minimum relative humidity (RH_{min}, %), mean wind speed ($Wind_{mean}$, m s^{-1}), soil pH (pH), and total soil phosphorus (P).

5.2.8 Genotyping

Dried leaf tissue samples were genotyped using DArTseq (Diversity Arrays Technology Australia Pty Ltd, Canberra, Australia), a reduced representation sequencing method (Sansaloni et al., 2010). Data quality and SNP filtering were formed using 'RRtools' v.0.1 (Bragg et al., 2020; Rossetto et al., 2019). SNPs with a reproducibility score below 0.96, over 20% missing data, or redundant loci were excluded. Individuals with 80% missing loci were also removed. A minor allele frequency threshold of 0.05 was applied, and loci with no population data were excluded. The cleaned dataset comprised 98 individuals and 8884 SNPs for *C. sublimis* (6.48 % missing data), 96 individuals and 8009 SNPs for *D. darlingiana* (8.15 % missing data), and 89 individuals and 4935 SNPs for *E. grandis* (6.65 % missing data).

5.2.9 Population genetic diversity and structure

I assessed population genetic diversity by estimating allelic richness, expected heterozygosity (H_e), observed heterozygosity (H_o) and the inbreeding coefficient (F_{IS}) using 'diveRsity' v1.9.90 (Keenan et al., 2013), with 1000 bootstrap replicates for confidence intervals. Genetic similarity was evaluated through Principal Component Analysis (PCA) using 'adegenet' v2.1.8 (Jombart, 2008). Ancestry coefficients were estimated via discriminant analysis of principal components (DAPC) and sparse non-negative matrix factorization (sNMF). For both methods, I tested genetic clusters (K) ranging from 1 to 16. DAPC was performed with K-means clustering on PCA-transformed genotypes, selecting the optimal K via the Bayesian information criterion and retaining 10 principal component axes using cross-validation. For sNMF, 'LEA' v.3.8.0 (Frichot & François, 2015) was used, selecting the optimal K based on the stabilization of cross-entropy values and choosing the best replicate with the lowest cross-entropy.

5.2.10 Signals of selection

To detect potentially adaptive loci, I used F_{ST} outlier analysis, genotype-environment association (GEA), and genotype-phenotype association (GPA). Association analyses were performed using latent factor mixed modelling (LFMM) and partial redundancy analysis (pRDA), combining univariate and multivariate methods to detect both single-locus and multi-locus signatures of selection with high power and low false-positive rates (Forester et al., 2018). For GPA, I tested two trait sets: 1) ΔT_{trait} as an integrative trait, and 2) a suite of leaf traits influencing leaf temperature.

To ensure complete SNP datasets, missing values were imputed with the most common SNP across individuals. Given the multiple potential values of K identified in prior population structure analyses, I conducted analyses for K = 1, 2, and 3, treating all significant SNPs as putatively adaptive. F_{ST} outlier analysis was done using 'pcadapt' v.4.3.3 (Luu et al., 2017) using default parameters, with SNPs considered putatively adaptive if the qvalue was < 0.05. LFMM was run with a lasso penalty using 'lfmm' v.1.1 (Caye

et al., 2019) testing multiple latent factors. Z scores were calibrated for genomic inflation before being converted into p-values. Candidate SNPs were identified using a false discovery threshold of $q < 0.1$. The pRDA analyses in both GPA and GEA were conducted using 'vegan' v.2.6-4 (Oksanen et al., 2022), with two principal components for genetic structure (see previous section) as conditional variables. For GPA, elevation was also included as a conditional variable to account for non-genetic variation in leaf traits. SNPs associated with phenotypes (GPA), or environments (GEA) were identified by extreme loadings, defined as 3 standard deviations along pRDA axes.

5.2.11 Generalised dissimilarity modelling

I employed generalised dissimilarity modelling (GDM) to investigate genotype-environment and phenotype-environment associations and identify potential environmental drivers of variation. This approach assesses multivariate, nonlinear patterns of genomic or trait turnover along environmental gradients, accounting for isolation by distance (Ferrier et al., 2007; Mokany et al., 2022). GDM is useful for evaluating the relative importance of environmental predictors (via the sum of I-spline coefficients) and for identifying where steepest gradients of change occur (by observing the change in slope).

For the genomic data, I ran GDMs on three SNP datasets. First, I used the putatively adaptive SNPs identified by GPA analysis, including all those identified by LFMM and pRDA with leaf traits or estimated ΔT_{trait}. The second dataset included SNPs identified by FST outlier and GEA analysis. I used both GEA and GPA because GPA was not measured in a common garden; thus, GEA helps determine if the environmental variables linked to trait variation also drive adaptive variation. While the environmental drivers of genomic variation are already inherently assessed within the LFMM and pRDA analyses in GEA, I performed GDM on this SNP set to allow direct comparison of driver relative importance across the different genomic GDMs. The third dataset combined adaptive and neutral SNPs by including the original cleaned SNP set. For these analyses, I used a population-level pairwise FST distance matrix generated with 'SNPRelate' v.1.30.1 (Zheng et al., 2012) using the relative beta estimator in Weir & Hill (2002).

Additionally, I conducted two trait GDMs to assess environmental drivers of ΔT_{trait} and leaf trait variation. I calculated population-level means for ΔT_{trait} and other leaf traits. For the leaf trait GDM, I reduced variables to two principal component axes. Euclidean distance matrices were computed for each dataset using the 'dist' function.

All five GDMs were fit using 'gdm' v.1.5.9-9.1 (Ferrier et al., 2007; Mokany et al., 2022). Predictor significance was tested with matrix permutation (n = 50 permutations) using the 'gdm.varImp' function, with predictor significance defined by increases in explained deviance. Variables with the highest sum of I-Spline Coefficients were considered most important. I estimated model sensitivity with bootstrapping (n = 1,000 iterations), retaining 90% of populations (Shryock et al., 2015).

5.2.12 Glasshouse experiment

I collected 59 naturally germinated *E. grandis* seedlings from the base of 11 likely mother trees across six sites and grew these in pots at James Cook University's Environmental Research Complex in Cairns (Figure 5. 1). The number of mother trees per site ranged from one to three, and seedlings per mother tree ranged from one to two. Seedlings originated from sites with mean annual temperatures between 18.8°C and 24.9°C.

To assess genotype × environment effects on leaf thermal traits while controlling for temperature and vapor pressure deficit (VPD) variations, I conducted a glasshouse experiment with three treatments: a low T_{air} low VPD_{air} chamber (26°C, 1 kPa VPD), a high T_{air} low VPD_{air} chamber (32°C, 1 kPa VPD), and a high T_{air} high VPD_{air} chamber (32°C, 2 kPa VPD). These treatments simulated typical upland summer conditions (low T_{air} low VPD_{air}) and lowland conditions (high T_{air} high VPD_{air}), with the high T_{air} low VPD_{air} chamber used to isolate VPD effects from temperature effects (Appendix C: Table 1).

In August 2022, seedlings were allocated to their respective chambers, with at least one seedling from each mother tree in each chamber. After two months, leaf-level gas exchange and functional traits were measured on new, fully expanded sun leaves. Two seedlings in the low T_{air} low VPD_{air} treatment died, leaving 57 seedlings but maintaining the total number of mother trees in that treatment. Detailed measurement protocols are described in Appendix C: Methods S2.

5.2.13 Data analysis

Our goal was to assess how genotype and environment contribute to intraspecific variation in leaf thermoregulation and to determine if plants acclimated or adapted to warmer conditions have lower predicted ΔT_{trait} compared to those acclimated or adapted to cooler conditions.

I first quantified intraspecific variation, population differentiation, and the association of trait variation with thermal gradients. This involved using the quartile coefficient of variation to account for issues with standard CV (Botta-Dukát, 2023). Linear regressions assessed the relationship between leaf functional traits (e.g., LMA, LDMC, leaf thickness, $\delta^{13}C$) and thermal parameters (e.g., T_{crit}, T_{50}, ΔT_{trait}, TSM) with population identity or mean annual temperature (MAT) as dependent variables. Population differentiation was measured using R^2, which is analogous to P_{ST} but does not assume trait heritability. A negative slope in ΔT_{trait} with increasing MAT was interpreted as evidence of limited homeothermy.

To examine if trait variation was an adaptation to temperature across species distributions, signals of selection were identified using association analysis and the relative importance of environmental predictors were compared in genomic vs trait generalized dissimilarity modelling. To complement association analyses and explicitly test the contribution of genotype and environment to intraspecific variation in leaf traits and ΔT_{trait} for *E. grandis* saplings grown in a glasshouse, I used mixed effects models

to test the influence of MAT of origin (continuous) and treatment (categorical, 3 levels) on leaf traits and ΔT_{trait}. 'Mother tree' was included as a random effect nested within 'site'. I then removed non-significant variables and presented estimated marginal means for the final models.

5.3 Results

5.3.1 Extent of intraspecific leaf trait variation in natural populations

In most cases, the extent of intraspecific trait variation (defined as the quartile coefficient of variation, CV) for each trait was similar across the three species (Figure 5. 2). Traits with the lowest quartile CV (< 0.05) included LDMC, Abs, Ref, $\delta^{13}C$, T_{crit}, and T_{50}. The trait g_1, which is calculated from $\delta^{13}C$ (but accounts for some influence of the environment) had the highest levels of variation and showed the greatest differences in CV across species, with CV = 0.14, 0.28, and 0.21 in *C. sublimis*, *D. darlingiana*, and *E. grandis* respectively. For most traits, population effects on trait variation were significant ($P < 0.05$), except for leaf C/N ratio, $\delta^{13}C$, g_1, and T_{50} in *C. sublimis*; stomatal density, T_{crit} and T_{50} in *D. darlingiana*; and stomatal density, theoretical g_{max}, and T_{crit} in *E. grandis* (Figure 5. 2, Appendix C: Table 2). Where significant effects of population on trait variation were observed, the proportion of trait variation explained by population ranged from R^2 = 23% to 85% across all species and traits, with the strongest effects observed for leaf thickness (Figure 5. 2, Appendix C: Table 2).

5.3.2 Patterns of leaf trait variation with mean annual temperature

I observed differences in the relationship between traits and mean annual temperature (MAT) across the three target species (Figure 5. 2, Appendix C: Table 3 & Figure 1). In *C. sublimis*, g_1 was the only trait associated with MAT despite other traits having levels of CV similar to the other species and significant population effects on trait variation (Figure 5. 2, Appendix C: Table 3 & Figure 1). For *D. darlingiana*, as MAT increased, LMA, leaf thickness, Absorptance, and $\delta^{13}C$ all decreased, whereas leaf width and g_1 increased (Figure 5. 2, Appendix C: Table 3 & Figure 1). For *E. grandis*, as MAT increased, LMA, leaf width, $\delta^{13}C$, and stomatal size decreased, whereas LDMC, g_1 and stomatal density increased (Figure 5. 2, Appendix C: Table 3 & Figure 1). For *D. darlingiana* and *E. grandis*, the covariation between stomatal density and size resulted in no change in theoretical g_{max} with MAT (Figure 5. 2, Appendix C: Table 3 & Figure 1).

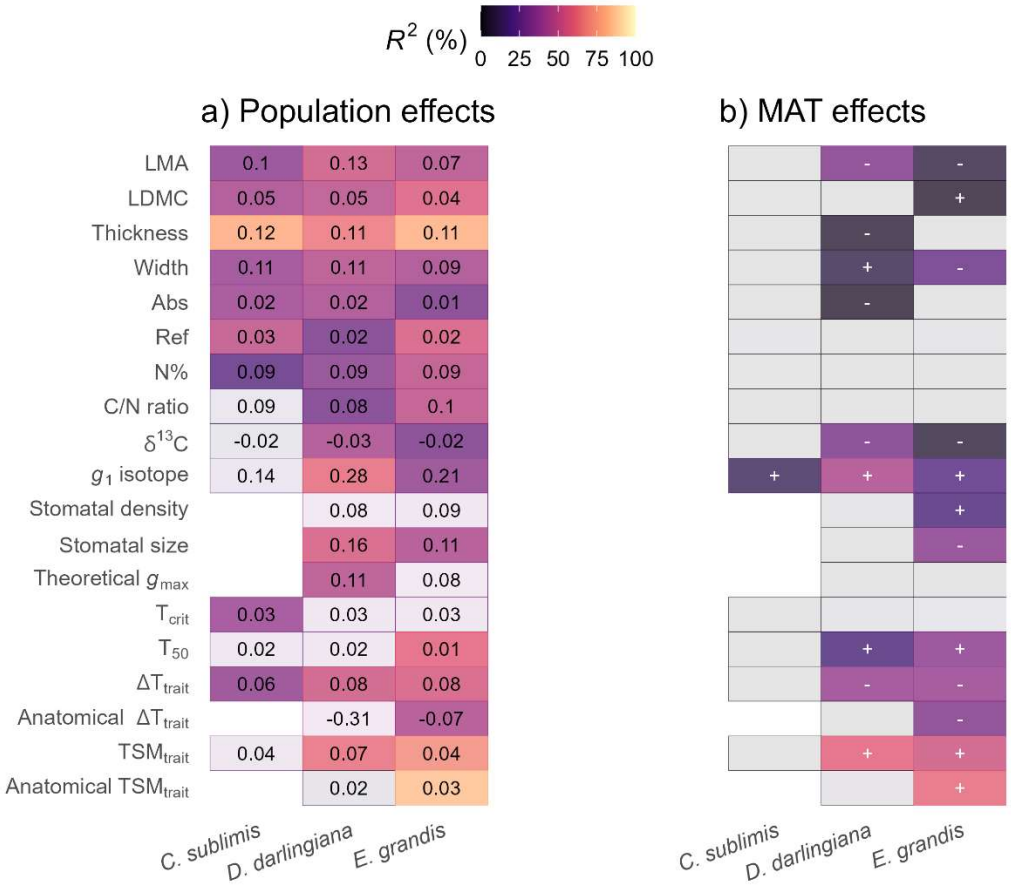

Figure 5. 2. Comparison of regression results for the effect of population or mean annual temperature on trait variation for each species. Tiles are coloured by R^2, with transparent tiles indicating non-significant ($P > 0.05$) results. Values within tiles for panel a) show the quartile coefficient of variation, and symbols in panel b) show the sign of the slope estimate for the linear regression. For more information on model results see Appendix C: Table 2 & 3.

5.3.3 Implications of intraspecific trait variation on leaf thermoregulation and thermal safety margins

The consequences of intraspecific trait trade-offs for leaf thermoregulation were investigated through the prediction of trait-based leaf-to-air temperature differences (ΔT_{trait}) and how this varies with MAT. Note that ΔT_{trait} is calculated using a single set of microclimate parameters and thus represents the influence of traits only. Mean ΔT_{trait} was 6.0, 5.1, and 4.2°C in *C. sublimis*, *D. darlingiana*, and *E. grandis* respectively (Appendix C: Table 2). Levels of intraspecific variation in ΔT_{trait} were similar across the three species, with quartile CV = 0.06 to 0.08 (Figure 5. 2). Population was a significant predictor of ΔT_{trait} for all species, although the proportion explained was slightly higher for *D. darlingiana* and *E. grandis* than *C. sublimis* (Figure 5. 2, Appendix C: Table 2). I found evidence of leaf thermoregulation for two of the three species, with ΔT_{trait} decreasing with increasing MAT for *D. darlingiana* ($R^2 = 0.39$, $P < 0.001$) and *E.*

grandis (R^2 = 0.39, P < 0.001) but not *C. sublimis* (Figure 5. 2, Figure 5. 3, Appendix C: Table 3). This represented a 0.21°C (95th C.I. 0.15, 0.26) and a 0.16°C (95th C.I. 0.12, 0.20) decrease in ΔT_{trait} per 1°C increase in MAT for *D. darlingiana* and *E. grandis* respectively (Appendix C: Table 3).

Unsurprisingly, using theoretical g_{max} from stomatal anatomy to calculate trait-based leaf-to-air temperature differences (anatomical ΔT_{trait}) led to substantially lower values of ΔT_{trait} (Appendix C: Figure 2). Mean anatomical ΔT_{trait} was equal to −0.6°C for *D. darlingiana* and −1.8°C for *E. grandis* (with negative values indicating T_{leaf} cooler than T_{air}). Levels of intraspecific variation for anatomical ΔT_{trait} in *D. darlingiana* and *E. grandis* were different, with a quartile CV = −0.31 for *D. darlingiana* and −0.07 for *E. grandis* (Figure 5. 2). Population was only a significant predictor of anatomical ΔT_{trait} for *E. grandis*, with R^2 = 0.45, P = 0.0139 (Figure 5. 2, Appendix C: Table 2). This time I found evidence of thermoregulation only for *E. grandis* (R^2 = 0.33, P < 0.001) where anatomical ΔT_{trait} decreased 0.06°C (95th C.I. 0.03, 0.09) per 1°C increase in MAT (Figure 5. 2, Appendix C: Table 3 & Figure 2).

Thermal tolerance metrics were similar for all three species, with species-mean T_{crit} ranging from 44.3 to 45.1°C and species-mean T_{50} ranging from 49.5, to 49.8°C (Appendix C: Table 2). Levels of intraspecific variation were low relative to other traits, and population differences were only significant in *C. sublimis* for T_{crit} and *E. grandis* for T_{50} (Figure 5. 2, Appendix C: Table 2). I observed significant positive relationships between T_{50} and MAT for both *D. darlingiana* and *E. grandis*, but not *C. sublimis*, and no relationship between MAT and T_{crit} for any species (Figure 5. 2, Figure 5. 3, Appendix C: Table 3). T_{50} increased by 0.22°C per 1°C rise in MAT for *D. darlingiana* (R^2 = 0.19, P = 0.044), and 0.28 °C per 1°C rise in MAT for *E. grandis* (R^2 = 0.28, P < 0.001, Figure 5. 3).

The combined variation in T_{50} and ΔT_{trait} were assessed through calculation of trait-based thermal safety margins ($TSM_{trait} = T_{50} - T_{leaf}$ °C). I observed a significant increase in TSM_{trait} with MAT for *D. darlingiana* and *E. grandis*, but not *C. sublimis*, representing an increase in TSM_{trait} of 0.52°C (95th C.I. 0.32, 0.72) and 0.42°C (95th C.I. 0.26, 0.58) per 1°C increase in MAT for *D. darlingiana* and *E. grandis* respectively (Figure 5. 2, Figure 5. 3, Appendix C: Table 3). In contrast, when calculating trait-based thermal safety margins using stomatal anatomical traits (anatomical TSM_{trait}), I only observed a relationship with MAT in *E. grandis* (R^2 = 0.62, P < 0.0001), representing an increase in TSM_{trait} of 0.4°C (95th C.I. 0.22, 0.58 per 1°C increase in MAT (Figure 5. 2, Appendix C: Table 3 & Figure 2).

To evaluate how effective intraspecific trait variation was at avoiding heat stress in-situ, I compare the above results with ΔT (and TSMs) calculated using tree-level variation in both traits and microclimate (ΔT_{clim} and TSM_{clim}) (Figure 5. 3). A comparison of slope estimates for the linear regression of ΔT_{trait} and ΔT_{clim} with MAT indicated that the approach of excluding the passive effects of site microclimate in ΔT_{trait} leads to a 0.08 and 0.09°C shallower decrease in ΔT_{trait} with MAT compared to ΔT_{clim} for *D. darlingiana* and *E. grandis* respectively, and no change for *C. sublimis* (Figure 5. 3, Appendix C: Table 3). Comparing

slopes for the linear regression of TSM_{clim} with MAT across species that exhibited ΔT_{trait} variation consistent with limited homeothermy (*D. darlingiana* and *E. grandis*), with that which did not (*C. sublimis*) highlights how effective thermoregulation could be at offsetting increasing air temperatures in TSM_{clim}. I found that the TSM_{clim} decline with MAT was significantly shallower for *D. darlingiana* (Slope = −0.55, R^2 = 0.59, P < 0.001) and *E. grandis* (Slope = −0.63, R^2 = 0.66, P < 0.001) compared to *C. sublimis* (Slope = −1.11, R^2 = 0.85, P < 0.001) (Figure 5. 3, Appendix C: Table 3).

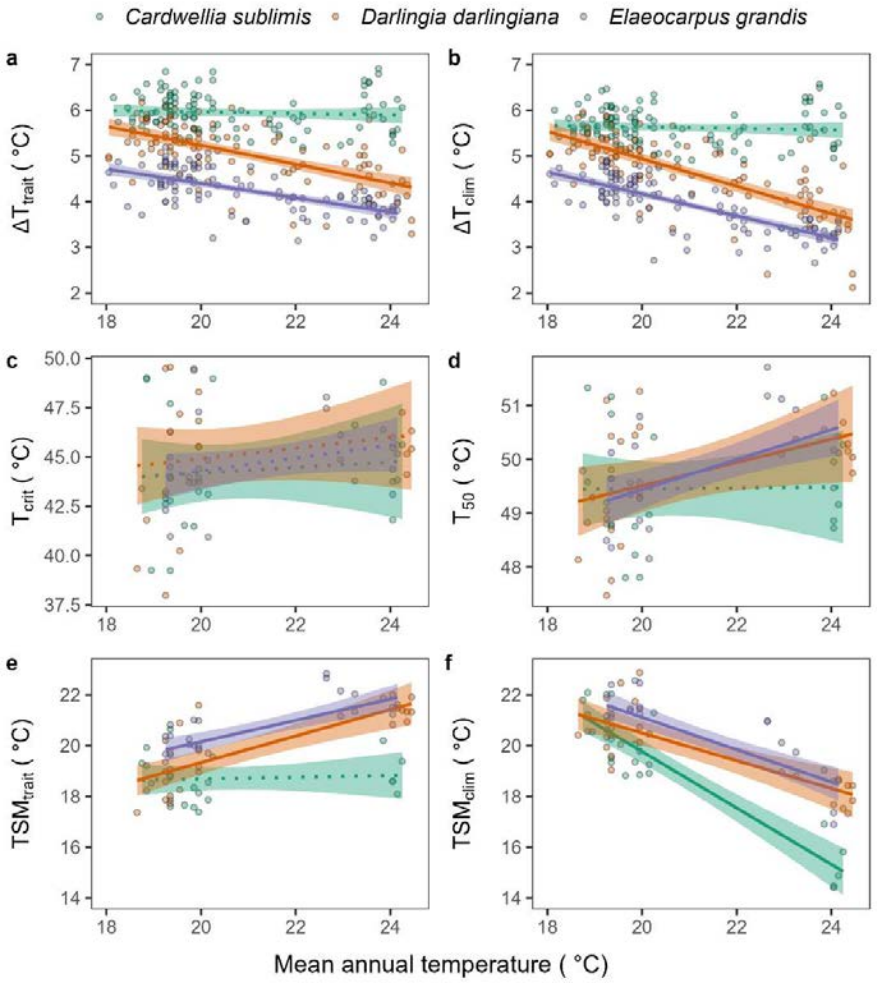

Figure 5. 3. Variation in leaf-to-air temperature differences (ΔT; a-b), thermal tolerance metrics (T_{crit} & T_{50}; c, d) and thermal safety margins (TSM; e, f) with mean annual temperature across the distribution of three tropical tree species. Note in a, b, and e ΔT is based on leaf trait variation with the same microclimate inputs for all trees (ΔT_{trait}), whereas in f, microclimate inputs also vary with each individual tree (ΔT_{clim}). Each point represents an individual-tree level average. Significant correlations with mean annual temperature are denoted by solid regression lines whereas non-significant correlations are dotted. Shaded region represents standard errors.

5.3.4 Genetic diversity and population structure

Genetic diversity was relatively low in these study species. Expected heterozygosity across all populations was 0.19 (±0.012 SD) in *C. sublimis*, 0.19 (±0.011 SD) in *D. darlingiana*, and 0.23 (±0.013 SD) in *E. grandis* (Appendix C: Table 4). Observed heterozygosity was less than expected heterozygosity for all populations of all species and was 0.15 (±0.014 SD) in *C. sublimis*, 0.12 (±0.010 SD) in *D. darlingiana*, and 0.18 (±0.016 SD) in *E. grandis* (Appendix C: Table 4). All three species showed strong isolation by distance, with Mantel tests showing R^2 of 0.86 ($P = 0.001$) in *C. sublimis* (Appendix C: Figure 3), R^2 of 0.77 ($P = 0.001$) in *D. darlingiana* (Appendix C: Figure 4), and R^2 of 0.51 ($P = 0.011$) in *E. grandis* (Appendix C: Figure 5). Ancestry analysis indicated the presence of 1, 2, or 3 genetic clusters across the sampled range, with the main break for all species corresponding to the Black Mountain Corridor, a biogeographic barrier for multiple taxa coinciding with a break in the Great Dividing Range (Schneider et al., 1998).

5.3.5 Signals of Selection

Signals of selection were identified in all three species through the detection of candidate SNPs that were associated with either environmental (GEA) or phenotypic (GPA) variables or were identified F_{ST} outliers. For *C. sublimis*, the genotype-phenotype association (GPA) analyses identified 118 candidate SNPs associated with ΔT_{trait} or leaf traits themselves (Figure 5. 4, Appendix C: Table 5). LFMM identified 1 SNP associated with leaf thickness and no SNPS associated with predicted ΔT_{trait}. The leaf trait pRDA had an $adjR^2 = 0.0031$ and identified 66 SNPs with the highest contributing variables including leaf thickness, LMA, Absorptance, and V_{cmax25} (Appendix C: Figure 6). The ΔT_{trait} pRDA had an $adjR^2$ of 0.0006 and identified 63 candidate SNPs. The combined F_{ST} outlier and GEA analyses identified 321 unique candidate SNPs, including 243 SNPs identified by F_{ST} outlier analysis and 85 SNPs identified by GEA (Figure 5. 4, Appendix C: Table 5). For the GEA SNPs, LFMM identified 13 SNPs including 1 associated with Bio1, 4 with RH_{min}, 3 with $Wind_{mean}$, 1 with Bio14, 2 with Soil P and 2 with Soil pH. The environment pRDA had an $adjR^2 = 0.0173$ and identified 72 candidate SNPs, with highest contributing variables including Bio1, Bio14, RH_{min} and $Wind_{mean}$ (Appendix C: Figure 6). In *C. sublimis*, 1 candidate SNP was identified by GPA, GEA, and outlier analyses, 4 candidate SNPs were identified both by GPA and GEA analyses, and 4 SNPs were identified by both GPA and outlier analyses (Figure 5. 4).

For *D. darlingiana*, the GPA analyses identified 151 candidate SNPs associated with ΔT_{trait} or leaf traits themselves (Figure 5. 4, Appendix C: Table 5). LFMM identified 43 SNPs associated with one or more leaf traits including 2 SNPs associated with leaf width, 11 with g_1, 25 with V_{cmax25}, 2 with LMA and 3 with modelled ΔT_{trait}. The trait pRDA had an $adjR^2 = 0.0022$ and identified 63 SNPs with the highest

contributing variable being Absorptance, g_1, and LMA (Appendix C: Figure 6). The ΔT_{trait} pRDA had an adjR^2 of 0.0006 and identified 69 candidate SNPs. The combined F_{ST} outlier and GEA analyses identified a total of 140 unique candidate SNPs, including 60 SNPs identified by F_{ST} outlier analysis and 87 SNPs identified by GEA (Figure 5. 4, Appendix C: Table 5). For the GEA SNPs, LFMM identified 24 SNPs, including 3 SNPs associated with Bio1, 3 with RH_{min}, 1 with $Wind_{mean}$, 3 with Bio14, 13 with Soil P, and 2 with Soil pH. The environment pRDA had an adjR^2 = 0.0083 and identified 63 candidate SNPs, with highest contributing variables including Bio1 and soil pH, followed by Bio14, RH_{min}, and $Wind_{mean}$ (Appendix C: Figure 6). In *D. darlingiana*, 2 candidate SNPs were identified both by GPA and GEA analyses, and 1 SNP was identified by both GPA and outlier analyses (Figure 5. 4).

For *E. grandis*, the GPA analyses identified 73 candidate SNPs associated with ΔT_{trait} or leaf traits themselves (Figure 5. 4, Appendix C: Table 5). LFMM identified 4 SNPs including 1 SNP associated with leaf width, 2 with LMA, and 1 with ΔT_{trait}. The trait pRDA had an adjR^2 = 0.0019 and identified 28 candidate SNPs, with the highest contributing variables including V_{cmax25}, leaf thickness, and LMA, followed by Absorptance and leaf width (Appendix C: Figure 6). The ΔT_{trait} pRDA had an adjR^2 of 0.0006 and identified 45 candidate SNPs. The combined F_{ST} outlier and GEA analyses identified 156 unique candidate SNPs, including 126 SNPs identified by F_{ST} outlier analysis and 30 SNPs identified by GEA (Figure 5. 4, Appendix C: Table 5). For the GEA SNPs, LFMM identified 1 SNP associated with Bio1. The environment pRDA had an adjR^2 of 0.0064 and identified 29 SNPs, with the highest contributing environmental variables including Bio14, RH_{min}, soil P, and Bio1 (Appendix C: Figure 6). In *E. grandis*, no candidate SNPs were identified both by GPA and GEA analyses, however 1 SNP was identified by both GPA and outlier analyses (Figure 5. 4, Appendix C: Table 5).

5.3.6 Generalised dissimilarity modelling

I used generalized dissimilarity modelling to investigate the relative importance of environmental predictors in explaining deviance in the genotypic turnover based on GPA SNPs, GEA & Outlier SNPs, and all SNPs, as well as trait turnover in ΔT_{trait}, and in the principal components of leaf functional traits as the response matrices. Across all three species, the GDMs based on SNP datasets had generally high explained deviance (27.47–76.89%) and low intercepts (0–0.07), indicating the included predictors had good explanatory power, whereas the GDMs based on ΔT_{trait} or the leaf trait PCA values had a higher level of unexplained variance in the response variables (explained deviance 20.93–44.07%, intercepts 0.07–0.44) (Appendix C: Table 6).

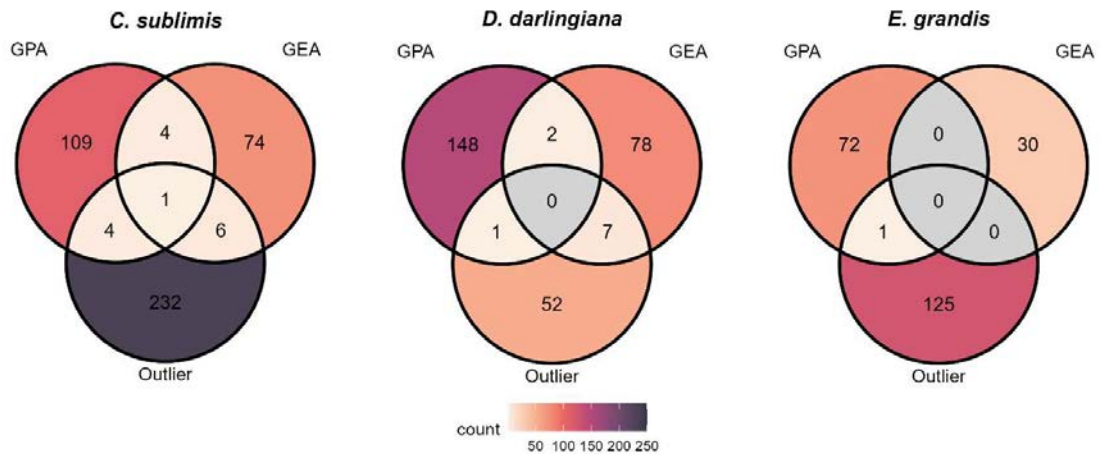

Figure 5. 4. Overlap of candidate SNPs identified using F_{ST} outlier analysis, and genotype phenotype (GPA) and genotype environment (GEA) association analyses for three tropical tree species. Numbers indicate the total number of overlapping SNPs with each analysis. Candidate SNPs identified using GPA or GEA association analyses include all identified by either latent factor mixed modelling (LFMM) or partial redundancy analysis (pRDA). For GPA analyses, candidate SNPs include those identified from two sets of response variables; 'ΔT_{trait}', based on modelled leaf-to-air temperature differences with individual tree level traits and common microclimate inputs, and 'Trait PCA', based on the principal component axes of a suite of leaf traits. Intersections are coloured by total number of SNPs and with grey panels = no SNPs detected.

In *C. sublimis*, geographic distance was the top predictor of allele frequency turnover for all three SNP-based GDMs, followed by soil pH and Bio14 for the GPA-SNPs, Bio14 and RH_{min} for the GEA & Outlier SNPs, and Bio14 and $Wind_{mean}$ for the All SNPs GDMs (Figure 5. 5, Appendix C: Table 6). For the trait GDMs, Soil pH was the most important predictor of ΔT_{trait} variation, whereas Bio14, followed by soil P were the most important predictors of variation in the Trait PCA (Figure 5. 5, Appendix C: Table 6).
For *D. darlingiana*, Geographic distance, followed by Bio1 and Bio14 were the top environmental predictors for all three SNP-based GDMs (Figure 5. 5, Appendix C: Table 6). For the trait GDMs, variation in ΔT_{trait} was best explained by Bio1, whereas both Bio1 and Bio14 were importance predictors in the Trait PCA GDM (Figure 5. 5, Appendix C: Table 6).

In *E. grandis*, geographic distance and Bio14 were the top two predictors for all SNP-based GDMs, with the third most explanatory variable switching between Bio1 and RH_{min} (Figure 5. 5). In the trait GDMs, mean annual temperature (Bio1) was the single most important predictor for variation in both ΔT_{trait} and the trait PCA (Figure 5. 5, Appendix C: Table 6).

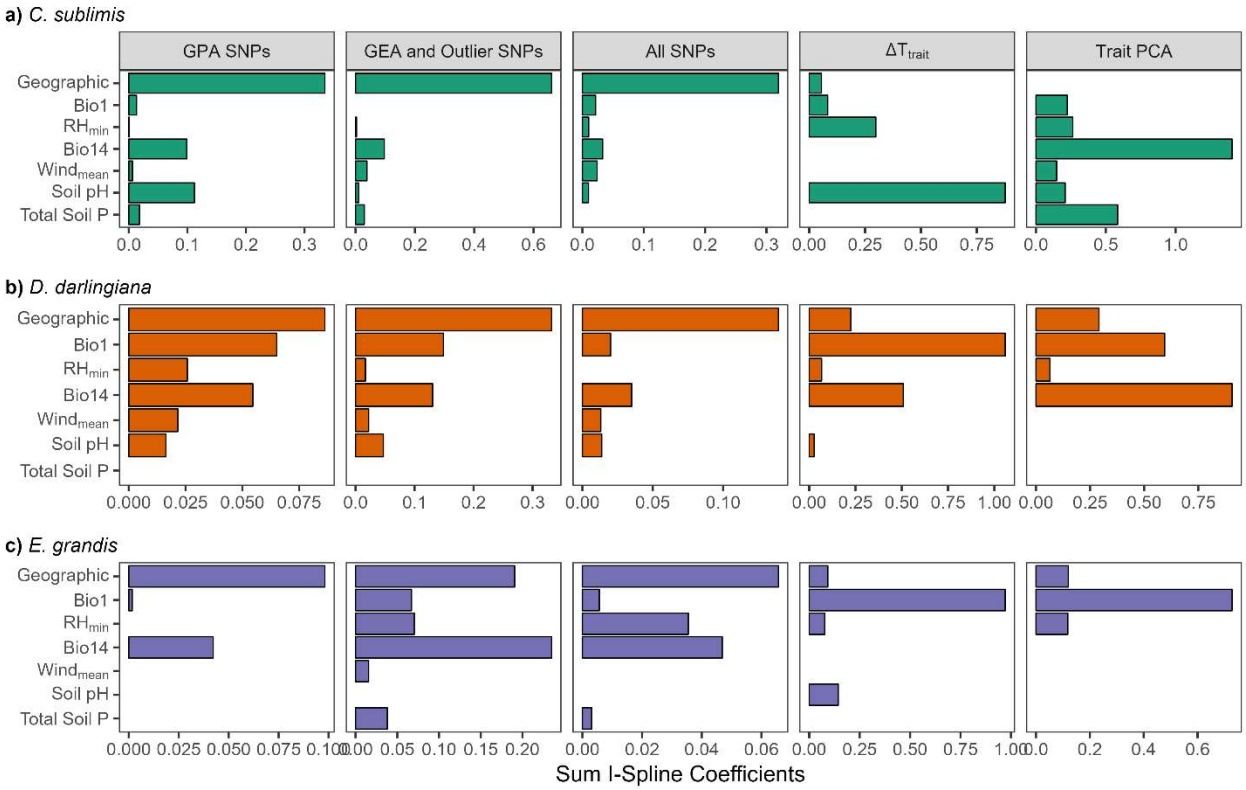

Figure 5. 5. Relative importance of predictors in generalised dissimilarity models (GDM) for three tropical tree species. Relative importance is calculated as the sum of I-Spline coefficients for that predictor in the model. For each species there are five separate analyses presented, with the response variable a population-level pairwise F_{ST} matrix on SNPs identified by GPA analyses (GPA SNPs), the SNPs identified from GEA or F_{ST} outlier analyses (GEA and Outlier SNPs), or the entire suite of neutral and non-neutral SNPs (All SNPs). For the last two columns, the response variable was a Euclidean distance matrix based on either population-mean ΔT_{trait} or principal component axes on a suite of leaf traits (Trait PCA). Model performance metrics can be found in Appendix C: Table 6. For the predictor variables, Geographic = geographic distance, Bio1 = mean annual temperature, RH_{min} = minimum relative humidity, Bio14 = precipitation of the driest month, $Wind_{mean}$ = mean wind speed.

5.3.7 Genotype × Environment glasshouse trial

In the climate-controlled glasshouse experiment, *E. grandis* showed trait variation resulting from both plastic responses to treatment conditions, and adaptation to mean annual temperature of origin, but not their interaction (Figure 5. 6, Table 5. 2). Leaf width had a negative correlation with MAT of origin and had significant effects of treatment, exhibiting narrower leaves when grown under warmer conditions. I observed a significant positive correlation between g_1 and MAT of origin, but no effect of treatment. When excluding seedlings from the highest MAT site (Cedar Bay), this relationship was no longer significant,

suggesting the association between g_1 and MAT of origin was primarily driven by the population at the hottest part of its distribution. Variation in V_{cmax25} was not associated with MAT of origin, but was influenced by treatment, with plants grown under low T_{air} low VPD_{air} conditions having a higher V_{cmax25} than plants grown under both high T_{air} low VPD_{air} and high T_{air} high VPD_{air} conditions (Figure 5. 6, Table 5. 2).

When these traits were input into a leaf energy balance model paramaterised with standard microclimate to determine ΔT_{trait} I found evidence for adaptation to MAT of origin but no effect of treatment (Figure 5. 6, Table 5. 2). Seedlings from warm-origin provenance had lower ΔT_{trait} than seedlings from cool-origin provenance (Figure 5. 6, Table 5. 2). These patterns were driven by intraspecific variation in both leaf width and g_1. The decline in ΔT_{trait} with an increase in MAT of origin is likely due to the combined effects of narrower leaves, and a higher g_1 (so lower water use efficiency), which both result in cooler T_{leaf} under common conditions and thus a decrease ΔT_{trait}. The lack of a treatment effect on ΔT_{trait} is likely due to the treatment effects on V_{cmax25} and leaf width cancelling each other out. i.e. for leaves with common g_1, a higher V_{cmax25} will result in a higher modelled conductance which will cool leaves.

Table 5. 2. ANOVA results from *E. grandis* glasshouse trial

Trait	Variable	Chisq	Df	*P* value	Sig
	MAT	11.26	1	0.0008	***
ΔT_{trait}	Treatment	1.94	2	0.3793	ns
	MAT × Treatment	1.66	2	0.4362	ns
	MAT	6.78	1	0.0092	**
Leaf width	Treatment	13.55	2	0.0011	**
	MAT × Treatment	1.33	2	0.5155	ns
	MAT	5.82	1	0.0158	*
Log10(g_1)	Treatment	4.01	2	0.1347	ns
	MAT × Treatment	2.13	2	0.3451	ns
	MAT	0.09	1	0.7617	ns
$V_{cmax.leafN}$	Treatment	8.12	2	0.0173	*
	MAT × Treatment	0.77	2	0.6799	ns

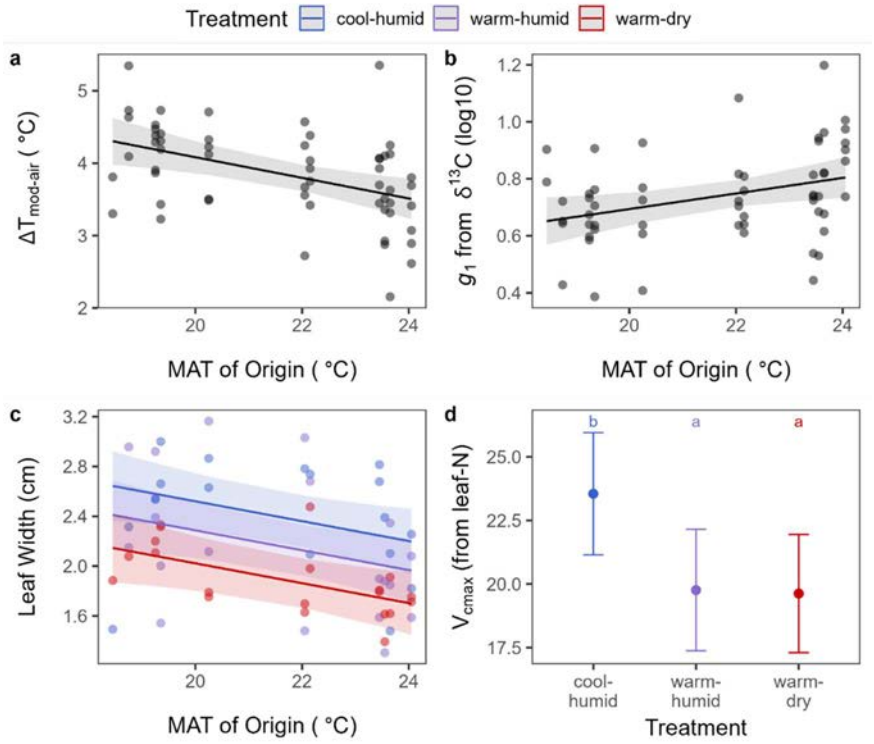

Figure 5. 6. Results from the glasshouse experiment showing significant effects of both treatment conditions and mean annual temperature of origin in *E. grandis*. Panels show a) response of predicted leaf-to-air temperature differences based on leaf traits (ΔT_{trait}), b) g_1 calculated from leaf $\delta^{13}C$ plotted as log transformed values, c) leaf width, and d) V_{cmax25} estimated from leaf N_{mass}. Points represent observed plant level averages, and lines and shaded regions show the estimated margin means and 95% confidence intervals. Letters in panel d) show significant differences.

5.4 Discussion

Globally increasing temperatures threaten to push tropical rainforest plants beyond their physiological limits. However, populations adapted to contrasting climates may exhibit phenotypic divergence due to local adaptation that affects their capacity to cope with warming. Intraspecific variation of leaf traits across species distributions can enhance leaf cooling, thereby avoiding lethal temperatures in warmer regions. Yet, evidence of this thermoregulatory ability and the roles of acclimation or adaptation remain limited despite it being key information to assess population resilience to global warming impacts. In this study, I show how leaf energy balance modelling combined with population/ecological genomics can be used to assess the patterns and drivers of local adaptation of thermoregulatory traits in mature tropical rainforest trees. I found intraspecific variation of field-measured leaf traits was associated with enhanced leaf cooling and partial maintenance of modelled thermal safety margins in warmer sites for two of the

three species, providing partial support for my first hypothesis. Despite relatively low sample size for genomic analysis, signals of selection were detected in all species, however contrary to my second hypothesis, adaptive genomic variation associated with predicted ΔT_{trait} was best explained by geographic distance and precipitation of the driest month rather than temperature. Finally, the genotype × environment trial of *E. grandis* seedlings supported my third hypothesis: clines in ΔT_{trait} with MAT of origin were a result of both phenotypic plasticity and adaptation.

5.4.1 Intraspecific trait variation leads to enhanced leaf cooling in warmer climates.

Our expectation that leaf trait variation would enhance leaf cooling in plants from warmer sites was observed in two of the three species, consistent with the limited homeothermy hypothesis (Gates et al., 1964; Mahan & Upchurch, 1988; Michaletz et al., 2015) which suggests that trait-based regulation of leaf temperatures may help maintain carbon uptake in suboptimal environments. Although evidence for this phenomenon varies across biomes and species (Blonder et al., 2020; Drake et al., 2020; Fauset et al., 2018; Guo et al., 2023; Guo et al., 2022; Helliker & Richter, 2008; Helliker et al., 2018; Liancourt et al., 2020; Song et al., 2011; Still et al., 2022; Zhou et al., 2023), the theory is debated due to inconsistencies in its definition and testing (Still et al., 2023). By using a leaf energy balance model paramaterised with observed leaf trait variations and common microclimate inputs, I isolate ΔT variations resulting from leaf trait covariation, excluding passive changes due to radiation, humidity, wind speed, and air temperature.

I found that traits varied significantly with MAT in *E. grandis* and *D. darlingiana,* but their responses differed: leaf width increased with MAT for *D. darlingiana* and decreased for *E. grandis*. Wider leaves have lower boundary layer conductance leading to higher leaf temperatures (Leigh et al., 2017; Wright et al., 2017). Despite this, both species showed similar declines in ΔT_{trait} with increasing MAT. This suggests that variables associated with stomatal conductance (g_s) played crucial roles in offsetting the heating effect of wider leaves in *D. darlingiana*. When comparing predicted ΔT_{trait} using the coupled photosynthesis-stomatal conductance model with predictions based on theoretical maximum conductance (which itself did not change with MAT), the ΔT_{trait} trends aligned for *E. grandis* but not for *D. darlingiana*. Differences between the methods may partly explain the lack of thermoregulation observed by Kullberg et al. (2023) who used stomatal anatomical traits to calculate g_s. The primary model I used assumes g_s is coupled with photosynthesis (Medlyn et al., 2011), but this may not be true under high temperatures (De Kauwe et al., 2019; Diao et al., 2024b; Drake et al., 2018; Marchin et al., 2023; Urban et al., 2017a), particularly in high humidity conditions typical of tropical rainforests. Given the impact of g_s modelling on these results, it is crucial to develop approaches that accurately account for how g_s varies with temperature.

I examined whether variation in leaf traits and thermal tolerance help maintain thermal safety margins across a wide thermal gradient. Thermal tolerance increased with MAT while predicted ΔT_{trait}

decreased for two of the three species. These adjustments worked together to increase both heat tolerance and avoidance in mature trees at warmer sites. This supports other studies that show how trait variation (both intra- and inter- specific) increases thermal safety margins in plants grown under warm environments compared to cooler environments (Kitudom et al., 2022; Kullberg et al., 2023; Perez & Feeley, 2020). When accounting for observed microclimate, this trait variation was not sufficient to perfectly maintain thermal safety margins but did lead to a shallower decrease in thermal safety margin with MAT than for *C. sublimis* which showed no variation in either ΔT_{trait} or thermal tolerance. Failure to consider intraspecific trait variation in trait-based thermal safety margins may bias assessment of species vulnerability to heat stress.

5.4.2 Genome-wide signals of selection

I hypothesised that intraspecific variation in ΔT_{trait} could be explained by selection across thermal gradients. Genomic analysis revealed putative signals of selection in all species, linked to either climatic or edaphic factors. Precipitation of the driest month (Bio14) was a strong predictor of both adaptive and neutral variation across all species, particularly *D. darlingiana* and *E. grandis*. For these species, mean annual temperature (Bio1) was another key explanatory variable in the SNP-based GDMs, while soil pH was significant for *C. sublimis*. These species-specific differences in environmental drivers of adaptive genomic variation were also reflected in GDMs assessing population mean leaf trait values. Climate, particularly Bio1, was most influential for *D. darlingiana* and *E. grandis,* while both edaphic factors (soil pH and Phosphorus) and climate were important for *C. sublimis*. Moisture availability and temperature are well-established drivers of mortality (Aleixo et al., 2019; Bauman et al., 2022b), growth (Bauman et al., 2022a), regeneration (Comita & Engelbrecht, 2017) and thereby species distributions (Gaviria et al., 2017) in tropical trees. The importance of edaphic variables for *C. sublimis* may be related to its proteoid roots (Cheesman et al., 2018), an adaptation of Proteaceae species that enhances phosphorus availability in nutrient-poor soils (Lamont, 2003). Interestingly, similar edaphic factors were not significant for *D. darlingiana*, suggesting species-specific responses to soil conditions despite common adaptations.

Geographic distance emerged as a stronger driver of SNP variation than any single environmental variable across all species. The consistent emergence of the same environmental predictors for both adaptive and neutral variation suggests that the distribution patterns of adaptive loci may align with those of neutral loci. This correlation highlights the need for caution in interpreting these results, as much of the adaptive signal may be embedded within neutral variation. This aligns with evidence that functional genetic variation might be influenced by neutral processes rather than selection alone (Kardos et al., 2021; Mathur et al., 2023). Alternatively, it could indicate that loci under selection, which contribute to trait clines, may not form monotonic allele frequency clines in response to environmental gradients (Lotterhos, 2023). This does not negate the presence of adaptive signals but highlights the complexity of adaptation, driven by

intricate genetic systems. The polygenic nature of plant traits is well established, and many complex traits are influenced by numerous loci with small effects. To account for this, I combined both univariate (LFMM) and multivariate (pRDA) approaches to identify SNPs associated with environmental variables. While the sample size in this study was relatively small compared to many genome-wide association studies, the power of these approaches are also affected by the species population structure and sampling design. All three species exhibited strong isolation by distance, rather than complex population structure, which can help improve the power and reduce the likelihood of false positives in analyses like redundancy analysis (Forester et al., 2018). Additionally, the sampling design was carefully structured to enhance the ability to detect signals of selection. By sampling both lowland and upland populations across the full latitudinal range, the study maximized differences in adaptive environments while minimizing confounding effects of neutral genetic structure, substantially increasing the power to detect weak signals of selection. Despite the limitations of reduced-representation sequencing, which inherently excludes parts of the genome and structural variants, and the challenges posed by small sample sizes, this study still identified clear evidence of selection. While the number of overlapping SNPs across methods was low, the total putatively adaptive SNPs identified using LFMM and pRDA was compelling. Additionally, the R^2 values from the multivariate pRDA analyses, while low, are consistent with expectations given that most SNPs in the genome are neutral. Notably, the R^2 values for GEA analyses were higher than those for GPA analyses, reflecting the strength of the signals associated with environmental variables. However, it is possible that other traits not measured in this study also contribute to local adaptation and remain undetected.

5.4.3 Local adaptation drives leaf thermoregulation in E. grandis

The climate-controlled experiment with *E. grandis* seedlings revealed clinal variation in ΔT_{trait} that suggests divergent selection along a gradient of MAT of origin. The observed negative correlation between ΔT_{trait} and MAT of origin aligns with traits that would enhance leaf cooling in hotter environments, supporting the idea that ecotypic variation reflects adaptation to the local climate. This was further evidenced by genomic signals of selection associated with climatic variables, suggesting that local adaptation contributes to patterns of ΔT_{trait}. However, it is important to clarify that the glasshouse study does not directly demonstrate local adaptation, as it lacks explicit measures of fitness (i.e. lifetime growth or reproductive success) necessary to establish a home environment advantage. Instead, ΔT_{trait} was used as a proxy for thermoregulatory performance, which may contribute to fitness under specific environmental conditions. While this approach highlights meaningful variation, future studies will need to explore the relationship between ΔT_{trait} and fitness outcomes, particularly in reciprocal transplant experiments or natural settings, to fully validate these findings. Plasticity also played a role in shaping trait responses, as evidenced by acclimation of traits like V_{cmax25} (predicted from leaf N_{mass}) and leaf width to growth conditions. Yet, the

net effect of this plasticity on ΔT_{trait} appeared neutral, with ecotypic variation in leaf width and water use efficiency driving much of the observed variation in ΔT_{trait} with MAT. This suggests that both plastic and adaptive responses interact to shape thermoregulation, but their relative contributions may vary across species and environments (Chapters 2, 3, and 4). Across the Wet Tropics of Australia, warmer areas are usually wetter due to the lowlands being located along the coast and the tablelands being in a rain shadow. Trees in warm-moist sites may benefit from less conservative water use strategies that enhance carbon uptake and cooling compared to those in warm-dry sites that prioritise hydraulic safety. While the seedling provenance collection for the glasshouse experiment was guided by contrasting MAT of origin, I tested how genotype × environment effects to different growth temperature were impacted by vapour pressure deficit. Moreover, the generalized dissimilarity modelling on outlier SNPs identified using GPA indicated that precipitation of the driest month was a more important explanatory variable than the mean annual temperature. It is possible then that ecotypic variation observed in the glasshouse was driven by changes in precipitation rather than temperature, however the included provenances did not cover as even a distribution of precipitation of origin as they did for MAT of origin.

5.4.4 Conclusions and recommendations for future research

This study supports growing evidence that while some tropical tree species exhibit acclimation and/or adaptation in leaf thermal traits, patterns of intraspecific variation differ across species (Blonder et al., 2020; Kullberg & Feeley, 2022; Middleby et al., 2024; Tarvainen et al., 2022). These findings indicate that limited homeothermy is present in some, but not all, tropical tree species, and that divergent selection to climate influences variation in leaf thermoregulatory traits for certain species. This underscores the importance of considering intraspecific variation in leaf thermal traits when evaluating plant responses to climate change, as it may affect the adaptive capacity and resilience of tropical rainforest trees. However, it remains unclear whether observed ecotypic variation is a response to thermal or moisture gradients, and whether leaf thermoregulation itself is under selection or if this is just a byproduct of adaptive variation to maintain carbon uptake or avoid water stress. Additionally, a central challenge in advancing our understanding of leaf thermal ecology is the inability to accurately model or measure the distribution of leaf temperatures within canopies. Current models provide only coarse approximations, and measurements are typically confined to a small number of leaves, which may not adequately represent the majority of leaf area within a canopy. Until we develop improved methods for modelling and measuring canopy-wide leaf temperature distributions, drawing definitive conclusions about the role of leaf thermoregulation in tropical tree resilience will remain difficult. Future research should address these gaps by expanding studies of plant thermoregulation, leveraging existing trait- and genetic datasets, and refining approaches to better understand the vulnerability and resilience of tropical rainforest trees in the face of climate change.

Chapter 6: General discussion

Leaf temperature is a key determinant of leaf function, influencing processes such as photosynthesis, respiration, and transpiration, which in turn affect the overall productivity and survival of tropical forests. These forests, vital for their biodiversity and role in global carbon cycling (Mitchard, 2018), face increasing threats from rising global temperatures (IPCC, 2022). Prolonged increases in leaf and whole canopy temperatures can push trees beyond their physiological limits, leading to reduced net primary productivity and, in extreme cases, widespread mortality (Bauman et al., 2022b; Doughty et al., 2023b; Hammond et al., 2022). This jeopardizes not only ecosystem services but also undermines forest restoration efforts (Jordan et al., 2024). Understanding the mechanisms by which tropical trees tolerate or avoid extremes in leaf temperature is therefore essential for predicting their resilience to climate change and ensuring the persistence of these ecosystems in a warming world.

Leaf temperature is influenced by a combination of external climatic factors – such as air temperature, vapour pressure deficit, and solar radiation – and intrinsic leaf functional traits. These leaf thermal traits, including stomatal conductance, absorptance to radiation, and leaf size, can vary substantially within canopies and across individuals, leading to differences in the offset between leaf and air temperature ($\Delta T_{leaf\text{-}air}$) across species or environmental gradients. How this offset shifts across thermal gradients may affect a tree's capacity to maintain optimal leaf temperatures for photosynthesis and growth (Gates et al. 1964; Mahan & Upchurch, 1988; Michaletz et al., 2015), potentially influencing species distributions and evolutionary trajectories (Lynch et al., 2014; Zimmermann et al., 2009). However, the complexity of factors driving leaf energy balance makes it challenging to disentangle temperature variation resulting from intrinsic trait differences versus external environmental influences. Leaf energy balance modelling serves as a valuable tool in this regard, allowing for the passive effects of microclimate to be accounted for using a standard set of microclimatic inputs alongside observed variation in leaf traits.

While most research to date has focused on interspecific patterns in leaf thermoregulation, relatively little attention has been given to intraspecific variation. I combined extensive field measurements across the species home range, with genomic analyses, provenance trials, and detailed climate-controlled experiments to address this knowledge gap, specifically:

1. ***To identify patterns of leaf thermoregulation:*** Determine how leaf thermal traits vary within species across different temperature environments and assess whether this variation enhances cooling in warmer conditions.
2. ***To explore the roles of acclimation and genetic adaptation:*** Assess the relative contributions of short-term physiological acclimation and longer-term genetic adaptation to leaf thermoregulation.

3. ***To disentangle thermal trait variation that is due to temperature:*** Investigate how vapor pressure deficit and other environmental factors interact with temperature to affect leaf thermoregulation.

6.1 Impact of coordinated thermal trait variation on leaf thermoregulation and thermal safety margins

When assessing plant vulnerability to heat stress, it is important to consider changes in both physiological limits (i.e. heat tolerance) and the operating temperature of leaves, as both aspects are important in evaluating thermal safety margins and the impact of climate warming. Throughout this thesis, I examined both photosynthetic heat tolerance (i.e. T_{crit}, T_{50}) and leaf thermal trait variation to evaluate their combined impact on thermal safety margins in tropical trees (Chater 4 & 5). While increased thermal tolerance can prevent damage to leaves during heat stress, this adjustment is often attributed to either acclimation or adaptation to higher leaf temperatures (Bison & Michaletz, 2024; Perez & Feeley, 2020). Indeed, in two of the three species studied in Chapter 5, thermal tolerance increased with mean annual temperature (MAT), and therefore absolute leaf temperatures. Furthermore, covariation in leaf thermal traits led to enhanced leaf cooling under warmer temperatures at the same time that there was an increase in thermal tolerance. As a result, both factors contributed equally to the increase in thermal safety margins in warmer climates, with plants from the warmest sites exhibiting ~3°C higher thermal safety margins than those from the coolest sites (~6°C difference in MAT). Conversely, two populations from contrasting climates may exhibit no differences in vulnerability to heat stress when grown under common conditions, despite showing phenotypic divergence in leaf thermoregulation and/or heat tolerance if they cancel each other out. Indeed, this was observed in Chapter 4, where, despite substantial differences in leaf thermal traits and heat tolerance between upland and lowland provenances of two species, there were no significant differences in thermal safety margins when grown under common garden conditions.

6.2 Site acclimation or genetic adaptation

It is important to consider whether intraspecific variation observed in leaf thermal traits across the distribution of tropical trees is due to phenotypic plasticity (i.e. site acclimation), or genetic adaptation as this will determine plant responses to climate change. Acclimation allows for reversible adjustments in leaf traits and enables trees to respond to short-term environmental changes. This can be particularly important in allowing a species to persist when climate change outpaces adaptation in long-lived organisms such as trees. Adaptation, on the other hand, involves genetic changes over multiple generations, enabling populations to evolve traits that can be better suited to the new environmental conditions. Across this work I observed acclimation of leaf thermal traits and heat tolerance in Chapters 2, 3 and 5, and adaptation or genetic variation in Chapters 4 and 5, however patterns differed greatly across species.

In Chapter 2, plants grown under elevated temperature and VPD showed some common responses, with thermal tolerance showing a degree of acclimation for all species examined (+0.31°C per 1°C increase in air temperature). However, observed changes in leaf morphology and leaf-level gas exchange were much more species-specific. Evaluating the impact of this trait acclimation through leaf energy balance modelling in Chapter 3 revealed that trait coordination in response to different environmental conditions led to acclimation of the $\Delta T_{leaf\text{-}air}$ and/or the thermal time constant in only 2 of the 6 species. Similarly, in Chapter 5, the glasshouse experiment of *E. grandis* seedlings showed that despite acclimation of individual traits to contrasting growth climates, their combined effect on leaf energy balance cancelled out, leaving variation in leaf thermoregulation apparently reflecting local adaptation.

Genomic analysis in Chapter 5 supported the role of genetic variation and local adaptation in thermoregulation, showing climate-driven selection on putative adaptive loci related to leaf thermal traits. However, adaptive variation does not always enhance leaf cooling, as seen in *C. sublimis*. The species-specific patterns of adaptive variation were also apparent in Chapter 4 where I explored ecotypic variation in thermal tolerance and leaf temperatures in tropical trees by measuring leaf and canopy temperatures, thermal tolerance, and leaf thermal traits in lowland and upland provenances of four species in a common garden experiment. In that chapter, only one species exhibited the expected enhanced leaf cooling capacity in warm-adapted plants, despite most of the species showing ecotypic variation in at least one thermal trait. Notably, despite ecotypic variation in leaf temperatures and thermal tolerance, there were no significant provenance differences in thermal safety margins among the species. These results indicate that if aiming to select 'future-adapted' provenances for rainforest restoration, it is essential to consider variation in both leaf temperature and thermal tolerance together, as warm-adapted provenances may not necessarily be more resilient to warming. Together, these findings show evidence that the diverse patterns of leaf thermoregulation in tropical trees are a result of species differences in their capacity to acclimate (Chapters 2, 3 and 5) and adapt (Chapters 4 and 5) to warmer climates.

6.3 Environmental drivers of thermoregulation

Predicting how thermal safety margins, and thereby risk of canopy decline, will change in a warmer climate is complicated by changes in other environmental factors that correlate with air temperature such as precipitation, nutrient availability and VPD. While air temperature and precipitation are often inversely correlated across elevation gradients, the sites sampled in the Australian Wet Tropics presented the opposite pattern: cooler areas in the tablelands generally receive less annual precipitation compared to the warmer lowland areas along the coast. Across this thesis, I was interested in how temperature affects thermal trait variation and addressed confounding factors through either climate-controlled glasshouse experiments (Chapters 2, 3 and 5) or generalised dissimilarity modelling across species distributions (Chapter 5). In

Chapter 5, I found that phenotypic variation in modelled leaf-air temperature offsets was overwhelmingly driven by temperature in two species that exhibited limited homeothermy, whereas edaphic factors explained leaf thermal trait variation in a species that did not. Further analysis of genetic data provided evidence that adaptive genetic variation in leaf thermal traits across species' geographic ranges was influenced not only by temperature but also by precipitation. This may explain the lower intrinsic water use efficiency (as estimated by the g_1 parameter) observed in lowland populations in Chapter 5, where plants are presumably less constrained by soil water availability.

Many studies have examined tropical tree gas exchange (i.e. photosynthetic biochemistry, stomatal conductance, water use efficiency) in response to altered temperatures and soil drought, but Chapter 2 disentangles the effect of atmospheric dryness (elevated VPD) from elevated air temperature. This provides new insights into the mechanisms by which plants respond to warming. Chapter 2 revealed that many species reduced stomatal conductance when grown under drier atmospheric conditions, rather than warmer temperatures. Although the magnitude of this response varied across species, it suggests that water conservation is prioritized over thermoregulation, a strategy which may leave tropical trees more vulnerable to heat than drought stress as climate warming continues. However, the effects of elevated VPD on thermal safety margins and evapotranspiration are complex. As VPD rises, the difference in water vapour concentration between the leaf interior and the surrounding air increases (Cernusak et al., 2024; Diao et al., 2024a), causing the latent heat flux to increase and cool leaves, which explains why leaf temperatures were cooler in the high T_{air} high VPD_{air} chamber compared to the high T_{air} low VPD_{air} chamber.

6.4 Future directions

6.4.1 Patterns of plant thermoregulation across species

Throughout this thesis I examined intraspecific variation in leaf thermal traits across a range of tropical tree species. While I predicted that plant thermoregulation would reflect a strategy of limited homeothermy, with enhanced leaf cooling in warmer climates, this was not always the case. Limited homeothermy was observed in two of six species in Chapters 2 and 3, one of four species in Chapter 4, and two of three species in Chapter 5. This indicates that a diversity of thermoregulation strategies can exist in speciose tropical rainforests. Diving deeper into intraspecific patterns of how $\Delta T_{leaf\text{-}air}$ acclimates and adapts to growth temperatures in a broad range of species should be the focus of future research. The techniques I implemented throughout this thesis, i.e. using commonly measured leaf functional traits to predict T_{leaf} under common microclimatic conditions provide a blueprint for assessing leaf thermoregulation and could be applied to other provenance trials or existing trait databases. This would allow assessment of whether the ability to thermoregulate is more prevalent in different life history strategies, for populations on the edge of their distribution, or for those inhabiting particular biomes.

6.4.2 Accurate T_{leaf} estimates rely on improved modelling of stomatal conductance

Assessing the prevalence of leaf thermoregulation in a larger number of species using trait databases will in some cases rely upon the modelling of stomatal conductance from leaf functional traits such as leaf stable isotope ratios (see Chapter 5). However, accurate T_{leaf} estimates rely on appropriate estimates of stomatal conductance and how this itself is affected by temperature. Some of the modelling approaches used in this thesis employ the unified stomatal optimisation (USO) model (Medlyn et al., 2011) for stomatal conductance (i.e. Chapters 3 and 5). However, this model assumes that stomatal conductance and photosynthesis are tightly coupled, declining together at temperatures surpassing the photosynthetic temperature optima, it can underestimate stomatal conductance at high temperatures (Marchin et al., 2023). This has implications on findings from Chapters 3 and 5, in which I use the USO model to estimate stomatal conductance throughout a species range. While I complemented that analysis with stomatal conductance calculated using theoretical maximum conductance (g_{max}) from stomatal anatomical traits, this further highlighted the discrepancy between the two approaches (i.e. limited homeothermy was observed for two of three species using the USO model, but only one of the three species using theoretical g_{max}). Improving stomatal models will allow us to better predict how vulnerable tropical forests are to warming, as well as how the carbon and water cycling services they provide may be altered with global change.

6.4.3 Linking extreme leaf temperatures to mortality

While there is evidence that global tree mortality increases during hot, dry periods (Hammond et al., 2022), and that tropical forest canopy temperatures can exceed optimal levels (Doughty et al., 2023b), directly linking exposure to extreme leaf temperatures with tree mortality remains challenging. Plants exhibit modularity, complicating the direct connection between extreme leaf temperatures and mortality, which is critical for understanding natural selection processes. Thermal stress can impair carbon uptake and affect ecosystem function, but the precise relationship between extreme leaf temperatures and mortality has not been thoroughly explored. Notably, leaf temperature distribution within a canopy varies significantly due to differences in light interception and boundary layer conditions (Rey-Sanchez et al., 2017). Sun-exposed leaves, particularly at the canopy edge, are more likely to exceed their thermal limits (Miller et al., 2021). While sun-exposed upper canopy leaves contribute significantly to total tree carbon uptake due to their high photosynthetic capacity and exposure to high light levels, shade leaves also play a vital role. Their contribution stems from the vertical distribution of leaf area index within the canopy, with sub-canopy positions hosting a greater number of leaves (depending on the species canopy architecture) (De Castro, 2000), enhancing their cumulative productivity. Additionally, the cooler microclimates of shade leaves buffer them from heat stress, enabling continued carbon uptake during periods when sun-exposed canopy leaves experience shutdown. Feeley et al. (2020) observed that changes in species' relative abundance over

time were not correlated with their thermal tolerances. Similarly, another study found that warm-adapted plants did not consistently outperform cool-adapted species during a heatwave, suggesting that thermal tolerance alone may not determine survival outcomes (Bucharova, Durka, Hermann, Holzel, et al., 2016). Furthermore, even when high temperatures contribute to mortality, the mechanisms–whether heat damage or water stress–are not well understood. Future research should address these issues, focusing on the trade-offs between leaf cooling and hydraulic damage, and identifying the specific temperatures and exposure durations that lead to mortality. Moreover, understanding how different species or functional groups balance these trade-offs could provide insights into species vulnerability. Such research would help clarify whether heat stress alone drives mortality, or if other factors, such as hydraulic failure and drought-induced damage, play a more significant role (Mcdowell et al., 2008). This will be critical for improving models of forest resilience and predicting how tropical ecosystems will respond to ongoing climate change. By establishing these relationships, we can better identify species that are at greater risk, refine restoration strategies, and improve our capacity to conserve and manage tropical forests under future conditions.

6.5 Conclusions

The research I present in this thesis has advanced our understanding of thermoregulation in tropical rainforest trees by demonstrating the critical role of inter and intraspecific trait variation in mitigating heat stress and offsetting warmer climates. Key findings reveal that while some species exhibit limited homeothermy, the capacity for acclimation and adaptation varies among species, leading to diverse thermal responses. This will likely influence future species compositions and impact the functioning of tropical forests, which are vital for global carbon cycling. This work is novel in its comprehensive analysis of the limited homeothermy hypothesis in tropical trees and its implications for predicting species responses to climate change. By providing insights into how tropical trees adapt to rising temperatures, this research contributes valuable knowledge for improving predictive provenancing and parameterizing climate-vegetation models, informing conservation and restoration strategies to preserve these crucial ecosystems.

While this research highlights the importance of thermal ecology for restoration planning, its application must account for the broader complexities of genotype and species selection. Restoration efforts should not rely solely on single thermal trait metrics but instead consider provenance trials that evaluate multiple phenotypic traits to ensure fitness across diverse environmental conditions. Additionally, maintaining genetic diversity within and across restoration sites is essential to preserve adaptive potential along axes that may not yet be fully understood. This is particularly critical given the expected increase in temperatures over the next century, which exceeds the range currently explored and encompasses correlated changes in other climate variables, such as moisture availability.

References

Abasolo, M., Lee, D. J., Brooks, L., Raymond, C., & Shepherd, M. (2014). Genetic control of flowering in spotted gum, Corymbia citriodora subsp. variegata and C. maculata. *Australian Journal of Botany*, *62*(1), 22-35. https://doi.org/10.1071/bt13223

Aitken, S. N., & Whitlock, M. C. (2013). Assisted Gene Flow to Facilitate Local Adaptation to Climate Change. In D. J. Futuyma (Ed.), *Annual Review of Ecology, Evolution, and Systematics, Vol 44* (Vol. 44, pp. 367-388). Annual Reviews. https://doi.org/10.1146/annurev-ecolsys-110512-135747

Aleixo, I., Norris, D., Hemerik, L., Barbosa, A., Prata, E., Costa, F., & Poorter, L. (2019). Amazonian rainforest tree mortality driven by climate and functional traits. *Nature Climate Change*, *9*, 384-388. https://doi.org/10.1038/s41558-019-0458-0

Anderegg, W. R. L., Martinez-Vilalta, J., Cailleret, M., Camarero, J. J., Ewers, B. E., Galbraith, D., et al. (2016). When a Tree Dies in the Forest: Scaling Climate-Driven Tree Mortality to Ecosystem Water and Carbon Fluxes. *Ecosystems*, *19*(6), 1133-1147. https://doi.org/10.1007/s10021-016-9982-1

Ansari, A. Q., & Loomis, W. E. (1959). Leaf Temperatures [Article]. *American Journal of Botany*, *46*(10), 713-717. https://doi.org/10.2307/2439126

Arab, M. M., Marrano, A., Abdollahi-Arpanahi, R., Leslie, C. A., Cheng, H., Neale, D. B., & Vahdati, K. (2020). Combining phenotype, genotype, and environment to uncover genetic components underlying water use efficiency in Persian walnut. *Journal of Experimental Botany*, *71*(3), 1107-1127. https://doi.org/10.1093/jxb/erz467

Araujo, I., Marimon, B. S., Scalon, M. C., Fauset, S., Junior, B. M., Tiwari, R., et al. (2021). Trees at the Amazonia-Cerrado transition are approaching high temperature thresholds. *Environmental Research Letters*, *16*(3), 7, Article 034047. https://doi.org/10.1088/1748-9326/abe3b9

Armstrong Mckay, D. I., Staal, A., Abrams, J. F., Winkelmann, R., Sakschewski, B., Loriani, S., et al. (2022). Exceeding 1.5°C global warming could trigger multiple climate tipping points. *Science*, *377*(6611), eabn7950. https://doi.org/10.1126/science.abn7950

Barlow, J., Gardner, T. A., Araujo, I. S., Avila-Pires, T. C., Bonaldo, A. B., Costa, J. E., et al. (2007). Quantifying the biodiversity value of tropical primary, secondary, and plantation forests. *Proceedings of the National Academy of Sciences of the United States of America*, *104*(47), 18555-18560. https://doi.org/10.1073/pnas.0703333104

Barton, K. E., Jones, C., Edwards, K. F., Shiels, A. B., & Knight, T. (2020). Local adaptation constrains drought tolerance in a tropical foundation tree. *Journal of Ecology*, *108*(4), 1540-1552. https://doi.org/10.1111/1365-2745.13354

Bates, D., Mächler, M., Bolker, B., & Walker, S. (2015). Fitting Linear Mixed-Effects Models Using lme4. In *Journal of Statistical Software* (Vol. 67, pp. 1-48). https://doi.org/10.18637/jss.v067.i01

Bauman, D., Fortunel, C., Cernusak, L. A., Bentley, L. P., Mcmahon, S. M., Rifai, S. W., et al. (2022). Tropical tree growth sensitivity to climate is driven by species intrinsic growth rate and leaf traits. *Global Change Biology*, *28*(4), 1414-1432. https://doi.org/10.1111/gcb.15982

Bauman, D., Fortunel, C., Delhaye, G., Malhi, Y., Cernusak, L. A., Bentley, L. P., et al. (2022). Tropical tree mortality has increased with rising atmospheric water stress. *Nature*, *608*(7923), 528-533. https://doi.org/10.1038/s41586-022-04737-7

Binks, O., Cernusak, L. A., Liddell, M., Bradford, M., Coughlin, I., Bryant, C., et al. (2023). Vapour pressure deficit modulates hydraulic function and structure of tropical rainforests under nonlimiting soil water supply. *New Phytologist*, *240*(4), 1405-1420. https://doi.org/10.1111/nph.19257

Bison, N. N., & Michaletz, S. T. (2024). Variation in leaf carbon economics, energy balance, and heat tolerance traits highlights differing timescales of adaptation and acclimation. *New Phytologist*, *242*(5), 1919-1931. https://doi.org/10.1111/nph.19702

Blasini, D. E., Koepke, D. F., Bush, S. E., Allan, G. J., Gehring, C. A., Whitham, T. G., et al. (2022). Tradeoffs between leaf cooling and hydraulic safety in a dominant arid land riparian tree species. *Plant, Cell & Environment*, *45*(6), 1664-1681. https://doi.org/10.1111/pce.14292

Blonder, B., Escobar, S., Kapas, R. E., & Michaletz, S. T. (2020). Low predictability of energy balance traits and leaf temperature metrics in desert, montane and alpine plant communities. *Functional Ecology*, *34*(9), 1882-1897. https://doi.org/10.1111/1365-2435.13643

Blonder, B., & Michaletz, S. T. (2018). A model for leaf temperature decoupling from air temperature. *Agricultural and Forest Meteorology*, *262*, 354-360. https://doi.org/10.1016/j.agrformet.2018.07.012

Blonder, B. W., Aparecido, L. M. T., Hultine, K. R., Lombardozzi, D., Michaletz, S. T., Posch, B. C., et al. (2023). Plant water use theory should incorporate hypotheses about extreme environments, population ecology, and community ecology. *New Phytologist*, *238*(6), 2271-2283. https://doi.org/10.1111/nph.18800

Bonan, G. B. (2008). Forests and climate change: Forcings, feedbacks, and the climate benefits of forests. *Science*, *320*(5882), 1444-1449. https://doi.org/10.1126/science.1155121

Botta-Dukát, Z. (2023). Quartile coefficient of variation is more robust than CV for traits calculated as a ratio. *Scientific Reports*, *13*(1). https://doi.org/10.1038/s41598-023-31711-8

Bradford, M. G., Murphy, H. T., Ford, A. J., Hogan, D. L., & Metcalfe, D. J. (2014). Long-term stem inventory data from tropical rain forest plots in Australia. *Ecology*, *95*(8), 2362-2362. https://doi.org/10.1890/14-0458r.1

Bragg, J. G., Cuneo, P., Sherieff, A., & Rossetto, M. (2020). Optimizing the genetic composition of a translocation population: Incorporating constraints and conflicting objectives. *Molecular Ecology Resources*, *20*(1), 54-65. https://doi.org/10.1111/1755-0998.13074

Brancalion, P. H. S., Oliveira, G. C. X., Zucchi, M. I., Novello, M., van Melis, J., Zocchi, S. S., et al. (2018). Phenotypic plasticity and local adaptation favor range expansion of a Neotropical palm. *Ecology and Evolution*, *8*(15), 7462-7475. https://doi.org/https://doi.org/10.1002/ece3.4248

Breed, M. F., Harrison, P. A., Blyth, C., Byrne, M., Gaget, V., Gellie, N. J. C., et al. (2019). The potential of genomics for restoring ecosystems and biodiversity. *Nature Reviews Genetics*, *20*(10), 615-628. https://doi.org/10.1038/s41576-019-0152-0

Breed, M. F., Stead, M. G., Ottewell, K. M., Gardner, M. G., & Lowe, A. J. (2013). Which provenance and where? Seed sourcing strategies for revegetation in a changing environment. *Conservation Genetics*, *14*(1), 1-10. https://doi.org/10.1007/s10592-012-0425-z

Brienen, R. J. W., Phillips, O. L., Feldpausch, T. R., Gloor, E., Baker, T. R., Lloyd, J., et al. (2015). Long-term decline of the Amazon carbon sink. *Nature*, *519*(7543), 344-348. https://doi.org/10.1038/nature14283

Brun, P., Zimmermann, N. E., Hari, C., Pellissier, L., & Karger, D. N. (2022). Global climate-related predictors at kilometer resolution for the past and future. *Earth System Science Data*, *14*(12), 5573-5603. https://doi.org/10.5194/essd-14-5573-2022

Bucharova, A., Durka, W., Hermann, J. M., Holzel, N., Michalski, S., Kollmann, J., & Bossdorf, O. (2016). Plants adapted to warmer climate do not outperform regional plants during a natural heat wave. *Ecology and Evolution*, *6*(12), 4160-4165. https://doi.org/10.1002/ece3.2183

Bucharova, A., Durka, W., Hermann, J. M., Hölzel, N., Michalski, S., Kollmann, J., & Bossdorf, O. (2016). Plants adapted to warmer climate do not outperform regional plants during a natural heat wave. *Ecology and Evolution*, *6*(12), 4160-4165. https://doi.org/10.1002/ece3.2183

Campbell, G. S., & Norman, J. M. (1998). *Introduction to environmental biophysics*. Springer. https://doi.org/http://dx.doi.org/10.1007/978-1-4612-1626-1

Carter, K. R., Wood, T. E., Reed, S. C., Butts, K. M., & Cavaleri, M. A. (2021). Experimental warming across a tropical forest canopy height gradient reveals minimal photosynthetic and respiratory acclimation. *Plant Cell and Environment*, *44*(9), 2879-2897. https://doi.org/10.1111/pce.14134

Caye, K., Jumentier, B., Lepeule, J., & François, O. (2019). LFMM 2: Fast and Accurate Inference of Gene-Environment Associations in Genome-Wide Studies. *Molecular Biology and Evolution*, *36*(4), 852-860. https://doi.org/10.1093/molbev/msz008

Cernusak, L. A., Wong, S. C., Stuart-Williams, H., Márquez, D. A., Pontarin, N., & Farquhar, G. D. (2024). Unsaturation in the air spaces of leaves and its implications. *Plant, Cell & Environment*, *47*(10), 3685-3698. https://doi.org/10.1111/pce.15001

Chardon, N. I., Pironon, S., Peterson, M. L., & Doak, D. F. (2020). Incorporating intraspecific variation into species distribution models improves distribution predictions, but cannot predict species traits for a wide-spread plant species. *Ecography*, *43*(1), 60-74. https://doi.org/10.1111/ecog.04630

Charles, L. S., Dwyer, J. M., Smith, T. J., Connors, S., Marschner, P., & Mayfield, M. M. (2018). Seedling growth responses to species-, neighborhood-, and landscape-scale effects during tropical forest restoration. *Ecosphere*, *9*(8), e02386. https://doi.org/10.1002/ecs2.2386

Chave, J., Coomes, D., Jansen, S., Lewis, S. L., Swenson, N. G., & Zanne, A. E. (2009). Towards a worldwide wood economics spectrum. *Ecology Letters*, *12*(4), 351-366. https://doi.org/10.1111/j.1461-0248.2009.01285.x

Cheesman, A. W., Preece, N. D., van Oosterzee, P., Erskine, P. D., & Cernusak, L. A. (2018). The role of topography and plant functional traits in determining tropical reforestation success. *Journal of Applied Ecology*, *55*(2), 1029-1039. https://doi.org/10.1111/1365-2664.12980

Cheesman, A. W., & Winter, K. (2013). Growth response and acclimation of CO2 exchange characteristics to elevated temperatures in tropical tree seedlings [Article]. *Journal of Experimental Botany*, *64*(12), 3817-3828. https://doi.org/10.1093/jxb/ert211

Chen, S. G., Yang, J., Zhang, M. S., Strasser, R. J., & Qiang, S. (2016). Classification and characteristics of heat tolerance in *Ageratina adenophora* populations using fast chlorophyll a fluorescence rise O-J-I-P. *Environmental and Experimental Botany*, *122*, 126-140. https://doi.org/10.1016/j.envexpbot.2015.09.011

Choury, Z., Wujeska-Klause, A., Bourne, A., Bown, N. P., Tjoelker, M. G., Medlyn, B. E., & Crous, K. Y. (2022). Tropical rainforest species have larger increases in temperature optima with warming than warm-temperate rainforest trees. *New Phytologist*, *234*(4), 1220-1236. https://doi.org/10.1111/nph.18077

Coast, O., Posch, B. C., Rognoni, B. G., Bramley, H., Gaju, O., Mackenzie, J., et al. (2022). Wheat photosystem II heat tolerance: evidence for genotype-by-environment interactions. *The Plant Journal*, *111*(5), 1368-1382. https://doi.org/10.1111/tpj.15894

Cochard, H. (2021). A new mechanism for tree mortality due to drought and heatwaves. *Peer Community Journal*, *1*, article e36. https://doi.org/10.24072/pcjournal.45

Colwell, R. K., & Feeley, K. J. (2024). Still little evidence of poleward range shifts in the tropics, but lowland biotic attrition may be underway. *Biotropica*, e13358. https://doi.org/https://doi.org/10.1111/btp.13358

Comita, L. S., & Engelbrecht, B. M. J. (2017). Drought as a driver of tropical tree species regeneration dynamics and distribution patterns. In D. A. Coomes, D. Burslem, & W. D. Simonson (Eds.), *Forests and Global Change* (pp. 261-308). Cambridge University Press.

Commander, L. E. (2021). *Florabank Guidelines – best practice guidelines for native seed collection and use* (L. E. Commander, Ed. 2nd ed.). Florabank Consortium: Australia.

Conti, L., Valencia, E., Galland, T., Götzenberger, L., Lepš, J., E-Vojtkó, A., et al. (2023). Functional trait trade-offs define plant population stability across different biomes. *Proceedings of the Royal Society B: Biological Sciences*, *290*(2001). https://doi.org/10.1098/rspb.2023.0344

Cook, A. M., Berry, N., Milner, K. V., & Leigh, A. (2021). Water availability influences thermal safety margins for leaves. *Functional Ecology*, *35*(10), 2179-2189. https://doi.org/10.1111/1365-2435.13868

Cook, A. M., Rezende, E. L., Petrou, K., & Leigh, A. (2024). Beyond a single temperature threshold: Applying a cumulative thermal stress framework to plant heat tolerance. *Ecology Letters*, *27*(3), e14416. https://doi.org/10.1111/ele.14416

Cooper, S. L., Catterall, C., & Bundock, P. C. (2018). Local provenancing in subtropical rainforest restoration: For better or worse? A review of practitioners' perspectives. *Ecological Management & Restoration*, *19*(2), 156-165. https://doi.org/10.1111/emr.12305

Cordero, I., Jiménez, M. D., Delgado, J. A., Balaguer, L., Pueyo, J. J., & Rincón, A. (2021). Local adaptation optimizes photoprotection strategies in a Neotropical legume tree under drought stress. *Tree Physiology*, *41*(9), 1641-1657. https://doi.org/10.1093/treephys/tpab034

Corlett, R. T. (2011). Impacts of warming on tropical lowland rainforests. *Trends in Ecology & Evolution*, *26*(11), 606-613. https://doi.org/10.1016/j.tree.2011.06.015

Corlett, R. T., & Westcott, D. A. (2013). Will plant movements keep up with climate change? *Trends in Ecology & Evolution*, *28*(8), 482-488. https://doi.org/10.1016/j.tree.2013.04.003

Corripio, J. G. (2021). insol: Solar Radiation. In (Vol. R Package 1.2.2).

Crous, K. Y., Cheesman, A. W., Middleby, K., Rogers, E. I. E., Wujeska-Klause, A., Bouet, A. Y. M., et al. (2023). Similar patterns of leaf temperatures and thermal acclimation to warming in temperate and tropical tree canopies. *Tree Physiology*, *43*(8), 1383-1399. https://doi.org/10.1093/treephys/tpad054

Crous, K. Y., Uddling, J., & De Kauwe, M. G. (2022). Temperature responses of photosynthesis and respiration in evergreen trees from boreal to tropical latitudes. *New Phytologist*, *234*(2), 353-374. https://doi.org/10.1111/nph.17951

Cunningham, S., & Read, J. (2003). Comparison of temperate and tropical rainforest tree species: growth responses to temperature. *Journal of Biogeography*, *30*(1), 143-153. https://doi.org/10.1046/j.1365-2699.2003.00811.x

Cunningham, S. C. (2004). Stomatal sensitivity to vapour pressure deficit of temperate and tropical evergreen rainforest trees of Australia. *Trees-Structure and Function*, *18*(4), 399-407. https://doi.org/10.1007/s00468-004-0318-y

Cunningham, S. C. (2005). Photosynthetic responses to vapour pressure deficit in temperate and tropical evergreen rainforest trees of Australia. *Oecologia*, *142*(4), 521-528. https://doi.org/10.1007/s00442-004-1766-1

Curtis, E. M., Knight, C. A., & Leigh, A. (2019). Intracanopy adjustment of leaf-level thermal tolerance is associated with microclimatic variation across the canopy of a desert tree (*Acacia papyrocarpa*). *Oecologia*, *189*(1), 37-46. https://doi.org/10.1007/s00442-018-4289-x

Davies-Colley, R. J., Payne, G. W., & van Elswijk, M. (2000). Microclimate gradients across a forest edge. *New Zealand Journal of Ecology*, *24*(2), 111-121. https://doi.org/http://www.jstor.org/stable/24054666

De Castro, F. (2000). Light spectral composition in a tropical forest: measurements and model. *Tree Physiology, 20(1), 49–56.* https://doi.org/10.1093/treephys/20.1.49

De Kauwe, M. G., Medlyn, B. E., Pitman, A. J., Drake, J. E., Ukkola, A., Griebel, A., et al. (2019). Examining the evidence for decoupling between photosynthesis and transpiration during heat extremes. *Biogeosciences*, *16*(4), 903-916. https://doi.org/10.5194/bg-16-903-2019

de Villemereuil, P., Gaggiotti, O. E., Mouterde, M., & Till-Bottraud, I. (2016). Common garden experiments in the genomic era: new perspectives and opportunities. *Heredity*, *116*(3), 249-254. https://doi.org/10.1038/hdy.2015.93

Deacon, N. J., & Cavender-Bares, J. (2015). Limited Pollen Dispersal Contributes to Population Genetic Structure but Not Local Adaptation in *Quercus oleoides* Forests of Costa Rica. *Plos One*, *10*(9), Article e0138783. https://doi.org/10.1371/journal.pone.0138783

Degen, B., & Sebbenn, A. (2015). Genetics and Tropical Forests. In L. Pancel & M. Köhl (Eds.), *Tropical Forestry Handbook* (2 ed., Vol. 2, pp. 885-920). Springer Nature. https://doi.org/0.1007/978-3-642-41554-8_75-1

Deva, C. R., Urban, M. O., Challinor, A. J., Falloon, P., & Svitakova, L. (2020). Enhanced Leaf Cooling Is a Pathway to Heat Tolerance in Common Bean. *Frontiers in Plant Science*, *11*, 17, Article 19. https://doi.org/10.3389/fpls.2020.00019

Diao, H., Cernusak, L. A., Saurer, M., Gessler, A., Siegwolf, R. T. W., & Lehmann, M. M. (2024a). Dry inside: progressive unsaturation within leaves with increasing vapour pressure deficit affects

estimation of key leaf gas exchange parameters. *New Phytologist*. https://doi.org/10.1111/nph.20078

Diao, H., Cernusak, L. A., Saurer, M., Gessler, A., Siegwolf, R. T. W., & Lehmann, M. M. (2024b). Uncoupling of stomatal conductance and photosynthesis at high temperatures: mechanistic insights from online stable isotope techniques. *New Phytologist*, *241*(6), 2366-2378. https://doi.org/10.1111/nph.19558

Dong, N., Prentice, I. C., Harrison, S. P., Song, Q. H., & Zhang, Y. P. (2017). Biophysical homoeostasis of leaf temperature: A neglected process for vegetation and land-surface modelling. *Global Ecology and Biogeography*, *26*(9), 998-1007. https://doi.org/10.1111/geb.12614

Dormann, C. F. (2007). Assessing the validity of autologistic regression. *Ecological Modelling*, *207*(2-4), 234-242. https://doi.org/10.1016/j.ecolmodel.2007.05.002

Doughty, C. E., Keany, J. M., Wiebe, B. C., Rey-Sanchez, C., Carter, K. R., Middleby, K. B., et al. B. (2023). Tropical forests are approaching critical temperature thresholds. *Nature*, *621*, 105–111. https://doi.org/10.1038/s41586-023-06391-z

Drake, J. E., Harwood, R., Varhammar, A., Barbour, M. M., Reich, P. B., Barton, C. V. M., & Tjoelker, M. G. (2020). No evidence of homeostatic regulation of leaf temperature in *Eucalyptus parramattensis* trees: integration of CO(2)flux and oxygen isotope methodologies. *New Phytologist*, *228*(5), 1511-1523. https://doi.org/10.1111/nph.16733

Drake, J. E., Tjoelker, M. G., Varhammar, A., Medlyn, B. E., Reich, P. B., Leigh, A., et al. (2018). Trees tolerate an extreme heatwave via sustained transpirational cooling and increased leaf thermal tolerance. *Global Change Biology*, *24*(6), 2390-2402. https://doi.org/10.1111/gcb.14037

Duursma, R. A. (2015). Plantecophys - An R Package for Analysing and Modelling Leaf Gas Exchange Data. *Plos One*, *10*(11), 13, Article e0143346. https://doi.org/10.1371/journal.pone.0143346

Duursma, R. A., Blackman, C. J., Lopez, R., Martin-StPaul, N. K., Cochard, H., & Medlyn, B. E. (2019). On the minimum leaf conductance: its role in models of plant water use, and ecological and environmental controls. *New Phytologist*, *221*(2), 693-705. https://doi.org/10.1111/nph.15395

Engert, J. E., Vogado, N. O., Freebody, K., Byrne, B., Murphy, J., Sheather, G., et al. (2020). Functional trait representation differs between restoration plantings and mature tropical rainforest. *Forest Ecology and Management*, *473*, 9, Article 118304. https://doi.org/10.1016/j.foreco.2020.118304

Escribano-Rocafort, A. G., Ventre-Lespiaucq, A. B., Granado-Yela, C., López-Pintor, A., Delgado, J. A., Muñoz, V., et al. (2014). Simplifying data acquisition in plant canopies- Measurements of leaf angles with a cell phone. *Methods in Ecology and Evolution*, *5*(2), 132-140. https://doi.org/10.1111/2041-210x.12141

Everingham, S., Offord, C., Sabot, M., & Moles, A. (2024). Leaf morphological traits show greater responses to changes in climate than leaf physiological traits and gas exchange variables. *Ecology and Evolution*, *14*, Article e10941. https://doi.org/10.1002/ece3.10941

Fakhet, D., Morales, F., Jauregui, I., Erice, G., Aparicio-Tejo, P. M., González-Murua, C., et al. (2021). Short-Term Exposure to High Atmospheric Vapor Pressure Deficit (VPD) Severely Impacts Durum Wheat Carbon and Nitrogen Metabolism in the Absence of Edaphic Water Stress. *Plants*, *10*(1), 120. https://doi.org/10.3390/plants10010120

Fang, Z., Zhang, W., Brandt, M., Abdi, A. M., & Fensholt, R. (2022). Globally Increasing Atmospheric Aridity Over the 21st Century. *Earth's Future*, *10*(10). https://doi.org/10.1029/2022ef003019

Fanourakis, D., Heuvelink, E., & Carvalho, S. M. P. (2013). A comprehensive analysis of the physiological and anatomical components involved in higher water loss rates after leaf development at high humidity. *Journal of Plant Physiology*, *170*(10), 890-898. https://doi.org/10.1016/j.jplph.2013.01.013

Farquhar, G. D., Caemmerer, S. V., & Berry, J. A. (1980). A biochemical-model of photosynthetic CO2 assimilation in leaves of C-3 species. *Planta*, *149*(1), 78-90. https://doi.org/10.1007/bf00386231

Farquhar, G. D., & Sharkey, T. D. (1982). Stomatal Conductance and Photosynthesis. *Annual Review of Plant Physiology*, *33*(1), 317-345. https://doi.org/10.1146/annurev.pp.33.060182.001533

Faske, T. M., Agneray, A. C., Jahner, J. P., Sheta, L. M., Leger, E. A., & Parchman, T. L. (2021). Genomic and common garden approaches yield complementary results for quantifying environmental drivers of local adaptation in rubber rabbitbrush, a foundational Great Basin shrub. *Evolutionary Applications*, *14*(12), 2881-2900. https://doi.org/10.1111/eva.13323

Fauset, S., Freitas, H. C., Galbraith, D. R., Sullivan, M. J. P., Aidar, M. P. M., Joly, C. A., et al. (2018). Differences in leaf thermoregulation and water use strategies between three co-occurring Atlantic forest tree species. *Plant Cell and Environment*, *41*(7), 1618-1631. https://doi.org/10.1111/pce.13208

Fauset, S., Oliveira, L., Buckeridge, M. S., Foyer, C. H., Galbraith, D., Tiwari, R., & Gloor, M. (2019). Contrasting responses of stomatal conductance and photosynthetic capacity to warming and elevated CO2 in the tropical tree species Alchomea glandulosa under heatwave conditions. *Environmental and Experimental Botany*, *158*, 28-39. https://doi.org/10.1016/j.envexpbot.2018.10.030

Feeley, K.J., Silman, M.R., Bush, M.B., Farfan, W., Cabrera, K.G., Malhi, Y., Meir, P., Revilla, N.S., Quisiyupanqui, M.N.R. & Saatchi, S. (2011). Upslope migration of Andean trees. *Journal of Biogeography*, 38: 783-791. https://doi.org/10.1111/j.1365-2699.2010.02444.x

Feeley, K., Martinez-Villa, J., Perez, T., Duque, A. S., Gonzalez, D. T., & Duque, A. (2020). The Thermal Tolerances, Distributions, and Performances of Tropical Montane Tree Species. *Frontiers in Forests and Global Change*, *3*, Article 25. https://doi.org/10.3389/ffgc.2020.00025

Ferrier, S., Manion, G., Elith, J., & Richardson, K. (2007). Using generalized dissimilarity modelling to analyse and predict patterns of beta diversity in regional biodiversity assessment. *Diversity and Distributions*, *13*(3), 252-264. https://doi.org/10.1111/j.1472-4642.2007.00341.x

Fordham, D. A., Brown, S. C., Wigley, T. M. L., & Rahbek, C. (2019). Cradles of diversity are unlikely relics of regional climate stability. *Current Biology*, *29*(10), R356-R357. https://doi.org/10.1016/j.cub.2019.04.001

Forester, B. R., Lasky, J. R., Wagner, H. H., & Urban, D. L. (2018). Comparing methods for detecting multilocus adaptation with multivariate genotype-environment associations. *Molecular Ecology*, *27*(9), 2215-2233. https://doi.org/10.1111/mec.14584

Franks, P. J., & Beerling, D. J. (2009). Maximum leaf conductance driven by CO_2 effects on stomatal size and density over geologic time. *Proceedings of the National Academy of Sciences*, *106*(25), 10343-10347. https://doi.org/10.1073/pnas.0904209106

Franks, P. J., & Farquhar, G. D. (1999). A relationship between humidity response, growth form and photosynthetic operating point in C3 plants. *Plant, Cell & Environment*, *22*(11), 1337-1349. https://doi.org/10.1046/j.1365-3040.1999.00494.x

Frichot, E., & François, O. (2015). LEA: An R package for landscape and ecological association studies. *Methods in Ecology and Evolution*, *6*(8), 925-929. https://doi.org/10.1111/2041-210x.12382

Friedlingstein, P., Jones, M. W., O'Sullivan, M., Andrew, R. M., Bakker, D. C. E., Hauck, J., et al. (2022). Global Carbon Budget 2021. *Earth System Science Data*, *14*(4), 1917-2005. https://doi.org/10.5194/essd-14-1917-2022

Fürstenau Togashi, H., Prentice, I. C., Atkin, O. K., Macfarlane, C., Prober, S. M., Bloomfield, K. J., & Evans, B. J. (2018). Thermal acclimation of leaf photosynthetic traits in an evergreen woodland, consistent with the coordination hypothesis. *Biogeosciences*, *15*(11), 3461-3474. https://doi.org/10.5194/bg-15-3461-2018

Gamliel, I., Buba, Y., Guy-Haim, T., Garval, T., Willett, D., Rilov, G., & Belmaker, J. (2020). Incorporating physiology into species distribution models moderates the projected impact of warming on selected Mediterranean marine species. *Ecography*, *43*(7), 1090-1106. https://doi.org/10.1111/ecog.04423

Gates, D.M., Hiesey, W.M., Milner, H.W. & Nobs, M.A., (1964). Temperatures of Mimulus leaves in natural environments and in a controlled chamber. Carnegie Inst. Wash. Yearbook, 63, pp.418-428.

Gauthey, A., Bachofen, C., Deluigi, J., Didion-Gency, M., D'Odorico, P., Gisler, J., et al. (2023). Absence of canopy temperature variation despite stomatal adjustment in *Pinus sylvestris* under multidecadal soil moisture manipulation. *New Phytologist*. https://doi.org/10.1111/nph.19136

Gaviria, J., Turner, B., & Engelbrecht, B. (2017). Drivers of tree species distribution across a tropical rainfall gradient. *Ecosphere*, *8*, Article e01712. https://doi.org/10.1002/ecs2.1712

GBIF. (2024). Derived dataset GBIF.org (17 July 2024) Filtered export of GBIF occurrence data https://doi.org/10.15468/dd.a4mjzn

Geange, S. R., Arnold, P. A., Catling, A. A., Coast, O., Cook, A. M., Gowland, K. M., et al. (2021). The thermal tolerance of photosynthetic tissues: a global systematic review and agenda for future research. *New Phytologist*, 229, 2497-2513. https://doi.org/10.1111/nph.17052

Gellie, N. J. C., Breed, M. F., Thurgate, N., Kennedy, S. A., & Lowe, A. J. (2016). Local maladaptation in a foundation tree species: Implications for restoration. *Biological Conservation*, *203*, 226-232. https://doi.org/10.1016/j.biocon.2016.08.036

Gibson, L., Lee, T. M., Koh, L. P., Brook, B. W., Gardner, T. A., Barlow, J., et al. (2011). Primary forests are irreplaceable for sustaining tropical biodiversity. *Nature*, *478*(7369), 378-381. https://doi.org/10.1038/nature10425

Gimeno, T. E., Pias, B., Lemos-Filho, J. P., & Valladares, F. (2008). Plasticity and stress tolerance override local adaptation in the responses of Mediterranean holm oak seedlings to drought and cold. *Tree Physiology*, *29*(1), 87-98. https://doi.org/10.1093/treephys/tpn007

Girardin, C. A. J., Jenkins, S., Seddon, N., Allen, M., Lewis, S. L., Wheeler, C. E., et al. (2021). Nature-based solutions can help cool the planet - if we act now. *Nature*, *593*(7858), 191-194. https://doi.org/10.1038/d41586-021-01241-2

Girardin, C. A. J., Jenkins, S., Seddon, N., Allen, M., Lewis, S. L., Wheeler, C. E., et al. (2021). Nature-based solutions can help cool the planet — if we act now. *Nature*, *593*(7858), 191-194. https://doi.org/10.1038/d41586-021-01241-2

Goosem, S., & Tucker, N. (2013). *Repairing the Rainforest* (2 ed.). Wet Tropics Management Authority, Cairns, Queensland, Australia, & Biotropica Australia, Tarzali, Queensland, Australia.

Goosem, S. P., & Tucker, N. J. (1995). Repairing the rainforest: Theory and practice of rainforest re-establishment in North Queensland's wet tropics. In. Cairns: Wet Tropics Management Authority.

Griscom, B. W., Adams, J., Ellis, P. W., Houghton, R. A., Lomax, G., Miteva, D. A., et al. (2017). Natural climate solutions. *Proceedings of the National Academy of Sciences*, *114*(44), 11645-11650. https://doi.org/10.1073/pnas.1710465114

Grossiord, C., Buckley, T. N., Cernusak, L. A., Novick, K. A., Poulter, B., Siegwolf, R. T. W., et al. (2020). Plant responses to rising vapor pressure deficit. *New Phytologist*, *226*(6), 1550-1566. https://doi.org/10.1111/nph.16485

Gu, L., Meyers, T., Pallardy, S. G., Hanson, P. J., Yang, B., Heuer, M., et al. (2006). Direct and indirect effects of atmospheric conditions and soil moisture on surface energy partitioning revealed by a prolonged drought at a temperate forest site. *Journal of Geophysical Research*, *111*(D16). https://doi.org/10.1029/2006jd007161

Guo, Z., Still, C. J., Lee, C. K. F., Ryu, Y., Blonder, B., Wang, J., et al. (2023). Does plant ecosystem thermoregulation occur? An extratropical assessment at different spatial and temporal scales. *New Phytologist*, *238*(3), 1004-1018. https://doi.org/10.1111/nph.18632

Guo, Z. F., Yan, Z. B., Majcher, B. M., Lee, C. K. F., Zhao, Y. Y., Song, G. Q., et al. (2022). Dynamic biotic controls of leaf thermoregulation across the diel timescale. *Agricultural and Forest Meteorology*, *315*, 11, Article 108827. https://doi.org/10.1016/j.agrformet.2022.108827

Halbritter, A. H., Fior, S., Keller, I., Billeter, R., Edwards, P. J., Holderegger, R., et al. (2018). Trait differentiation and adaptation of plants along elevation gradients. *Journal of Evolutionary Biology*, *31*(6), 784-800. https://doi.org/10.1111/jeb.13262

Hammond, W. M., Williams, A. P., Abatzoglou, J. T., Adams, H. D., Klein, T., López, R., et al. (2022). Global field observations of tree die-off reveal hotter-drought fingerprint for Earth's forests. *Nature Communications*, *13*(1), Article 1761. https://doi.org/10.1038/s41467-022-29289-2

Helliker, B. R., & Richter, S. L. (2008). Subtropical to boreal convergence of tree-leaf temperatures. *Nature*, *454*(7203), 511-U516. https://doi.org/10.1038/nature07031

Helliker, B. R., Song, X., Goulden, M. L., Clark, K., Bolstad, P., Munger, J. W., et al. (2018). Assessing the interplay between canopy energy balance and photosynthesis with cellulose delta O-18: large-scale patterns and independent ground-truthing. *Oecologia*, *187*(4), 995-1007. https://doi.org/10.1007/s00442-018-4198-z

Hereford, J. (2009). A Quantitative Survey of Local Adaptation and Fitness Trade-Offs. *The American Naturalist*, *173*(5), 579-588. https://doi.org/10.1086/597611

Hernández, G. G., Winter, K., & Slot, M. (2020). Similar temperature dependence of photosynthetic parameters in sun and shade leaves of three tropical tree species. *Tree Physiology*, *40*(5), 637-651. https://doi.org/10.1093/treephys/tpaa015

Hijmans, R. (2022). raster: Geographic Data Analysis and Modeling. In (Vol. R package version 3.6-11).

Hijmans, R. J. (2022). *geosphere: Spherical Trigonometry*.

Hikosaka, K., Ishikawa, K., Borjigidai, A., Muller, O., & Onoda, Y. (2006). Temperature acclimation of photosynthesis: mechanisms involved in the changes in temperature dependence of photosynthetic rate. *Journal of Experimental Botany*, *57*(2), 291-302. https://doi.org/10.1093/jxb/erj049

Hultine, K. R., Allan, G. J., Blasini, D., Bothwell, H. M., Cadmus, A., Cooper, H. F., et al. (2020). Adaptive capacity in the foundation tree species Populus fremontii: implications for resilience to climate change and non-native species invasion in the American Southwest. *Conservation Physiology*, *8*(1), 2020, coaa2061. https://doi.org/10.1093/conphys/coaa061

Héroult, A., Lin, Y.-S., Bourne, A., Medlyn, B. E., & Ellsworth, D. S. (2013). Optimal stomatal conductance in relation to photosynthesis in climatically contrasting Eucalyptus species under drought. *Plant, Cell & Environment*, *36*(2), 262-274. https://doi.org/10.1111/j.1365-3040.2012.02570.x

IPCC. (2022). *Climate Change 2022: Impacts, Adaptation, and Vulnerability* (Contribution of Working Group II to the Sixth Assessment Report of the Intergovernmental Panel on Climate Change [H.-O. Pörtner, D.C. Roberts, M. Tignor, E.S. Poloczanska, K. Mintenbeck, A. Alegría, M. Craig, S. Langsdorf, S. Löschke, V. Möller, A. Okem, B. Rama (eds.)]. , Issue.

Jarvis, P. G. (1976). Interpretation of variations in leaf water potential and stomatal conductance in canopies in field. *Philosophical Transactions of the Royal Society of London Series B-Biological Sciences*, *273*(927), 593-610. https://doi.org/10.1098/rstb.1976.0035

Jayalakshmy, M. S., & Philip, J. (2010). Thermophysical Properties of Plant Leaves and Their Influence on the Environment Temperature. *International Journal of Thermophysics*, *31*(11-12), 2295-2304. https://doi.org/10.1007/s10765-010-0877-7

Jombart, T. (2008). *adegenet*: a R package for the multivariate analysis of genetic markers. *Bioinformatics*, *24*(11), 1403-1405. https://doi.org/10.1093/bioinformatics/btn129

Jones, H. G. (2013). *Plants and Microclimate: A Quantitative Approach to Environmental Plant Physiology* (3 ed.). Cambridge University Press. https://doi.org/10.1017/CBO9780511845727

Jordan, R., Harrison, P., & Breed, M. (2024). The eco-evolutionary risks of not changing seed provenancing practices in changing environments. *Ecology Letters,* *27*(1), e14248. https://doi.org/10.22541/au.168570191.19000524/v1

Kardos, M., Armstrong, E. E., Fitzpatrick, S. W., Hauser, S., Hedrick, P. W., Miller, J. M., et al. (2021). The crucial role of genome-wide genetic variation in conservation. *Proceedings of the National Academy of Sciences*, *118*(48), e2104642118. https://doi.org/10.1073/pnas.2104642118

Karger, D. N., Conrad, O., Böhner, J., Kawohl, T., Kreft, H., Soria-Auza, R. W., et al. (2017). Climatologies at high resolution for the earth's land surface areas. *Scientific Data*, *4*(1), 170122. https://doi.org/10.1038/sdata.2017.122

Karger, D. N., Conrad, O., Böhner, J., Kawohl, T., Kreft, H., Soria-Auza, R. W., et al. (2018). *Data from: Climatologies at high resolution for the earth's land surface areas* (Dryad. https://doi.org/doi.org/10.5061/dryad.kd1d4

Kawecki, T. J., & Ebert, D. (2004). Conceptual issues in local adaptation. *Ecology Letters*, *7*(12), 1225-1241. https://doi.org/10.1111/j.1461-0248.2004.00684.x

Kearney, M. R., & Porter, W. P. (2020). NicheMapR - an R package for biophysical modelling: the ectotherm and Dynamic Energy Budget models. *Ecography*, *43*(1), 85-96. https://doi.org/10.1111/ecog.04680

Keenan, K., Mcginnity, P., Cross, T. F., Crozier, W. W., & Prodöhl, P. A. (2013). diveRsity: An R package for the estimation and exploration of population genetics parameters and their associated errors. *Methods in Ecology and Evolution*, *4*(8), 782-788. https://doi.org/10.1111/2041-210x.12067

Kelly, J. W. (2014). *Productivity and water use of Australian tree species under climate change* [Thesis, Macquarie University].

Kitudom, N., Fauset, S., Zhou, Y. Y., Fan, Z. X., Li, M. R., He, M. J., et al. (2022). Thermal safety margins of plant leaves across biomes under a heatwave. *Science of the Total Environment*, *806*, Article 150416. https://doi.org/10.1016/j.scitotenv.2021.150416

Krause, G. H., Cheesman, A. W., Winter, K., Krause, B., & Virgo, A. (2013). Thermal tolerance, net CO2 exchange and growth of a tropical tree species, Ficus insipida, cultivated at elevated daytime and nighttime temperatures. *Journal of Plant Physiology*, *170*(9), 822-827. https://doi.org/10.1016/j.jplph.2013.01.005

Krause, G. H., Winter, K., Krause, B., Jahns, P., Garcia, M., Aranda, J., & Virgo, A. (2010). High-temperature tolerance of a tropical tree, Ficus insipida: methodological reassessment and climate change considerations. *Functional Plant Biology*, *37*(9), 890-900. https://doi.org/10.1071/fp10034

Kruse, J., Adams, M., Winkler, B., Ghirardo, A., Alfarraj, S., Kreuzwieser, J., et al. (2019). Optimization of photosynthesis and stomatal conductance in the date palm Phoenix dactylifera during acclimation to heat and drought. *New Phytologist*, *223*(4), 1973-1988. https://doi.org/10.1111/nph.15923

Kullberg, A. T., Coombs, L., Soria Ahuanari, R. D., Fortier, R. P., & Feeley, K. J. (2023). Leaf thermal safety margins decline at hotter temperatures in a natural warming 'experiment' in the Amazon. *New Phytologist*, *241*(4), 1447-1463. https://doi.org/10.1111/nph.19413

Kullberg, A. T., & Feeley, K. J. (2022). Limited acclimation of leaf traits and leaf temperatures in a subtropical urban heat island. *Tree Physiology*, *42*(11), 2266-2281. https://doi.org/10.1093/treephys/tpac066

Kumarathunge, D. P., Medlyn, B. E., Drake, J. E., Tjoelker, M. G., Aspinwall, M. J., Battaglia, M., et al. (2019). Acclimation and adaptation components of the temperature dependence of plant photosynthesis at the global scale. *New Phytologist*, *222*(2), 768-784. https://doi.org/10.1111/nph.15668

Lamont, B. (2003). Structure, ecology and physiology of root clusters - a review. *Plant and Soil*, *248*, 1-19. https://doi.org/https://doi.org/10.1023/A:1022314613217

Lancaster, L. T., & Humphreys, A. M. (2020). Global variation in the thermal tolerances of plants. *Proceedings of the National Academy of Sciences*, *117*(24), 13580-13587. https://doi.org/10.1073/pnas.1918162117

Lapidot, O., Ignat, T., Rud, R., Rog, I., Alchanatis, V., & Klein, T. (2019). Use of thermal imaging to detect evaporative cooling in coniferous and broadleaved tree species of the Mediterranean maquis. *Agricultural and Forest Meteorology*, *271*, 285-294. https://doi.org/10.1016/j.agrformet.2019.02.014

Lee, A. P., Upchurch, G., Murchie, E. H., & Lomax, B. H. (2015). Leaf energy balance modelling as a tool to infer habitat preference in the early angiosperms. *Proceedings of the Royal Society B-Biological Sciences*, *282*(1803), 7, Article 20143052. https://doi.org/10.1098/rspb.2014.3052

Leigh, A., Sevanto, S., Ball, M. C., Close, J. D., Ellsworth, D. S., Knight, C. A., et al. (2012). Do thick leaves avoid thermal damage in critically low wind speeds? *New Phytologist*, *194*(2), 477-487. https://doi.org/10.1111/j.1469-8137.2012.04058.x

Leigh, A., Sevanto, S., Close, J. D., & Nicotra, A. B. (2017). The influence of leaf size and shape on leaf thermal dynamics: does theory hold up under natural conditions?. *Plant Cell and Environment*, *40*(2), 237-248. https://doi.org/10.1111/pce.12857

Leimu, R., & Fischer, M. (2008). A Meta-Analysis of Local Adaptation in Plants. *Plos One*, *3*(12), 8, Article e4010. https://doi.org/10.1371/journal.pone.0004010

Leites, L., & Garzón, B., Marta. (2023). Forest tree species adaptation to climate across biomes: Building on the legacy of ecological genetics to anticipate responses to climate change. *Global Change Biology*, *29*(17), 4711-4730. https://doi.org/10.1111/gcb.16711

Lenth, R. (2022). *EMMEANS: Estimated Marginals Means, aka Least-Square Means.* In (Version R package v.1.8.3.) https://CRAN.R-project.org/package=emmeans

Leon-Garcia, I. V., & Lasso, E. (2019). *Heat tolerance in plant leaves*. protocols.io. https://dx.doi.org/10.17504/protocols.io.29fgh3n

Leon-Garcia, I. V., & Lasso, E. (2019). High heat tolerance in plants from the Andean highlands: Implications for paramos in a warmer world. *Plos One*, *14*(11), Article e0224218. https://doi.org/10.1371/journal.pone.0224218

Leuzinger, S., & Korner, C. (2007). Tree species diversity affects canopy leaf temperatures in a mature temperate forest. *Agricultural and Forest Meteorology*, *146*(1-2), 29-37. https://doi.org/10.1016/j.agrformet.2007.05.007

Liancourt, P., Song, X., Macek, M., Santrucek, J., & Dolezal, J. (2020). Plant's-eye view of temperature governs elevational distributions. *Global Change Biology*, *26*(7), 4094-4103. https://doi.org/10.1111/gcb.15129

Liang, X., Ye, Q., Liu, H., & Brodribb, T. J. (2021). Wood density predicts mortality threshold for diverse trees. *New Phytologist*, *229*(6), 3053-3057. https://doi.org/10.1111/nph.17117

Lin, D., Xia, J., & Wan, S. (2010). Climate warming and biomass accumulation of terrestrial plants: a meta-analysis. *New Phytologist*, *188*(1), 187-198. https://doi.org/10.1111/j.1469-8137.2010.03347.x

Lopez, J., Way, D. A., & Sadok, W. (2021). Systemic effects of rising atmospheric vapor pressure deficit on plant physiology and productivity. *Global Change Biology*, *27*(9), 1704-1720. https://doi.org/10.1111/gcb.15548

Lotterhos, K. (2023). The paradox of adaptive trait clines with nonclinal patterns in the underlying genes. *PNAS*, *120*, Article e2220313120. https://doi.org/10.1073/pnas.2220313120

Luu, K., Bazin, E., & Blum, M. G. B. (2017). *pcadapt*: an R package to perform genome scans for selection based on principal component analysis. *Molecular Ecology Resources*, *17*(1), 67-77. https://doi.org/10.1111/1755-0998.12592

Lynch, H. J., Rhainds, M., Calabrese, J. M., Cantrell, S., Cosner, C., & Fagan, W. F. (2014). How climate extremes—not means—define a species' geographic range boundary via a demographic tipping point. *84*(1), 131-149. https://doi.org/https://doi.org/10.1890/12-2235.1

Maclean, I. M. D., Mosedale, J. R., & Bennie, J. J. (2019). Microclima: An r package for modelling meso- and microclimate. *Methods in Ecology and Evolution*, *10*(2), 280-290. https://doi.org/10.1111/2041-210x.13093

Mahan, J. R., & Upchurch, D. R. (1988). Maintenance of constant leaf temperature by plants. 1. Hypothesis limited homeothermy. *Environmental and Experimental Botany*, *28*(4), 351-357. https://doi.org/10.1016/0098-8472(88)90059-7

Malavasi, M. D., Davis, A. S., & Malavasi, U. C. (2018). Tree seed sourcing for landscape restoration under climate changes. *Ciencia Florestal*, *28*(1), 446-455. https://doi.org/10.5902/1980509831628

Malcolm, D. T., Nagel, B. K. A., Sinclair, I., & Heiner, I.J. . (1999). *Soils and agricultural land suitability of the Atherton Tablelands*.

Manishimwe, A., Ntirugulirwa, B., Zibera, E., Nyirambangutse, B., Mujawamariya, M., Dusenge, M. E., et al. (2022). Warming Responses of Leaf Morphology Are Highly Variable among Tropical Tree Species. *Forests*, *13*(2), 219. https://doi.org/10.3390/f13020219

Marchin, R. M., Medlyn, B. E., Tjoelker, M. G., & Ellsworth, D. S. (2023). Decoupling between stomatal conductance and photosynthesis occurs under extreme heat in broadleaf tree species regardless of water access. *Global Change Biology*, *29*(22), 6319-6335. https://doi.org/10.1111/gcb.16929

Marias, D. E., Meinzer, F. C., Woodruff, D. R., & Mcculloh, K. A. (2016). Thermotolerance and heat stress responses of Douglas-fir and ponderosa pine seedling populations from contrasting climates. *Tree Physiology*, *37*(3), 301-315. https://doi.org/10.1093/treephys/tpw117

Massmann, A., Gentine, P., & Lin, C. (2019). When Does Vapor Pressure Deficit Drive or Reduce Evapotranspiration? *Journal of Advances in Modeling Earth Systems*, *11*(10), 3305-3320. https://doi.org/10.1029/2019ms001790

Matesanz, S., & Ramirez-Valiente, J. A. (2019). A review and meta-analysis of intraspecific differences in phenotypic plasticity: Implications to forecast plant responses to climate change. *Global Ecology and Biogeography*, *28*(11), 1682-1694. https://doi.org/10.1111/geb.12972

Mathias, J., & Hudiburg, T. (2022). *isocalcR*: An R package to streamline and standardize stable isotope calculations in ecological research. *Global Change Biology*, *28*, 7428-7436. https://doi.org/10.1111/gcb.16407

Mathur, S., Agrawal, D., & Jajoo, A. (2014). Photosynthesis: Response to high temperature stress. *Journal of Photochemistry and Photobiology B-Biology*, *137*, 116-126. https://doi.org/10.1016/j.jphotobiol.2014.01.010

Mathur, S., Mason, A., Bradburd, G., & Gibbs, L. (2023). Functional genomic diversity is correlated with neutral genomic diversity in populations of an endangered rattlesnake. *PNAS*, *120*, Article e2303043120. https://doi.org/10.1073/pnas.2303043120

Mau, A. C., Reed, S. C., Wood, T. E., & Cavaleri, M. A. (2018). Temperate and Tropical Forest Canopies are Already Functioning beyond Their Thermal Thresholds for Photosynthesis. *Forests*, *9*(1), 24, Article 47. https://doi.org/10.3390/f9010047

Maxwell, K., & Johnson, G. N. (2000). Chlorophyll fluorescence - a practical guide. *Journal of Experimental Botany*, *51*(345), 659-668. https://doi.org/10.1093/jexbot/51.345.659

McAdam, S. A. M., & Brodribb, T. J. (2015). The Evolution of Mechanisms Driving the Stomatal Response to Vapor Pressure Deficit. *Plant Physiology*, *167*(3), 833-843. https://doi.org/10.1104/pp.114.252940

McDonald, T., Jonson, J., & Dixon, K. W. (2016). National standards for the practice of ecological restoration in Australia. *Restoration Ecology*, *24*, S6-S32. https://doi.org/10.1111/rec.12359

Mcdowell, N., Pockman, W. T., Allen, C. D., Breshears, D. D., Cobb, N., Kolb, T., et al. (2008). Mechanisms of plant survival and mortality during drought: why do some plants survive while

others succumb to drought? *New Phytologist*, *178*(4), 719-739. https://doi.org/10.1111/j.1469-8137.2008.02436.x

Mcelwain, J. C., Yiotis, C., & Lawson, T. (2016). Using modern plant trait relationships between observed and theoretical maximum stomatal conductance and vein density to examine patterns of plant macroevolution. *New Phytologist*, *209*(1), 94-103. https://doi.org/10.1111/nph.13579

Medlyn, B. E., Duursma, R. A., Eamus, D., Ellsworth, D. S., Prentice, I. C., Barton, C. V. M., et al. (2011). Reconciling the optimal and empirical approaches to modelling stomatal conductance. *Global Change Biology*, *17*(6), 2134-2144. https://doi.org/10.1111/j.1365-2486.2010.02375.x

Meek, M. H., Beever, E. A., Barbosa, S., Fitzpatrick, S. W., Fletcher, N. K., Mittan-Moreau, C. S., et al. (2022). Understanding Local Adaptation to Prepare Populations for Climate Change. *Bioscience*, *73*(1), 36-47. https://doi.org/10.1093/biosci/biac101

Merila, J., & Hendry, A. P. (2014). Climate change, adaptation, and phenotypic plasticity: the problem and the evidence. *Evolutionary Applications*, *7*(1), 1-14. https://doi.org/10.1111/eva.12137

Michaletz, S. T., Weiser, M. D., McDowell, N. G., Zhou, J. Z., Kaspari, M., Helliker, B. R., & Enquist, B. J. (2016). The energetic and carbon economic origins of leaf thermoregulation. *Nature Plants*, *2*(9), Article 16129. https://doi.org/10.1038/nplants.2016.129

Michaletz, S. T., Weiser, M. D., Zhou, J. Z., Kaspari, M., Helliker, B. R., & Enquist, B. J. (2015). Plant Thermoregulation: Energetics, Trait-Environment Interactions, and Carbon Economics. *Trends in Ecology & Evolution*, *30*(12), 714-724. https://doi.org/10.1016/j.tree.2015.09.006

Middleby, K. B., Cheesman, A. W., & Cernusak, L. A. (2024). Impacts of elevated temperature and vapour pressure deficit on leaf gas exchange and plant growth across six tropical rainforest tree species. *New Phytologist*. https://doi.org/10.1111/nph.19822

Miller, B. D., Carter, K. R., Reed, S. C., Wood, T. E., & Cavaleri, M. A. (2021). Only sun-lit leaves of the uppermost canopy exceed both air temperature and photosynthetic thermal optima in a wet tropical forest. *Agricultural and Forest Meteorology*, *301*, 10, Article 108347. https://doi.org/10.1016/j.agrformet.2021.108347

Mitchard, E. T. A. (2018). The tropical forest carbon cycle and climate change. *Nature*, *559*(7715), 527-534. https://doi.org/10.1038/s41586-018-0300-2

Mokany, K., Ware, C., Woolley, S. N. C., Ferrier, S., & Fitzpatrick, C., Matthew. (2022). A working guide to harnessing generalized dissimilarity modelling for biodiversity analysis and conservation assessment. *Global Ecology and Biogeography*, *31*(4), 802-821. https://doi.org/10.1111/geb.13459

Monteith, J., & Unsworth, M. (2013). *Principles of Environmental Physics* (4 ed.). Academic Press. https://doi.org/https://doi.org/10.1016/B978-0-12-386910-4.00020-2.

Muehleisen, A. J., Engelbrecht, B. M. J., Jones, F. A., Manzane-Pinzon, E., & Comita, L. S. (2020). Local adaptation to herbivory within tropical tree species along a rainfall gradient. *Ecology*, *101*(11). https://doi.org/10.1002/ecy.3151

Muggeo, V. M. (2003). Estimating regression models with unknown break-points. *Statistics in Medicine*, *22*, 3055-3071. https://doi.org/https://doi.org/10.1002/sim.1545

Mujawamariya, M., Wittemann, M., Dusenge, M. E., Manishimwe, A., Ntirugulirwa, B., Zibera, E., et al. (2023). Contrasting warming responses of photosynthesis in early- and late-successional tropical trees. *Tree Physiology*, *43*(7), 1104-1117. https://doi.org/10.1093/treephys/tpad035

Murtha, G. G. (1989). *Soils of the Mossman Cape Tribulation Area, North Queensland* (Division of Soils Divisional Report; no. 102)

Mushagalusa, F. C., Bauman, D., Bazirake, B. M., Mleci, Y., Kalenga, M., Shutcha, M. N., & Meerts, P. (2020). Phenotypic plasticity, not ecotype differentiation, explains the broad ecological niche of a tree species in African dry woodlands. *Environmental and Experimental Botany*, *178*, 8, Article 104186. https://doi.org/10.1016/j.envexpbot.2020.104186

Muñoz, M. (2022). The Bogert effect, a factor in evolution. *Evolution*, *76*, 49-66. https://doi.org/10.1111/evo.14388

Muñoz, M. M., & Bodensteiner, B. L. (2019). Janzen's Hypothesis Meets the Bogert Effect: Connecting Climate Variation, Thermoregulatory Behavior, and Rates of Physiological Evolution. *Integrative Organismal Biology*, *1*(1). https://doi.org/10.1093/iob/oby002

Müller, K., & Albach, D. C. (2010). Evolutionary Rates in Veronica L. (Plantaginaceae): Disentangling the Influence of Life History and Breeding System. *Journal of Molecular Evolution*, *70*(1), 44-56. https://doi.org/10.1007/s00239-009-9307-5

Neri, P., Gu, L., & Song, Y. (2024). The effect of temperature on photosystem II efficiency across plant functional types and climate. In *Biogeosciences* (Vol. 21, pp. 2731-2758).

O'Sullivan, O. S., Heskel, M. A., Reich, P. B., Tjoelker, M. G., Weerasinghe, L. K., Penillard, A., et al. (2017). Thermal limits of leaf metabolism across biomes [Article]. *Global Change Biology*, *23*(1), 209-223. https://doi.org/10.1111/gcb.13477

Offord, C. A., & Meagher, P. F. (2009). *Plant germplasm conservation in Australia: strategies and guidelines for developing, managing and utilising ex situ collections.* Australian Network for Plant Conservation Inc.

Oksanen, J., Simpson, G., Blanchet, F., Kindt, R., Legendre, P., Minchin, P., & al., e. (2022). vegan: Community Ecology Package. In (Vol. R package version 2.6-4).

Olsoy, P. J., Zaiats, A., Delparte, D. M., Germino, M. J., Richardson, B. A., Roop, S., et al. (2023). High-resolution thermal imagery reveals how interactions between crown structure and genetics shape

plant temperature. *Remote Sensing in Ecology and Conservation*, *10*(1), 106-120. https://doi.org/10.1002/rse2.359

Pau, S., Detto, M., Kim, Y., & Still, C. J. (2018). Tropical forest temperature thresholds for gross primary productivity. *Ecosphere*, *9*(7), Article e02311. https://doi.org/10.1002/ecs2.2311

Peak, D., & Mott, K. A. (2011). A new, vapour-phase mechanism for stomatal responses to humidity and temperature. *Plant, Cell & Environment*, *34*(1), 162-178. https://doi.org/10.1111/j.1365-3040.2010.02234.x

Pearcy, R. W. E., J.R., Mooney, H. A., & Rundel, P. W. (1989). *Plant Physiological Ecology: Field methods and instrumentation* (1 ed.). Springer. https://doi.org/https://doi.org/10.1007/978-94-009-2221-1

Perera, R. S., Cullen, B. R., & Eckard, R. J. (2020). Using Leaf Temperature to Improve Simulation of Heat and Drought Stresses in a Biophysical Model. *Plants-Basel*, *9*(1), 20, Article 8. https://doi.org/10.3390/plants9010008

Perez, T. M., & Feeley, K. J. (2018). Increasing Humidity Threatens Tropical Rainforests. *Frontiers in Ecology and Evolution*, *6*, 2, Article 68. https://doi.org/10.3389/fevo.2018.00068

Perez, T. M., & Feeley, K. J. (2020). Photosynthetic heat tolerances and extreme leaf temperatures. *Functional Ecology*, *34*(11), 2236-2245. https://doi.org/10.1111/1365-2435.13658

Perez-Harguindeguy, N., Diaz, S., Garnier, E., Lavorel, S., Poorter, H., Jaureguiberry, P., et al. H. C. (2013). New handbook for standardised measurement of plant functional traits worldwide. *Australian Journal of Botany*, *61*(3), 167-234. https://doi.org/10.1071/bt12225

Ponce De León, M. A., & Bailey, B. N. (2024). Quantifying water-use efficiency in plant canopies with varying leaf angle and density distribution. *Annals of Botany*, *133*(4), 605-620. https://doi.org/10.1093/aob/mcae018

Poorter, L., Wright, S. J., Paz, H., Ackerly, D. D., Condit, R., Ibarra-Manríques, G., et al. (2008). Are functional traits good predictors of demographic rates?: Evidence from five Neotropical forests [Article]. *Ecology*, *89*(7), 1908-1920. https://doi.org/10.1890/07-0207.1

Posch, B. C., Hammer, J., Atkin, O. K., Bramley, H., Ruan, Y. L., Trethowan, R., & Coast, O. (2022). Wheat photosystem II heat tolerance responds dynamically to short- and long-term warming. *Journal of Experimental Botany*, *73*(10), 3268-3282. https://doi.org/10.1093/jxb/erac039

Preece, N. D., Lawes, M. J., Rossman, A. K., Curran, T. J., & van Oosterzee, P. (2015). Modelling the growth of young rainforest trees for biomass estimates and carbon sequestration accounting. *Forest Ecology and Management*, *351*, 57-66. https://doi.org/10.1016/j.foreco.2015.05.003

Preece, N. D., van Oosterzee, P., Unda, G. C. H., & Lawes, M. J. (2017). National carbon model not sensitive to species, families and site characteristics in a young tropical reforestation project. *Forest Ecology and Management*, *392*, 115-124. https://doi.org/10.1016/j.foreco.2017.02.052

Quebbeman, J. A., & Ramirez, J. A. (2016). Optimal allocation of leaf-level nitrogen: Implications for covariation of V_{cmax} and J_{max} and photosynthetic downregulation. *Journal of Geophysical Research: Biogeosciences*, *121*(9), 2464-2475. https://doi.org/10.1002/2016jg003473

R Core Team. (2022). *R: A language and environmental for statistical computing*. In (Version 4.2.2) R Foundation for Statistical Computing. http://www.R-project.org

Ramesh, A. S., Cheesman, A. W., Flores-Moreno, H., Preece, N. D., Crayn, D. M., & Cernusak, L. A. (2023). Temperature, nutrient availability, and species traits interact to shape elevation responses of Australian tropical trees. *Frontiers in Forests and Global Change*, *6*, Article 1089167. https://doi.org/10.3389/ffgc.2023.1089167

Ravn, J., Taylor, A. R., Lavigne, M. B., & D'Orangeville, L. (2024). Local adaptation of balsam fir seedlings improves growth resilience to heat stress. *Canadian Journal of Forest Research*, *54*(3), 331-343. https://doi.org/10.1139/cjfr-2023-0128

Reed, D. H., & Frankham, R. (2003). Correlation between fitness and genetic diversity. *Conservation Biology*, *17*(1), 230-237. https://doi.org/10.1046/j.1523-1739.2003.01236.x

Rehm, E. M., Olivas, P., Stroud, J., & Feeley, K. J. (2015). Losing your edge: climate change and the conservation value of range-edge populations. *Ecology and Evolution*, *5*(19), 4315-4326. https://doi.org/10.1002/ece3.1645

Reich, P. B. (2014). The world-wide 'fast-slow' plant economics spectrum: a traits manifesto. *Journal of Ecology*, *102*(2), 275-301. https://doi.org/10.1111/1365-2745.12211

Rey-Sanchez, A. C., Slot, M., Posada, J. M., & Kitajima, K. (2017). Spatial and seasonal variation in leaf temperature within the canopy of a tropical forest. *Climate Research*, *71*(1), 75-89. https://doi.org/10.3354/cr01427

Riahi, K., Schaeffer, R., Arango, J., Calvin, K., Guivarch, C., Hasegawa, T., et al. (2022). Mitigation pathways compatible with long-term goals. In P. R. Shukla, J. Skea, R. Slade, A. Al-Khourdajie, R. van Diemen, D. McCollum, M. Pathak, S. Some, P. Vuyas, R. Fradera, M. Belkacemi, A. Hasija, G. Lisboa, S. Luz, & J. Malley (Eds.), *In IPCC, 2022: Climate Change 2022: Mitigation of Climate Change. Contribution of Working Group III to the Sixth Assessment Report of the Intergovernmental Panel on Climate Change*. Cambridge University Press.

Ritz, C., Baty, F., Streibig, J. C., & Gerhard, D. (2015). Dose-Response Analysis Using R. *PLOS ONE*, *10*(12), e0146021. https://doi.org/10.1371/journal.pone.0146021

Rossetto, M., Bragg, J., Kilian, A., McPherson, H., van der Merwe, M., & Wilson, P. D. (2019). Restore and Renew: a genomics-era framework for species provenance delimitation. *Restoration Ecology*, *27*(3), 538-548. https://doi.org/10.1111/rec.12898

Ryan, M. G., & Yoder, B. J. (1997). Hydraulic Limits to Tree Height and Tree Growth. *BioScience*, *47*(4), 235-242. https://doi.org/10.2307/1313077

Réjou-Méchain, M., Tanguy, A., Piponiot, C., Chave, J., & Hérault, B. (2017). *biomass*: an r package for estimating above-ground biomass and its uncertainty in tropical forests. *Methods in Ecology and Evolution*, *8*(9), 1163-1167. https://doi.org/10.1111/2041-210x.12753

Sack, L., & Buckley, T. (2016). The Developmental Basis of Stomatal Density and Flux. *Plant Physiology*, *171*, 2358-2363. https://doi.org/10.1104/pp.16.00476

Sack, L., & Scoffoni, C. (2007). *Minimum epidermal conductance (gmin, a.k.a. cuticular conductance)*. Retrieved 10/01/2023 from https://prometheusprotocols.net/function/gas-exchange-and-chlorophyll-fluorescence/stomatal-and-non-stomatal-conductance-and-transpiration/minimum-epidermal-conductance-gmin-a-k-a-cuticular-conductance/

Sadok, W., Lopez, J. R., & Smith, K. P. (2021). Transpiration increases under high-temperature stress: Potential mechanisms, trade-offs and prospects for crop resilience in a warming world. *Plant, Cell & Environment*, *44*(7), 2102-2116. https://doi.org/10.1111/pce.13970

Sansaloni, C. P., Petroli, C. D., Carling, J., Hudson, C. J., Steane, D. A., Myburg, A. A., et al. (2010). A high-density Diversity Arrays Technology (DArT) microarray for genome-wide genotyping in *Eucalyptus*. *Plant Methods*, *6*, Article 16. https://doi.org/10.1186/1746-4811-6-16

Schlaepfer, D. R., Braschler, B., Rusterholz, H. P., & Baur, B. (2018). Genetic effects of anthropogenic habitat fragmentation on remnant animal and plant populations: a meta-analysis. *Ecosphere*, *9*(10), 17, Article e02488. https://doi.org/10.1002/ecs2.2488

Schneider, C. J., Cunningham, M., & Moritz, C. (1998). Comparative phylogeography and the history of endemic vertebrates in the Wet Tropics rainforests of Australia. *Molecular Ecology*, *7*(4), 487-498. https://doi.org/10.1046/j.1365-294x.1998.00334.x

Schonbeck, L., Schuler, P., Lehmann, M. M., Mas, E., Mekarni, L., Pivovaroff, A. L., et al. (2022). Increasing temperature and vapour pressure deficit lead to hydraulic damages in the absence of soil drought. *Plant, Cell & Environment*, *45*(11), 3275-3289. https://doi.org/10.1111/pce.14425

Schreiber, U. (1986). Detection of rapid induction kinetics with a new type of high-frequency modulated chlorophyll fluorometer. *Photosynthesis Research*, *9*(1-2), 261-272. https://doi.org/10.1007/bf00029749

Schuster, A. C., Burghardt, M., Alfarhan, A., Bueno, A., Hedrich, R., Leide, J.,…Riederer, M. (2016). Effectiveness of cuticular transpiration barriers in a desert plant at controlling water loss at high temperatures. *Aob Plants*, *8*, Article plw027. https://doi.org/10.1093/aobpla/plw027

Schwinning, S., Lortie, C. J., Esque, T. C., & DeFalco, L. A. (2022). What common-garden experiments tell us about climate responses in plants. *Journal of Ecology*, *110*(5), 986-996. https://doi.org/https://doi.org/10.1111/1365-2745.13887

Shane, M. W., McCully, M. E., & Lambers, H. (2004). Tissue and cellular phosphorus storage during development of phosphorus toxicity in Hakea prostrata (Proteaceae). *Journal of Experimental Botany*, *55*(399), 1033-1044. https://doi.org/10.1093/jxb/erh111

Shirke, P. A. (2004). Influence of leaf-to-air vapour pressure deficit (VPD) on the biochemistry and physiology of photosynthesis in Prosopis juliflora. *Journal of Experimental Botany*, *55*(405), 2111-2120. https://doi.org/10.1093/jxb/erh229

Shryock, D. F., Havrilla, C. A., Defalco, L. A., Esque, T. C., Custer, N. A., & Wood, T. E. (2015). Landscape genomics of Sphaeralcea ambigua in the Mojave Desert: a multivariate, spatially-explicit approach to guide ecological restoration. *Conservation Genetics*, *16*(6), 1303-1317. https://doi.org/10.1007/s10592-015-0741-1

Shryock, D. F., Washburn, L. K., DeFalco, L. A., & Esque, T. C. (2021). Harnessing landscape genomics to identify future climate resilient genotypes in a desert annual. *Molecular Ecology*, 20. https://doi.org/10.1111/mec.15672

Slot, M., Cala, D., Aranda, J., Virgo, A., Michaletz, S. T., & Winter, K. (2021). Leaf heat tolerance of 147 tropical forest species varies with elevation and leaf functional traits, but not with phylogeny. *Plant, Cell & Environment. In press.*, *44*(7), 2414-2427. https://doi.org/doi:10.1111/pce.14060

Slot, M., Krause, G. H., Krause, B., Hernandez, G. G., & Winter, K. (2019). Photosynthetic heat tolerance of shade and sun leaves of three tropical tree species. *Photosynthesis Research*, *141*(1), 119-130. https://doi.org/10.1007/s11120-018-0563-3

Slot, M., Nardwattanawong, T., Hernández, G. G., Bueno, A., Riederer, M., & Winter, K. (2021). Large differences in leaf cuticle conductance and its temperature response among 24 tropical tree species from across a rainfall gradient. *New Phytologist*, *232*(4), 1618-1631. https://doi.org/10.1111/nph.17626

Smith, M. N., Taylor, T. C., van Haren, J., Rosolem, R., Restrepo-Coupe, N., Adams, J., et al. (2020). Empirical evidence for resilience of tropical forest photosynthesis in a warmer world. *Nature Plants*, *6*(10), 1225-1230. https://doi.org/10.1038/s41477-020-00780-2

Smith, S. A., & Beaulieu, J. M. (2009). Life history influences rates of climatic niche evolution in flowering plants. *Proceedings of the Royal Society B-Biological Sciences*, *276*(1677), 4345-4352. https://doi.org/10.1098/rspb.2009.1176

Smith, S. A., & Donoghue, M. J. (2008). Rates of molecular evolution are linked to life history in flowering plants. *Science*, *322*(5898), 86-89. https://doi.org/10.1126/science.1163197

Song, X., Barbour, M. M., Saurer, M., & Helliker, B. R. (2011). Examining the large-scale convergence of photosynthesis-weighted tree leaf temperatures through stable oxygen isotope analysis of multiple data sets. *New Phytologist*, *192*(4), 912-924. https://doi.org/10.1111/j.1469-8137.2011.03851.x

Sork, V. L., Aitken, S. N., Dyer, R. J., Eckert, A. J., Legendre, P., & Neale, D. B. (2013). Putting the landscape into the genomics of trees: approaches for understanding local adaptation and population responses to changing climate. *Tree Genetics & Genomes*, *9*(4), 901-911. https://doi.org/10.1007/s11295-013-0596-x

Stanton, M. L., & Thiede, D. A. (2005). Statistical convenience vs biological insight: consequences of data transformation for the analysis of fitness variation in heterogeneous environments. *New Phytologist*, *166*(1), 319-338. https://doi.org/10.1111/j.1469-8137.2004.01311.x

Steane, D. A., Potts, B. M., McLean, E., Prober, S. M., Stock, W. D., Vaillancourt, R. E., & Byrne, M. (2014). Genome-wide scans detect adaptation to aridity in a widespread forest tree species. *Molecular Ecology*, *23*(10), 2500-2513. https://doi.org/10.1111/mec.12751

Stephens, R., Sauquet, H., Guerin, G., Jiang, M., Falster, D., & Gallagher, R. (2022). Climate shapes community flowering periods across biomes. In *Journal of Biogeography* (Vol. 49, pp. 1205-1218).

Still, C. J., Page, G., Rastogi, B., Griffith, D. M., Aubrecht, D. M., Kim, Y., et al. (2022). No evidence of canopy-scale leaf thermoregulation to cool leaves below air temperature across a range of forest ecosystems. *Proceedings of the National Academy of Sciences*, *119*(38). https://doi.org/10.1073/pnas.2205682119

Still, C. J., Page, G. F. M., Rastogi, B., Griffith, D. M., Aubrecht, D. M., Kim, Y., et al. (2023). Reply to Garen et al.: Within-canopy temperature data also do not support limited homeothermy. *Proceedings of the National Academy of Sciences*, *120*(15). https://doi.org/10.1073/pnas.2302515120

Tarvainen, L., Wittemann, M., Mujawamariya, M., Manishimwe, A., Zibera, E., Ntirugulirwa, B., et al. (2022). Handling the heat – photosynthetic thermal stress in tropical trees. *New Phytologist*, *233*(1), 236-250. https://doi.org/10.1111/nph.17809

Threatened Species Scientific Comittee (2021). *Approved Conservation Advice for the Lowland tropical rainforest of the Wet Tropics*. Department of Agriculture, Water and the Environment.

Tito, R., Vasconcelos, H. L., & Feeley, K. J. Multi-population seedling and soil transplants show possible responses of a common tropical montane tree species (*Weinmannia bangii*) to climate change. *Journal of Ecology*. https://doi.org/10.1111/1365-2745.13443

Tiwari, R., Gloor, E., da Cruz, W. J. A., Marimon, B. S., Marimon, B., Reis, S. M., et al. (2020). Photosynthetic quantum efficiency in south-eastern Amazonian trees may be already affected by climate change. *Plant Cell and Environment*. https://doi.org/10.1111/pce.13770

Trew, B. T., & Maclean, I. M. D. (2021). Vulnerability of global biodiversity hotspots to climate change. *Global Ecology and Biogeography*, *30*(4), 768-783. https://doi.org/10.1111/geb.13272

Tserej, O., & Feeley, K. J. (2021). Variation in leaf temperatures of tropical and subtropical trees are related to leaf thermoregulatory traits and not geographic distributions. *Biotropica*, 11. https://doi.org/10.1111/btp.12919

UNESCO World Heritage Centre (1988). Inscription: Wet Tropics of Queensland (Australia). In *World Heritage List*.

Resolution adopted by the General Assembly on 1 March 2019: United Nations Decade on Ecosystem Restoration (2021–2030) (2019).

Urban, J., Ingwers, M., McGuire, M. A., & Teskey, R. O. (2017a). Stomatal conductance increases with rising temperature. *Plant Signaling & Behavior*, *12*(8), 3, Article e1356534. https://doi.org/10.1080/15592324.2017.1356534

Urban, J., Ingwers, M. W., McGuire, M. A., & Teskey, R. O. (2017b). Increase in leaf temperature opens stomata and decouples net photosynthesis from stomatal conductance in Pinus taeda and Populus deltoides x nigra [Article]. *Journal of Experimental Botany*, *68*(7), 1757-1767. https://doi.org/10.1093/jxb/erx052

Vancutsem, C., Achard, F., Pekel, J. F., Vieilledent, G., Carboni, S., Simonetti, D., et al. (2021). Long-term (1990-2019) monitoring of forest cover changes in the humid tropics. *Science Advances*, *7*(10), Article eabe1603. https://doi.org/10.1126/sciadv.abe1603

Vogado, N. O., Liddell, M. J., Laurance, S. G. W., Campbell, M. J., Cheesman, A. W., Engert, J. E., et al. (2020). The effects of an experimental drought on the ecophysiology and fruiting phenology of a tropical rainforest palm. *Journal of Plant Ecology*, *13*(6), 744-753. https://doi.org/10.1093/jpe/rtaa069

Wadgymar, S., DeMarche, M., Josephs, E., Sheth, S., & Anderson, J. (2022). Local Adaptation: Causal Agents of Selection and Adaptive Trait Divergence. In *Annual Review of Ecology Evolution and Systematics* (Vol. 53, pp. 87-111).

Wahid, A., Gelani, S., Ashraf, M., & Foolad, M. R. (2007). Heat tolerance in plants: An overview. *Environmental and Experimental Botany*, *61*(3), 199-223. https://doi.org/10.1016/j.envexpbot.2007.05.011

Walker, A. P., Beckerman, A. P., Gu, L., Kattge, J., Cernusak, L. A., Domingues, T. F., et al. (2014). The relationship of leaf photosynthetic traits -Vcmax and Jmax- to leaf nitrogen, leaf phosphorus, and specific leaf area: a meta-analysis and modeling study. *Ecology and Evolution*, *4*(16), 3218-3235. https://doi.org/10.1002/ece3.1173

Wang, H., Prentice, I. C., Keenan, T. F., Davis, T. W., Wright, I. J., Cornwell, W. K., et al. (2017). Towards a universal model for carbon dioxide uptake by plants. *Nature Plants*, *3*(9), 734-741. https://doi.org/10.1038/s41477-017-0006-8

Wang, R., Li, L., Gentine, P., Zhang, Y., Chen, J., Chen, X., et al. (2022). Recent increase in the observation-derived land evapotranspiration due to global warming. *Environmental Research Letters*, *17*(2), 024020. https://doi.org/10.1088/1748-9326/ac4291

Watson, J. E. M., Evans, T., Venter, O., Williams, B., Tulloch, A., Stewart, C., et al. (2018). The exceptional value of intact forest ecosystems. *Nature Ecology & Evolution*, *2*(4), 599-610. https://doi.org/10.1038/s41559-018-0490-x

Weigand, H., & Leese, F. (2018). Detecting signatures of positive selection in non-model species using genomic data. *Zoological Journal of the Linnean Society*, *184*(2), 528-583. https://doi.org/10.1093/zoolinnean/zly007

Weir, B. S., & Hill, W. G. (2002). Estimating F-statistics. In (Vol. 36, pp. 721-750): Annu. Rev. Genet.

Westerband, A. C., Funk, J. L., & Barton, K. E. (2021). Intraspecific trait variation in plants: a renewed focus on its role in ecological processes. *Annals of Botany*, *127*(4), 397-410. https://doi.org/10.1093/aob/mcab011

Willi, Y., & Van Buskirk, J. (2022). A review on trade-offs at the warm and cold ends of geographical distributions. *Philosophical Transactions of the Royal Society B: Biological Sciences*, *377*(1848). https://doi.org/10.1098/rstb.2021.0022

Woods, H. A., Saudreau, M., & Pincebourde, S. (2018). Structure is more important than physiology for estimating intracanopy distributions of leaf temperatures. *Ecology and Evolution*, *8*(10), 5206-5218. https://doi.org/10.1002/ece3.4046

Wright, I. J., Dong, N., Maire, V., Prentice, I. C., Westoby, M., Diaz, S., et al. (2017). Global climatic drivers of leaf size. *Science*, *357*(6354), 917-921. https://doi.org/10.1126/science.aal4760

Wright, I. J., Reich, P. B., Westoby, M., Ackerly, D. D., Baruch, Z., Bongers, F., et al. (2004). The worldwide leaf economics spectrum. *Nature*, *428*(6985), 821-827. https://doi.org/10.1038/nature02403

Wright, S. J., Kitajima, K., Kraft, N. J. B., Reich, P. B., Wright, I. J., Bunker, D. E., et al. (2010). Functional traits and the growth-mortality trade-off in tropical trees. *Ecology*, *91*(12), 3664-3674. https://doi.org/10.1890/09-2335.1

Wu, J., Serbin, S. P., Ely, K. S., Wolfe, B. T., Dickman, L. T., Grossiord, C., et al. (2020). The response of stomatal conductance to seasonal drought in tropical forests. *Global Change Biology*, *26*(2), 823-839. https://doi.org/10.1111/gcb.14820

Yamori, W., Hikosaka, K., & Way, D. A. (2014). Temperature response of photosynthesis in C3, C4, and CAM plants: temperature acclimation and temperature adaptation. *Photosynthesis Research*, *119*(1-2), 101-117. https://doi.org/10.1007/s11120-013-9874-6

Yang, J., Duursma, R. A., De Kauwe, M. G., Kumarathunge, D., Jiang, M., Mahmud, K., et al. (2019). Incorporating non-stomatal limitation improves the performance of leaf and canopy models at high vapour pressure deficit. *Tree Physiology*, *39*(12), 1961-1974. https://doi.org/10.1093/treephys/tpz103

Yang, X., Li, R., Jablonski, A., Stovall, A., Kim, J., Yi, K., et al. (2023). Leaf angle as a leaf and canopy trait: Rejuvenating its role in ecology with new technology. *Ecology Letters*, *26*(6), 1005-1020. https://doi.org/10.1111/ele.14215

Yuan, W. P., Zheng, Y., Piao, S. L., Ciais, P., Lombardozzi, D., Wang, Y. P., et al. (2019). Increased atmospheric vapor pressure deficit reduces global vegetation growth. *Science Advances*, *5*(8), 12, Article eaax1396. https://doi.org/10.1126/sciadv.aax1396

Zhang, D. L., Jiao, X. C., Du, Q. J., Song, X. M., & Li, J. M. (2018). Reducing the excessive evaporative demand improved photosynthesis capacity at low costs of irrigation via regulating water driving force and moderating plant water stress of two tomato cultivars. *Agricultural Water Management*, *199*, 22-33. https://doi.org/10.1016/j.agwat.2017.11.014

Zheng, X., Levine, D., Shen, J., Gogarten, S. M., Laurie, C., & Weir, B. S. (2012). A high-performance computing toolset for relatedness and principal component analysis of SNP data. *Bioinformatics*, *28*(24), 3326-3328. https://doi.org/10.1093/bioinformatics/bts606

Zhou, S. X., Duursma, R. A., Medlyn, B. E., Kelly, J. W. G., & Prentice, I. C. (2013). How should we model plant responses to drought? An analysis of stomatal and non-stomatal responses to water stress. *Agricultural and Forest Meteorology*, *182*, 204-214. https://doi.org/10.1016/j.agrformet.2013.05.009

Zhou, Y. Y., Kitudom, N., Fauset, S., Slot, M., Fan, Z. X., Wang, J. P., et al. (2023). Leaf thermal regulation strategies of canopy species across four vegetation types along a temperature and precipitation gradient. *Agricultural and Forest Meteorology*, *343*, Article 109766. https://doi.org/10.1016/j.agrformet.2023.109766

Zhu, L. L., Bloomfield, K. J., Hocart, C. H., Egerton, J. J. G., O'Sullivan, O. S., Penillard, A., et al. (2018). Plasticity of photosynthetic heat tolerance in plants adapted to thermally contrasting biomes. *Plant Cell and Environment*, *41*(6), 1251-1262. https://doi.org/10.1111/pce.13133

Zimmermann, N. E., Yoccoz, N. G., Edwards, T. C., Meier, E. S., Thuiller, W., Guisan, A., et al. (2009). Climatic extremes improve predictions of spatial patterns of tree species. *Proceedings of the*

National Academy of Sciences of the United States of America, *106*, 19723-19728. https://doi.org/10.1073/pnas.0901643106

Zuleta, D., Muller-Landau, H., Duque, A., Caro, N., Cardenas, D., Castaño, N., et al. (2022). Interspecific and intraspecific variation of tree branch, leaf and stomatal traits in relation to topography in an aseasonal Amazon forest. *Functional Ecology*, *36*, 2955-2968. https://doi.org/10.1111/1365-2435.14199

Appendix A: Supporting information for Chapter 2

The following Supporting Information is available for Chapter 2:

Table 1. Table with trait means and one standard deviation for each species, treatment, and trait studied.

Figure 1. Treatment impacts on acclimation of g1 (a), leaf minimum conductance, gmin (b) and leaf width (c) for each species.

Figure 2. Treatment impacts on Vcmax25 (a), Jmax25 (b) and their ratio, JVr (c) for each species.

Figure 3. Treatment impacts on thermal tolerance, Tcrit (a), specific leaf area, SLA (b), and leaf dry matter content, LDMC (c) for each species.

Appendix A: Table 1. Table with trait means and one standard deviation for each species, treatment, and trait studied.

Species	Variable	Low T_{air} Low VPD		High T_{air} Low VPD		High T_{air} High VPD	
		Mean	SD	Mean	SD	Mean	SD
Melicope elleryana	A_{net}	15.88	2.99	15.72	1.78	13.00	3.30
	g_s	0.38	0.14	0.53	0.14	0.22	0.10
	iWUE	49.01	25.85	31.08	6.84	63.83	17.13
	g_1	4.70	1.63	7.20	1.81	3.10	0.98
	V_{cmax25}	52.08	5.17	47.94	5.69	45.72	9.96
	J_{max25}	107.21	14.88	95.21	12.48	94.11	18.50
	JV_r	2.06	NA	1.99	NA	2.07	NA
	T_{crit}	44.06	1.34	47.47	1.08	45.64	1.13
	g_{min}	0.71	0.26	0.76	0.37	0.79	0.49
	Leaf width	6.90	0.63	6.92	0.54	6.43	1.25
	SLA	18.49	4.11	20.91	3.02	18.76	3.27
	LDMC	275.37	43.94	259.28	35.58	269.48	37.02
	Total biomass	177.30	26.18	217.40	33.7	181.81	28.36
Ficus racemosa	A_{net}	16.89	1.74	14.84	1.96	14.64	1.59
	g_s	0.49	0.12	0.43	0.23	0.31	0.13
	iWUE	35.23	6.18	40.33	15.86	54.22	20.47
	g_1	6.07	1.15	5.86	2.54	4.10	1.97
	V_{cmax25}	57.31	5.31	47.34	3.90	50.38	6.51
	J_{max25}	103.52	7.37	72.97	9.06	81.42	16.25
	JV_r	1.81	NA	1.54	NA	1.60	NA
	T_{crit}	45.61	1.38	47.42	0.84	46.73	0.40
	g_{min}	1.64	0.53	1.86	1.18	1.47	0.74
	Leaf width	6.50	0.65	7.07	0.74	6.29	0.71
	SLA	16.57	0.50	15.62	1.56	16.14	1.65
	LDMC	300.65	13.98	305.55	4.05	300.34	20.29
	Total biomass	162.56	12.39	236.53	14.68	188.11	19.64
Atractocarpus fitzalanii	A_{net}	12.45	1.54	11.89	1.05	11.68	1.32
	g_s	0.28	0.07	0.30	0.11	0.26	0.05
	iWUE	47.66	13.28	44.71	18.05	46.47	12.32
	g_1	4.47	1.05	5.23	2.30	4.60	1.29
	V_{cmax25}	40.45	3.17	37.68	2.79	39.33	6.29
	J_{max25}	113.14	9.37	95.6	8.94	99.07	16.70
	JV_r	2.80	NA	2.54	NA	2.52	NA
	T_{crit}	47.76	0.72	49.17	1.79	48.89	1.12
	g_{min}	0.07	0.04	0.13	0.04	0.08	0.02
	Leaf width	12.30	1.15	9.32	1.44	9.89	0.74
	SLA	8.07	0.75	8.29	0.67	8.61	0.72
	LDMC	343.10	31.06	333.48	16.54	339.17	19.26
	Total biomass	126.08	30.35	148.84	21.87	153.36	29.92

Nauclea orientalis	A_{net}	10.82	2.11	15.16	2.50	13.40	1.47
	g_s	0.17	0.08	0.66	0.07	0.29	0.09
	iWUE	70.84	21.74	23.43	4.82	52.14	20.88
	g_1	2.84	1.07	9.86	2.95	4.38	1.81
	V_{cmax25}	39.55	6.53	48.27	5.44	44.07	7.89
	J_{max25}	79.33	8.44	76.65	7.64	75.49	15.62
	JV_r	2.03	NA	1.59	NA	1.71	NA
	T_{crit}	48.15	1.04	48.54	0.71	48.83	0.91
	g_{min}	0.50	0.27	0.29	0.21	0.40	0.10
	Leaf width	13.09	1.12	14.64	1.48	12.31	2.28
	SLA	15.48	2.19	15.8	2.32	15.76	1.81
	LDMC	212.11	25.39	220.83	17.38	226.18	21.93
	Total biomass	172.11	22.05	219.62	25.32	190.62	31.37
Buckinghamia celssisima	A_{net}	9.66	1.77	9.29	1.74	8.03	1.26
	g_s	0.31	0.05	0.26	0.09	0.15	0.03
	iWUE	32.22	8.89	38.57	12.14	57.75	15.28
	g_1	7.08	2.02	5.84	1.58	3.62	1.32
	V_{cmax25}	29.61	8.05	29.1	5.28	28.43	6.55
	J_{max25}	73.55	18.51	65.26	9.17	65.57	8.46
	JV_r	2.52	NA	2.26	NA	2.37	NA
	T_{crit}	45.93	1.19	47.16	0.87	47.02	0.80
	g_{min}	0.24	0.05	0.57	0.32	0.45	0.10
	Leaf width	2.60	0.34	2.15	0.46	2.39	0.54
	SLA	9.98	0.98	10.07	0.70	10.42	0.89
	LDMC	466.54	15.37	452.75	19.26	436.04	31.56
	Total biomass	151.55	18.81	180.61	23.92	153.73	23.99
Endiandra microneura	A_{net}	8.53	1.97	7.71	1.88	6.00	1.29
	g_s	0.09	0.03	0.09	0.03	0.05	0.01
	iWUE	100.97	9.30	95.31	24.91	126.53	13.93
	g_1	1.56	0.20	1.87	0.75	1.05	0.20
	V_{cmax25}	39.56	4.11	35.78	8.77	38.72	9.56
	J_{max25}	94.98	14.64	77.42	13.76	83.43	10.07
	JV_r	2.40	NA	2.20	NA	2.24	NA
	T_{crit}	46.40	1.11	48.64	0.69	48.65	0.79
	g_{min}	0.41	0.16	0.27	0.08	0.26	0.11
	Leaf width	6.00	1.58	6.85	1.26	6.16	1.03
	SLA	11.04	1.01	12.21	1.17	12.2	1.19
	LDMC	372.60	37.03	339.54	31.90	342.5	38.98
	Total biomass	70.87	15.90	99.37	24.54	94.36	22.90

Note: JV_r = ratio of J_{max25} to V_{cmax25} and LDMC = leaf dry matter content.

Appendix A: Figure 1. Treatment impacts on acclimation of g_1 (a), leaf minimum conductance, g_{min} (b) and leaf width (c) for each species. Species are ordered in decreasing stomatal sensitivity to VPD (top panel is high sensitivity, bottom panel is low sensitivity). Box and whisker plots show the median, the 25th and 75th percentile, along with 1.5*interquartile range. Colours represent the different treatments. Significant differences between treatments from Tukey Post Hoc results ($p < 0.05$) denoted with letters. Note that data for g_{min} were transformed for analysis, but untransformed values are presented here.

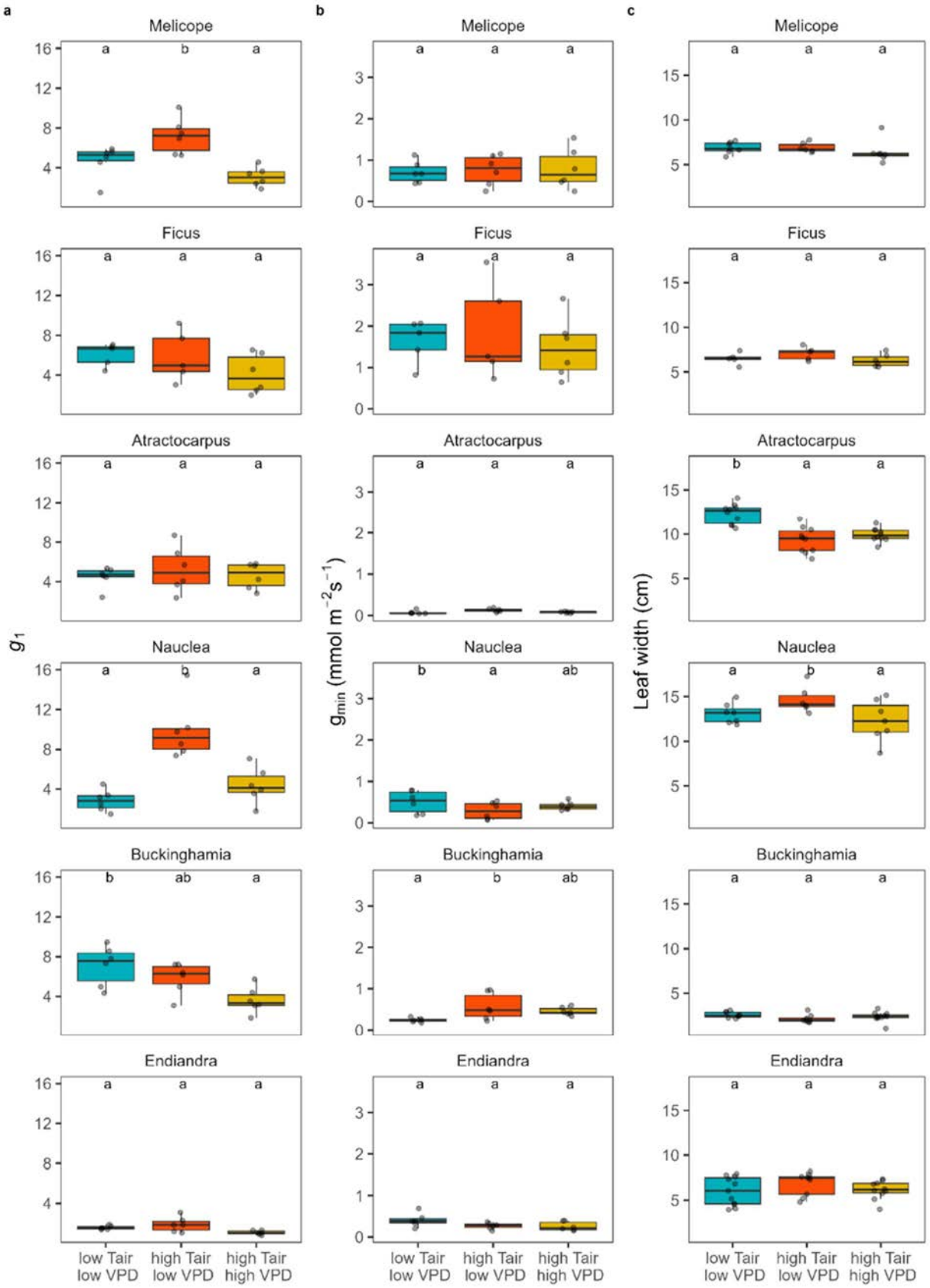
a
b
c
Melicope
Ficus
Atractocarpus
Nauclea
Buckinghamia
Endiandra
g_1
g_{min} (mmol m^{-2}s^{-1})
Leaf width (cm)
low Tair low VPD
high Tair low VPD
high Tair high VPD

Appendix A: Figure 2. Treatment impacts on Vcmax25 (a), Jmax25 (b) and their ratio, JVr (c) for each species. Species are ordered in decreasing stomatal sensitivity to VPD (top panel is high sensitivity, bottom panel is low sensitivity). Box and whisker plots show the median, the 25th and 75th percentile, along with 1.5*interquartile range. Colours represent the different treatments

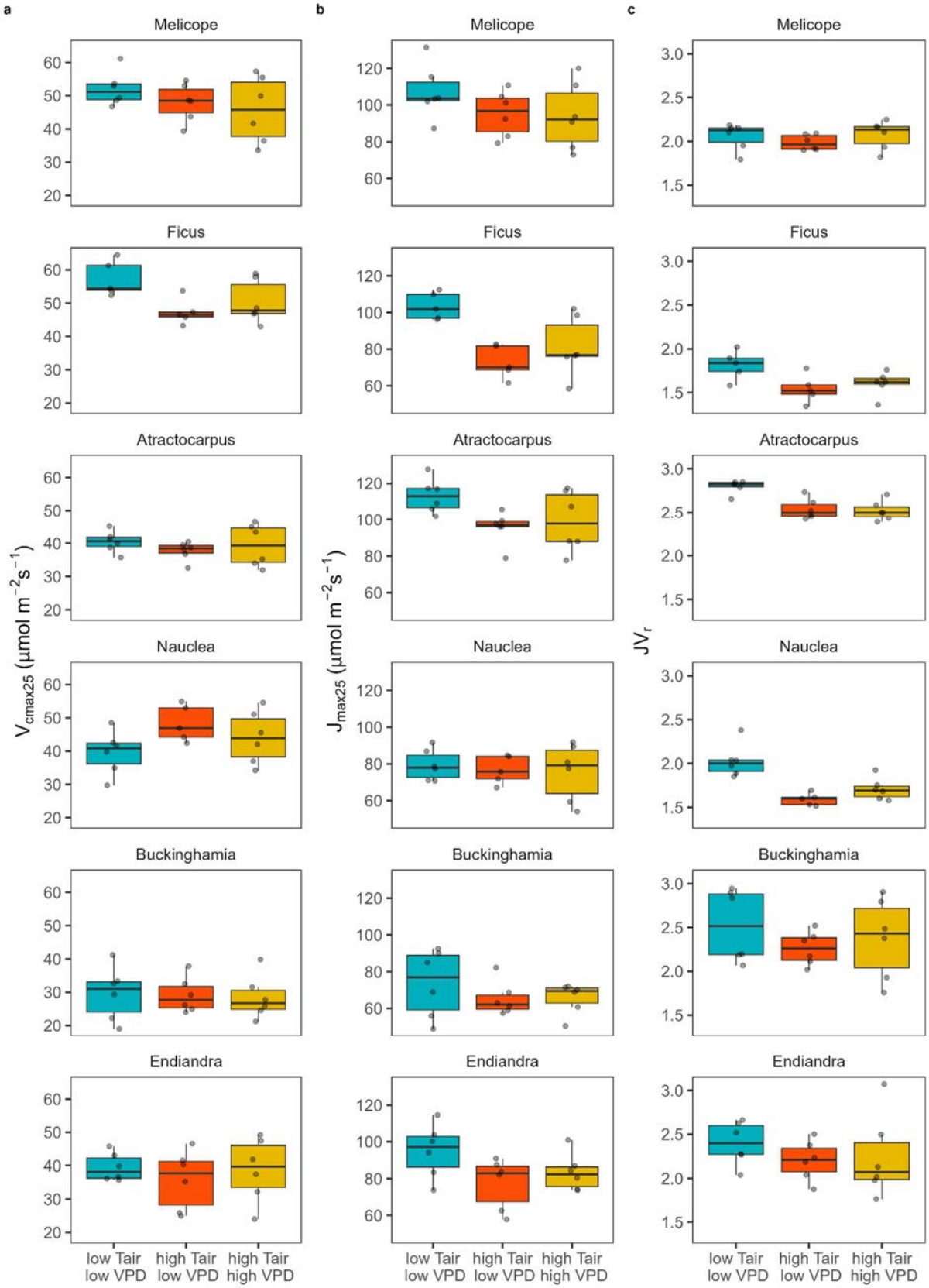
a
b
c
Melicope
Ficus
Atractocarpus
Nauclea
Buckinghamia
Endiandra
V_{cmax25} (µmol $m^{-2}s^{-1}$)
J_{max25} (µmol $m^{-2}s^{-1}$)
JV_r
low Tair low VPD
high Tair low VPD
high Tair high VPD

Appendix A: Figure 3. Treatment impacts on thermal tolerance, Tcrit (a), specific leaf area, SLA (b), and leaf dry matter content, LDMC (c) for each species. Species are ordered in decreasing stomatal sensitivity to VPD (top panel is high sensitivity, bottom panel is low sensitivity). Box and whisker plots show the median, the 25th and 75th percentile, along with 1.5*interquartile range. Colours represent the different treatments.

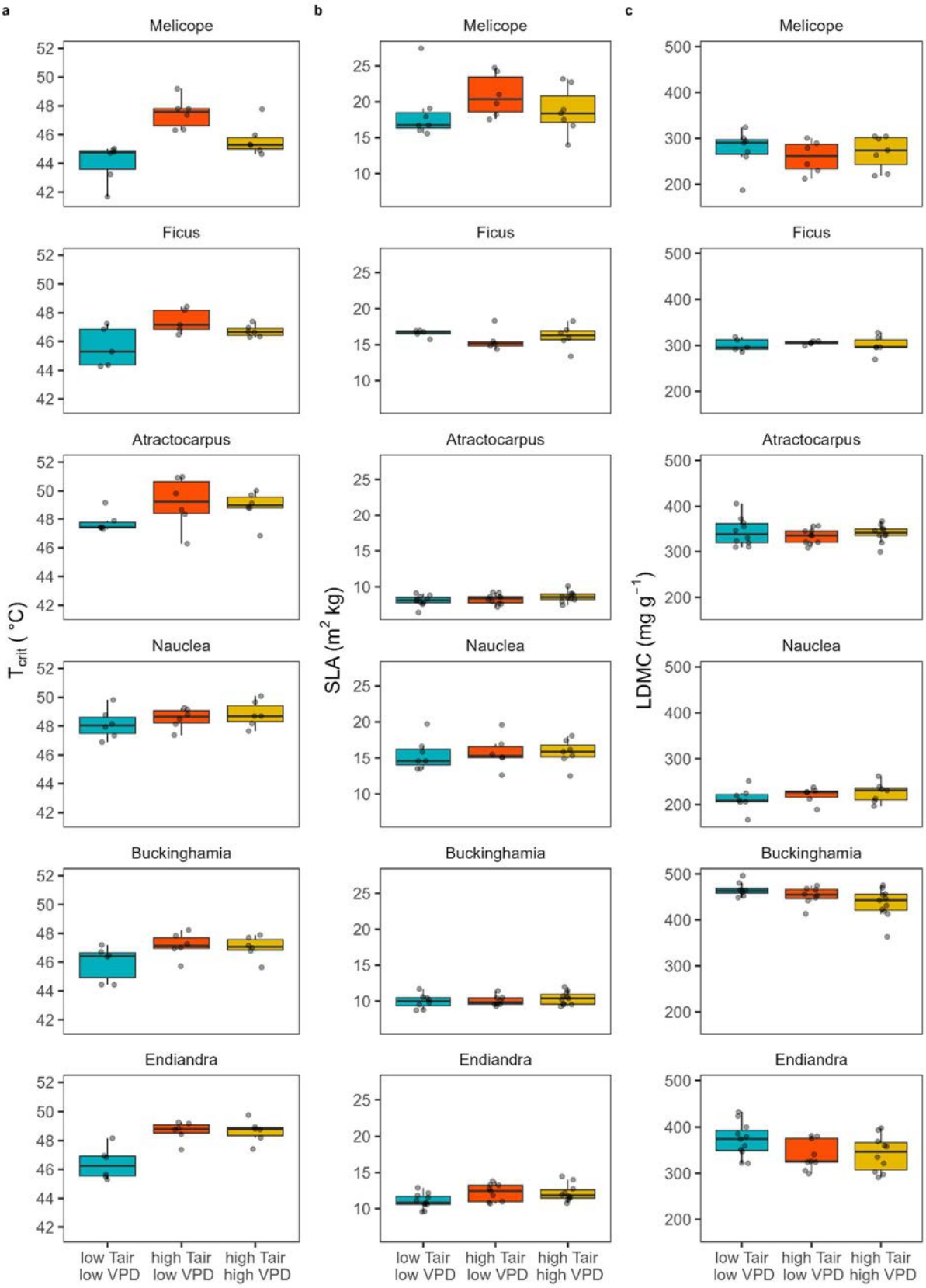
a
b
c
Melicope
Ficus
Atractocarpus
Nauclea
Buckinghamia
Endiandra
T_{crit} (°C)
SLA (m^2 kg)
LDMC (mg g^{-1})
low Tair low VPD
high Tair low VPD
high Tair high VPD

Appendix B: Supporting information for Chapter 4:

The following Supporting Information is available for Chapter 4:

Appendix B: Figure 1. Thermal niche of each species.

Appendix B: Figure 2. Climate envelopes of each species.

Appendix B: Figure 3. Sampling heights for each species and treatment group.

Appendix B: Figure 4. Daily course of (a) air temperature and (b) vapour pressure deficit during the 30 days prior to the experiment and during measurement campaigns.

Appendix B: Figure 5. Time-series based on 10-min averaged meteorology during the measurement campaigns of leaf temperature and stomatal conductance.

Appendix B: Figure 6. Histogram of individual leaf temperatures for each species.

Appendix B: Figure 7. Evaluation of model performance and the influence of plant height.

Appendix B: Figure 8. Within-canopy variation in leaf traits and thermal tolerance for the lowland provenance of *C. australe* (Ca) and *H. novo-guineensis* (Hn).

Appendix B: Figure 9. Provenance differences in thermal safety margin (TSM) of four tropical tree species grown under common environmental conditions.

Description of GBIF record collection and cleaning for determination of species thermal envelope.
Species georeferenced occurrence records were retrieved from the GBIF database: Derived dataset GBIF.org (17 July 2024) Filtered export of GBIF occurrence data https://doi.org/10.15468/dd.a4mjzn In A. Cheesman (Ed.). For each species, occurrence records were cleaned to exclude duplicate coordinates, any records that were not living occurrence records, records with a coordinate precision of greater than 25km, or old records (earlier than 1950). I also used the 'clean_coordinates' function to identify any issues due to records being in capital cities, centroids, equal, located at GBIF headquarters, institutions, and zeros. I did not filter for records in the sea as these species are present on small islands that might be excluded using this method. I then excluded occurrences from each species based on unrealistic latitude and longitude from their known natural distribution. Following this procedure, I used spatially thinned occurrences to a minimum radius of 1km to match the resolution of our climate data.

Climate data was obtained from the CHELSA database V.2.1. and included the 1981-2010 Climatologies of mean annual temperature (BIO1) and mean annual precipitation (BIO12) at 1km resolution. Using the quantiles of mean annual temperature to assess the thermal niche of each species, I observed that for *C. australe*, the climate of origin for the upland provenance was close to the median of its thermal niche, whilst the climate of origin for the lowland provenance and DRO common garden site was closer to the 95th percentile of mean annual temperature and thus located in the warm edge of the species thermal niche. For *T. microcarpa*, the climate of origin of the upland provenance was cooler than the 5th percentile of mean annual temperature and thus located in the cool edge of the species thermal niche, whilst the lowland provenance and DRO common garden site occupied a slightly warmer part of the thermal niche, but still cooler than the median. For *H. novo-guineensis* and *M. elleryana*, the climate of origin of the upland provenance was in the cool edge of the species thermal niche, whilst the climate of origin of the lowland provenance and the DRO common garden site was around the median of the species thermal niche.

Appendix B: Figure 1. Thermal niche of each species. Violin and boxplots show the distribution of mean annual temperature (MAT, BIO1) from the CHELSA database (1981-2010 V.2.1) across the species occurrences. Boxplots show the median along with 1.5 times the interquartile range along with outliers. Coloured points represent the MAT from the seed collection locations of each provenance, and the red dashed line represents the MAT of the DRO common garden site.

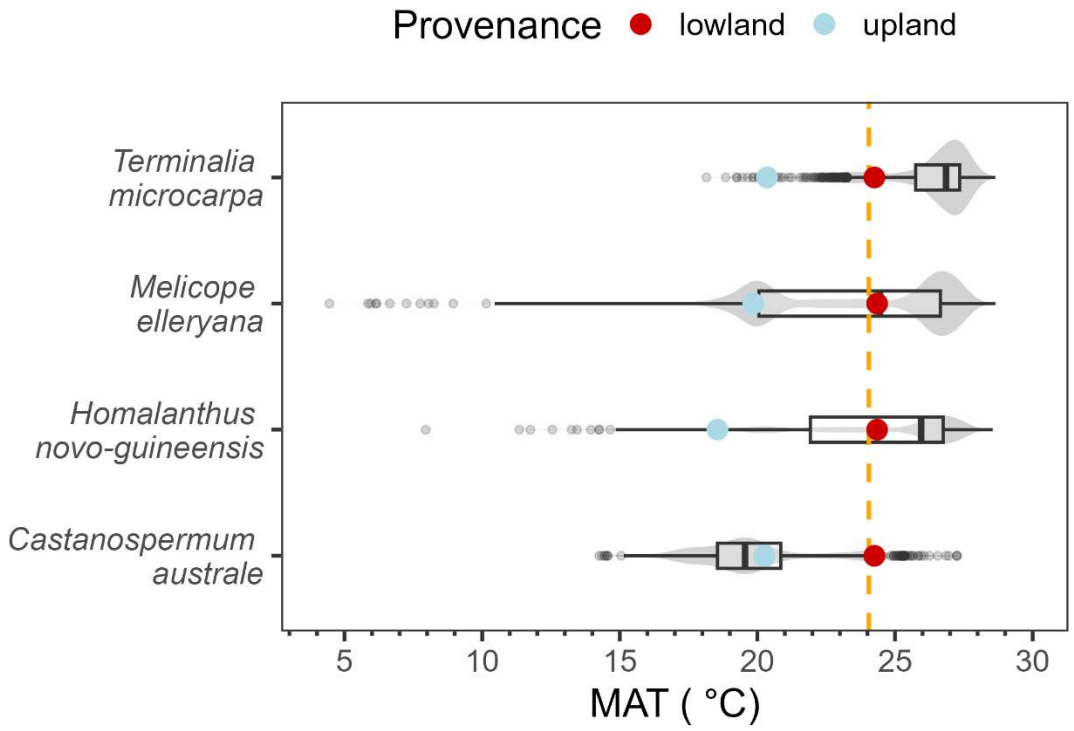

Appendix B: Figure 2. Climate envelopes of each species. Points represent cleaned occurrence records obtained from GBIF, coloured by density of points within climate space. Mean annual temperature (MAT, BIO1) and mean annual precipitation (MAP, BIO12) obtained from the CHELSA database (1981-2010 V.2.1) across species distributions. The larger triangles show the climate space where upland and lowland provenances were collected, while the orange circle shows the climate space of the common garden planting location.

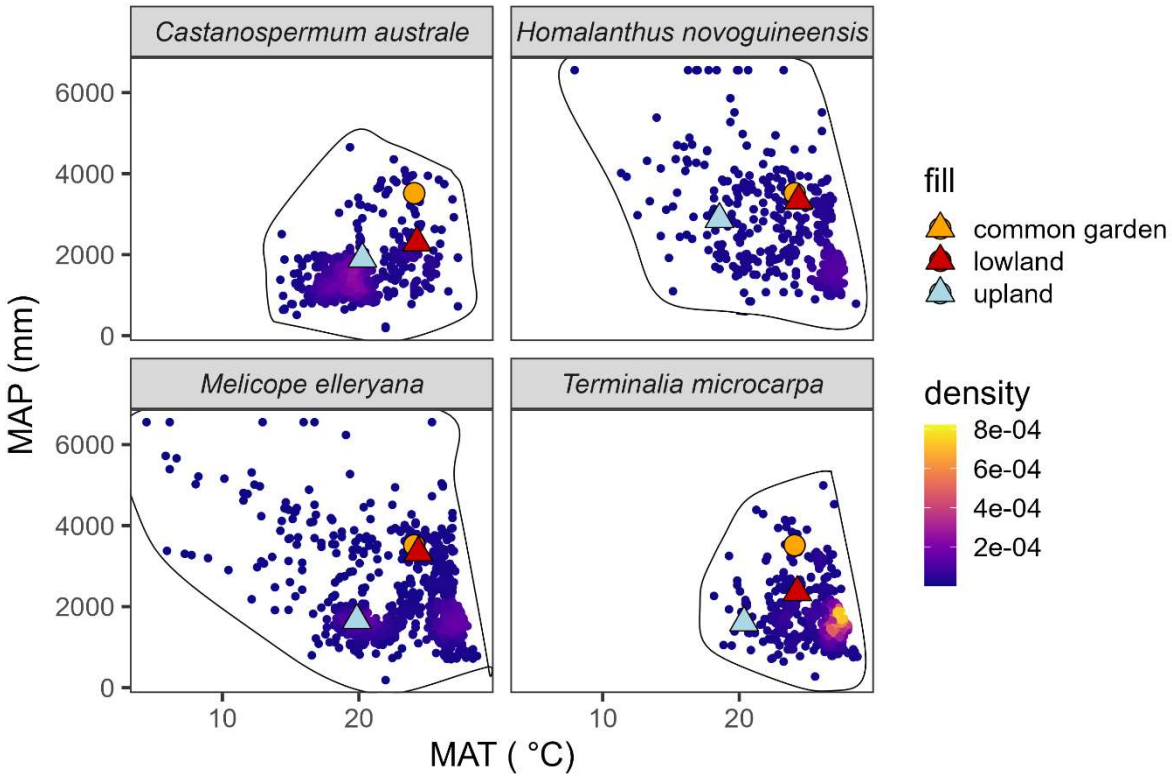

Appendix B: Figure 3. Sampling heights for each species and treatment group. LO = lowland provenance and UP = upland provenance both sampled within the top ~1m of the canopy. LOX indicates approximate sampling heights for individuals from the LO provenance that were resampled at the mid canopy. Ca = *Castanospermum australe*, Hn = *Homalanthus novo-guineensis*, Me = *Melicope elleryana*, Tm = *Terminalia microcarpa.*

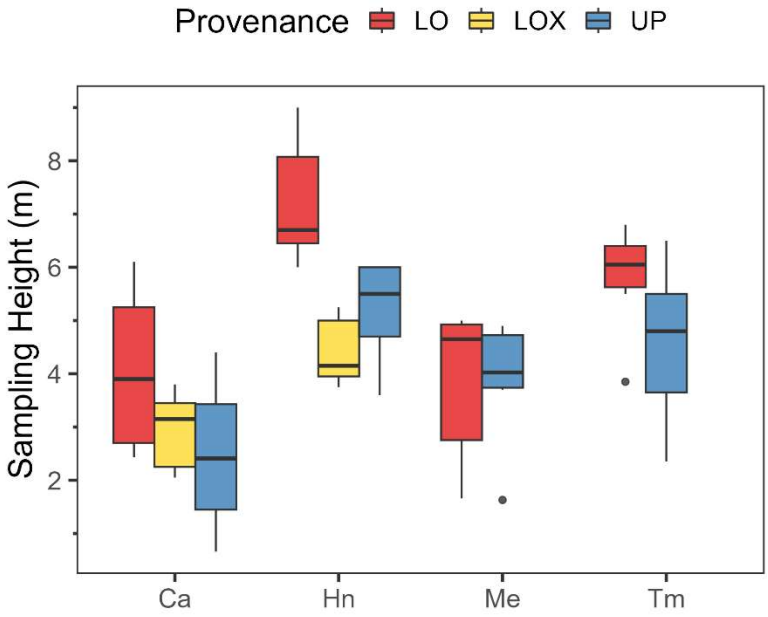

Appendix B: Figure 4. Daily course of (a) air temperature and (b) vapour pressure deficit during the 30 days prior to the experiment and during measurement campaigns. Solid line represents daily average, with grey shaded region representing range of daily max and min. Coloured vertical shaded areas show time periods that measurements took place. The red shaded region is the first week of measurements when thermal tolerance and leaf traits were measured along with hand-held leaf temperature and stomatal conductance. The blue shaded region represents the 3 days that extra campaigns were made to measure just leaf temperature and stomatal conductance. The green shaded region represents the day the UAV thermal imaging was conducted.

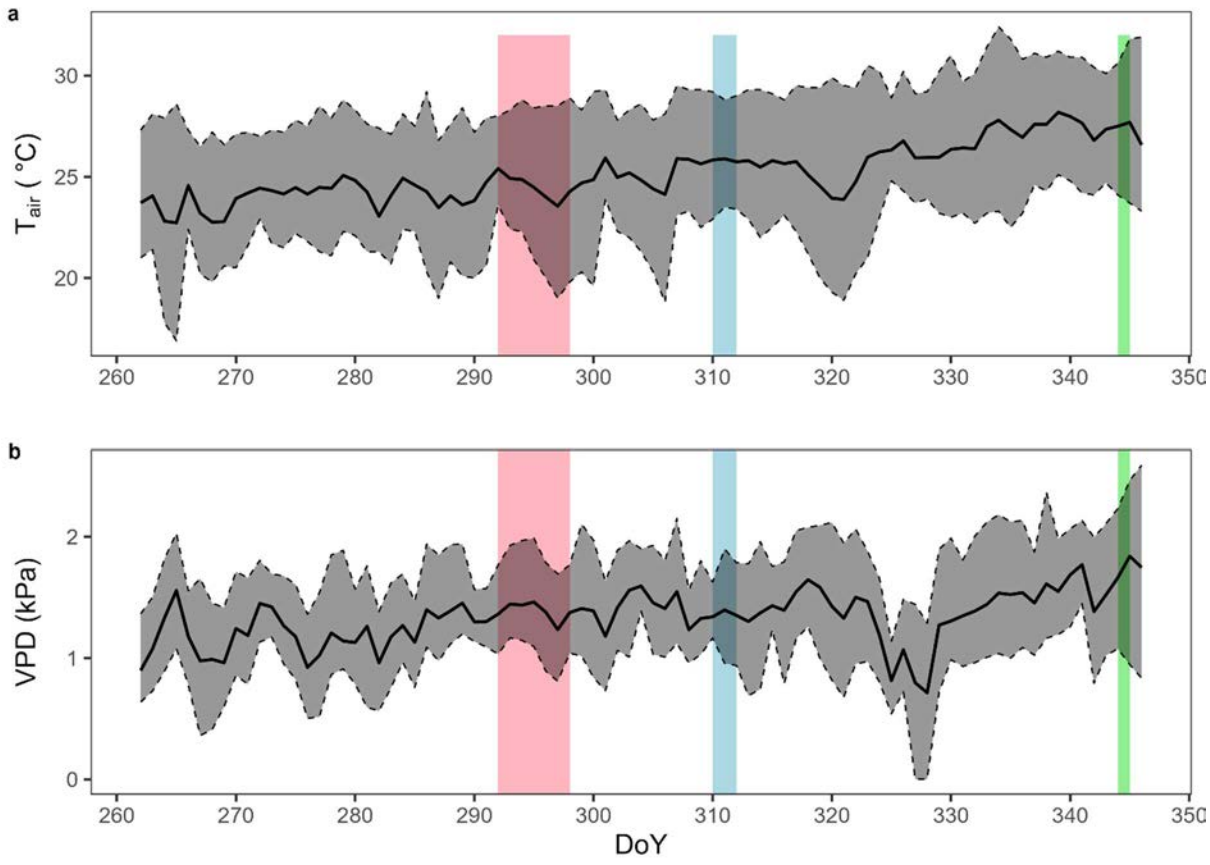

Appendix B: Figure 5. Time-series based on 10-min averaged meteorology during the measurement campaigns of leaf temperature and stomatal conductance. Measurements on each day took place between 10am and 4pm. Lines represent the variables observed on each measurement day of year. Note DoY 292-312 were days hand-held leaf temperature and stomatal conductance were measured, whilst DoY 345 was the day UAV thermal imaging took place.

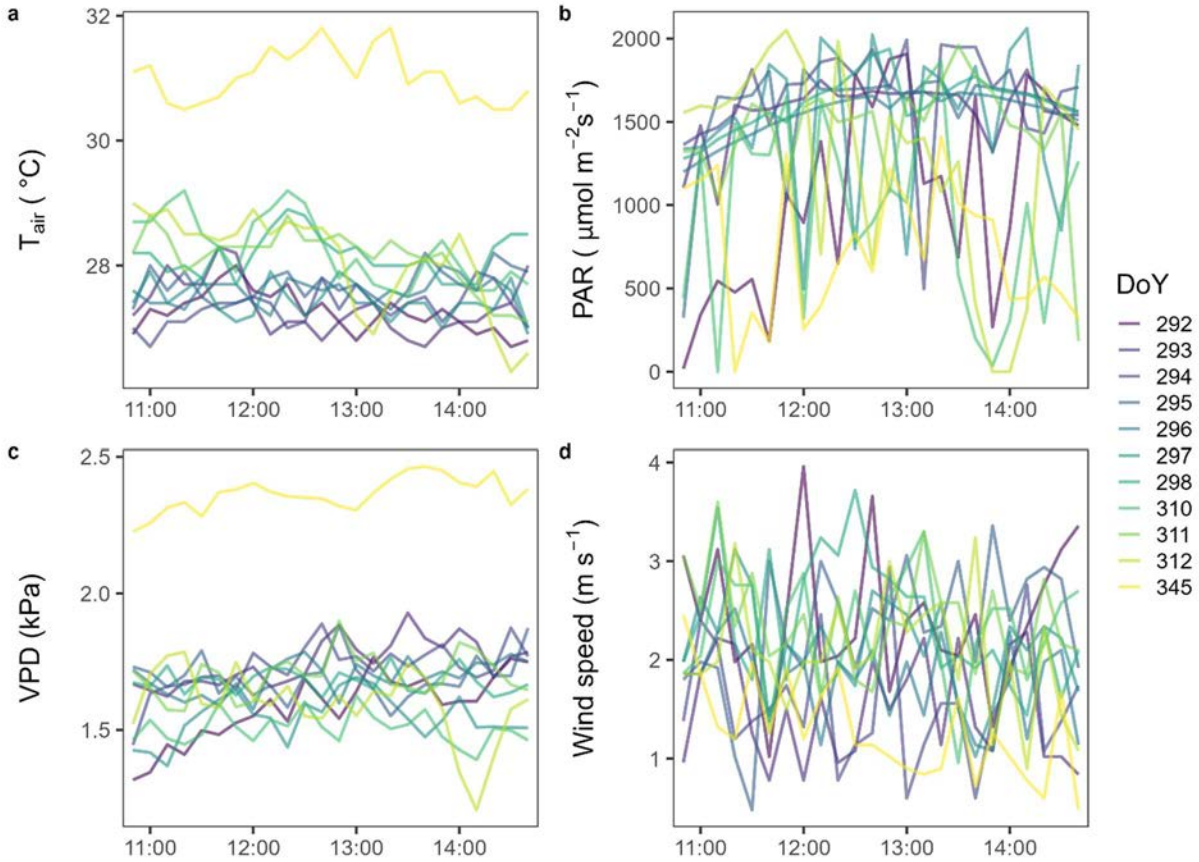

Appendix B: Figure 6. Histogram of individual leaf temperatures for each species. Each observation represents a recording of leaf temperature on a single leaf at one time point. For each plant and time point, 10 leaves were measured. Each plant was revisited 3 to 5 times. Total *n* = 1990. Air temperature during measurements averaged 28 °C. LO = lowland and UP = upland

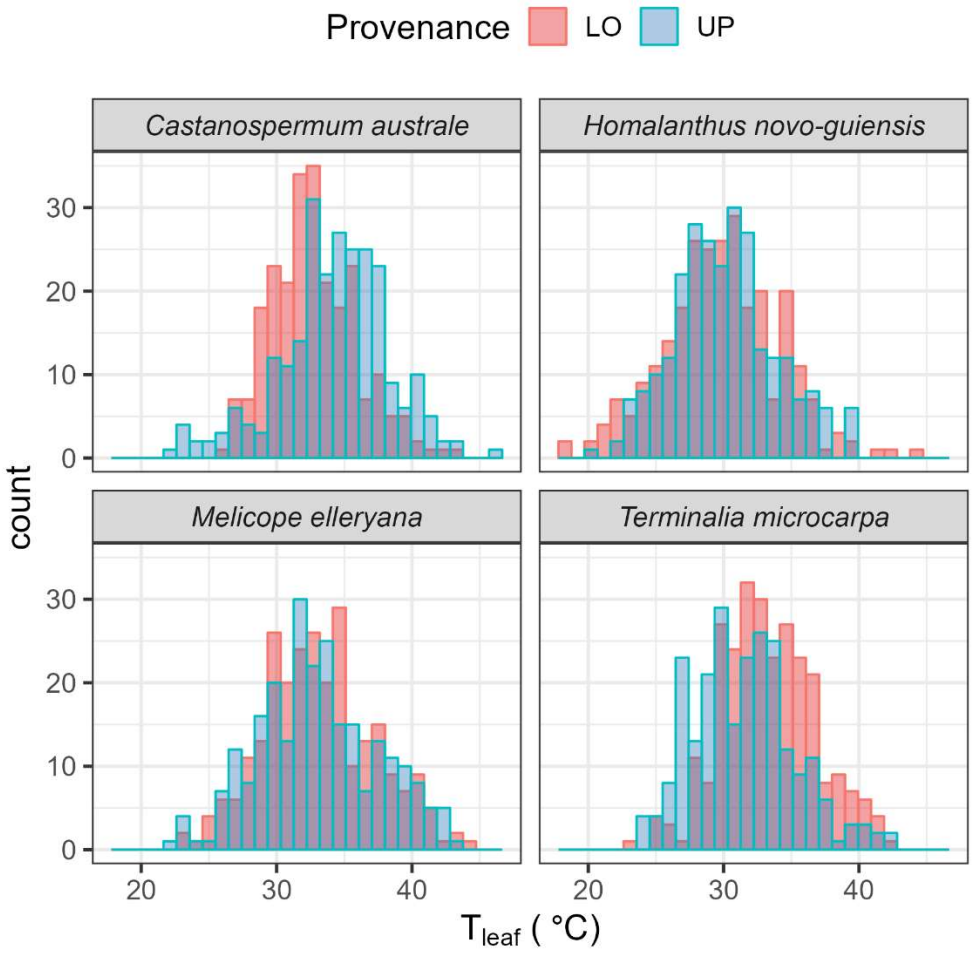

Appendix B: Figure 7. Evaluation of model performance and the influence of plant height. Panel (a) shows the observed ΔT_{leaf} and modelled ΔT_{mod} compared to a 1:1 line (dashed). In (b) the difference between observed and modelled ΔT is plotted against plant height. Panel (c) shows that the trend is driven by a decrease in measured ΔT_{leaf} with plant height, and (d) shows no trend of modelled ΔT_{mod} with plant height. Each point represents a plant-level average, with different species represented by different colours. Statistics represent the linear regression applied across the entire dataset, with regression line depicted (solid black line) only if significant.

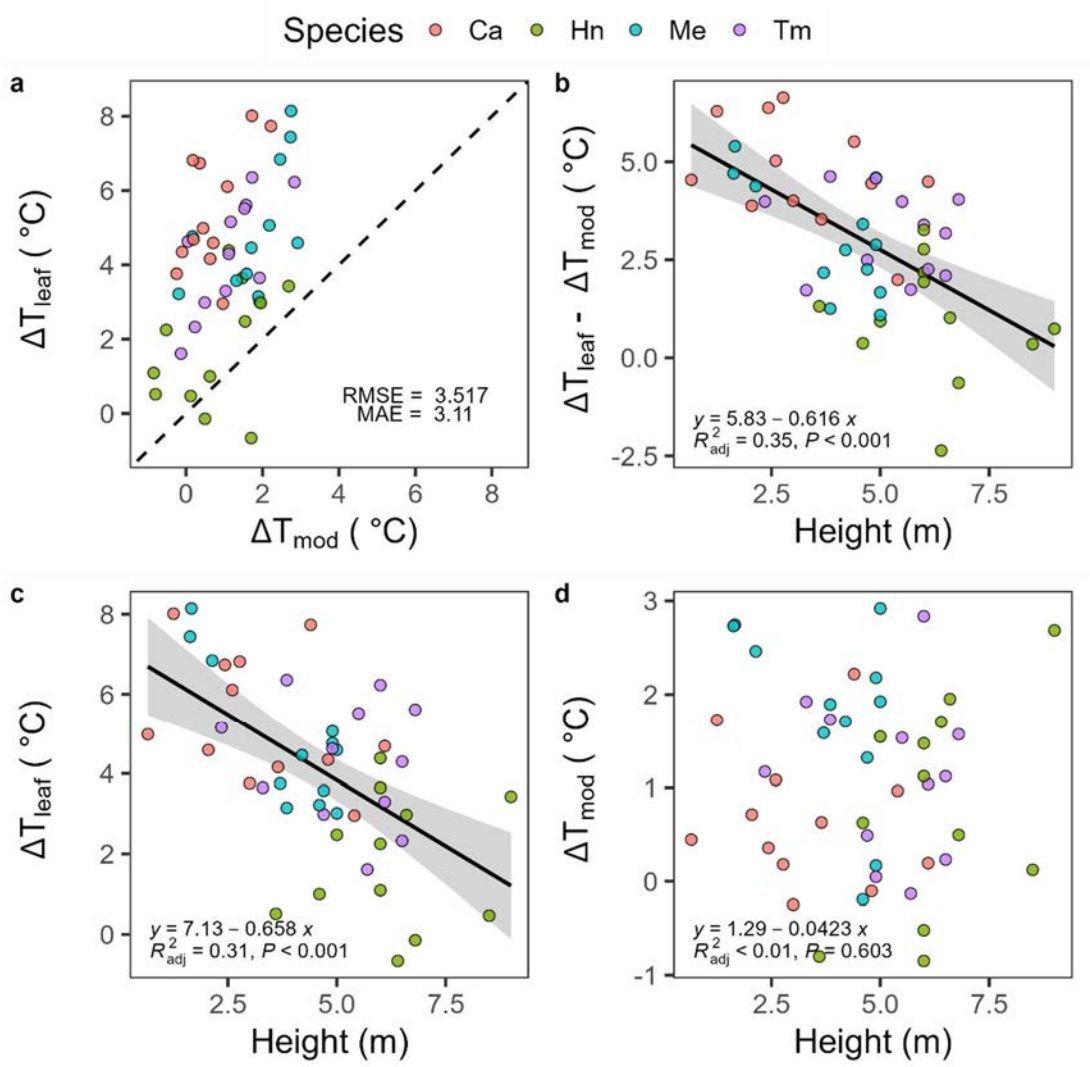

Appendix B: Figure 8. Within-canopy variation in leaf traits and thermal tolerance for the lowland provenance of *C. australe* (Ca) and *H. novo-guineensis* (Hn). Colour indicates the provenance, and patterns of boxplots indicate leaf collection locations within the canopy. Data are tree averages (n=5) presented as box and whisker plots showing median and interquartile range, with the average marked by an X. Results of paired t-test to detect within canopy differences indicated by subscript ns=not significant, with marginal significance of $p < 0.1$ represented by +. Note for statistical analysis, LMA was log transformed, but untransformed values are shown here.

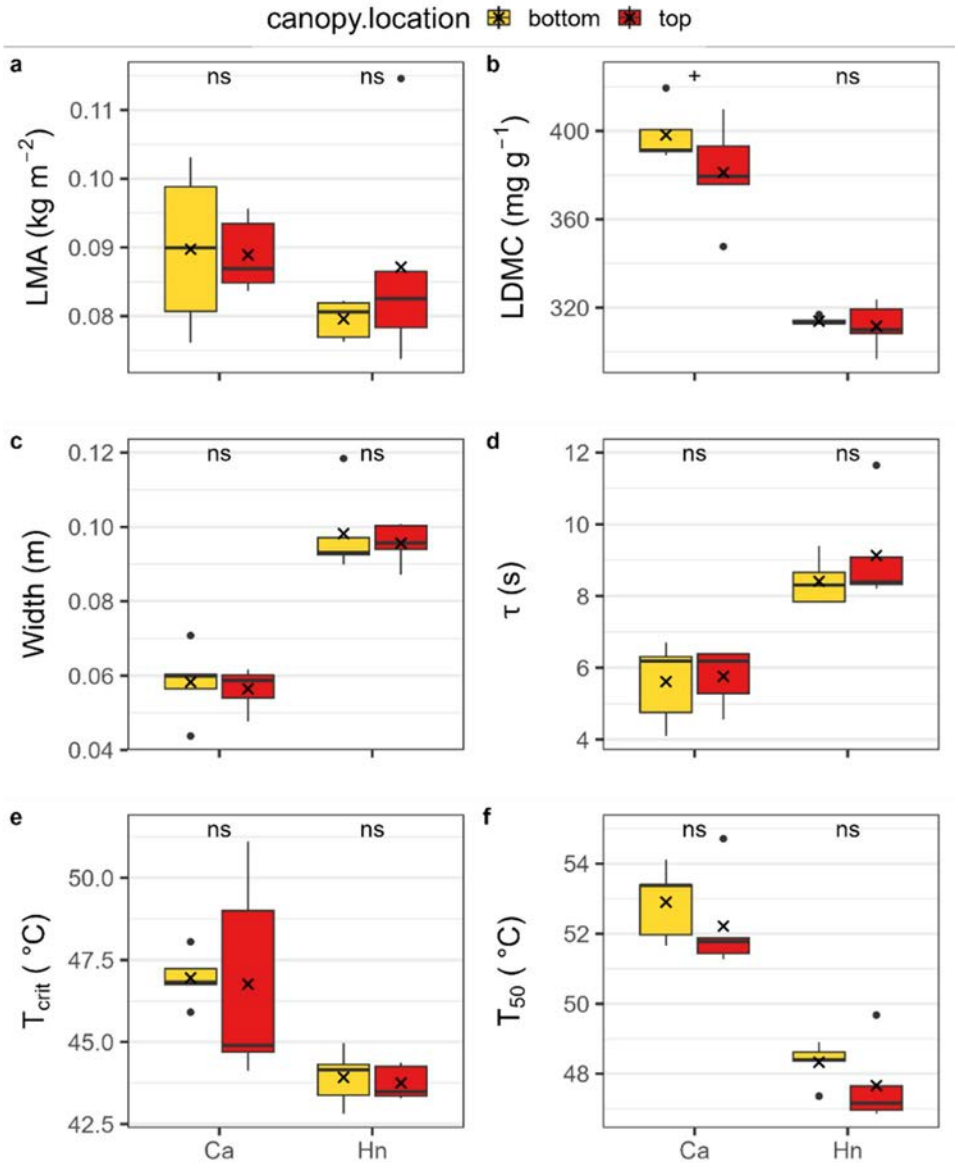

Appendix B: Figure 9. Provenance differences in thermal safety margin (TSM) of four tropical tree species grown under common environmental conditions. TSM calculated using T_{50} as upper threshold in all panels, with operating temperature defined as 32 °C (mean max air temperature of the site) plus ΔT_{leaf} in (a), ΔT_{can} in (b), and ΔT_{mod} in (c). Ca = *Castanospermum australe,* Hn = *Homalanthus novo-guineensis,* Me= *Melicope elleryana,* and Tm = *Terminalia microcarpa*. Data is of tree averages (*n*=6) presented as a box and whisker plots showing median and interquartile range, with the average marked by an X. Results of intraspecific t-test of provenance differences indicated by subscript ns=not significant

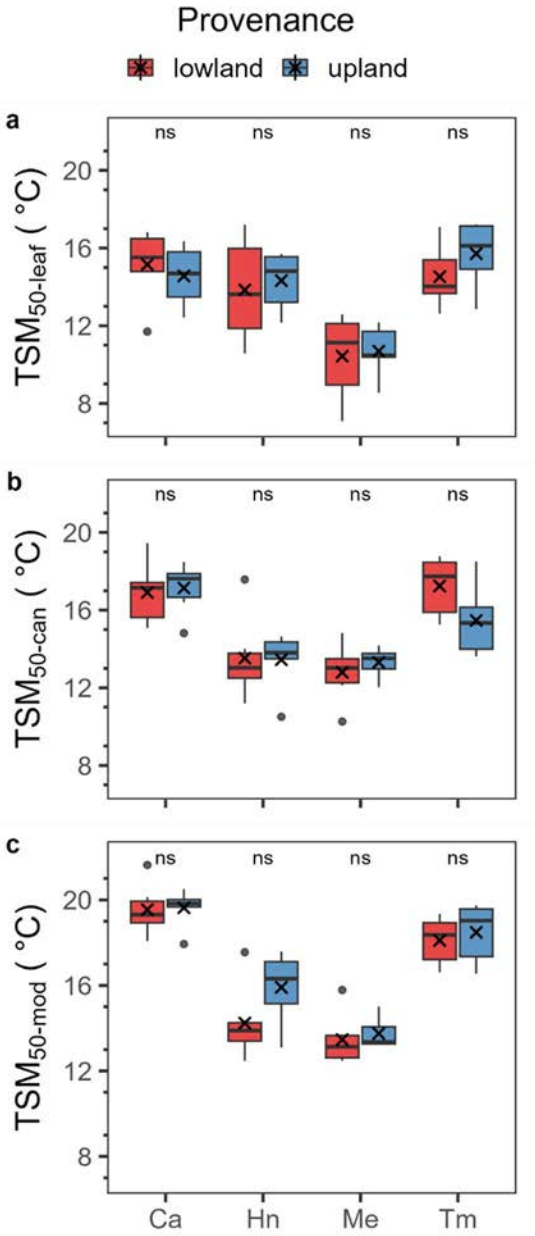

Appendix B: Figure 10. Positive correlation between T_{leaf} and the thermal tolerance metrics T_{crit} (a) and T_{50} (b) across four tropical tree species. Each point represents a plant-level average, with different species represented by different colours. Statistics represent the linear regression applied across the entire dataset (solid black line), whereas regression lines for each species were not significant ($p > 0.1$) and are represented with coloured dashed lines.

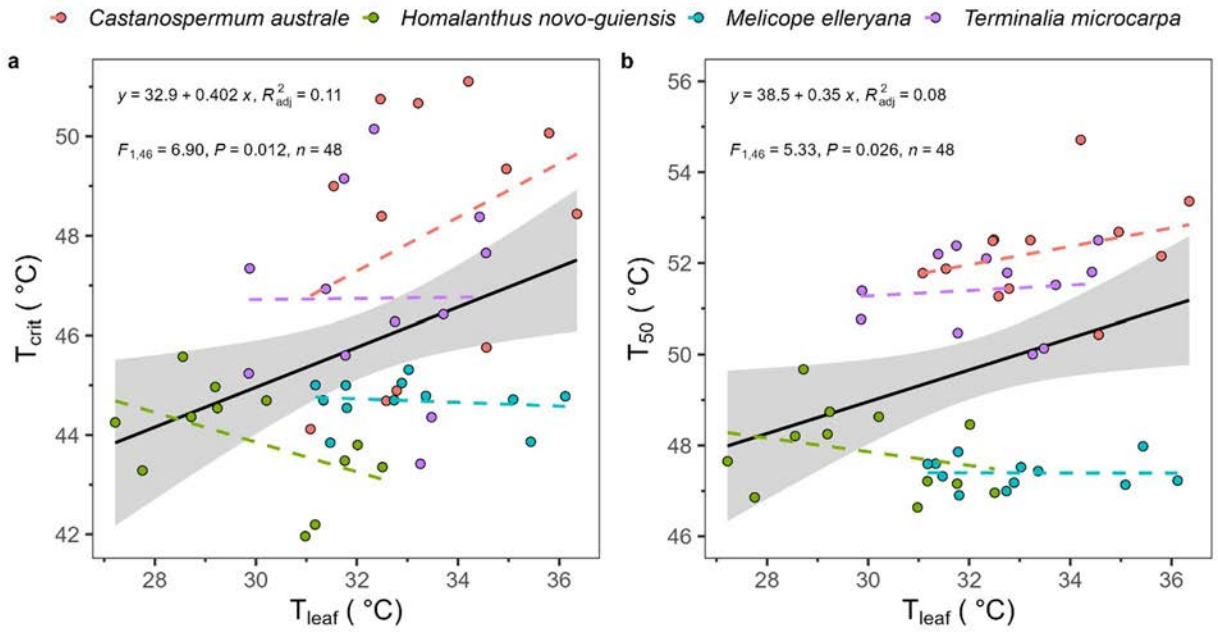

Appendix C: Supporting information for Chapter 5

The following Supporting Information is available for Chapter 5:

Appendix C: Method S1. Extended method descriptions from field measurements

Appendix C: Method S2. Extended method descriptions from climate-controlled glasshouse trial

Appendix C: Table 1. Glasshouse conditions and licor set points. Values are means ± 1 SD. Mean glasshouse conditions are based on data from 9:00 to 15:00, whereas means for gas exchange survey are from licor measurements. Licor set points represent Tleaf, VPDleaf and RHsample

Appendix C: Table 2. Population effects on trait variation. For each species I report the overall trait mean, along with the model results for the linear regression with population as the independent variable. Tests with $P < 0.05$ are bolded

Appendix C: Table 3. Mean annual temperature effects on trait variation. For each species I report the slope estimate, along with model results for the linear regression with mean annual temperature as the independent variable. Tests with $P < 0.05$ are bolded

Appendix C: Figure 1. Leaf trait relationships with mean annual temperature across the Wet Tropics for three tropical tree species. Each point represents an individual tree average of 10 leaves (or 3 for Abs and stomatal anatomy). Significant correlations ($P < 0.05$) are denoted by solid lines whereas nonsignificant relationships are denoted by dashed lines. Shaded regions represent standard error.

Appendix C: Figure 2. Variation in anatomical trait-based leaf-to-air temperature differences (anatomical ΔT; a-b), and thermal safety margins (anatomical TSM; *c,* d) *with mean* annual temperature across the distribution of *D. darlingiana* and *E. grandis*. Note in a and c ΔT is based on leaf trait variation with the same microclimate inputs for all trees, whereas in b and d, microclimate inputs also vary with each individual tree. Each point represents an individual-tree level average. Significant correlations with mean annual temperature are denoted by solid regression lines whereas non-significant correlations are dotted. Shaded region represents standard errors.

Appendix C: Figure 3. Population structure results for *Cardwellia sublimis*. Map with pie charts (top left) representing proportion of ancestry contribution corresponding to bar plot, ordered by latitude (bottom) with dark and light green colours representing the two different ancestry groups. Principal component plot (top right) shows the genetic similarity of individuals with point colours corresponding to latitude, and isolation by distance plot (centre, right).

Appendix C: Figure 4. Population structure results for *Darlingia darlingiana*. Map with pie charts (top left) representing proportion of ancestry contribution corresponding to bar plot, ordered by latitude (bottom) with dark and light green colours representing the two different ancestry groups. Principal component plot

(top right) shows the genetic similarity of individuals with point colours corresponding to latitude, and isolation by distance plot (centre, right).

Appendix C: Figure 5. Population structure results for *Elaeocarpus grandis*. Map with pie charts (top left) representing proportion of ancestry contribution corresponding to bar plot, ordered by latitude (bottom) with dark and light green colours representing the two different ancestry groups. Principal component plot (top right) shows the genetic similarity of individuals with point colours corresponding to latitude, and isolation by distance plot (centre, right).

Appendix C: Table 4. Population genetic diversity metrics for each species.

Appendix C: Figure 6. Partial redundancy analysis (pRDA) of genotype variation for each species. The plot displays the relationship between the SNPs with traits (a, c, e) or environment (b, d, f) along the first two pRDA axes.

Appendix C: Table 5. Number of candidate SNPs identified by each method.

Appendix C: Table 6. Generalised dissimilarity modelling results.

Appendix C: Figure 7. Correlation between photosynthetic parameters and leaf nitrogen determined in the glasshouse trial. Vcmax25 = maximum carboxylation rate and Jmax25 = maximum rate of electron transport. Each point represents a plant level mean. Coefficients from linear regressions used to predict Vcmax25 and Jmax25 in the field.

Appendix C: Method S1: Extended method descriptions from field measurements

Leaf spectra

Reflectance and transmittance spectra from wavelengths 390-1100 nm were collected for the adaxial side of leaves using a spectrometer (Jaz Spectrometer, Ocean Optics, Ocean Insight, Orlando, FL, US) and external type integrating sphere with a halogen light source 'illuminator' (LI-1800-12, LI-COR Biosciences, Lincoln, NE, US). Spectra were obtained using the 'OceanView' software (Ocean Optics, Ocean Insight, Orlando, FL, US). The scanning parameters were set to average 40 scans with a boxcar width of 5, nonlinearity correction enabled, and default settings for integrating time. Barium sulphate was used as reference material. For each leaf, reflectance and transmittance sample and reference measurements were taken, with a dark reference collected every 10-15 minutes. Absorptance was then calculated using the formula: Absorptance = 1 – Reflectance – Transmittance.

Stomatal anatomy

Leaf stomatal imprints were obtained on 3 leaves per plant using nail varnish and tape on the abaxial mid-lamina. Stomatal imprints for *C. sublimis* were impacted by leaf hairs so stomatal anatomical traits are only presented for *E. grandis* and *D. darlingiana*. Microscope images were obtained at ×20 magnification and were processed using ImageJ to obtain stomatal density (d, pores mm^{-2}), as well as stomatal length (μm) on 10 stomata per leaf. Stomatal length was converted to size (s, μm^2) assuming stomatal width is 0.5×stomatal length. Maximum theoretical conductance (g_{max}, mol m^{-2} s^{-1}) was calculated as a function of stomatal size and density as per (Franks & Beerling, 2009; Mcelwain et al., 2016; Sack & Buckley, 2016);

$$g_{max} = bmds^{0.5}$$

where b is a biophysical constant equal to D (diffusivity of water vapour in air, m^2 s^{-1}) / v (molar volume of air, m^3 mol^{-1}) and m is a morphological constant that represents the allometric relationships between pore length and depth, and stomatal length and width. Here I used scaling factors assuming kidney bean-shaped guard cells, and as such m = 0.432. For b factors were calculated assuming an air temperature of 25°C so that D = 0.0000249 m^2 s^{-1} and v = 0.0224 m^3 mol^{-1}. Thereby g_{max} accounts for variation in stomatal anatomy, and not in the increase in diffusivity of water as temperature increases.

Stomatal conductance modelling

To obtain g_s, traits that impact gas exchange are required, such as the maximum rate of carboxylation (V_{cmax25}) and light-saturated rate of electron transport (J_{max25}), as well as the slope parameter (g_1) that describes the relationship between photosynthesis and stomatal conductance and responses to changes in VPD (Medlyn et al., 2011). Since characterizing V_{cmax25}, J_{max25} and g_1 in the field for each tree

was not feasible, I varied these according to observed relationships with leaf N_{mass} (V_{cmax25}), and as a ratio of V_{cmax25} (J_{max}) (Appendix C: Figure 7) and used thermal sensitivity of V_{cmax} and J_{max} parameters determined in Australian tropical trees (Kelly, 2014). The parameter g_1 was calculated using the following equation (2011):

$$g_1 = \frac{(\frac{C_i}{C_a}\sqrt{VPD})}{(1 - \frac{C_i}{C_a})}$$

where VPD is the tree-level mean daytime vapour pressure deficit (kPa), and C_i/C_a is the ratio of intercellular to ambient CO_2 concentrations, estimated from leaf $\delta^{13}C$ using the 'isocalcr' package in R (Mathias & Hudiburg, 2022).

An assumption of the USO model used to predict g_s is that plants maximize carbon gain while minimizing water loss. This model effectively captures dynamic gas exchange and produces realistic leaf temperatures under non-stressful conditions (Guo et al., 2022). However, evidence suggests that at higher temperatures, g_s and photosynthesis decouple, with g_s maintained or even increasing (De Kauwe et al., 2019; Diao et al., 2024b; Drake et al., 2018; Marchin et al., 2023; Urban et al., 2017a). This decoupling may reflect a strategy to enhance transpirational cooling rather than optimizing carbon gain, especially under heat stress. Relying solely on the USO model could thus overlook plant responses aimed at maintaining T_{leaf} within a viable range. In addition, this parameterisation relies on a within-species correlation between V_{cmax25} and leaf N_{mass} that was only determined in *E. grandis*. To address these assumptions, I also calculated ΔT_{trait} and ΔT_{clim} using theoretical g_{max} determined from stomatal anatomy, via the 'FindTleaf' function, which estimates T_{leaf} independently of photosynthesis. By incorporating g_{max}, I aim to account for the upper limits of stomatal conductance that plants may employ in response to heat stress.

Appendix C: Method S2: Extended method descriptions from climate-controlled glasshouse trial

Gas exchange measurements

Photosynthesis-CO_2 response curves (A-Ci) were conducted using a portable gas exchange system (LiCor 6400xt; LiCor Inc., Lincoln, NE, USA) to determine V_{cmax25} and J_{max25} for comparison with leaf nitrogen content (described below). Measurements were conducted on 6 plants per chamber (8 for the high T_{air} low VPD_{air}) representing one unique mother tree per plant. The cuvette conditions were conducted under ambient midday treatment temperatures (32°C for the two warm chambers, and 29°C for the cool chamber), with a flow rate of 500 µmol s^{-1}, a PAR of 1000 µmol m^{-2} s^{-1}, and an RH in the reference air stream of 73%. The 'Photosyn' function in the 'plantecophys' package was used to fit V_{cmax} and J_{max} standardized to 25°C using temperature response parameters from Kelly (2014).

Leaf traits

Upon completion, leaf traits (leaf width, leaf area, and fresh and dry leaf mass) were measured on 10 healthy, new, full expanded leaves per plant, including those measured for gas exchange, using standard techniques (Perez-Harguindeguy et al., 2013). The leaf material was oven-dried at 70°C for 3 days and ground for analysis of leaf $\delta^{13}C$ and % nitrogen. These traits were compared with observed measurements of g_1 and V_{cmax25} to assess assumptions used for leaf energy balance modelling in the field campaign data. To convert $\delta^{13}C$ values to estimates of g_1 in the glasshouse, I assumed a value of −10‰ for the $d^{13}C$ of CO_2 in air in the glasshouse chambers.

T_{leaf} parameterisation

I estimated ΔT_{trait} for plants in the glasshouse experiment using the same leaf energy balance modelling approach as for the field campaign, with leaf traits varying by individual, and microclimate inputs standardised across all individuals to isolate the effect of trait variation on ΔT_{trait}. Microclimate inputs were T_{air} = 25°C, VPD = 1.4 kPa, PPFD = 1400 µmol m^{-2} s^{-1} and Wind = 0.5 m s^{-1}. Leaf trait inputs included leaf width, V_{cmax25} calculated from the observed relationship between Leaf N %, and g_1 calculated from leaf $\delta^{13}C$.

Appendix C: Table 1. Glasshouse conditions and licor set points. Values are means ± 1 SD. Mean glasshouse conditions are based on data from 9:00 to 15:00, whereas means for gas exchange survey are from licor measurements. Licor set points represent T_{leaf}, VPD_{leaf} and RH_{sample}

	Tair (°C)		VPD (kPa)		RH (%)	
	Mean	SD	Mean	SD	Mean	SD
Daytime mean glasshouse conditions						
low T_{air} high VPD_{air}	25.7	1.67	1.0	0.21	71.1	4.76
high T_{air} low VPD_{air}	31.6	1.68	1.1	0.20	76.2	3.21
high T_{air} high VPD_{air}	31.7	1.70	2.0	0.45	58.7	7.02
Total 24 hour mean glasshouse conditions						
low T_{air} high VPD_{air}	21.5	3.63	0.6	0.27	76.5	5.51
high T_{air} low VPD_{air}	27.3	3.69	0.8	0.29	78.7	3.99
high T_{air} high VPD_{air}	27.4	3.70	1.2	0.67	70.4	11.31
Set points for gas exchange survey						
low T_{air} high VPD_{air}	28.9	1.69	1.2	0.19	75.7	3.98
high T_{air} low VPD_{air}	32.1	1.27	1.5	0.28	75.3	4.75
high T_{air} high VPD_{air}	32.7	1.51	1.5	0.50	77.6	4.52

Appendix C: Table 2. Population effects on trait variation. For each species I report the overall trait mean, along with the model results for the linear regression with population as the independent variable. Tests with $P < 0.05$ are bolded

Trait	*Cardwellia sublimis*					*Darlingia darlingiana*					*Elaeocarpus grandis*				
	Mean	R^2	df	F	*P*	Mean	R^2	df	F	P	Mean	R^2	df	F	*P*
LMA	137	0.36	14, 91	3.6	**< 0.0001**	169	0.54	14, 81	6.73	**< 0.0001**	116	0.47	15, 88	5.2	**< 0.0001**
LDMC	410	0.43	14, 91	4.98	**< 0.0001**	456	0.48	14, 81	5.34	**< 0.0001**	433	0.58	15, 88	8.15	**< 0.0001**
Thickness	26.34	0.8	14, 91	26.37	**< 0.0001**	34.5	0.65	14, 81	10.85	**< 0.0001**	22.49	0.81	15, 88	24.43	**< 0.0001**
Width	5.66	0.39	14, 91	4.16	**< 0.0001**	5.55	0.47	14, 81	5.17	**< 0.0001**	3.33	0.43	15, 88	4.41	**< 0.0001**
Abs	0.56	0.41	14, 90	4.42	**< 0.0001**	0.55	0.43	14, 81	4.41	**< 0.0001**	0.56	0.31	15, 88	2.65	**0.0024**
Ref	0.25	0.5	14, 90	6.46	**< 0.0001**	0.27	0.3	14, 81	2.45	**0.0062**	0.26	0.56	15, 88	7.53	**< 0.0001**
N %	0.95	0.23	14, 91	1.94	**0.0324**	0.98	0.35	14, 81	3.07	**0.0008**	1.55	0.49	15, 88	5.73	**< 0.0001**
C/N ratio	47.4	0.15	14, 91	1.14	0.339	48.91	0.3	14, 81	2.43	**0.0066**	28.85	0.49	15, 88	5.61	**< 0.0001**
$\delta^{13}C$	−28.9	0.1	14, 91	0.72	0.752	−30.7	0.44	14, 81	4.63	**< 0.0001**	−29.3	0.31	15, 88	2.65	**0.0024**
g_1	3.18	0.21	14, 91	1.68	0.0731	5.71	0.62	14, 81	9.29	**< 0.0001**	3.75	0.37	15, 88	3.38	**0.0002**
Stomatal density	NA	NA	NA	NA	NA	335	0.4	8, 26	2.13	0.0694	816	0.35	10, 33	1.78	0.104
Stomatal size	NA	NA	NA	NA	NA	429	0.56	8, 26	4.15	**0.0027**	188	0.45	10, 33	2.67	**0.0164**
g_{max}	NA	NA	NA	NA	NA	3.3	0.47	8, 26	2.9	**0.0189**	5.31	0.36	10, 33	1.86	0.0883
T_{crit}	44.26	0.4	3, 17	3.83	**0.0291**	45.12	0.33	3, 18	2.95	0.0603	44.73	0.33	4, 22	2.74	0.0546
T_{50}	49.46	0.3	3, 17	2.38	0.105	49.68	0.34	3, 18	3.04	0.056	49.82	0.6	4, 22	8.33	**0.0003**
ΔT_{trait}	5.95	0.37	14, 90	3.83	**< 0.0001**	5.06	0.54	14, 81	6.79	**< 0.0001**	4.25	0.56	15, 88	7.34	**< 0.0001**
Anatomical ΔT_{trait}	NA	NA	NA	NA	NA	−0.63	0.41	8, 26	2.23	0.0579	−1.84	0.45	10, 33	2.75	**0.0139**
TSM_{trait}	18.71	0.31	3, 17	2.56	0.0893	19.75	0.63	3, 18	10.16	**0.0004**	20.72	0.71	4, 22	13.7	**< 0.0001**
Anatomical TSM_{trait}	NA	NA	NA	NA	NA	25.88	0.09	2, 8	0.39	0.692	26.81	0.85	3, 12	21.99	**< 0.0001**

Appendix C: Table 3. Mean annual temperature effects on trait variation. For each species I report the slope estimate, along with model results for the linear regression with mean annual temperature as the independent variable. Tests with $P < 0.05$ are bolded

Trait	*Cardwellia sublimis*				*Darlingia darlingiana*				*Elaeocarpus grandis*			
	Slope	df	F	*P*	Slope	df	F	P	Slope	df	F	*P*
LMA	0.6	1, 104	0.29	0.59	−6.84	1, 94	45.64	**< 0.0001**	−2.09	1, 102	8.46	**0.0045**
LDMC	3.23	1, 104	3.23	0.0753	−1.44	1, 94	0.78	0.379	3.65	1, 102	4.99	**0.0277**
Thickness	−0.04	1, 104	0.03	0.86	−0.7	1, 94	6.53	**0.0122**	−0.2	1, 102	1.17	0.282
Width	0.05	1, 104	1.07	0.303	0.14	1, 94	10.01	**0.0021**	−0.12	1, 102	35	**< 0.0001**
Abs	0	1, 103	0.21	0.652	0	1, 94	4.79	**0.0312**	0	1, 102	1.37	0.245
Ref	0	1, 103	3.76	0.0552	0	1, 94	0.14	0.713	0	1, 102	2.39	0.125
N %	−0.01	1, 104	3.26	0.0739	0	1, 94	0.17	0.679	0	1, 102	0.16	0.691
C/N ratio	0.46	1, 104	1.42	0.237	0.03	1, 94	0.01	0.939	0.18	1, 102	0.8	0.372
$\delta^{13}C$	−0.01	1, 104	0.04	0.837	−0.31	1, 94	41.85	**< 0.0001**	−0.15	1, 102	7.83	**0.0061**
g_1	0.13	1, 104	15.62	**0.0001**	0.86	1, 94	77.15	**< 0.0001**	0.27	1, 102	28.74	**< 0.0001**
Stomatal density	NA	NA	NA	NA	2.65	1, 33	0.64	0.43	23.48	1, 42	9.69	**0.0033**
Stomatal size	NA	NA	NA	NA	−4.86	1, 33	0.38	0.541	−9.01	1, 42	22.93	**< 0.0001**
g_{max}	NA	NA	NA	NA	0.02	1, 33	0.18	0.676	0.02	1, 42	0.28	0.596
T_{crit}	0.14	1, 19	0.17	0.683	0.27	1, 20	0.75	0.396	0.33	1, 25	2.85	0.104
T_{50}	0.01	1, 19	0	0.945	0.22	1, 20	4.61	**0.0441**	0.28	1, 25	14.27	**0.0009**
ΔT_{trait}	−0.02	1, 103	0.56	0.457	−0.21	1, 94	59.24	**< 0.0001**	−0.16	1, 102	65.16	**< 0.0001**
Anatomical ΔT_{trait}	NA	NA	NA	NA	0.02	1, 33	0.49	0.487	−0.06	1, 42	20.6	**< 0.0001**
TSM_{trait}	0.03	1, 19	0.09	0.765	0.52	1, 20	30.15	**< 0.0001**	0.42	1, 25	29.94	**< 0.0001**
Anatomical TSM_{trait}	NA	NA	NA	NA	0.09	1, 9	0.61	0.455	0.4	1, 14	22.62	**0.0003**

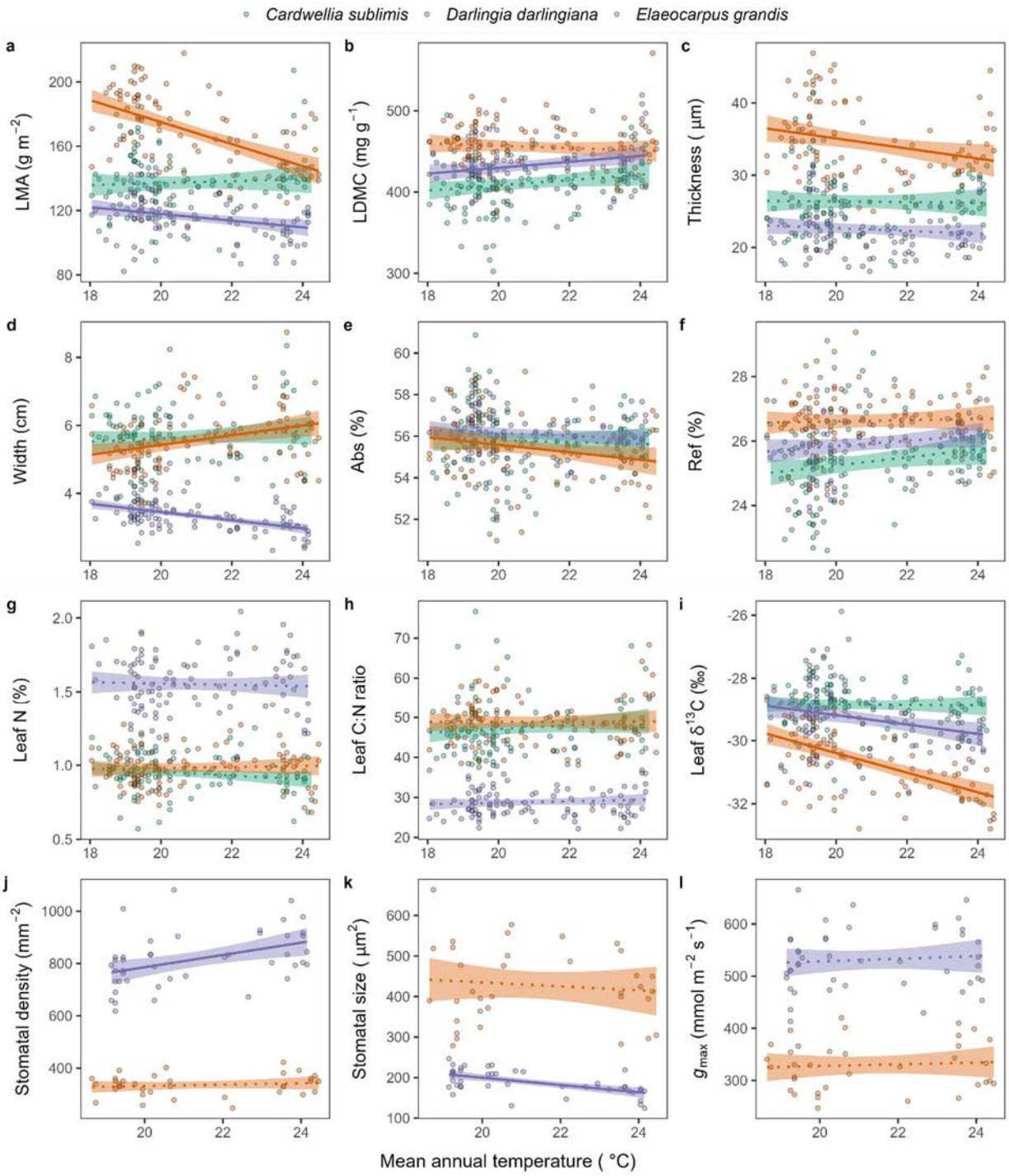

Appendix C: Figure 1. Leaf trait relationships with mean annual temperature across the Wet Tropics for three tropical tree species. Each point represents an individual tree average of 10 leaves (or 3 for Abs and stomatal anatomy). Significant correlations ($P < 0.05$) are denoted by solid lines whereas nonsignificant relationships are denoted by dashed lines. Shaded regions represent standard error.

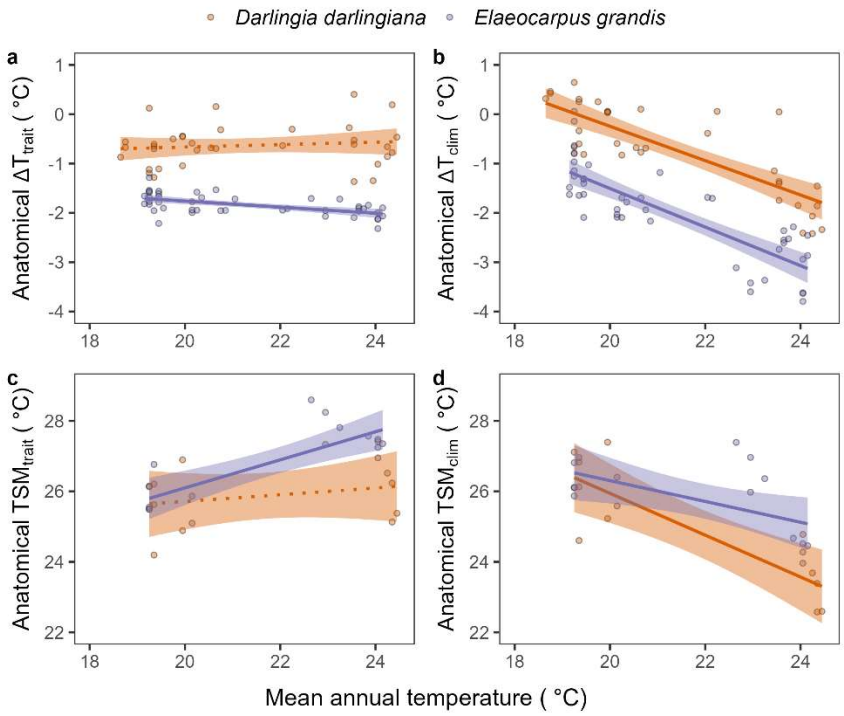

Appendix C: Figure 2. Variation in anatomical trait-based leaf-to-air temperature differences (anatomical ΔT; a-b), and thermal safety margins (anatomical TSM; c, d) with mean annual temperature across the distribution of *D. darlingiana* and *E. grandis*. Note in a and c ΔT is based on leaf trait variation with the same microclimate inputs for all trees, whereas in b and d, microclimate inputs also vary with each individual tree. Each point represents an individual-tree level average. Significant correlations with mean annual temperature are denoted by solid regression lines whereas non-significant correlations are dotted. Shaded region represents standard errors.

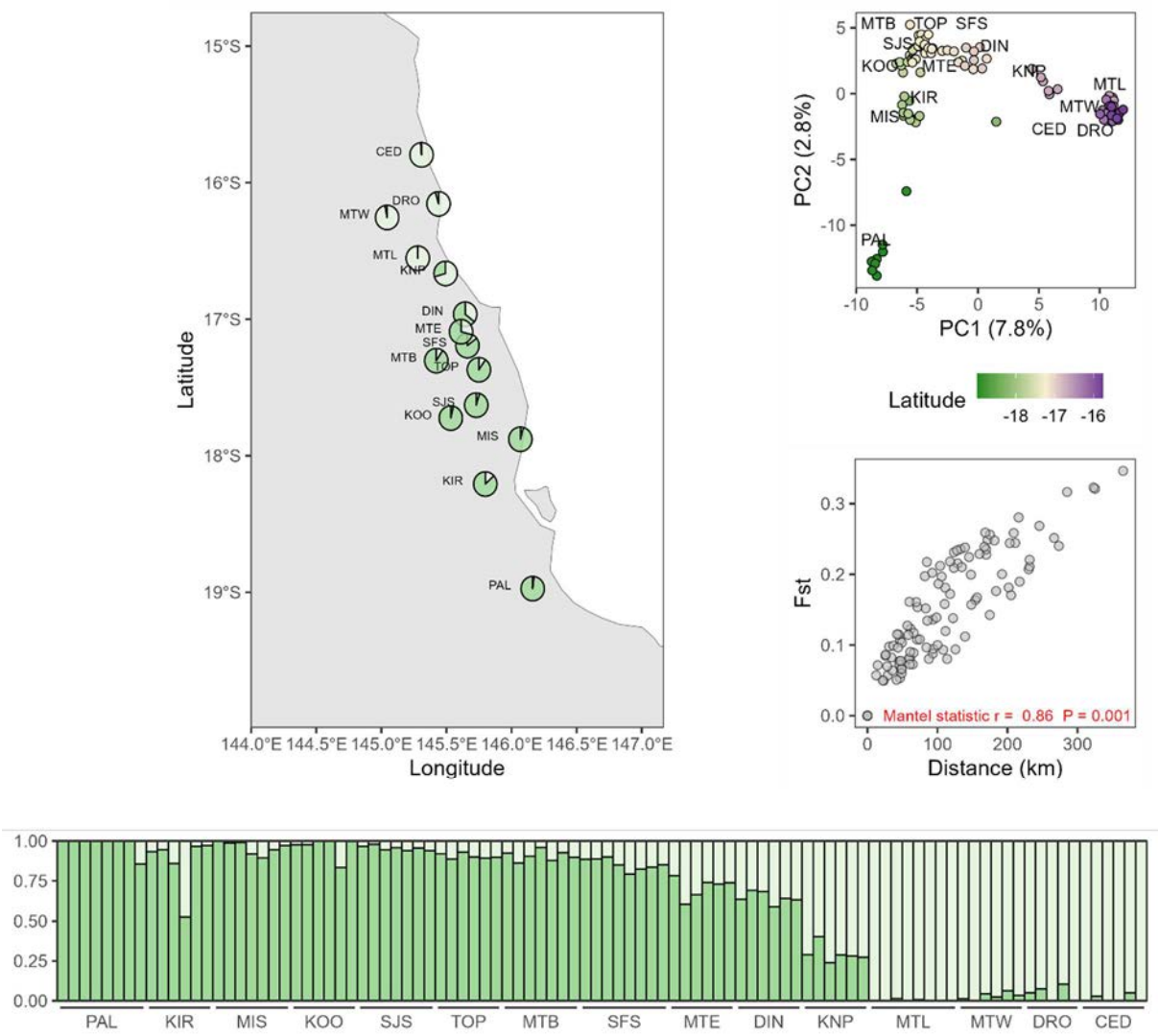

Appendix C: Figure 3. Population structure results for Cardwellia sublimis. Map with pie charts (top left) representing proportion of ancestry contribution corresponding to bar plot, ordered by latitude (bottom) with dark and light green colours representing the two different ancestry groups. Principal component plot (top right) shows the genetic similarity of individuals with point colours corresponding to latitude, and isolation by distance plot (centre, right).

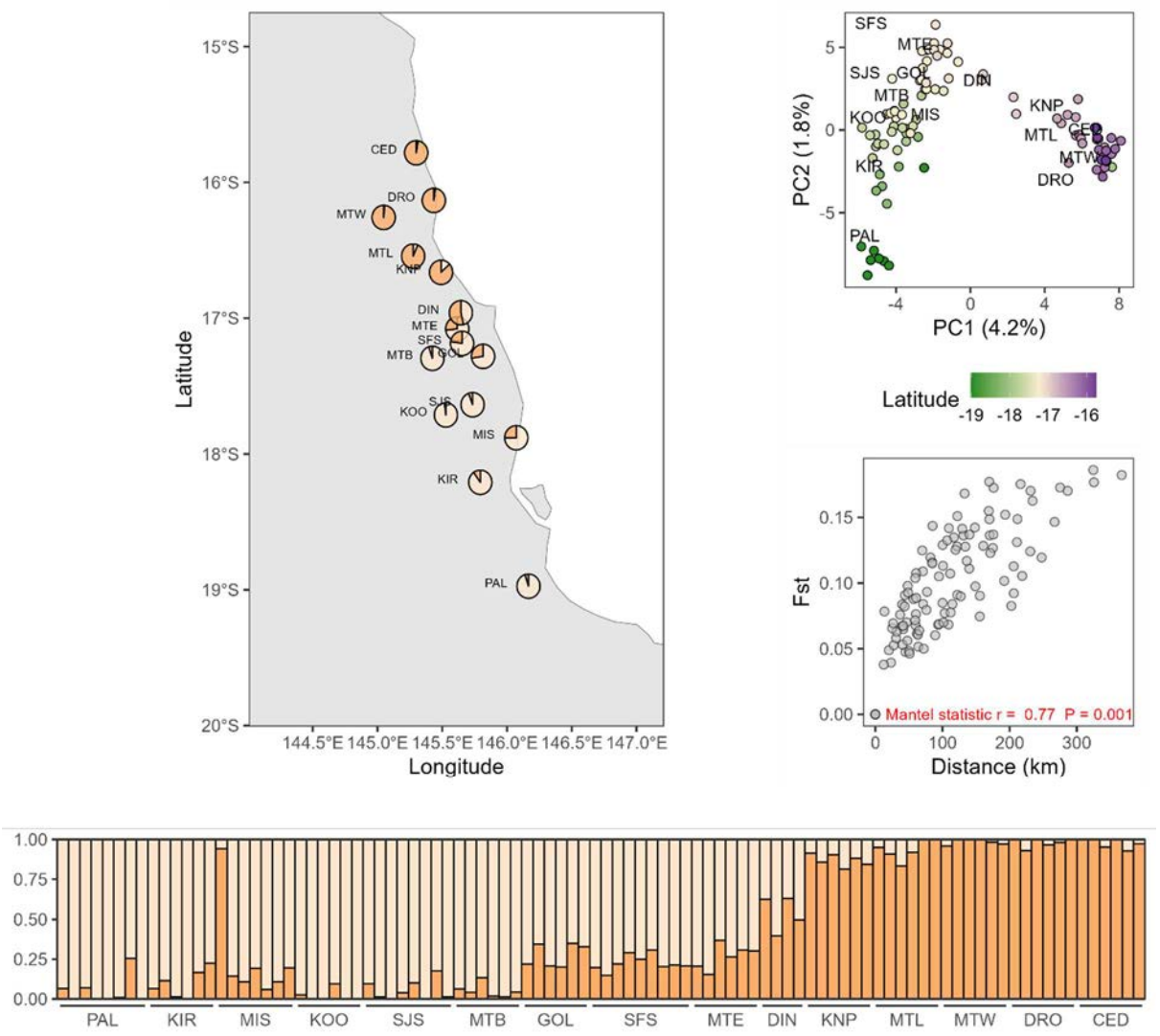

Appendix C: Figure 4. Population structure results for Darlingia darlingiana. Map with pie charts (top left) representing proportion of ancestry contribution corresponding to bar plot, ordered by latitude (bottom) with dark and light green colours representing the two different ancestry groups. Principal component plot (top right) shows the genetic similarity of individuals with point colours corresponding to latitude, and isolation by distance plot (centre, right).

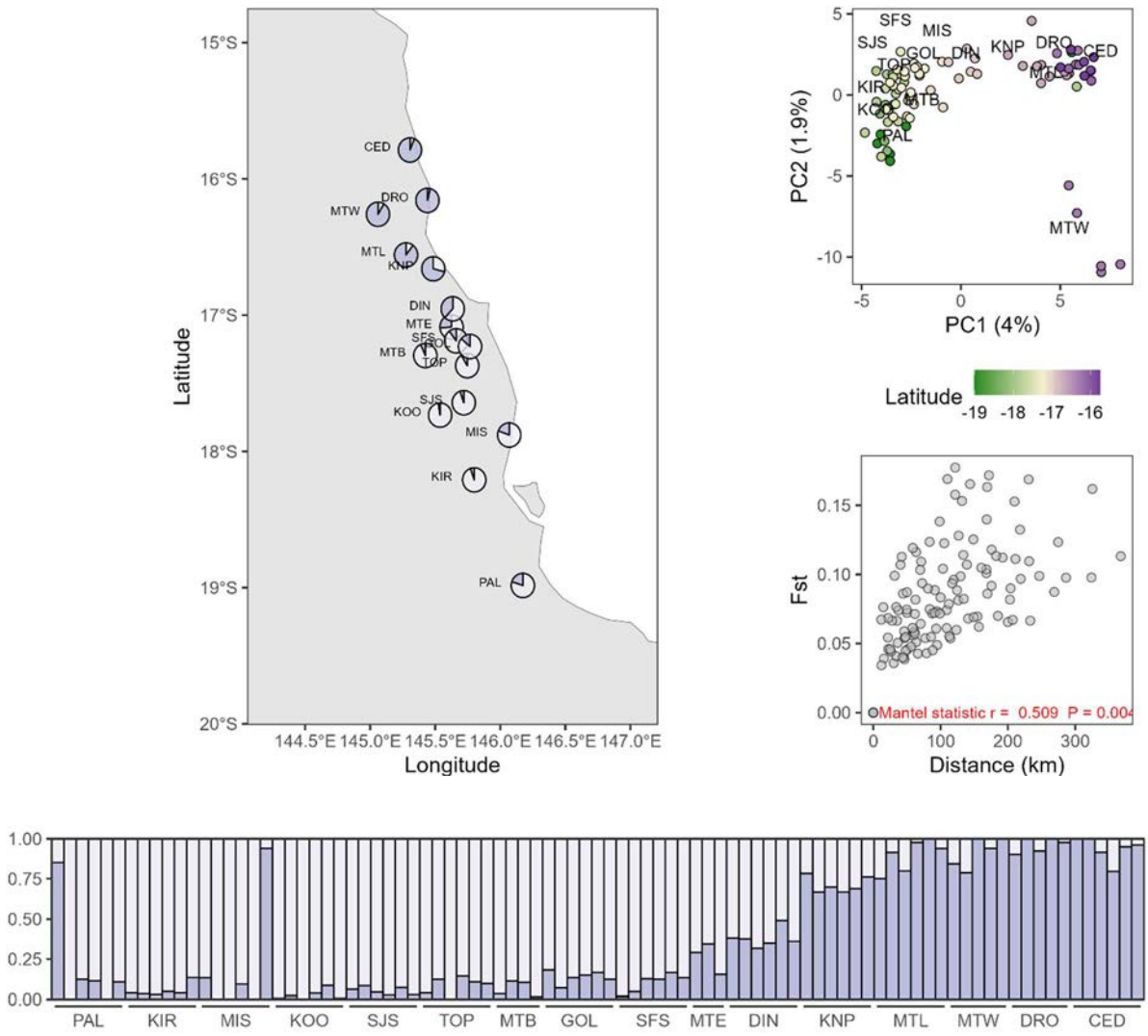

Appendix C: Figure 5. Population structure results for Elaeocarpus grandis. Map with pie charts (top left) representing proportion of ancestry contribution corresponding to bar plot, ordered by latitude (bottom) with dark and light green colours representing the two different ancestry groups. Principal component plot (top right) shows the genetic similarity of individuals with point colours corresponding to latitude, and isolation by distance plot (centre, right).

Appendix C: Table 4. Population genetic diversity metrics for each species.

Population	*Cardwellia sublimis*				*Darlingia darlingiana*				*Elaeocarpus grandis*			
	AR (C.I.)	H_{obs}	H_{exp}	F_{IS} (C.I.)	AR	H_{obs}	H_{exp}	F_{IS} (C.I.)	AR	H_{obs}	H_{exp}	F_{IS} (C.I.)
1. Cedar Bay	1.41 (1.28, 1.49)	0.13	0.17	0.19 (0, 0.18)	1.36 (1.22, 1.44)	0.11	0.17	0.28 (0.08, 0.28)	1.42 (1.14, 1.53)	0.17	0.23	0.21 (-0.05, 0.23)
2. Daintree	1.4 (1.24, 1.49)	0.12	0.17	0.2 (-0.12, 0.2)	1.37 (1.24, 1.45)	0.11	0.17	0.26 (0.06, 0.26)	1.48 (1.19, 1.57)	0.21	0.23	0.04 (-0.23, 0.04)
3. Mt Windsor	1.41 (1.26, 1.49)	0.12	0.18	0.24 (0.03, 0.24)	1.37 (1.25, 1.45)	0.12	0.17	0.24 (0.04, 0.24)	1.39 (1.13, 1.48)	0.16	0.2	0.15 (-0.16, 0.15)
4. Mt Lewis	1.46 (1.38, 1.52)	0.14	0.18	0.18 (0.04, 0.17)	1.37 (1.25, 1.46)	0.12	0.17	0.25 (0.04, 0.24)	1.45 (1.18, 1.54)	0.18	0.23	0.16 (-0.04, 0.16)
5. Kuranda	1.48 (1.33, 1.58)	0.16	0.19	0.13 (-0.06, 0.12)	1.41 (1.26, 1.5)	0.13	0.19	0.23 (0.05, 0.23)	1.46 (1.19, 1.56)	0.19	0.24	0.16 (-0.05, 0.16)
6. Dinden	1.5 (1.34, 1.59)	0.16	0.2	0.11 (-0.04, 0.1)	1.38 (1.28, 1.5)	0.12	0.18	0.22 (-0.08, 0.22)	1.46 (1.34, 1.55)	0.18	0.24	0.19 (0, 0.18)
7. Mt Edith	1.5 (1.34, 1.6)	0.16	0.2	0.15 (-0.11, 0.13)	1.41 (1.24, 1.52)	0.12	0.19	0.27 (0.08, 0.27)	1.35 (0.87, 1.49)	0.16	0.19	0.11 (-1, 0.11)
8. Danbulla	1.51 (1.39, 1.59)	0.14	0.21	0.24 (0.1, 0.23)	1.47 (1.31, 1.53)	0.14	0.2	0.25 (0.14, 0.24)	1.44 (1.21, 1.55)	0.18	0.23	0.19 (-0.05, 0.21)
9. Goldsborough	NA	NA	NA	NA	1.43 (1.28, 1.52)	0.13	0.19	0.22 (0.03, 0.22)	1.49 (1.2, 1.55)	0.21	0.23	0.06 (-0.12, 0.04)
10. Mt Baldy	1.48 (1.32, 1.57)	0.14	0.2	0.21 (0.04, 0.21)	1.43 (1.29, 1.52)	0.14	0.19	0.21 (0.01, 0.21)	1.39 (1.04, 1.5)	0.17	0.21	0.13 (-0.16, 0.13)
11. Topaz	1.48 (1.32, 1.58)	0.15	0.2	0.2 (0.01, 0.19)	NA	NA	NA	NA	1.43 (1.26, 1.53)	0.17	0.23	0.2 (-0.01, 0.22)
12. South Johnstone	1.5 (1.43, 1.59)	0.15	0.2	0.19 (0.04, 0.18)	1.46 (1.3, 1.54)	0.14	0.2	0.25 (0.12, 0.23)	1.46 (1.17, 1.54)	0.18	0.23	0.16 (-0.04, 0.16)
13. Tully Falls	1.46 (1.31, 1.56)	0.14	0.19	0.19 (-0.02, 0.19)	1.4 (1.27, 1.49)	0.12	0.19	0.26 (0.1, 0.25)	1.42 (1.18, 1.54)	0.16	0.23	0.22 (0, 0.23)
14. Mission Beach	1.5 (1.35, 1.58)	0.15	0.2	0.19 (0.01, 0.18)	1.43 (1.28, 1.51)	0.12	0.2	0.29 (0.11, 0.28)	1.48 (1.37, 1.57)	0.19	0.24	0.15 (-0.04, 0.14)
15. Kirrama	1.51 (1.32, 1.62)	0.17	0.21	0.13 (-0.14, 0.18)	1.38 (1.21, 1.47)	0.11	0.19	0.32 (0.09, 0.33)	1.42 (1.11, 1.52)	0.16	0.23	0.25 (0.06, 0.23)
16. Paluma Range	1.42 (1.3, 1.49)	0.13	0.18	0.2 (0.05, 0.21)	1.4 (1.22, 1.49)	0.13	0.19	0.26 (0.12, 0.26)	1.44 (1.32, 1.53)	0.17	0.23	0.18 (-0.04, 0.19)

Note: AR=Allelic richness, H_{obs}=observed Heterozygosity, H_{exp}=expected Heterozygosity, F_{IS}=inbreeding coefficient. Bootstrapped confidence intervals (C.I.) based on 1000 replicates.

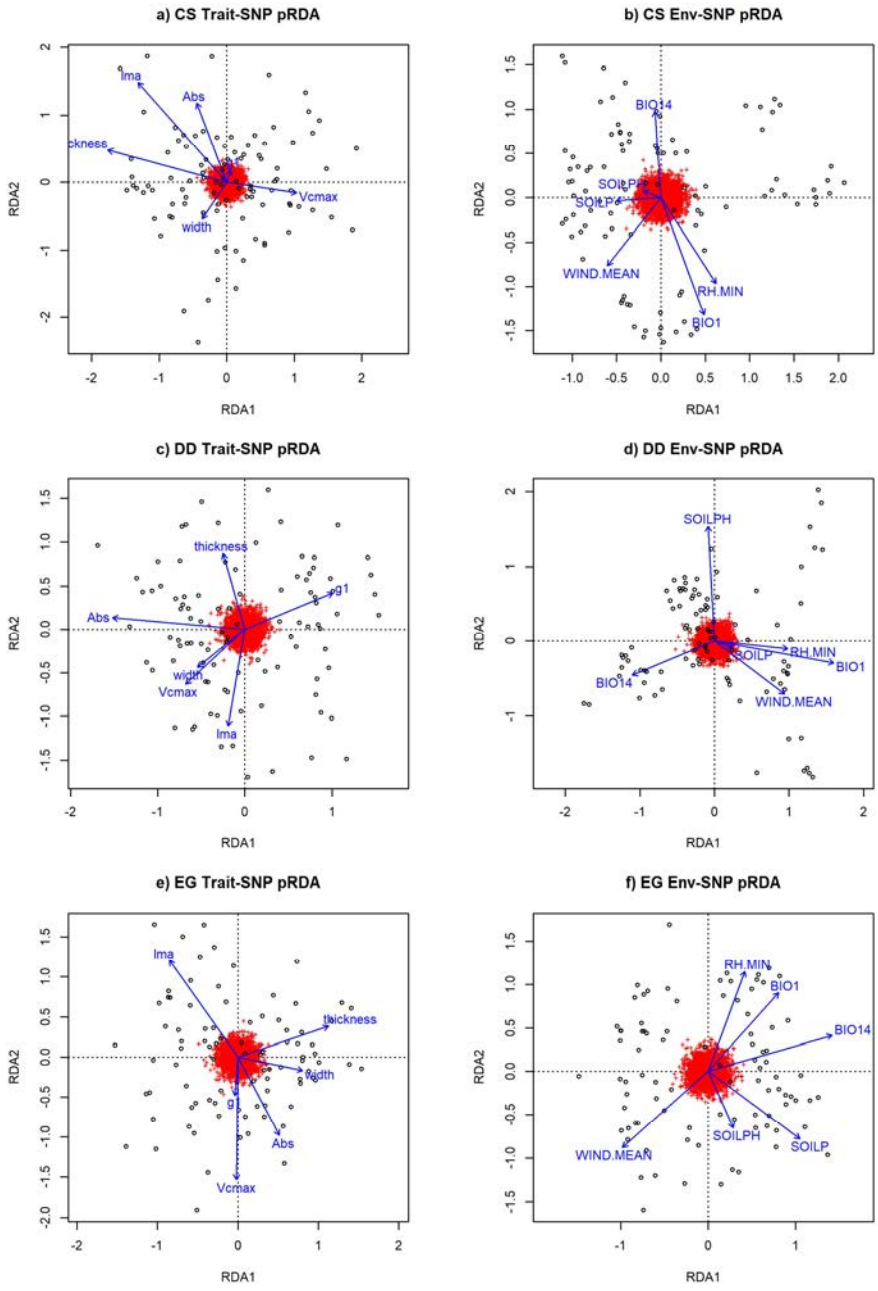

Appendix C: Figure 6. Partial redundancy analysis (pRDA) of genotype variation for each species. The plot displays the relationship between the SNPs with traits (a, c, e) or environment (b, d, f) along the first two pRDA axes.

Appendix C: Table 5. Number of candidate SNPs identified by each method.

		Number of Candidate SNPs		
Analysis	Method	*C. sublimis*	*D. darlingiana*	*E. grandis*
GPA	ΔT_{trait} LFMM	0	3	1
GPA	ΔT_{trait} pRDA	63	69	45
GPA	Leaf trait LFMM	1	40	3
GPA	Leaf trait pRDA	66	63	28
GEA	Environment LFMM	13	24	1
GEA	Environment pRDA	72	63	29
Outlier	PCADAPT	243	60	126

Appendix C: Table 6. Generalised dissimilarity modelling results.

Species	Response variable	Deviance explained (%)	Intercept	Top 6 significant predictors (ordered by % deviance explained)
Cardwellia sublimis	All SNPs	76.89	0.04	Geographic, Bio14, $Wind_{mean}$, Bio1, RH_{min}, Soil pH
	GEA & Outlier SNPs	61.93	0.07	Geographic, Bio14, RH_{min}, Soil pH, $Wind_{mean}$, Soil P
	GPA SNPs	66.6	0.05	Geographic, Soil pH, Bio14, $Wind_{mean}$, RH_{min}
	ΔT_{trait}	36.45	0.16	Soil pH, RH_{min}, Bio1, Geographic
	Trait PCA	34.1	0.22	Bio14, Soil P, Bio1, Soil pH, $Wind_{mean}$, RH_{min}
Darlingia darlingiana	All SNPs	68.08	0.03	Geographic, Bio14, Bio1, $Wind_{mean}$, Soil pH
	GEA & Outlier SNPs	61.9	0	Geographic, Bio1, Bio14, Soil pH, $Wind_{mean}$, RH_{min}
	GPA SNPs	49.05	0.04	Geographic, Bio1, Bio14, RH_{min}, Soil pH, $Wind_{mean}$
	ΔT_{trait}	44.07	0.07	Bio1, Bio14, Soil pH, Geographic, RH_{min}
	Trait PCA	21.69	0.44	Bio14, Bio1, Geographic, RH_{min}
Elaeocarpus grandis	All SNPs	65.8	0.04	Geographic, Bio14, RH_{min}, Bio1, Soil P
	GEA & Outlier SNPs	58.98	0.01	Geographic, Bio14, Bio1, RH_{min}, Soil P, $Wind_{mean}$
	GPA SNPs	27.47	0.07	Geographic, Bio14, Bio1
	ΔT_{trait}	37.27	0.07	Bio1, Soil pH, RH_{min}, Geographic
	Trait PCA	20.93	0.32	Bio1, RH_{min}, Geographic

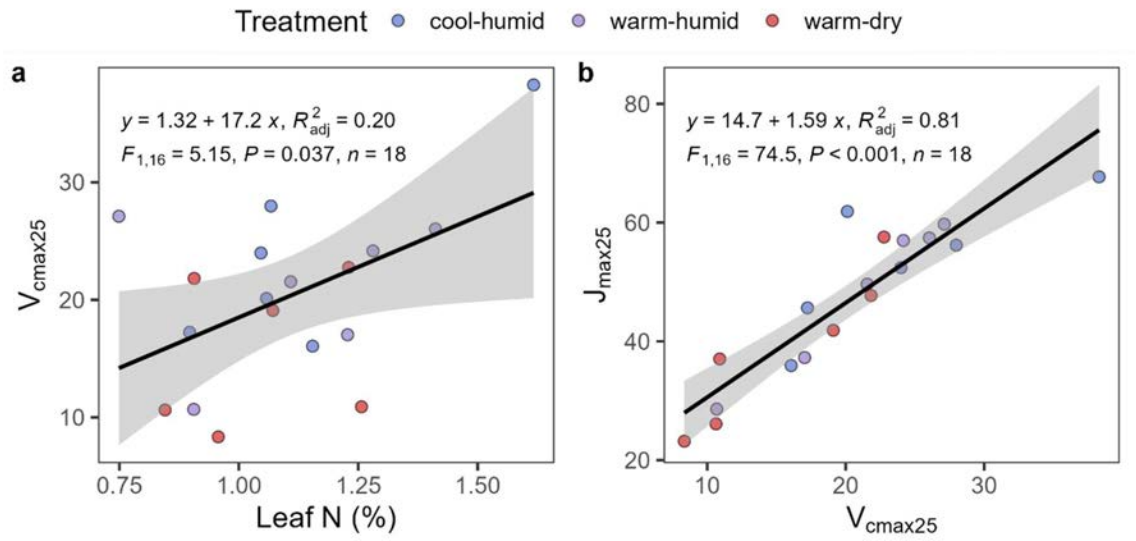

Appendix C: Figure 7. Correlation between photosynthetic parameters and leaf nitrogen determined in the glasshouse trial. V_{cmax25} = maximum carboxylation rate and J_{max25} = maximum rate of electron transport. Each point represents a plant level mean. Coefficients from linear regressions used to predict V_{cmax25} and J_{max25} in the field.

Appendix D: Strong site and provenance effects on tropical tree growth and survival, but mixed evidence for local adaptation

Kali B. Middleby[1], Lucas A. Cernusak[1], Martin F. Breed[2], Darren M. Crayn[3,4], Susan G.W. Laurance[1], Noel Preece[1,5,6], Penny van Oosterrzee[1,5,6], Jayden Engert[1], and Alexander W. Cheesman[1]

[1] Centre for Tropical Environmental Sustainability Science, James Cook University Nguma-Bada Campus, McGregor Road, Smithfield, QLD, Australia

[2] College of Science and Engineering, Flinders University, Bedford Park, SA, Australia

[3] Australian Tropical Herbarium, James Cook University Nguma-Bada Campus, McGregor Road, Smithfield, QLD, Australia

[4] ARC Centre of Excellence for Indigenous and Environmental Histories and Futures, James Cook University Nguma-Bada Campus, McGregor Road, Smithfield, QLD, Australia

[5] Biome 5 Pty Ltd., Atherton, QLD, Australia

[6]Research Institute for the Environment and Livelihoods, Charles Darwin University, Darwin, NT 0909, Australia

ABSTRACT

Restoring tropical rainforests is vital for mitigating climate change and conserving biodiversity. Appropriate seed-sourcing strategies are important for ensuring the success of restoration efforts, but require species-specific and context-dependent information, such as the strength of local adaptation. With studies of local adaptation severely lacking for tropical rainforest tree species, the current industry default is to source seed locally, which may not be beneficial in a rapidly changing climate. We therefore sought to identify the effects of provenance, site, and their interaction on the growth and survival of 16 tropical tree species commonly used for rainforest restoration in the Australian Wet Tropics. Saplings from lowland and upland populations were planted in common gardens across three field sites with contrasting climatic and edaphic conditions. We observed consistent site effects on growth, with all species performing better at the lowland, high-nutrient site compared to the lowland, low-nutrient and upland sites. Provenance effects were observed for both growth and survival, but evidence for local adaptation was mixed, with the lowland provenance often outperforming the upland provenance across most sites. Interestingly, species-variation in the effects of provenance was related to species wood density, with provenance effects more pronounced in faster-growing species. Together, these findings highlight the complexity of local adaptation in tropical tree species, which brings a note of caution to the current practice of sourcing seed locally.

KEYWORDS

Provenance, reciprocal transplant, climate change, restoration, ecotypes

INTRODUCTION

Tropical rainforests represent a disproportionate and dynamic component of the world's carbon budget (Friedlingstein et al., 2022; Mitchard, 2018), contain a majority of Earth's terrestrial biodiversity (Barlow et al., 2007; Gibson et al., 2011), and provide a diverse array of ecosystem services (Watson et al., 2018). Despite their significance, these ecosystems are under severe anthropogenic pressure, with an estimated 17% reduction in moist tropical forest extent from 1990 to 2019 (Vancutsem et al., 2021). At the same time, active restoration of terrestrial ecosystems is essential for addressing global challenges such as climate change, biodiversity decline, and land degradation (Girardin et al., 2021). The latest IPCC report (Riahi et al., 2022), highlights afforestation, reforestation, and revegetation perhaps in addition to improved forest management, agroforestry, and soil carbon sequestration as the primary CO_2 removal methods currently in use. The United Nations (UN) declared 2021-2030 the Decade of Ecosystem Restoration (United Nations General Assembly, 2019). However, the increasing frequency of hot, dry periods is exacerbating global tree mortality (Hammond et al., 2022) and is predicted to increase the frequency of lethal canopy temperatures being reached in tropical forests (Doughty et al., 2023a), posing a significant threat to the success of restoration efforts.

In response to climate change, plants can migrate, adapt, or become extinct (Corlett & Westcott, 2013; Merila & Hendry, 2014). However, the rapid rate of anthropogenic climate change and the shallow latitudinal temperature gradient in the tropics mean that migration is largely restricted to upward shifts in elevation (Colwell & Feeley, 2024). Additionally, the long generation times of forest tree species limit their ability to adapt quickly, making intraspecific phenotypic variation – both genetic variation accumulated over generations and phenotypic plasticity – crucial for adaptation (Merila & Hendry, 2014). When variation exists for divergent selection to act on, local adaptation can result in local populations with a fitness advantage over nonlocal populations in their home site (Brancalion et al., 2018; Muehleisen et al., 2020). Understanding and leveraging intraspecific variation is therefore essential for assessing and enhancing the success of restoration plantings in the face of rapid climate change.

One strategy to ensure that restoration plantings are successful in establishing resilient forests is the appropriate choice of seed sources. Restoration guidelines provide advice on how to maintain the genetic diversity and adaptive capacity of restored forest populations through the consideration of the geographic origin of seed, i.e. provenance (Malavasi et al., 2018; McDonald et al., 2016; Offord & Meagher, 2009). Although a strategy of selecting local provenances has traditionally been preferred by practitioners (Cooper et al., 2018), this can reduce fitness in cases when forest fragmentation results in inbreeding (Schlaepfer et al., 2018) or when rapid climate change causes a mismatch between the current or future climate with the historic conditions a population is adapted (Aitken &

Whitlock, 2013; Gellie et al., 2016). These issues have led to the recommendation of alternative provenancing strategies incorporating non-local seed sources (Breed et al., 2013; Jordan et al., 2024). Given the strong role climate can have in driving selection (Cordero et al., 2021; Ravn et al., 2024; Steane et al., 2014), the matching of seed sources to future climates (known as predictive or climate-adjusted provenancing) aims to introduce to an area genetic material that is better adapted and therefore also more resilient to climate change (Breed et al., 2013).

Despite the known advantages that strategies such as climate-matching provenance can have for restoration outcomes, the current industry default in rainforest restoration plantings is to source seed locally (Cooper et al., 2018). A key challenge in adopting alternative provenance selection in tropical rainforests is the extensive genetic information required to recommend a suitable strategy. Evidence for local adaptation requires direct evidence of local populations having fitness advantages over non-local populations, with full life-cycle analysis under reciprocal common garden conditions being considered the gold standard for determining true local adaptation (Kawecki & Ebert, 2004; Meek et al., 2022; Schwinning et al., 2022). Synthesis studies to date are heavily biased toward temperate species of commercial importance with very few, if any, tropical trees included (Hereford, 2009; Matesanz & Ramirez-Valiente, 2019). Their findings also reveal how the presence and strength of local adaptation are species and context dependent. This limits our understanding of the prevalence and strength of local adaptation in tropical rainforest trees, which typically have lower population densities than temperate species, but high reproductive efficiency over large distances maintaining similar levels of genetic diversity (Degen & Sebbenn, 2015). However, provenance trials to test for local adaptation are highly resource-intensive (Sork et al., 2013) and typically focus on a single species. This has limited the broad applicability of climate-matching provenance strategies in tropical systems where forests are extremely speciose and understanding the genetic background of each species is not feasible.

While a ‘one-size fits all’ approach to provenancing is generally not recommended or ideal, the combination of extremely high species diversity in tropical rainforests, and the limited resources available for restoration activities necessitates a simplified, easy-to-implement provenancing strategy. One possibility could be grouping the strategy according to species plant functional traits, such as wood density, that describe the *slow-fast* life-history continuum (Reich, 2014). Faster-growing species such as pioneers have shorter lifespans and earlier reproductive capacity than slower-growing species such as mature-phase species. As such, early successional stage species may show higher rates of molecular evolution and may therefore be more likely to have developed local adaptation than slower-growing species (Müller & Albach, 2010; Smith & Beaulieu, 2009; Smith & Donoghue, 2008). However, with studies of local adaptation severely lacking for tropical rainforest tree species, there is currently insufficient experimental evidence to support this. Additionally, while meta-analyses are

useful to discern the patterns and drivers of local adaptation in studies across multiple species, these studies often vary in methodology, site maintenance, and conditions that are not easily accounted for. There is therefore a need for multi-species studies of local adaptation in tropical trees that are key to rainforest restoration.

We investigated the prevalence of local adaptation in tropical rainforest tree species commonly used in restoration plantings in the Australian Wet Tropics. To do so we established three field-based provenance trials, including an upland and lowland site that differ in climate but have similar high-nutrient soils, and an additional lowland site on a low-nutrient soil. Saplings of 16 species were sourced from lowland and upland populations and reciprocally planted at each site, where initial growth and survival were monitored over 1.5 years. Specifically, we tested the following questions:

1) How do provenance, site, and provenance × site interactions affect sapling growth and survival?
2) If provenance × site interactions exist, do local provenances outperform non-local provenances at their local site (i.e. local adaptation sensu Kawecki & Ebert (2004))
3) If there is variation across species in their provenance differentiation, is this more pronounced in faster-growing species?

METHODS

Common garden sites

This experiment, part of the 'TropAdapt' project (https://tropadapt.org/) was conducted across three common garden trials established within the Wet Tropics bioregion of far north Queensland, Australia: two in the coastal lowlands and one in the uplands. The first lowland site is located at the Daintree Rainforest Observatory (DRO) in Cape Tribulation (−16.10449 °S, 145.4511 °E) with an elevation of 52 m (a.s.l.), mean annual temperature (MAT) of 24.5 °C and a mean annual precipitation (MAP) of 3026 mm. The soil at the site is acidic, dystrophic, brown dermosol, formed in the colluvium from the metamorphic and granitic mountains to the west (Murtha 1989). The second lowland site was established on an old airstrip in Cow Bay (−16.22406 °S, 145.4220 °E) with a MAT of 24.4 °C and a MAP of 3439 mm. Although soils in the area were originally dominated by haplic, dystrophic, red ferrosols formed on an alluvial fan derived from basalt (Murtha 1989), an anthropogenic reworking of the site and augmentation with sand and gravels to form the airstrip have left the soils poorly structured. The upland study site is in the southern Atherton Tablelands (−17.43025 °S, 145.5153 °E) on Thiaki Creek Nature Reserve (https://www.biome5.com.au/thiaki) at an elevation of 980 m a.s.l. It has a MAT of 19 °C and receives a MAP of 2264 mm. The site is on a ~30° slope with an NW aspect. The soil is acidic ferrosol formed from Cainozoic Basalt (Malcolm et al., 1999). The property was previously managed as a cattle pasture for approximately 70 years, and subsequently used as a research site for several previous reforestation experiments (Charles et al.,

2018) (Preece et al., 2015; Preece et al., 2017). The common garden plot used for this study is dominated by exotic grass species (e.g. *Melinis minutiflora*, *Urochloa* (*Brachiaria*) *decumbens* and *Setaria sphacelata*) and receives no shading from nearby trees.

The two lowland sites, DRO and Cow Bay are both located within the Daintree Rainforest and as such are similar both geographically and climatically. They differ primarily in soil nutrient status. The upland site Thiaki provides a climate contrast with MAT differing by ~ 5.5 °C and MAP differing by ~ 969 mm compared to the two lowland sites but does not suffer in terms of soil nutrient availability like the Cow Bay site. Comparison of tree performance across these three sites allows assessment of the effects of both climatic (upland vs lowland sites) and edaphic factors (low nutrient vs high nutrient sites).

Study species and plant material

We selected 16 tropical rainforest tree species (Figure 1, Table S1, Figure S1) that are commonly used in revegetation plantings in the Australian Wet Tropics bioregion (Engert et al., 2020), taxonomically diverse (representing 13 families), and exhibit a broad range of plant functional traits and successional strategies (Goosem & Tucker, 2013). Plant material with verified coordinates or collection location descriptions were sourced from local nurseries including Cairns Regional Council, Rainforest Rescue, Douglas Shire Council, Tablelands Regional Council, and Kuranda Envirocare. For each species, we obtained 30 individual seedlings from either lowland or upland origin (n = 960 = 30 seedlings × 2 provenance × 16 species). For two species (*Davidsonia pruriens* and *Syzygium kuranda*) only 15 seedlings could be sourced from a single upland maternal location so seedlings from an additional upland maternal location were included to make up the 30 total replicate seedlings needed (Table S1). During seedling handling and planting, we made sure plant provenance could be tracked back to the maternal plant location, however for this study we consider any plants originating from above 300 m a.s.l to be of 'upland provenance' and any plants originating from below this threshold to be of 'lowland' provenance in downstream analyses.

Across the focal species, the lowland and upland provenances differed in their MAT by on average 4.0 °C (range 1.8 to 5.8 °C) and by 836 mm in their MAP (range 102 to 1890 mm) (Table S1). Lowland and upland provenance collection locations were on average 105 km (range 52 to 150 km) apart (great-circle distance calculated with 'geosphere' package (R. J. Hijmans, 2022)), with Lowland provenances sourced from the Daintree Rainforest and upland provenances sourced from the Atherton tablelands (with few exceptions). As such, the comparison between DRO and Thiaki planting sites represented a reciprocal transplant for many species.

Experiment setup and site maintenance

Before planting, each site was treated with a broad-spectrum herbicide (Roundup, active ingredient Glyphosate, SpecialistSales, Toowoomba, QLD, Australia) across the entire plot for the DRO and Cow Bay, or along the planting strips (~1m wide) across the slope at Thiaki. Saplings ~6 to 12 months (mean height 37 cm, range 5 to 107 cm) were planted at each of the three trial sites in late March to April 2022 at 3 m x 3 m spacing to provide for an even light environment as plants grew. This included ten replicate saplings each of the two provenances (lowland and upland) for 16 species planted at each of the three trial sites (n = 320 at each site). The order of plants was randomised within 'blocks' with 1 replicate plant from each of 16 species and provenance (upland or lowland) represented in each block (n = 32 plants per block x 10 blocks at each site). At planting, soil cores were augered (diameter 200mm, depth ~30 cm) with each hole receiving 50g of an organic fertilizer pellet (Organic Life, Terra Firma fertilizers, Beaudesert Qld, Australia), and the pre-soaked plants replanted and watered in immediately. At the Thiaki site, there was a lack of significant rainfall in the weeks immediately after planting, so seedlings were hand-watered every 3 days until the first rains. After seedling establishment, weed management consisted of periodic row spraying with a C_4-targeted herbicide (Fuzilade Forte 128C, active ingredient Fluazifop-p, SpecialistSales, Toowoomba, QLD, Australia).

Measurements of growth and survival

Two months after the initial planting 98.4% survival was observed across all sites. Supplementary planting of additional replicates was carried out to maintain the complete planting matrix; these replacement plants were not included in our survival analyses. Over the experiment, total plant height (m) and plant health (described below) were recorded: at planting, and 4, 12, 17, and 24 months after planting. For multi-stemmed individuals, the total height of the leading stem was measured. Health was assessed qualitatively using an index of 0 to 5, with 0 = dead, 1 = main stem dead but with resprouting evident, and levels 2 to 5 representing; <25%, 25 to 50%, 50 to 75%, and >75% healthy canopy respectively. For survival analysis, plants with a health class of 1 or lower were classified as functionally dead. For analysis of height data, all functionally dead individuals were excluded.

To account for potential within-site variation in environmental conditions (i.e. edaphic or light conditions) known to impact tree growth across the experimental sites (Cheesman et al., 2018) we tested for spatial autocorrelation present in the tree growth rates, using Moran's I. This test indicated significant spatial autocorrelation in growth data within each plot. As trees were not grouped by species in the plots, this autocorrelation is likely due to intra-site variation in soil properties such as rockiness or fertility. Therefore, to account for this spatial autocorrelation, we built a spatial autologistic term (Dormann, 2007) using height data from the August 2023 campaign normalised for each site. We generated autologistic terms using focal windows with diameters of three, five, and

seven trees, then selected the window size that addressed spatial autocorrelation while exerting the least influence on the model. All three autologistic terms accounted for spatial autocorrelation in model residuals, thus, we chose the term with a focal diameter of seven trees as it had the least influence on the model and was least likely to bias model parameter estimates (Figure S2).

Common Garden soil and meteorological data

Across each site, nine surface soil samples (0 to 10 cm) were taken for basic physiochemical and nutrient analysis to characterize soil nutrient availability and water-holding capacity (Table S2). In addition, actual site meteorological conditions (rainfall, and daily minimum and maximum temperatures) over the entire experimental period (Figure 2) were extracted from SILO climate database hosted by the Queensland Department of Environment, Science and Innovation (https://www.longpaddock.qld.gov.au). Average climatological data (1980 to 2010) for planting sites and seed provenances were taken from CHELSA-BIOCLIM V2.1 dataset (Karger *et al.* 2017, 2018).

Wood density

To explore whether species with different life-history strategies differ in their provenance differentiation, we examined the impact of species wood density, as an important component and continuous variable in the *slow-fast* life-history continuum (Reich, 2014). We assume that species with higher wood density generally grow more slowly, have longer lifespans, and exhibit lower mortality rates (Chave et al., 2009; Liang et al., 2021). We retrieved wood density values for each species from the global wood density database using the 'BIOMASS' package v.2.1.8 (Réjou‐Méchain et al., 2017). Although wood density data for Australian rainforest species are generally sparse, with many species having only one or a few data points, (Preece et al. 2015, Ilic et al 2000), we were able to extract species level averages of wood density for all species based on a sample size of 6 individuals on average (range 1 to 46). Given our interest in using this trait as an index of inherent species differences in life history strategies, we considered the data appropriate for our needs.

Data analysis

For each species, we analysed two performance metrics that have fitness consequences: overall survival and height increase after ~17 months of growth (503, 525, and 523 days in Cow Bay, DRO, and Thiaki respectively) – analysis was limited to just 17 months given a) partial canopy closure by some trees at the DRO was beginning to lead to neighbour shading b) this allowed us to exclude the impacts of ex-Tropical Cyclone Jasper, which made landfall close to the DRO and Cow Bay sites on the 13th Dec 2023 causing extensive regional flooding.

Probability of survival was assessed using a generalised linear model with a binomial response with a 'log-link' family. Due to data separation issues, a Firth's correction was required so we fit the model using the 'brglm' function. Survival data (1 = alive, 0 = dead) was the response variable. To identify the impact of provenance and site on growth for each species, we fitted a generalised linear model with a Gaussian distribution. We compared absolute fitness (growth increment over ~17 months) instead of log transforming the data because this can lead to misinterpretations of the data (Stanton & Thiede, 2005). For each model, we looked at the interaction effects of provenance (factor, two levels) and site (factor, three levels), and included covariates for initial height (numeric, continuous) and the underlying spatial autocorrelation as the autologistic term (numeric, continuous) (Dormann, 2007).

To determine if species-level wood density could explain the strength and direction of population differentiation, we performed ordinary least squares regression. We used wood density as the independent variable and the difference between lowland and upland populations estimated marginal means of height increment or survival probability from the previous analysis as the dependent variable. Initial analysis also used common garden 'site' location as a fixed term in the model, although site-specific regressions were also carried out to provide clarity. All analyses were performed using R Statistical Software (R Core Team, 2022).

Two species – *Alstonia scholaris* and *Toona ciliata* – were found to have a complex interaction between initial growth and insect herbivory in that once individuals (irrespective of provenance) obtained a certain size they were subject to devastating insect damage from either an unidentified caterpillar or native Cedar tip moth (*Hypsipyla robusta*) respectively. This damage caused loss of the apical meristem and a reduction in overall height in these species at sites where they first gained a larger height - as such these species were excluded from growth analyses (but retained in survival analyses).

RESULTS

Provenance and site differentiation in tree survival

After 17 months of growth, we had on average 79% survival from the original planting, however, losses were somewhat asymmetric across species. Eleven of the 16 species showed significant effects of provenance and/or planting location on survival, and five showed no effect (Figure 3, Table S1, Figure S3). In two species, *C. ramiflorus* and *M. elleryana*, site alone significantly affected survival, with both species exhibiting lower survival at the DRO site compared to the other two sites, where no mortality was observed. In two species (*S. luehmannii*, and *N. dealbata*) provenance alone affected survival: the lowland provenance had a higher survival rate than the upland provenance irrespective of site for each species. For two species (*A. fitzalanii* and *G. acutifolia*), survival was impacted by both provenance and site (with no interaction effect): the upland provenance had higher survival than the

lowland provenance at all sites, and survival was generally lower at Thiaki compared to the other two sites (Figure S3). For three species (*C. hypospodia*, *E. grandis*, and *T. ciliata*) there were significant provenance × site effects on survival. In *C. hypospodia* the lowland provenance had higher mean survival at all sites but had greater provenance differentiation at Cow Bay compared to other sites. For *E. grandis*, survival was greater for the upland provenance compared to the lowland provenance when grown at the Cow Bay and Thiaki sites, but the opposite was observed when grown at the DRO site. For *T. ciliata* provenance differentiation was only significant at the DRO site, where the lowland provenance had a higher probability of survival.

3.2 Provenance and site patterns in growth

Overall, both site and provenance had strong effects on growth. Across the ~17 months of growth, saplings grew on average 1.0±0.7 and 1.1±0.9 m at Cow Bay and Thiaki respectively but 2.6±1.8 m at the DRO, with an average growth of some species at the DRO (i.e. *E. grandis*, *H. novo-guineensis*, and *T. microcarpa*) being >4.4 m. Site consistently impacted growth (Figure 3, Figure S4, Table S4), with all species except *N. dealbata* showing significant site effects. All species exhibited greater growth at the DRO site compared to Cow Bay or Thiaki. For five species, provenance had a significant impact on growth (Figure 3b), and in each species, the lowland provenance was taller than the upland provenance. Only two species (*H. novo-guineensis*, *S. kuranda*) showed significant provenance × site effects on growth, with a greater difference in growth between provenances at the two lowland sites, than at Thiaki.

3.3 Wood density effects

The magnitude of provenance differentiation (difference between estimated marginal means of the lowland and upland provenances) for growth data was significantly associated with species-level wood density ($F_{1,35} = 4.42$, $P = 0.043$) but not site ($P > 0.05$), whereas marginal interaction effects were observed for survival data ($F_{1,42} = 2.62$, $P = 0.085$) when including site as a fixed factor. In the site-specific model of survivorship (Figure 4), the same overall trend was only observed at the DRO site (adj-$R^2 = 0.30$, $P = 0.016$), whereas for growth this was observed at both the DRO (adj-$R^2 = 0.56$, $P = 0.002$) and Cow Bay sites ($R^2 = 0.24$, $P = 0.062$).

DISCUSSION

Studies of local adaptation are severely lacking for rainforest tree species that are key to restoration efforts. While meta-analyses are useful to discern drivers of local adaptation in studies across multiple species (Hereford, 2009; Leimu & Fischer, 2008; Matesanz & Ramirez-Valiente, 2019), these studies often vary in methodology, site maintenance and conditions that are not easily accounted for. In this study, we used three common garden sites to investigate the effects of site, provenance, and their interaction on the growth and survival of 16 tree species commonly used in restoration plantings in

the Australian Wet Tropics. Site effects were observed in 93% of species for growth and 44% for survival, while provenance effects were noted in 36% of species for growth and 56% for survival. Of the three species that had significant site × provenance interactions in survival, only *E. grandis* exhibited local adaptation. None of the two species with site × provenance interactions in growth exhibited local adaptation; in both cases, the lowland provenance generally outperformed the upland provenance regardless of site. We found a correlation between species wood density and the magnitude and direction of provenance differentiation in both survival and growth, suggesting that provenance effects are more pronounced in faster-growing species. These results challenge the usefulness of a 'local is best' provenancing strategy for upland restoration plantings in the Australian Wet Tropics and help to fill the gap in our understanding of the extent of local adaptation in tropical rainforest trees globally.

Site effects on growth and survival

We used three common garden sites to contrast tree performance across two major environmental axes commonly encountered by restoration practitioners: nutrient availability (DRO vs Cow Bay) and climate (DRO vs Thiaki). We found a substantial impact of site on both survival and growth of tropical trees planted under common garden conditions (Figure S3, S4), with trees at the DRO gaining on average over twice the height increment seen at the other two sites. This resulted in the DRO planting site reaching effective site capture and partial canopy closure after 1.5 years of growth with a planting density of just 1100 trees ha^{-1}, far lower than the planting density commonly employed in the Australian Wet Tropics (Goosem & Tucker, 2013). In contrast, poor overall growth at the Cow Bay site necessitated continued site maintenance. The differences between the DRO and Cow Bay highlight the significant impact that edaphic context can have on tree growth and restoration success. The DRO and Thiaki sites were not limited in nutrient availability, and differed primarily in climate conditions, with the DRO site experiencing on average higher temperatures, vapour pressure deficit, and rainfall than Thiaki. The higher growth rates observed at the DRO compared to Thiaki are consistent with elevational patterns of growth observed in natural populations across the Australian Wet Tropics (Bauman et al., 2022a; Bradford et al., 2014). This has been linked to warmer temperatures stimulating growth and biomass accumulation in tropical tree species that can be masked or limited by the associated increase in vapour pressure deficit (Smith et al., 2020). While the contrasting temperatures of the DRO and Thiaki sites likely contributed to the growth differences across these sites, it is also important to note the site differences in precipitation and therefore soil moisture. Although both sites receive relatively high levels of mean annual precipitation, the cumulative rainfall at the DRO was over 2x higher during the study period compared to Thiaki. We therefore cannot rule out the effect that soil moisture may have had on plant performance during this trial.

Impacts of provenance but limited evidence for local adaptation

In comparing the growth and survival of upland and lowland provenances between the DRO and Thiaki we had hoped to isolate the impacts of temperature - and given the proximity of maternal populations to planting sites (Figure S1) the prevalence of local adaptation in our study species. Although we found that the lowland provenance outperformed the upland provenance at the lowland site, we did not find the reciprocal to be true *i.e.* upland provenances did not outperform lowland provenances in the upland site, indicating a partial lack of local adaptation. The notable exception was *E. grandis*, where the local provenance had higher survival rates than the nonlocal provenance at both DRO and Thiaki, consistent with local adaptation sensu Kawecki and Ebert (2004). While this contrasts with some studies that observed local adaptation, many examples supporting our results challenge the notion that this is widespread (Bucharova, Durka, Hermann, Hölzel, et al., 2016; Leimu & Fischer, 2008; Mushagalusa et al., 2020). Our findings resemble those observed in the reciprocal transplant of *Quercus oleoides* populations conducted by Deacon & Cavender-Bares (2015). In their study, the lowland provenance also exhibited higher mean fitness at all sites compared to the upland provenance. Given that faster growth rates are typically observed in lowland environments (Bauman et al., 2022a; Bradford et al., 2014), it is possible that lowland populations of rainforest trees generally have evolved higher growth rates than upland populations, potentially at the cost of stress tolerance or other fitness metrics (Willi & Van Buskirk, 2022). Another possibility is that the lowland provenance seedlings in our study were sourced from more intact populations with higher reproductive population size and therefore genetic diversity, which has been linked to higher fitness (Reed & Frankham, 2003). Confirming this requires further work assessing within-species genetic diversity and differentiation across populations. However, it is possible that upland provenances may possess greater stress tolerance, and a full life-cycle assessment is needed to determine any true differences in population fitness. Furthermore, in Deacon & Cavender-Bares (2015) study, the advantage of the lowland provenance was only temporary with provenance differences no longer evident by the third year, highlighting the importance of continued monitoring of such studies when assessing patterns of local adaptation.

Stronger provenance effects in fast vs. slow growth species

Provenance trials are highly resource-intensive (Sork et al., 2013), often restricting investigations to a single species. However, local adaptation can be highly species- and context-dependent, which limits the broad applicability of climate-matching provenance strategies in tropical systems with high species diversity. We differentiated between species that generally grow slower, live longer, and invest more resources into defences than those that grow fast and have a more rapid lifecycle using the fundamental plant trait wood density (Poorter et al., 2008; Wright et al., 2010). We found that species-level wood density was negatively associated with the magnitude of provenance

differentiation in growth and, to a lesser extent, in survival. This supports our hypothesis that faster-growing species with shorter generation times are more likely to exhibit pronounced provenance differentiation. However, since very few species showed interaction effects between site and provenance consistent with local adaptation, it remains unclear whether the observed provenance differences are due to higher rates of molecular evolution in faster-growing species (Smith & Donoghue, 2008). It is likely that after only 1.5 years of measurements, provenance variation is observable primarily in faster-growing species or at sites where resource limitations do not obscure growth potential.

Conclusions and implications for rainforest restoration in the Australian Wet Tropics

Although site and provenance effects were important in determining tree survival and growth across our 16 study species, evidence for local adaptation was observed in only one species. For most species the lowland provenance performed better than the upland provenance regardless of site. This highlights the complexity and context-dependency of local adaptation in tropical rainforest trees, challenging the 'local is best' strategy for sourcing seed for restoration plantings (Cooper et al., 2018). Our findings suggest that using lowland provenances, regardless of site, could optimize initial plant growth in some species. Restoration practitioners might consider expanding the sources of seed, particularly in higher altitude sites like the Atherton Tablelands, to meet seed demands and enhance genetic diversity and adaptive capacity. However, risks associated with both local and mixed provenancing approaches are well-documented (Jordan et al 2024). We urge researchers and practitioners in this region to focus on generating the necessary information for informed decision-making.

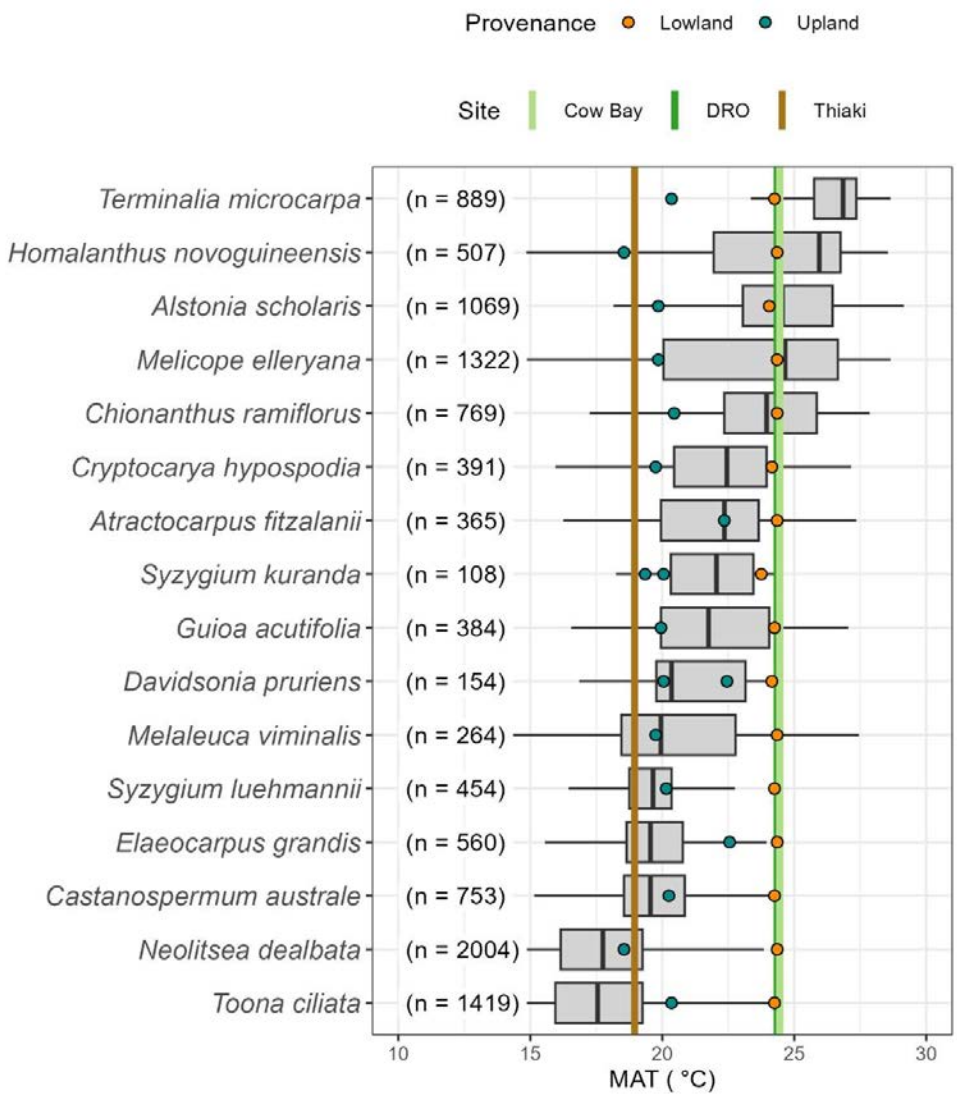

Figure 1. Comparison of mean annual temperature (MAT) of origin for seed source and planting locations within observed thermal niche of each species (GBIF, 2024). Boxplots show the MAT (1981-2010 CHELSA database V.2.1) distribution throughout each species global native range (occurrences obtained from GBIF, cleaned for errors, and spatially thinned to 1km resolution). The black line is the median, with the grey filled region equal to 1.5 × the interquartile range. Whiskers represent the 25th and 75th percentile, and outliers are not shown for clarity. The red and blue points represent the MAT of origin for the seed source locations of the lowland and upland provenances respectively. The three coloured vertical lines represent the MAT at the common garden sites. Species are arranged in order of their mean thermal niche.

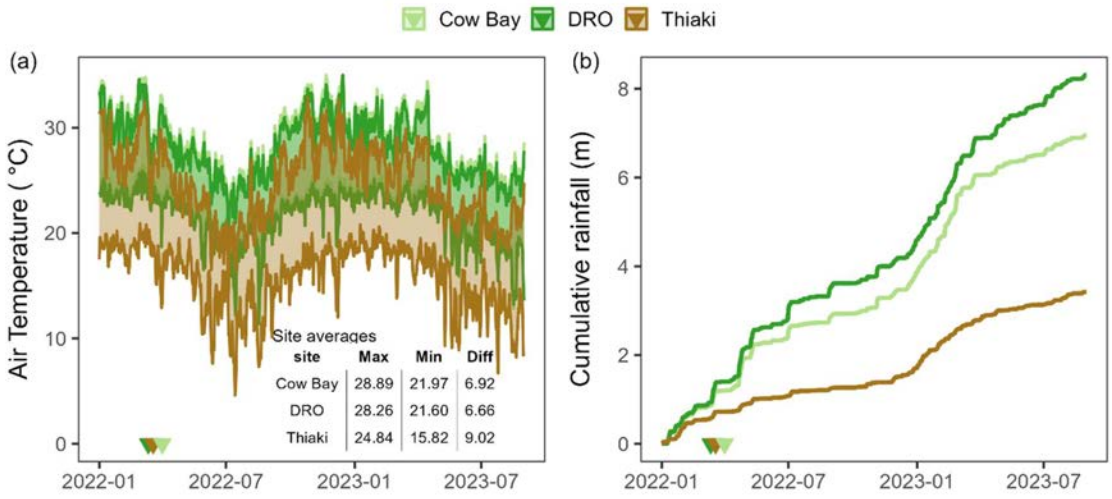

Figure 1. Meteorology at each site during the experiment. Plots show (a) daily max and min air temperature (°C) and (b) cumulative daily rainfall (m) from 01-01-2022 until the last census date 31-08-2023. The triangle points mark the planting dates. Table inset for panel (a) reports the overall means of daily max, min, and difference between max and min (diff) for air temperature (°C) at each site.

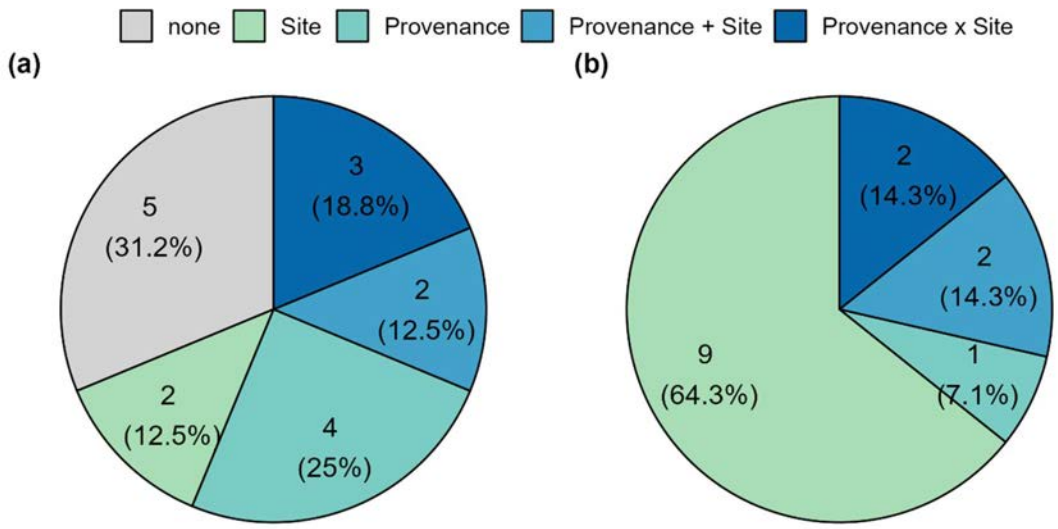

Figure 2. Proportion of species showing significant provenance and site effects on survival (a) and growth (b) in this study. Pie charts show the number and percentage of species that had significant ($P < 0.1$) effects of just 'Site', just 'Provenance', both 'Site' and 'Provenance', or their interaction 'Provenance x Site' ($n = 16$ species for survival and 14 species for growth). For full statistical details see Table S3 and Table S4.

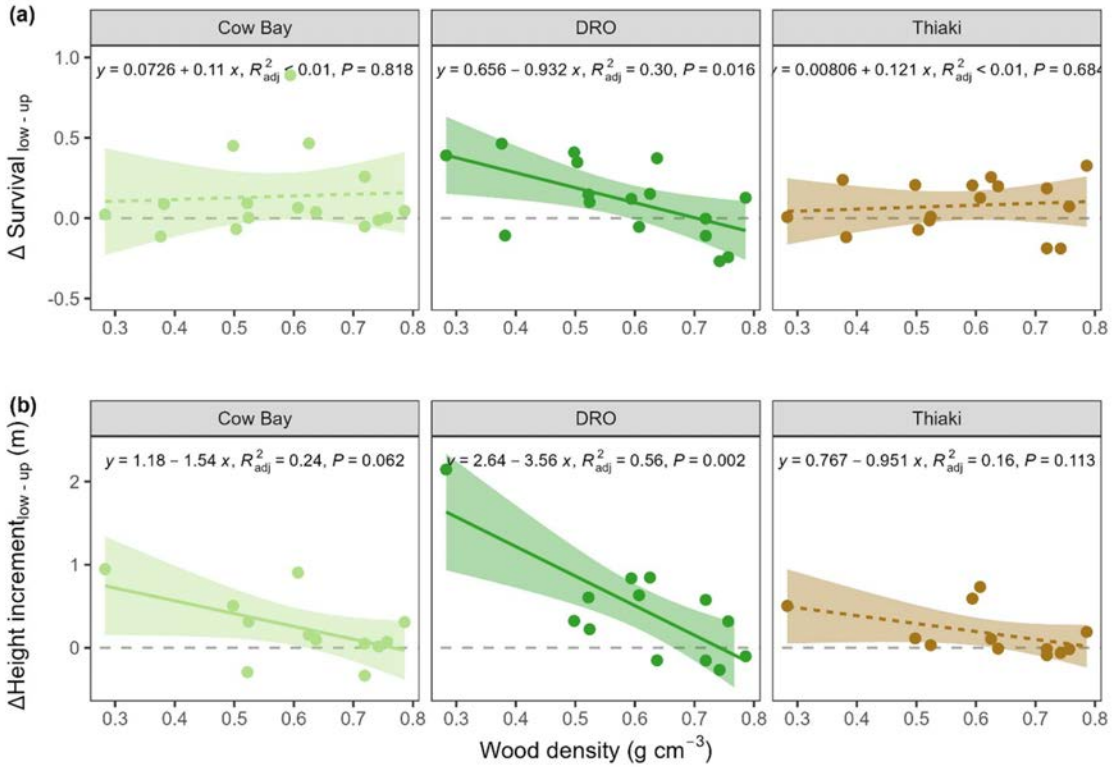

Figure 4: Relationship between species-level wood density and absolute population differentiation for either survival (a) or height increment (b) in tropical trees grown across three common garden experimental plots. All points represent the pairwise comparisons for lowland – upland provenances from the models. Values greater than 0 (grey horizontal line) indicate greater performance of the lowland provenance, and values < 0 indicate greater performance of the upland population, significant regression trends (P<0.05) are indicated by solid line.

SUPPLEMENTARY INFORMATION

Table S1. Provenance information for species used in study. Mean annual temperature (MAT, °C) and precipitation (MAP, mm) from between 1980 and 2010 as retrieved from CHELSA V2.1 (Karger et al., 2017, 2018). Letters in brackets within the provenance column denote separate information for species whose upland population was collected from two different locations. Latitude and Longitude are given in decimal degrees.

Species	Provenance	Latitude	Longitude	Locality	MAT (°C)	MAP (mm)
Alstonia scholaris	lowland	-16.8295	145.7023	Smithfield	24.1	1958
(Apocynaceae)	upland	-17.2893	145.6177	Yungaburra	19.9	2421
Atractocarpus fitzalanii	lowland	-16.2029	145.4041	Diwan	24.4	3077
(Rubiaceae)	upland	-16.8493	145.6208	Kuranda	22.4	1788
Castanospermum australe	lowland	-16.4725	145.3649	Mossman	24.3	2298
(Fabaceae)	upland	-17.3359	145.5003	Wongabel	20.3	1898
Chionanthus ramiflorus	lowland	-16.2029	145.4041	Diwan	24.4	3077
(Oleaceae)	upland	-17.2742	145.5805	Yungaburra	20.5	2068
Cryptocarya hypospodia	lowland	-16.2377	145.4279	Cow Bay	24.2	2959
(Lauraceae)	upland	-17.3687	145.6746	Glen Allyn	19.8	3092
Davidsonia pruriens	lowland	-16.2382	145.4324	Cow Bay	24.2	2959
(Cunoniaceae)	upland (a)	-17.3550	145.5878	Malanda	20.1	2444
	upland (b)	-16.8069	145.5806	Kuranda	22.5	1654
Elaeocarpus grandis	lowland	-16.1770	145.4128	Diwan	24.4	3334
(Elaeocarpaceae)	upland	-16.8053	145.6140	Kuranda	22.6	1796
Guioa acutifolia	lowland	-16.2620	145.3337	Daintree	24.3	2354
(Sapindaceae)	upland	-17.3090	145.6137	Peeramon	20.0	2457
Homalanthus novoguineensis	lowland	-16.1770	145.4128	Diwan	24.4	3334
(Euphorbiaceae)	upland	-17.5205	145.5679	Milla Milla	18.6	2874
Melaleuca viminalis	lowland	-16.1770	145.4128	Diwan	24.4	3334
(Myrtaceae)	upland	-17.3703	145.3904	Herberton	19.8	1444
Melicope elleryana	lowland	-16.1770	145.4128	Diwan	24.4	3334
(Rutaceae)	upland	-17.2995	145.4585	Carrington	19.9	1665
Neolitsea dealbata	lowland	-16.1770	145.4128	Diwan	24.4	3334
(Lauraceae)	upland	-17.5202	145.5691	Milla Milla	18.6	2874
Syzygium kuranda	lowland	-16.2344	145.4485	Cow Bay	23.8	3024
(Myrtaceae)	upland (a)	-17.3548	145.5861	Malanda	20.1	2444
	upland (b)	-16.2775	145.0675	Mt Windsor	19.4	1704
Syzygium luehmannii	lowland	-16.4725	145.3649	Mossman	24.3	2298
(Myrtaceae)	upland	-17.2769	145.4925	Atherton	20.2	1704
Terminalia microcarpa	lowland	-16.2620	145.3337	Daintree	24.3	2354
(Combretaceae)	upland	-17.2628	145.4817	Atherton	20.4	1604
Toona ciliata	lowland	-16.4725	145.3649	Mossman	24.3	2298
(Meliaceae)	upland	-17.2397	145.4801	Tolga	20.4	1530

Table S2. Surface soil characteristics for the three common garden sites.

Site	DRO			Cow Bay			Thiaki		
Soil Organic matter [1] (%)	16.58	±	1.99	8.43	±	1.44	22.16	±	0.95
Total Carbon [2] (mg g^{-1})	51.89	±	6.49	26.38	±	6.84	62.50	±	4.17
Total Nitrogen [2] (mg g^{-1})	4.32	±	0.61	2.16	±	0.73	4.28	±	0.41
pH[3]	5.23	±	0.11	5.20	±	0.15	5.63	±	0.31
CEC[4] ($cmol^{+}$ kg^{-1})	3.12	±	0.65	1.55	±	0.17	7.50	±	2.75
Available K (µg g^{-1})	71.22	±	12.30	32.63	±	8.12	196.75	±	189.79
Total Phosphorus (µg g^{-1})	873.33	±	151.58	297.50	±	39.91	3825.00	±	827.65

[1] determined by Loss on ignition (550°C, 4h)

[2] determined by Elemental Analysis

[3] pH determined in 1:5 DDI water

Cation Exchange capacity determined using ammonium acetate method, all base cations including aluminium

Available potassium determined using ammonium acetate

Total phosphorus determined after acid digestion and ICP-OES analysis

Table S3. Effects of provenance and site on survival. Table reports results for Bias Reduction in Binomial-Response Generalized Linear Models on the effect of provenance, site, and their interaction on probability of individual stem survival. Covariates include initial plant height, as well as spatial autocorrelation using a window based upon 7 trees. Binomial distribution was taken as the link function. Results with $P < 0.1$ are bolded.

Species	Spatial correlation		Initial Height		Site		Provenance		Provenance × Site	
	F	*P*	*F*	*P*	*F*	*P*	*F*	*P*	*F*	*P*
Alstonia scholaris	0.36	0.549	4.08	**0.043**	4.40	0.111	3.84	**0.050**	0.84	0.658
Atractocarpus fitzalanii	0.02	0.878	3.14	**0.077**	7.51	**0.023**	3.35	**0.067**	0.00	1.000
Castanospermum australe	0.19	0.660	1.83	0.176	2.46	0.292	0.00	1.000	0.00	1.000
Chionanthus ramiflorus	1.92	0.166	2.70	0.101	12.17	**0.002**	0.39	0.532	0.00	1.000
Cryptocarya hypospodia	4.40	**0.036**	0.46	0.499	17.13	**0.000**	17.62	**0.000**	7.99	**0.018**
Davidsonia pruriens	2.71	0.100	2.53	0.112	0.60	0.740	0.07	0.789	1.47	0.479
Elaeocarpus grandis	2.03	0.154	0.91	0.341	1.52	0.468	0.44	0.505	7.11	**0.029**
Guioa acutifolia	2.10	0.148	3.02	**0.082**	16.53	**0.000**	2.82	**0.093**	0.13	0.936
Homalanthus novoguineensis	9.20	**0.002**	4.63	**0.031**	2.25	0.324	0.95	0.330	0.00	1.000
Melaleuca viminalis	0.48	0.490	0.96	0.328	1.63	0.442	0.17	0.679	1.22	0.542
Melicope elleryana	0.82	0.364	0.43	0.512	4.90	**0.086**	0.17	0.679	0.00	1.000
Neolitsea dealbata	2.46	0.117	0.97	0.324	0.47	0.791	9.18	**0.002**	0.79	0.674
Syzygium kuranda	3.88	**0.049**	0.59	0.444	0.46	0.795	2.88	**0.089**	2.08	0.353
Syzygium luehmannii	2.71	0.100	0.00	1.000	1.18	0.553	3.10	**0.078**	0.92	0.630
Terminalia microcarpa	5.63	**0.018**	0.40	0.530	0.20	0.906	2.49	0.115	0.12	0.941
Toona ciliata	0.00	1.000	1.33	0.249	3.56	0.169	2.32	0.128	7.90	**0.019**

Table S3. Table of model on the effect of provenance and site and their interaction on incremental growth in tree heights using glm with gaussian distribution. Covariates include initial plant height and spatial autocorrelation. Spatial autocorrelation considered as a covariate (Spatial) using a window based upon 7 trees. Results with $P < 0.1$ are bolded.

Species	Spatial correlation		Initial Height		Site		Provenance		Provenance × Site	
	F	*P*	*F*	*P*	*F*	*P*	*F*	*P*	*F*	*P*
Atractocarpus fitzalanii	6.96	**0.008**	0.84	0.359	79.88	**0.000**	1.14	0.285	1.34	0.51
Castanospermum australe	5.50	**0.019**	0.03	0.875	55.48	**0.000**	1.01	0.315	2.51	0.28
Chionanthus ramiflorus	5.46	**0.0195**	0.96	0.328	9.68	**0.008**	0.26	0.613	0.56	0.756
Cryptocarya hypospodia	18.75	**0.000**	0.04	0.839	10.40	**0.006**	19.46	**0.000**	0.51	0.477
Davidsonia pruriens	5.64	**0.018**	2.80	**0.095**	39.08	**0.000**	0.55	0.460	2.82	0.244
Elaeocarpus grandis	28.55	**0.000**	3.02	**0.082**	46.66	**0.000**	2.48	0.115	0.44	0.801
Guioa acutifolia	2.80	**0.094**	0.68	0.411	9.10	**0.011**	12.56	**0.0004**	0.48	0.789
Homalanthus novoguineensis	20.11	**0.000**	0.77	0.381	94.27	**0.000**	25.69	**0.000**	8.24	**0.016**
Melaleuca viminalis	3.45	**0.063**	0.99	0.320	14.94	**0.0006**	1.68	0.195	2.06	0.357
Melicope elleryana	29.37	**0.000**	0.27	0.603	104.2	**0.000**	1.45	0.228	0.55	0.758
Neolitsea dealbata	23.45	**0.000**	0.14	0.710	4.30	0.116	4.49	**0.034**	1.38	0.502
Syzygium kuranda	0.08	0.781	1.89	0.170	9.86	**0.007**	0.62	0.431	4.91	**0.086**
Syzygium luehmannii	3.98	**0.046**	0.45	0.505	13.19	**0.001**	0.04	0.840	1.20	0.549
Terminalia microcarpa	1.28	0.257	0.56	0.454	51.15	**0.000**	0.14	0.710	2.66	0.264

Figure S3. Map of trial sites and seed collection locations for each species in the Wet Tropics Bioregion of Australia. Sites represented by black squares. Provenance locations for each species represented with coloured circles.

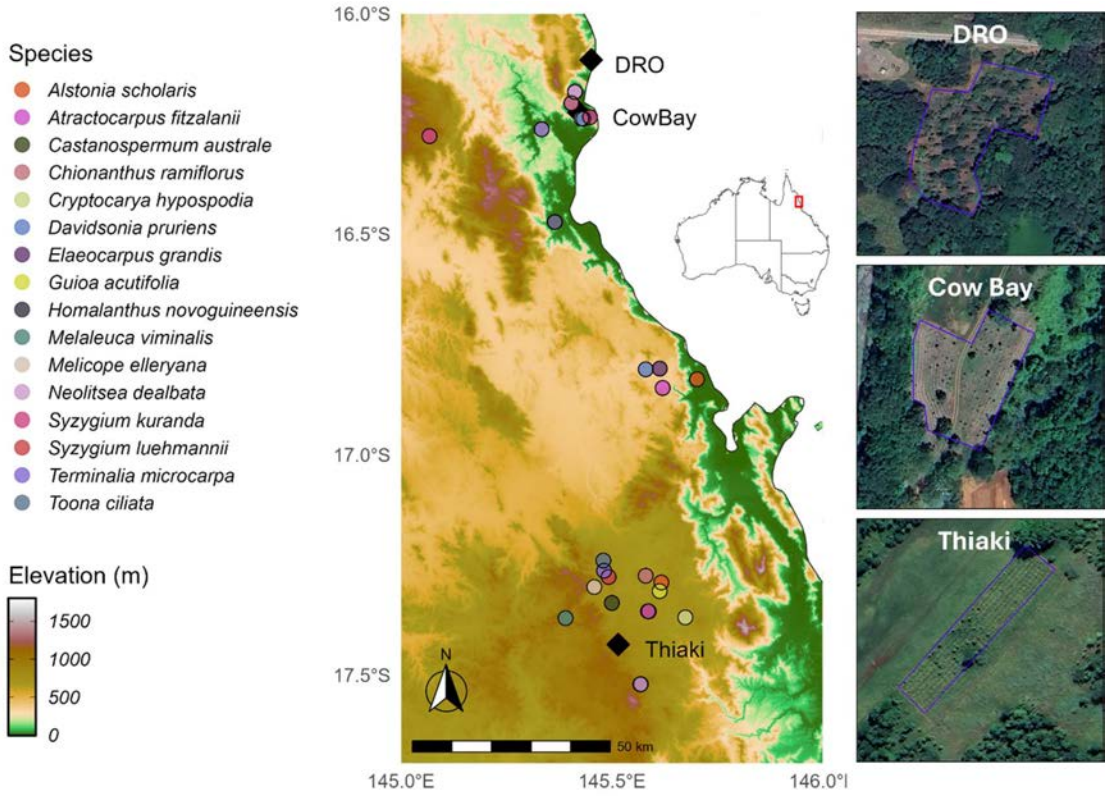

Figure S2: Map of spatial autocorrelation term built using a focal window of seven trees and used in the final model to account for spatial autocorrelation in observed growth rates across the three planting sites.

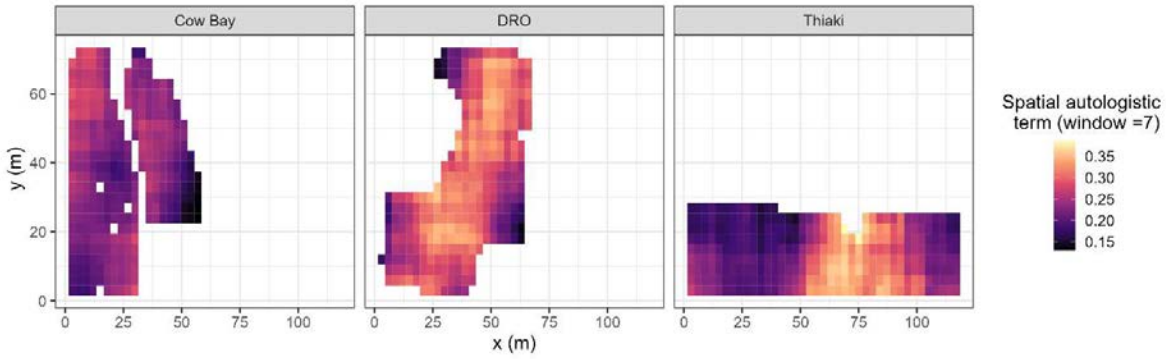

Figure S3: Proportion of planted saplings of 16 tropical tree species surviving to 1.5 years in one of three common garden planting sites in the Australian Wet Tropics. Points represent estimated marginal means of survival accounting for spatial correlation from full model (see text) for each species with lines indicating confidence interval.

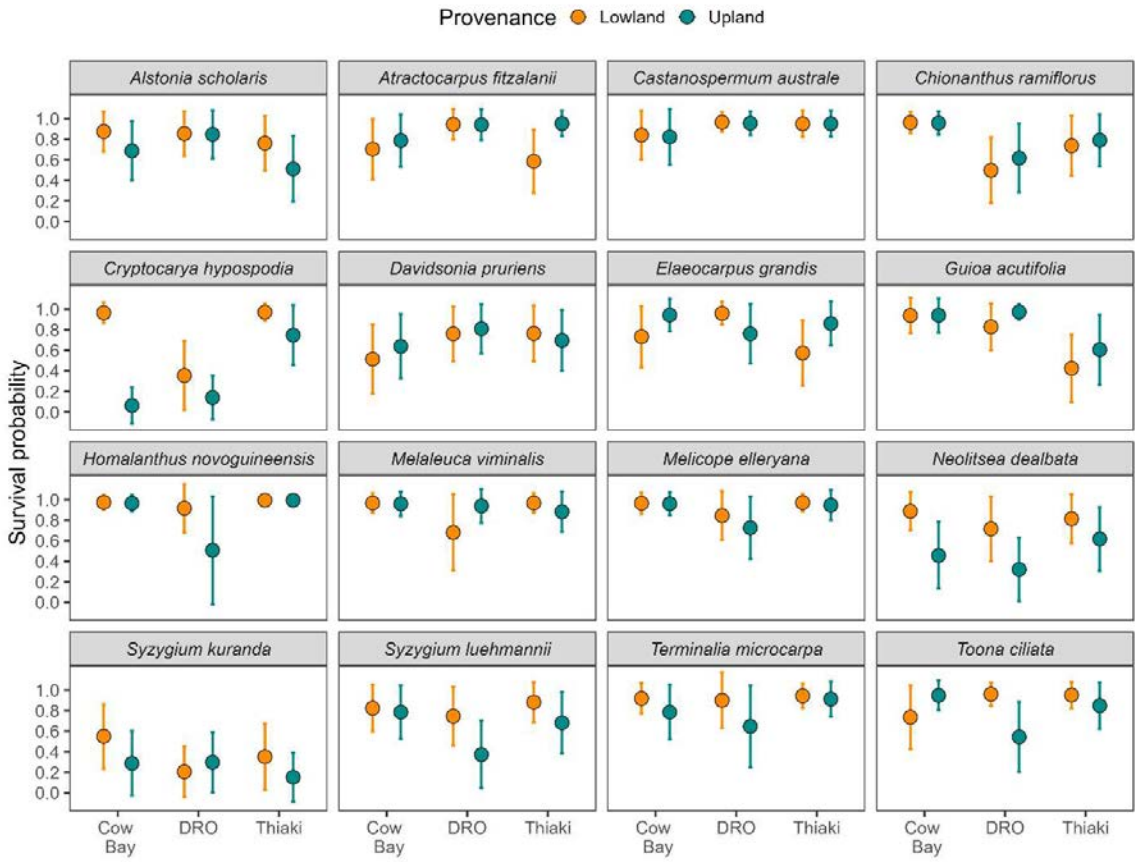

Figure S4. Growth increment across ~17 months in all surviving plants of 14 tropical tree species grown under three common garden conditions in the Australian Wet Tropics. Points represent estimated marginal means of absolute growth increment from full models (see text) for each species with lines indicating confidence interval. Note two species (*Alstonia scholaris* and *Toona ciliata*) removed from analysis given complex interaction with herbivory (see text)